The University of British Columbia

FACULTY OF GRADUATE STUDIES

PROGRAMME OF THE

FINAL ORAL EXAMINATION

FOR THE DEGREE OF

DOCTOR OF PHILOSOPHY

of

JEFFREY ERNEST HENTON

B.Sc., University of Leeds, 1964

MONDAY, OCTOBER 2, 1967, AT 3:30 P.M.

IN ROOM 207 CHEMICAL ENGINEERING BUILDING

COMMITTEE IN CHARGE

Chairman:　　　　　B. N. Moyls

Dr. K.L. Pinder　　　Dr. N. Epstein
Dr. J.S. Forsyth　　Dr. E. Peters
Dr. R.M.R. Branion　Dr. A. Mitchell

External Examiner:　T. Vermeulen
Professor, Department of Chemical Engineering
University of California,
Berkeley, California, U.S.A.

Research Supervisor:　S.D. Cavers

BACKMIXING IN LIQUID-LIQUID EXTRACTION SPRAY COLUMNS

ABSTRACT

Backmixing of the continuous phase was studied
in liquid-liquid spray columns of various geometries,
for various flowrates of the two phases, and for
various drop size distributions.

The dispersion or eddy diffusion model was used
to characterize the axial mixing of the continuous
phase, from a distributor of sodium chloride tracer
(soluble in the continuous phase only). The steady
state form of the model was utilized to calculate
axial eddy diffusivities from these results.

The tracer studies showed that the axial eddy
diffusivity is independent of the continuous phase
flowrate and the column height. Axial eddy diffusi-
vities between 7-ft.^{2}/hr. and 31-ft.^{2}/hr. were obtained
in a 1½-in. I. D. column. Low dispersed phase flow-
rates and large drop sizes resulted in high axial eddy
diffusivities. Increasing the column diameter to 3-in.
resulted in superficial axial eddy diffusivities
between 6.3 and 17.3 times larger.

The hold-up of dispersed phase was measured by
means of a piston sampler. The hold-up increases

approximately linearly with increasing dispersed phase superficial velocity and tends to be slightly higher for increased continuous phase superficial velocities. A smaller drop size resulted in an increased hold-up.

Drop size distributions were measured. They always show two peaks, one at 0.02-in. diameter, and the other at a much larger size, the actual value of which depends on the nozzle tip diameter used to disperse the drops.

The mixing cell-packed bed analogy was used to predict Peclet numbers in a spray column. The agreement between these and measured Peclet numbers is good for drops of about 0.15-in. equivalent diameter but becomes progressively worse as the drop size is reduced.

AWARDS

1964-1967   Commonwealth Scholarship
1966-1967   Finning Tractor Graduate Scholarship

GRADUATE STUDIES

Field of Study: Chemical Engineering

Related Studies

    Mass Transfer   S.D. Cavers

    Statistics   D.A. Ratkowsky

    Fluid and Particle Dynamics   R.M.R. Branion

    Linear Algebra   Wm.R. Simons

Other Studies

    Mass and Heat Transfer Analogies N. Epstein

    Surface Effects   J. Leja

    Optimization   K.L. Pinder

    Computer Programming   K. Teng

BACK-MIXING IN LIQUID-LIQUID EXTRACTION SPRAY COLUMNS

by

JEFFREY ERNEST HENTON

B. Sc., University of Leeds, 1964

A THESIS SUBMITTED IN PARTIAL FULFILMENT OF

THE REQUIREMENTS FOR THE DEGREE OF

DOCTOR OF PHILOSOPHY

in the Department

of

CHEMICAL ENGINEERING

We accept this thesis as conforming to the
required standard

THE UNIVERSITY OF BRITISH COLUMBIA

September, 1967

In presenting this thesis in partial fulfilment of the requirements

for an advanced degree at the University of British Columbia, I agree

that the Library shall make it freely available for reference and

study. I further agree that permission for extensive copying of this

thesis for scholarly purposes may be granted by the Head of my

Department or by his representatives. It is understood that copying

or publication of this thesis for financial gain shall not be allowed

without my written permission.

(

Department of _CHEMICAL ENGINEERING_

The University of British Columbia
Vancouver 8, Canada

Date _2 October 1967_

ABSTRACT

Backmixing of the continuous phase was studied in liquid-liquid spray columns of various geometries, for various flowrates of the two phases, and for various drop size distributions.

The dispersion or eddy diffusion model was used to characterize the axial mixing of the continuous phase. Axial concentration profiles were measured upstream, with respect to the continuous phase, from a distributor of sodium chloride tracer (soluble in the continuous phase only). The steady state form of the model was utilized to calculate axial eddy diffusivities from these results.

The tracer studies showed that the axial eddy diffusivity is independent of the continuous phase flowrate and the column height. Axial eddy diffusivities between 7-ft^2/hr. and 31-ft^2/hr. were obtained in a $1\frac{1}{2}$-in. I. D. column. Low dispersed phase flowrates and large drop sizes resulted in high axial eddy diffusivities. Increasing the column diameter to 3-in. resulted in superficial axial eddy diffusivities between 6.3 and 17.3 times larger.

The hold-up of dispersed phase was measured by means of a piston sampler. The hold-up increases approximately linearly with increasing dispersed phase superficial velocity and tends to be slightly higher for increased continuous phase superficial velocities. A smaller drop size resulted in an increased hold-up.

Drop size distributions were measured. They always show two peaks, one at 0.02-in. diameter, and the other at a much larger size, the actual value of which depends on the nozzle tip diameter used to disperse the drops.

The mixing cell-packed bed analogy was used to predict Peclet numbers in a spray column. The agreement between these and measured Peclet numbers is good for drops of about 0.15-in. equivalent diameter but becomes progressively worse as the drop size is reduced.

TABLE OF CONTENTS

LIST OF TABLES

LIST OF FIGURES

ACKNOWLEDGEMENTS

The author would like to express his sincere gratitude to
Dr. S. D. Cavers for his assistance, encouragement, and helpful criticisms
offered throughout the course of this project.

Thanks are extended to all members of the faculty and staff of
the Department of Chemical Engineering, The University of British
Columbia for their readiness and willingness in discussing both theoret-
ical and practical problems associated with the work. Particular
appreciation is offered to Dr. K. L. Pinder for the loan of a telephoto
lens and to Mr. R. Brandt for making most of the machined parts essential
for this study.

The author is indebted to Dr. Duncan of the British Columbia
Research Council for his suggesting the use of sodium chloride as a
tracer and for providing the use of the atomic absorption spectrophoto-
meter.

Financial support was most gratefully received in the form of
scholarships from the Commonwealth Scholarship and Fellowship Committee
of the External Aid Office, Ottawa, and from the Finning Tractor Company,
Ltd. Funds for the equipment were provided by the National Research
Council.

INTRODUCTION

1. PREVIOUS WORK

Liquid-liquid extraction is used widely for separating components which are more difficult or expensive to separate by other methods such as distillation, evaporation, or precipitation. Extraction processes usually are preferred if the two components to be separated have similar boiling points, or if one of the components is heat sensitive or present in small amounts.

Countercurrent extraction in vertical towers can be carried out when the raffinate and extract phases differ appreciably in density. Although sieve-plate, bubble cap, and packed towers are more commonly found in industrial use "...the spray tower is the more attractive for experimentation because of its inherent simplicity, and also because of the greater possible range of flowrates of the two (phases)..." (1)

Figure 1 shows diagrammatically how each phase is introduced into and removed from a spray tower. In the system shown the less dense phase is dispersed through nozzle tips located at the lower end of the column. The dispersed phase drops rise through the descending continuous phase and coalesce at the interface at the upper end of the column. Many workers have studied spray column operation. The knowledge gained in the main represents an accumulation of small contributions.
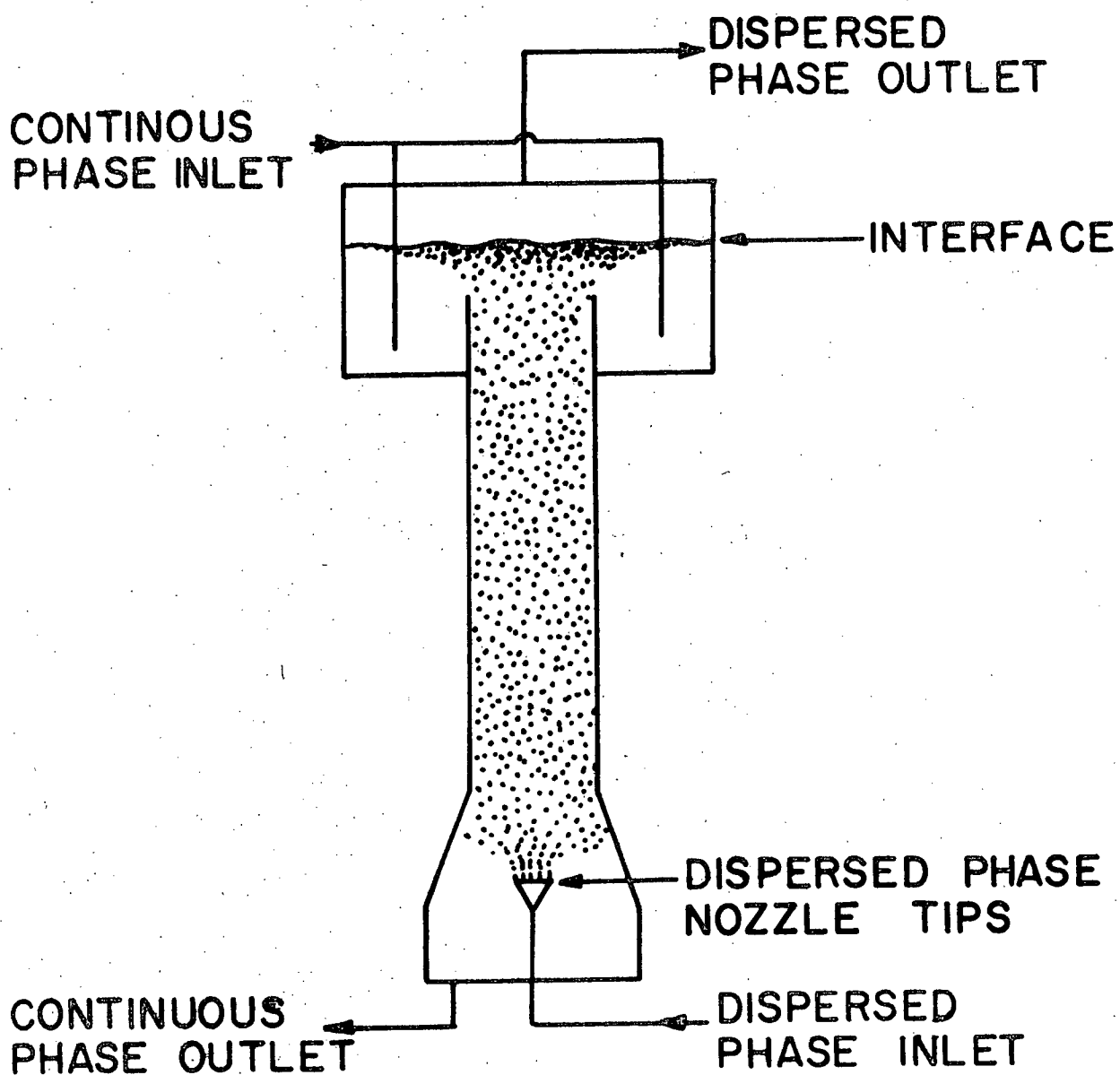
FIGURE 1. SCHEMATIC DIAGRAM OF A SPRAY COLUMN

The designs of the continuous phase inlet and dispersed phase outlet used in the present study were first proposed by Blanding and Elgin (2). Optimum nozzle tip diameters and dispersed phase flowrates in the nozzle tips for reproducible, more or less uniform drop size have been suggested by Johnson and Bliss (3) and later by others (4,5,6,7,8).

From about the early 1930's workers began to perform laboratory scale experiments in attempts to discover simple laws or to formulate correlations which applied to spray tower operation (2,3,9,10,11,12,13). Their results indicate that the extent of extraction is dependent upon the flowrates of the two phases, the direction of solute transfer (i.e. from dispersed phase to continuous phase or vice versa), which phase is dispersed, drop size, column dimensions, and sometimes upon inlet solute concentrations. All these workers analysed only the column inlet and outlet solute concentrations of each phase.

Licht and Conway (14) in 1950 pointed out that the mass transfer process should be considered as taking place in three separate stages - i) drop formation, ii) drop rise, and iii) drop coalescence. Geankoplis and Hixson (1), also in 1950, revolutionized techniques in spray column experimentation by taking samples of the continuous phase from within an operating column. This was accomplished by lowering a hook-shaped sampling probe, (as shown in the sketch below) into the column and then applying a slight vacuum to the upper end of the probe. Continuous phase was drawn into the probe without entraining any dispersed phase.
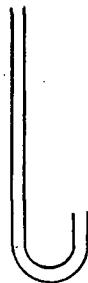
They observed that the basic flow pattern within the column did not

appear to be affected by the probe. In 1951 Geankoplis, Wells and

Hawk (15) extended Geankoplis and Hixson's work, again using an internal

sampling probe, to measure the solute concentration profile in the

continuous phase. A typical experimental solute concentration profile

in the continuous phase is shown in Figure 2.

Geankoplis and co-workers noticed a sharp change, or end-effect,

in solute concentration in the continuous phase at the interface.

They thought "...that the location of the end effect at the continuous

phase inlet may be caused by the inherent turbulence effect of coalescence

of bubbles at the interface..." (15). They made an allowance for this

end effect by calculating a fictitious height of column in which there

would occur the same amount of mass transfer as appeared to occur at

the interface. To calculate solute concentrations in the dispersed

phase at various elevations in the column the use of mass balances was

attempted. On the basis that the superficial flowrates of both phases
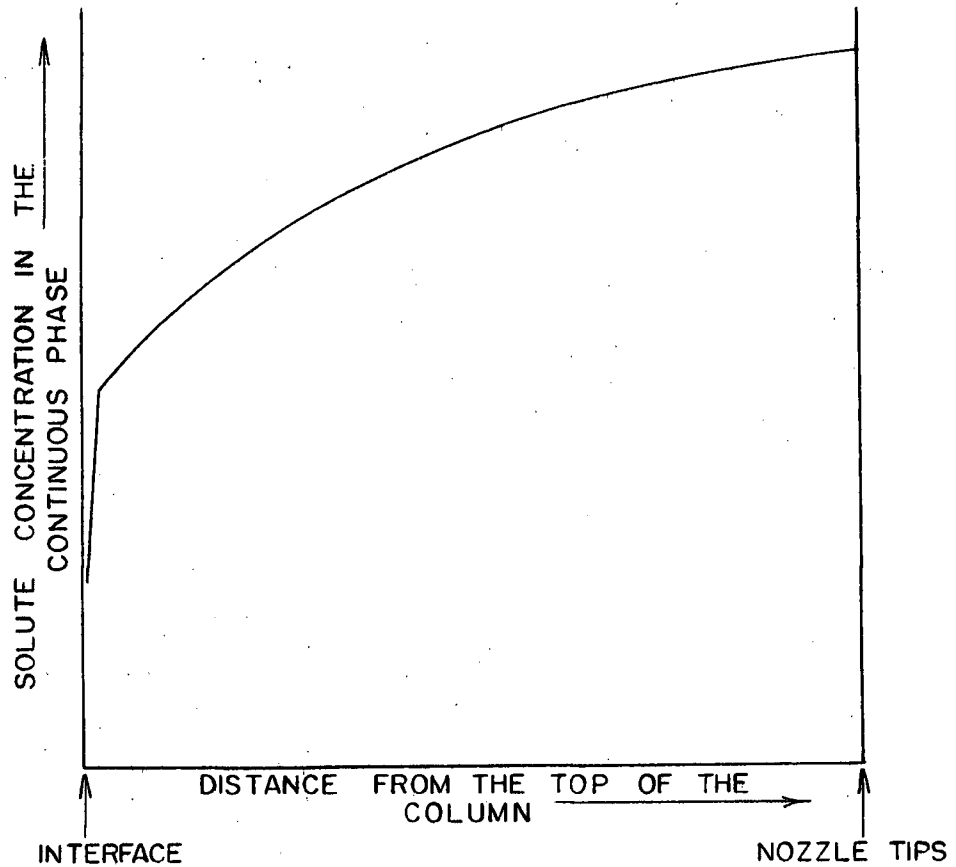
FIGURE 2. SOLUTE CONCENTRATION PROFILE IN A SPRAY COLUMN.

are not affected by solute concentration changes experienced in the column, a material balance on solute around the control zone shown in Figure 3 resulted in the following equation.

$$L_D c_D + L_C c_C^o = L_C c_C + L_D c_D^i$$
1

Thus

$$c_D = \frac{L_C}{L_D} \ (c_C - c_C^o) + c_D^i$$
2
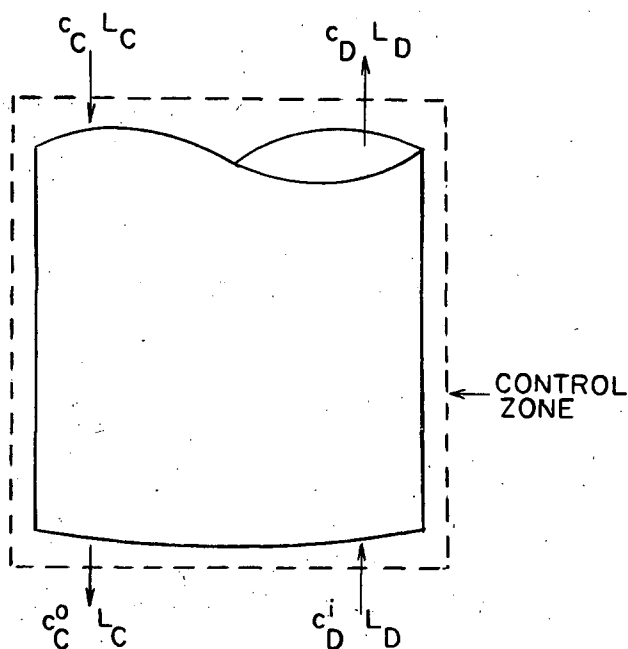
FIGURE 3. MASS BALANCE OVER A SECTION OF A SPRAY COLUMN.

Although some turbulence was observed in the continuous phase (1)
no allowance for its effect was included in the mass balance. Geankoplis
continued his work involving continuous phase sampling with Kreager (16)
and later with Vogt (17).

Morello and Poffenberger (18) were the first to suggest positively
that the continuous phase did not move through the column in effective
plug flow, but that there was recirculation within that phase. They
said that the recirculation, which was later to be called backmixing,
may be caused by thermal currents, density differences or by the friction
of the drops carrying some of the continuous phase along with them.

They portrayed the idea diagrammatically as shown in Figure 4.
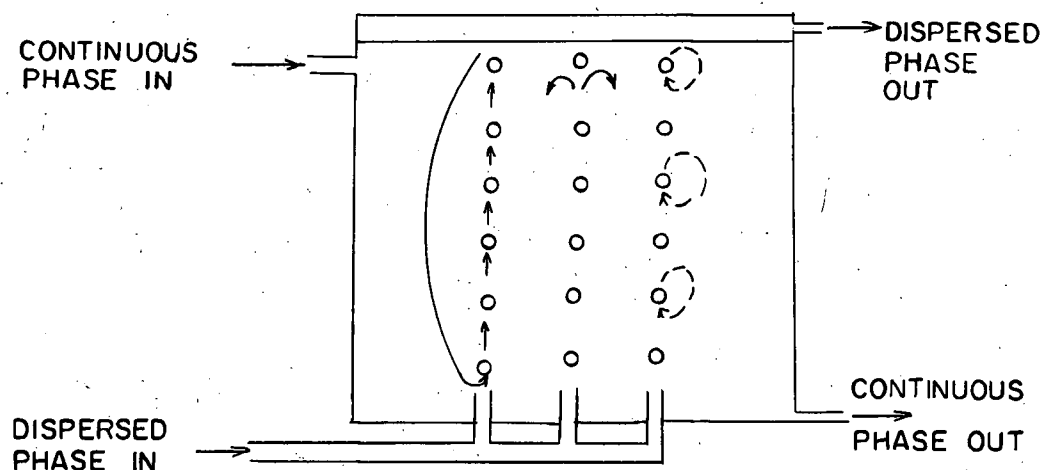
FIGURE 4. CONTINUOUS PHASE RECIRCULATION.

It can be seen that the simple mass balance given in Equation 1 based on plug flow of both phases is not valid.

Although Morello and Poffenberger (18) gave a physical picture of backmixing, Newman (19) pointed out that the end-effect which had been observed by earlier workers could be explained in terms of backmixing of the continuous phase. Also he presented the following argument to show that the solute concentration in the dispersed phase at some point in the column cannot be calculated by a mass balance over short sections of the column. Newman accounted for backmixing by considering a flow of continuous phase countercurrent to the main flow of continuous phase.

This backmixing flow was exactly compensated by an increased main flow of continuous phase. It was assumed that the resulting main flow of continuous phase was radially homogeneous at a given column elevation. The plug flow model and Newman's backmixing model are shown in the following sketch.
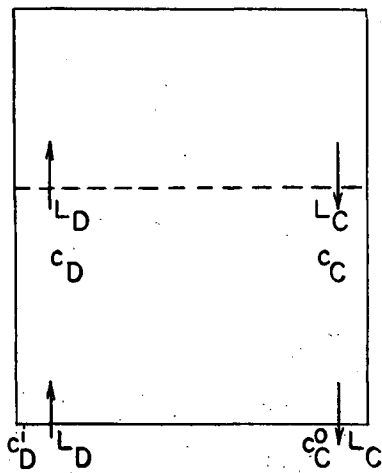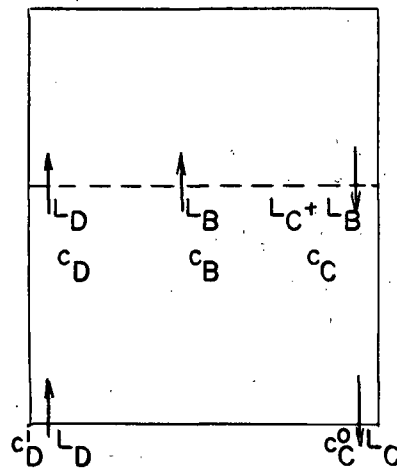
(a) PLUG FLOW MODEL   (b) BACKMIXING MODEL

For plug flow of both phases, as shown in (a) of the above sketch, c_D is given by Equation 2.

$$c_D = \frac{L_C}{L_D} (c_C - c_C^O) + c_D^i$$

2

For backmixing of the continuous phase, as shown in (b) above, a solute mass balance over the lower section of column yields

$$L_D c_D^i + (L_C + L_B) c_C = L_D c_D + L_C c_C^O + L_B c_B$$

3

Thus

$$c_D = \frac{L_C}{L_D} (c_C - c_C^o) + c_D^i + \frac{L_B}{L_D} (c_C - c_B)$$

4

As L_B and c_B cannot be determined it is not possible to use this equation to obtain c_D. For the same reason capacity coefficients and H.T.U. values for short sections of column cannot be derived from the knowledge of terminal conditions and the solute concentration profile in the continuous phase.

Campos (20) calculated the height of tower in which there would occur the same amount of mass transfer as appeared to have produced the end-effect at the continuous phase inlet of the column. He noted also that backmixing of the continuous phase may cause end-effects in spray towers. The existence of a backmixing stream in the form of wakes travelling with the dispersed phase drops has been demonstrated photographically (21, 22, 23, 24), and Li and Ziegler (25) say "In general the process of backmixing in spray towers is believed to be initiated largely in the wakes of droplets". Letan and Kehat (26, 27) have worked with spray column heat exchangers. They explain continuous phase backmixing effects by means of a model in which continuous phase is supposed to be carried along in the form of wakes, with the dispersed phase drops.

Gier and Hougen (28) used hypodermic syringes to draw off continuous phase samples and bell-shaped probes to collect dispersed phase samples.

The accompanying sketch shows an example of each sort of probe used by them. Probes of each sort were distributed along the length of the column.
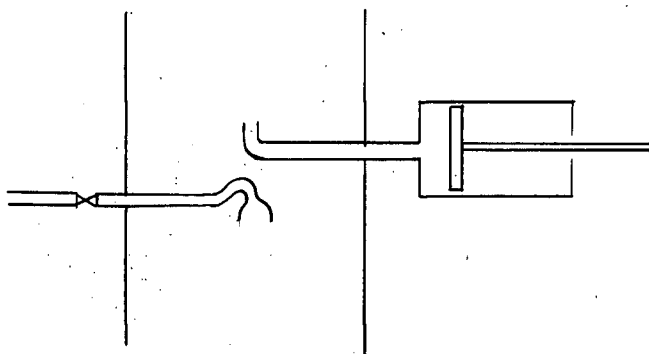
A bell-probe sample contained both dispersed and continuous phases. The sample was allowed to reach equilibrium* and then each phase was analysed for solute. A simple mass balance on solute in the bell-probe sample at the times of collection and analysis results in Equation 5.

$$V_D c_D + V_C c_C = V_D c_D^a + V_C c_C^a$$

5

Therefore

$$c_D = c_D^a + \frac{V_C}{V_D} (c_C^a - c_C)$$

6

In order to calculate c_D from Equation 6 an estimate of c_C, at the elevation of the bell-probe, was made from a plot of the concentration of solute in the hypodermic syringe samples versus column height.

---

* i.e. no change in concentration of either phase with time.

Gier and Hougen calculated values of H.T.U., based on concentration differences in the dispersed phase, by graphical integration using the measured concentration profiles. Their Figure 17 shows the solute concentration in the dispersed phase as determined by means of Equation 6 for one of their runs in which solute was transferred from the continuous phase to the dispersed phase. These concentrations are greater than those which could be obtained from calculation by means of Equation 2 which is based on plug flow of both phases. This result is in agreement with Newman's suggestions (Equation 4). As a result the H.T.U. values calculated by graphical integration were correspondingly lower than those calculated from the column terminal conditions assuming plug flow of both phases. Patton (29) took samples from an operating spray column using the hypodermic needle and inverted funnel technique of Gier and Hougen. He found a considerable drop in the continuous phase solute concentration at the interface which was not matched by a proportional drop in the solute concentration in the dispersed phase. He concluded that the discontinuity in the solute concentration profile in the continuous phase at the interface was due to bulk mixing of the continuous phase in the column.

A development of the sampling technique of Geankoplis and coworkers (1) and of Gier and Hougen (28) was used by Ewanchyna and Cavers (30, 31). They made use of a hook-shaped probe for continuous phase sampling and a bell-shaped probe for dispersed phase sampling. The probes were lowered into the operating column at the ends of stainless steel tubes as shown in Figure 5. Samples were drawn into the probes and
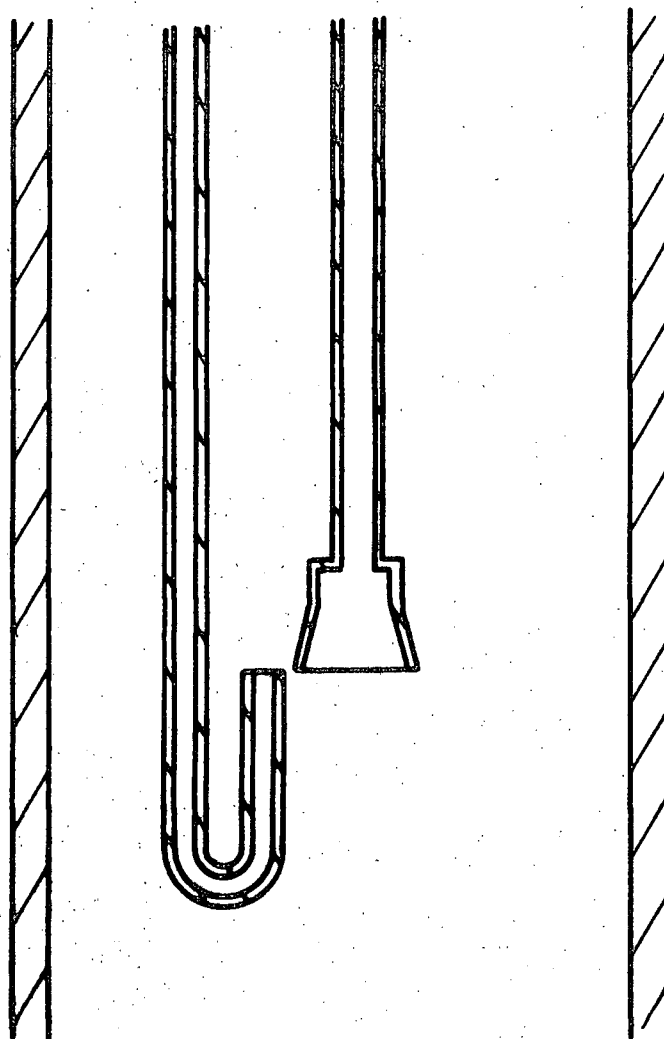
FIGURE 5. HOOK AND BELL-PROBES

and along the sample lines by the use of a water aspirator. Acetic acid was transferred between an aqueous continuous phase and a methyl isobutyl ketone (MIBK) dispersed phase. The aqueous phase was saturated with MIBK and the MIBK phase saturated with water. The solute concentration profile in each phase was measured at various combinations of phase flowrates. Plots were made showing the dependence of capacity coefficients on flowrates and also of H.T.U. values on flowrates. The causes of end effects in spray columns were explained clearly and verified experimentally.

The measured concentration profiles for a typical run with solute being transferred from the continuous aqueous phase to the dispersed MIBK phase are shown in Figure 6. The lines FB and GE are the measured concentration profiles for the dispersed phase and the continuous phase respectively. It was assumed that no backmixing took place in the dispersed phase. This assumption was based on the visual observation that the drops appeared to rise up the column without circulating back on their paths (28, 30, 31). If it is assumed in addition that no backmixing takes place in the continuous phase then Equation 2, which is based on plug flow of both phases, can be used to calculate the line GD. When the drops of dispersed phase arrive at the interface they do not coalesce immediately but remain as part of a drop layer there. Undoubtedly mass transfer takes place into these drops during their sojourn at the interface. Ewanchyna and Cavers attributed the concentration jumps BA (in the dispersed phase) and CD to this interface mass transfer.

The figure shows concentration profiles in a spray column with axes "SOLUTE CONCENTRATION" (vertical) and "HEIGHT UP COLUMN" (horizontal). Labeled points include C, D, E, H, A, B, G, F, with annotations "CONTINUOUS PHASE INLET", "CONTINUOUS PHASE OUTLET", "DISPERSED PHASE OUTLET", "DISPERSED PHASE INLET", "NOZZLE", and "INTERFACE".
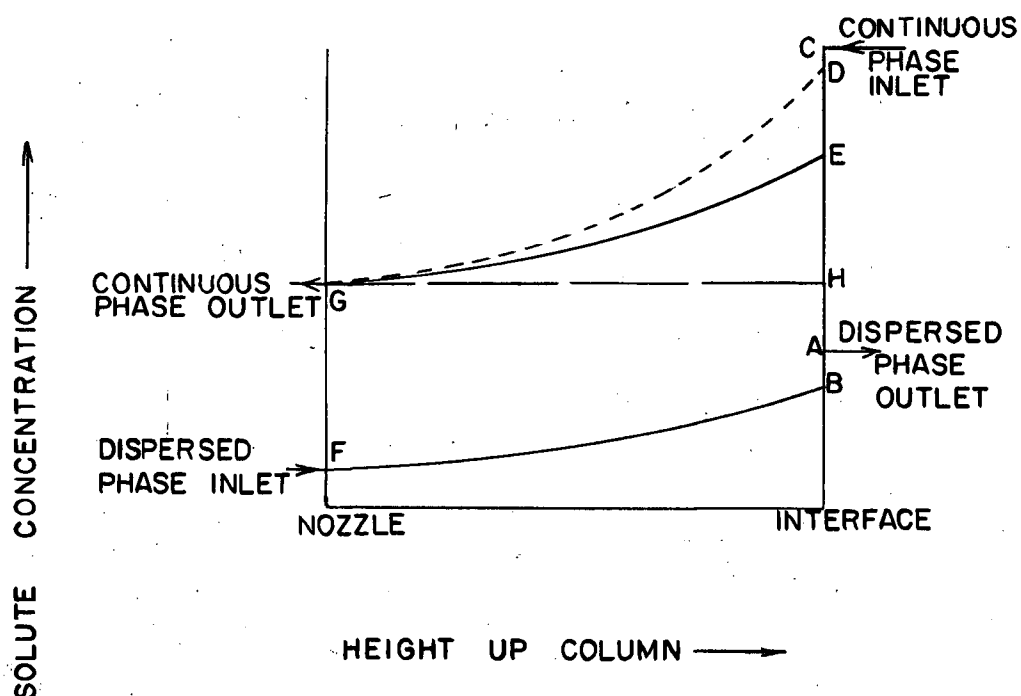
FIGURE 6. CONCENTRATION PROFILES IN A SPRAY COLUMN.

They attributed the change DE to axial mixing of the continuous phase. The line GH is the concentration profile which would be expected for perfect mixing of that phase under conditions such that the solute concentration in the aqueous stream leaving the column was that given by point G. It can be seen that the measured aqueous phase solute concentration profile (GE) lies between that expected for perfect mixing (GH) and that for true countercurrent flow (GD). Evidently the continuous phase does undergo some axial mixing.

Ewanchyna and Cavers (30, 31) found that the results of runs with solute transferred from the dispersed phase to the continuous phase supported the above ideas. With solute transferred to the continuous phase drops coalesce immediately on reaching the interface (31, 32, 33, 34). As a result there was negligible mass transfer at the interface and hence no jump in the dispersed phase concentration profile there. The results of a typical run are shown in Figure 7.
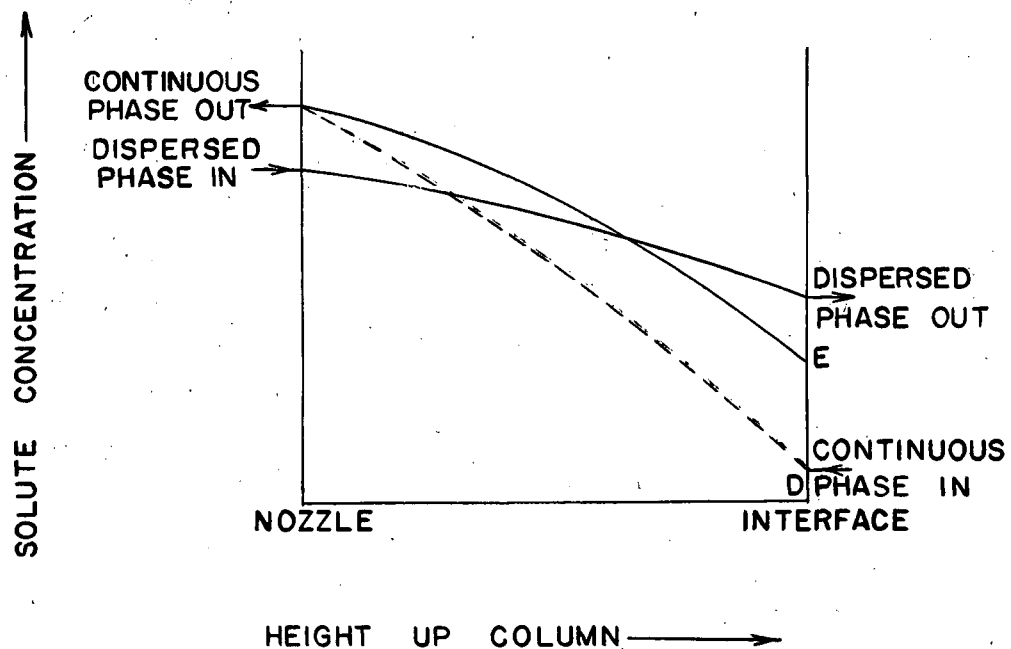
FIGURE 7. CONCENTRATION PROFILES IN A SPRAY COLUMN.

The whole of the solute concentration change (DE) in the continuous phase at the interface was attributed to backmixing of the continuous phase in the column.

Choudhury (35) continued Ewanchyna's work. To allow for backmixing of the continuous phase in the derivation of an expression for (H.T.U.) $_{overall}$ values, based on a logarithmic mean dispersed phase concentration driving force, he introduced a correction factor, F_m, as Pratt (36) had done for packed towers.

The question was raised as to whether the solute concentration in the continuous phase entering the bell-probe with the drops was the same as that entering the hook-probe. It was thought that the bell-probe might sample preferentially continuous phase which was in the immediate vicinity of the drops. If this continuous phase were not of the same solute concentration as that in the main bulk of the continuous phase the use in Equation 6 of c_C from a hook-probe sample in order to calculate c_D in a bell-probe sample would be invalid.

In order to test the hook and bell sampling technique Hawrelak (37) designed and constructed a piston sampler. A sketch of this device is shown in Figure 8. By moving the piston from one side of the piston block to the other it was possible to remove a bulk sample of both phases from the column and allow the column to continue operating. With this device Hawrelak (37), and later Bergeron (38),
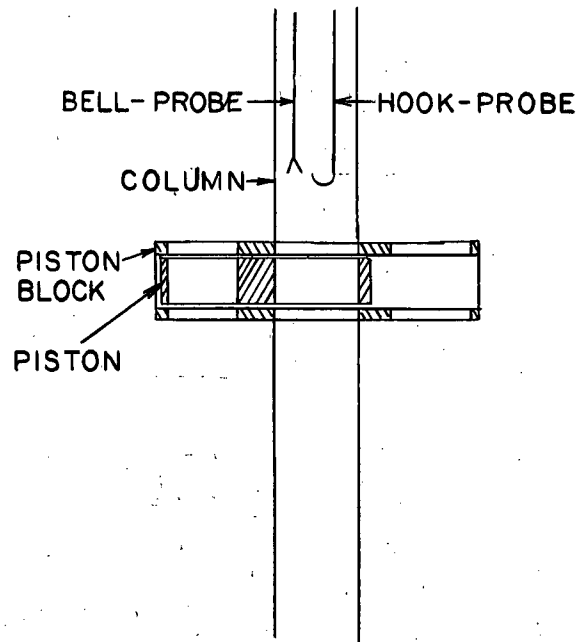
FIGURE 8. PISTON SAMPLER.

compared solute concentrations in the dispersed phase calculated

using the bell and hook-probes with those calculated from results

using the piston sampler and the hook-probe. It was necessary to

assume that the hook-probe sample was representative of the continuous

phase in the column at the sampling height. However, no definite

conclusions were drawn, mainly because the column was run under such

conditions that the two phases were near equilibrium at the sampling

elevation.

Rocchini (39, 40) studied drop shape and measured drop size

distributions in a spray column by examining close-up photographs

taken of an operating column.

Dispersed phase hold-ups in spray towers have been calculated largely from Equation 7 (3).

$$h = \frac{100\ L_D}{u}$$

7

However, Weaver, Lapidus and Elgin (41) determined hold-ups by isolating a section of column between two quick-acting ball valves and measuring the volume of each phase collected. Hawrelak (37) and Bergeron (38) measured dispersed phase hold-ups, without disrupting the column operation, with the aid of a piston sampler described earlier. It has been found (3, 30, 35, 42) that the dispersed phase hold-up increases only slightly with increasing continuous phase flowrate and is nearly linearly dependent on the dispersed phase flowrate.

Hayworth and Treybal (4) and Johnson and Bliss (3) have observed that the length of a jet of dispersed phase leaving a nozzle tip increases to a maximum and then decreases as the flowrate of dispersed phase increases. They noticed that the size of the drops formed at the ends of the jets of dispersed phase also increases to a maximum with increasing dispersed phase flowrate. However, the dispersed phase flowrate at which the maximum drop size occurs is lower than that at which the maximum jet length occurs. The claim was made that uniformly sized drops are produced at dispersed phase flowrates lower than those which give the maximum drop size. The formation of many small drops along with larger drops has been

observed under some operating conditions (4, 43). Weaver, Lapidus, and Elgin (41) found no noticeable change in drop size distribution along the length of a spray column. Garwin and Smith (43) report that the dispersed phase drop size is independent of the continuous phase flowrate.

2. MATHEMATICAL MODELS

In order to describe fully a turbulent field it is necessary to know the velocity vector at all points and at all times. However, such knowledge is unavailable. Therefore a measurement of some effect of the turbulence usually is made in order to characterize the extent of the turbulence. Even when the flow patterns in the turbulent field are of a complicated nature a simple mathematical model often adequately describes the mixing taking place. In the past the design of flow reactors has been based largely upon two idealized models: plug flow, and completely mixed flow. Plug flow assumes a flat velocity profile, whereas completely mixed flow assumes that the fluid in the vessel is perfectly mixed. The three most popular models which lie between the two extreme cases are the dispersion, mixing cell, and random walk models. For the case of fluid flow through a long column or bed the mathematical implications of all three models are essentially the same (44, 45, 46). However, there are fundamental differences between the premises upon which the models are based. Brief outlines of these models are presented below together with summaries of some of the more important researches

which have utilized them for interpreting experimental data. Axial

mixing of only one phase is considered in each case.

DISPERSION MODEL

It is assumed that axial mixing due to turbulence follows a

law similar to Fick's Law for molecular diffusion. On this basis

a mass balance on solute in the continuous phase over an incremental

section of column yields Equation 8 for the case of no mass transfer

to or from the continuous phase. (Also see Appendix 1.)

$$Ee \frac{\delta^2 c_C}{\delta z^2} - L_C \frac{\delta c_C}{\delta z} = e \frac{\delta c_C}{\delta t}$$

8

It is assumed that radial homogeneity prevails. Wilson (47)

solved an equation similar to Equation 8 for molecular diffusion

of heat from a point source into a flowing fluid. Wilson's solution

has been used together with experimental data (48, 49, 50) to

calculate eddy diffusivities in open ducts on the assumption of

isotropic homogeneous turbulence. Bernard and Wilhelm (51) used

a similar method to determine eddy diffusivities in packed columns.

In 1949 Gilliland and Mason (52) applied the model to the

steady state operation of an air-fluidized bed. At steady state c_C

is independent of t and Equation 8 can be integrated (Appendix I)

to give

$$Ee \frac{dc_C}{dz} = L_C c_C - J$$

9

where the constant of integration, J, is the net flux of solute down the column. If the test section is, from the viewpoint of the continuous phase, upstream from the feed point of tracer, then

$$J = 0$$

and Equation 9 yields Equation 10 on integration.

$$\ln \left[\frac{(c_C)}{(c_{CO})} \right] = \frac{L_C z}{Ee} \qquad 10$$

Gilliland and Mason (52, 53) injected a tracer gas at a constant rate into the bed and measured tracer concentrations at various points in the bed below the level of tracer injection. From the slope of a plot of $\ln (c_C)$ versus z they were able to calculate the superficial axial eddy diffusivity, (eE). The above method for estimating axial eddy diffusivities cannot be utilized for the cases of single phase or co-current flows because the process of axial mixing would not, in this case, carry the tracer upstream in the continuous phase with respect to the tracer injection point. The model has been applied subsequently to the study of pulsed sieve-plate extraction columns (54, 55), gas-sparged tubular vessels (56), rotating-disk contactors (57, 58), and commercial fluidized bed catalyst regenerators (59).

Continuous phase axial eddy diffusivities have been determined mostly by considering the effect downstream, with respect to the continuous phase, of an unsteady state injection of tracer. Equation 8 has been solved for injection of tracer according to a Dirac

Delta Function or single pulse, a step function, and a sinusoidal function. These three different methods of tracer injection are discussed briefly below.

Dirac Delta Function

With no axial mixing a transverse-homogeneous single pulse of tracer injected into a moving stream would appear downstream as a single pulse at all times. With some axial mixing, spreading with respect to distance within the column of the tracer pulse results. Danckwerts (60) and Levenspiel and Smith (61) showed how to interpret the plot of tracer concentration versus time for some point downstream from the place of tracer injection. Such a plot is called a C-curve (60) and the second moment or variance of this curve is related to the axial eddy diffusivity. Axial eddy diffusivities have been determined by the Dirac Delta Function method for packed columns (62, 63, 64), pulsed sieve-plate columns (54, 55, 100), coiled tube reactors (66), and liquid-fluidized beds (67). Van der Laan (68) showed how to determine the axial eddy diffusivity from the variance of a C-curve for a finite length of vessel by using the appropriate boundary conditions (60, 69). Aris (70) pointed out that it is impossible to inject a perfect pulse of tracer into a column. Also he showed, however, that it is not necessary for the tracer injection to be in the form of a perfect pulse if one takes the difference of the second moments of the C-curves measured at two different points in the column. Aris'

theory was later corrected by Bischoff (71) who, together with
Levenspiel (72, 73), presented the theory in detail. Axial eddy
diffusivities in liquid-liquid spray columns at flooding conditions
(74), in packed beds (75), and in orifice plate gas-liquid reactors
(76) have been determined by taking the difference of the variances
of C-curves.

Step Function

A step function of tracer can be introduced into a column by
suddenly stopping or starting the flow of tracer. A plot of down-
stream tracer concentration versus time is called an F-curve (60)
or breakthrough curve. The gradient of the F-curve at a particular
value on the time axis is related to the axial eddy diffusivity.
Gilliland and Mason (53) examined an F-curve for a fluidized bed
in 1952, but at that time a theoretical analysis of such a curve
had not been developed. In 1953 Danckwerts (60) showed how to
calculate the axial eddy diffusivity from an experimental F-curve.
Axial eddy diffusivities have been determined from breakthrough
curves for packed beds (46, 60, 77, 78, 79, 80, 81, 82), spray
columns (42), and rotating disk contactors (83). Brutvan (84)
determined axial eddy diffusivities from breakthrough curves in a
spray column where the dispersed phase was solid spheres. A
statistical analysis of experimental breakthrough curves has been
discussed by Klinkenberg (85). Levenspiel and Bischoff (73)
indicated how to eliminate the effect on the F-curve of the
particular method of tracer injection used. The procedure involved
taking measurements at two elevations in a column. Miller and

King (86) examined the slopes of F-curves measured at two axial distances in a packed bed to calculate axial eddy diffusivities. It should be noted that the F-curve is the time integral of the C-curve (79). This fact has been demonstrated experimentally (87).

Sinusoidal Function

Under the influence of axial mixing in a column a sinusoidal function of tracer concentration suffers both attenuation and phase lag. Levenspiel and Bischoff (73) derived equations relating the Peclet number to the attenuation and phase lag of a sinusoidal input of tracer. The sinusoidal input or frequency response method has been used to determine Peclet numbers for gas flow and liquid flow through random and ordered packed beds (63, 88, 89, 90, 91, 92, 93, 94, 104). Ebach and White (63) showed how to evaluate results for periodic tracer input functions which are not sinusoidal.

In liquid-liquid extraction columns two phase countercurrent flow with mass transfer is encountered. The performance of such columns has been predicted on the basis of Equation 8 modified to include a mass transfer term (95, 96, 97, 98) as shown below

$$E_e \left(\frac{\partial^2 c_C}{\partial z^2} \right) - L_C \left(\frac{\partial c_C}{\partial z} \right) - K_D a \left(\frac{c_C}{m} - c_D \right) = e \left(\frac{\partial c_C}{\partial t} \right)$$

I-1

Theoretical concentration profiles in extraction columns have been calculated for various operating conditions (99, 100, 101, 102, 103).

Theoretical concentration profiles have been compared with experimental profiles for various liquid-liquid extraction devices. Agreement was good for pulsed columns (58, 102) and moderately good for some conditions of spray column operation (103) and for gas absorption-tower operations (105).

Gottschlich (106) applied Equation 8 to a packed column. In doing so he modified the equation to take into account stagnant layers of fluid around the packing elements. He reports that the modification improves the agreement of experimental results and the theoretical model. Van Deemter, Zuiderweg, and Klinkenberg (107) used the dispersion model to correct for non-ideality in chromatography due to axial dispersion.

MIXING CELL MODEL

Kramers and Alberda (90) drew an analogy between single phase flow in a packed bed and a series of perfect mixing vessels. They assumed a long bed and restricted the magnitude of the particle Peclet number. On these bases they showed that the dispersion model and mixing cell model yield the same frequency response diagram for a sinusoidally varying tracer input. Other workers (44, 64, 92, 108, 109) have followed Kramers and Alberda's approach for single phase flow. It has been shown that for the analogy to be valid the Peclet number, Pe', must be given by Equation 11,

$$Pe' = \frac{2}{\lambda}$$

11

where λ is the ratio of the length of a mixing cell, d_i, to the characteristic packing dimension, d_p (See Appendix II.) In a packed bed the axial distance between layers of packing is taken to be equal to the height of a mixing cell.

Aris and Amundson (108) and Jacques and Vermeulen (46) used the Poisson probability distribution function to describe the residence time distribution of a tracer molecule on the basis of the mixing cell model.

Epstein (110) has developed charts for a correction factor which modifies log mean driving forces for single phase flow in packed beds. The model is based on the analogy between a fixed bed of particles and a series of perfect mixers.

Theoretical arguments have been presented relating the dispersion model to a series of perfect mixing cells with backflow between mixers (45, 100, 111, 112, 113). Li and Ziegler (25) recently have published a review of the experimental and theoretical work done on the application of the dispersion and the mixing cell models to spray and packed towers.

RANDOM WALK MODEL

The theory for the random walk model is based on Einstein's statistical treatment (115). Small packets of fluid are assumed to move in an intermittent fashion, the motion being over a

distance, and lasting for a length of time, both of which are taken to be purely random quantities. Jacques and Vermeulen (46) show that the random walk model, the mixing cell model, and the dispersion model result in the same mathematical equation for residence time distributions. Axial eddy diffusivities for packed beds have been determined using the random walk model and input of tracer according to a step function (46, 116, 117).

OBJECT OF THIS RESEARCH

In 1963 Gerster (127) summarized the work which had been done on the effect of axial mixing upon the performance of extraction columns. He suggested that much further work in the field of axial eddy diffusion was needed.

Previous work to determine axial eddy diffusivities in spray columns has been carried out by Hazlebeck and Geankoplis (42) and by Brutvan (84). The former investigation involved the use of water as the aqueous phase and MIBK as the dispersed phase in a $1\frac{1}{2}$-in. I.D. column. Only one set of nozzle tips, which produced drops of about 0.135-in. diameter, was used throughout the work. The step function input application of the dispersion model was used as described earlier. The axial eddy diffusivity was found to increase linearly between 12-ft^2/hr. and 22-ft^2/hr. for continuous phase superficial velocities between 10-ft^3/hr. ft^2 and 45-ft^3/hr. ft^2 respectively. For a given continuous phase

superficial velocity the axial eddy diffusivity was constant

for dispersed phase superficial velocities between 18.4-ft.^{3}/hr. ft.^{2}

and 50-ft.^{3}/hr. ft.^{2} Brutvan performed experiments in 1-in., $1\frac{1}{2}$-in.,

and 2-in. I.D. columns with water as the continuous phase and

glass beads, of diameters 3, 4, 5, and 6-mm. respectively, as

the dispersed phase. He, also, used the step function input

application of the dispersion model. Various dispersed phase

superficial velocities between 10-ft.^{3}/hr. ft.^{2} and 100-ft.^{3}/hr. ft.^{2}

and continuous phase superficial velocities between 140-ft.^{3}/hr. ft.^{2}

and 780-ft.^{3}/hr. ft.^{2} were studied. He found that the axial eddy

diffusivity increased with increasing column diameter, increasing

dispersed phase flowrate, decreasing continuous phase flowrate

and decreasing dispersed phase particle size. Both the investi-

gations of Hazlebeck and Geankoplis and of Brutvan did not take

into account the problems associated with the production of a

perfect step function as mentioned earlier. No work has been

reported where axial eddy diffusivities in spray columns were

determined by means of the steady state application of the

dispersion model.

Accordingly, the object of the present work was to measure

axial eddy diffusivities in an operating liquid-liquid spray

column. The steady state form of the dispersion model was used

in these investigations. Since little was known of the effect

of various operating parameters on eddy diffusivity it was

decided that the effects of flowrates of the two phases, column

length, and column diameter on the axial eddy diffusivity should
be investigated. A minor objective in the form of a preliminary
study was to find suitable methods for sampling the continuous
and dispersed phases of an operating spray column.

<u>THEORY</u>

APPLICATION OF THE DISPERSION MODEL TO RUNS WITH NO MASS TRANSFER

In the present work the dispersion model described in the Introduction was used. The general assumptions upon which this model is based are listed below.

1. Backmixing of the continuous phase can be represented by Fick's Second Law of Diffusion with a constant axial eddy diffusivity throughout the column.

2. The molecular diffusivity of any solute considered is negligible compared to the axial eddy diffusivity.

3. Radial homogeneity prevails at constant axial position.

4. The velocity profile in the continuous phase is flat.

5. Volumetric flowrates are constant throughout the column.

6. A test section of column is considered in which no hydrodynamic property is affected by the column terminal conditions.

7. There is no backmixing of the dispersed phase.

Determination of Axial Eddy Diffusivities

In addition to the above assumptions the following assumptions were made for determining axial eddy diffusivities.

1. The axial eddy diffusivity in the continuous phase is not

affected by the chemical nature of the solute.

2.   The solute dissolves only in the continuous phase.

The theory is developed for a test section of column which lies, from the viewpoint of the continuous phase, upstream from the point of injection of tracer.   The downstream flow of tracer due to bulk flow of the continuous phase is equated to the backflow of tracer by axial eddy diffusion to give

$$L_C\, c_C = Ee\, \frac{dc_C}{dz}$$

12

E is the axial eddy diffusivity and (Ee) is the superficial axial eddy diffusivity.   Obviously Equation 12 results from Equation 8 at steady state.   As mentioned earlier, also, the solution of Equation 12 is

$$\frac{L_C\, z}{Ee} = \ln\left[\frac{(c_C)}{(c_{CO})}\right] \quad ,$$

13

where c_{CO} is the value of c_C at $z = 0$.   It can be seen from Equation 13 that a plot of $\ln c_C$ versus z has a slope of $\frac{L_C}{Ee}$ if the model holds good.   Derivations of Equations 12 and 13 are given in Appendix I.

Prediction of Peclet Number by the Mixing Cell Analogy

As mentioned in the Introduction the analogy between single

phase flow through a packed bed and through a series of perfect
mixers results in the following limitation on the particle Peclet
Number, Pe'. (See Appendix II.)

$$Pe' = \frac{2}{\lambda}$$

where

$$\lambda = \frac{d_i}{d_p}$$

where d_i is the distance between layers of packing pieces.

It is suggested that the above analogy can be extended to
spray column operation by allowing the co-ordinate axes of reference
to move at the same velocity as the rising dispersed phase drops.
As shown in Appendix II, on this basis a spray column tends,
mathematically speaking, towards a packed bed. If the drops are
assumed to be arranged in some simple lattice structure, λ can be
expressed purely in terms of h . Therefore the predicted drop
Peclet number is a simple function of h only. Equations for
predicting the drop Peclet number, Pe, from the hold-up, h, have
been derived in Appendix II for six different lattice arrangements
of drops.

APPLICATION OF THE DISPERSION MODEL TO LIQUID-LIQUID EXTRACTION

On the basis of the dispersion model the reduced concentration
of solute in the continuous phase of a liquid-liquid extraction
column is given by Equation 14.

$$C_C = A \exp(\lambda_1 Z) + B \exp(\lambda_2 Z) - Q$$

14

where

$$\lambda_1 = \alpha + \sqrt{\alpha^2 + \beta} \quad ,$$

15

$$\lambda_2 = \alpha - \sqrt{\alpha^2 + \beta} \quad ,$$

16

$$2\alpha = \frac{L_C H}{Ee} + \frac{K_D aH}{L_D} \quad ,$$

17

$$\beta = \frac{(L_D - mL_C) K_D aH^2}{mL_D Ee} \quad ,$$

18

$$Q = \frac{Jm}{c_{CO}(L_D - mL_C)} \quad ,$$

19

and A and B are constants of integration. Equations 14 to 19 inclusive correspond to Equations I-13, I-14, I-15, I-10, I-11, and I-16 in Appendix I.

If the solute concentration profiles are available for both phases of a liquid-liquid extraction spray column the capacity coefficient, $(K_D a)$, can be calculated by means of Equation 20.

$$K_D a = \frac{L_D}{H} \int \frac{dc_D}{\left(\dfrac{c_C}{m} - c_D\right)}$$

20

The integral in Equation 20 is evaluated graphically over the length of test section, H. The volumetric fraction of continuous phase, e, in the column can be measured by means of a piston sampler (37). For steady-state operation the net flux, J, of solute down the column must be the same at any elevation in the column. J can be calculated from a knowledge of the superficial velocities of both phases and solute concentrations in the streams entering and leaving the column by means of Equation 21.

$$J = \tfrac{1}{2} \left[(L_C c_C^i - L_D c_D^o) + (L_C c_C^o - L_D c_D^i) \right]$$

21

Boundary conditions for Equation 14 have been suggested by Danckwerts (60). These could be used to calculate the values of A and B in that equation. Then, if an estimate of the axial eddy diffusivity, E, were available, the concentration profile of solute in the continuous phase could be predicted by means of Equation 14. However, the boundary conditions rely on the assumption that the dispersion model is applicable at the ends of the spray column. Some doubt exists as to whether this assumption is valid because the hydrodynamic flow patterns are much different in the Elgin head at the upper end of the column, and in the conical section at the lower end of the column, than in the column proper.

Another method for calculating values of A and B consists of fitting Equation 14 to a measured solute concentration profile in the continuous phase. In carrying out this curve fitting, an estimate of the axial eddy diffusivity, E, is obtained. Since Equations

15 to 18 inclusive involve E, values of E can be chosen by trial and error to produce the best fit of Equation 14 to the measured concentration profile.

One method of fitting Equation 14 to an experimental profile is by means of the least squares technique. Estimates of the values of A and B are obtained by minimizing the sum of the squares of the differences between measured concentrations and those given by Equation 14. That is, the value of Δ^2 given by Equation 22, must be a minimum.

$$\Delta^2 = \sum \left[C_C - A\exp(\lambda_1 Z) - B\exp(\lambda_2 Z) + Q \right]^2$$

22

If Equation 22 is differentiated partially with respect to A and this result equated to zero, and then again with respect to B, and that result equated to zero, two simultaneous equations in A and B, Equations 23 and 24, result.

$$A\sum(\exp(\lambda_1 Z))^2 + B\sum(\exp(\lambda_1 Z)\exp(\lambda_2 Z)) = \sum(C_C\exp(\lambda_1 Z)) + Q\sum\exp(\lambda_1 Z)$$

23

$$A\sum(\exp(\lambda_1 Z)\exp(\lambda_2 Z)) + B\sum(\exp(\lambda_2 Z))^2 = \sum(C_C\exp(\lambda_2 Z)) + Q\sum\exp(\lambda_2 Z)$$

24

Equations 23 and 24 can be solved for A and B. This process can be repeated for various assumed values of the axial eddy diffusivity, E. The value of E which results in the lowest value of Δ^2 is one estimate of the true value of E.

APPARATUS

The original apparatus was designed and built by Le Page (118). However, it has been modified by others (37, 38, 39) and by the author. A schematic flow diagram of one arrangement of the apparatus used in the present work is shown in Figure 9. This arrangement was used for tracer studies with no interphase mass transfer in a $1\frac{1}{2}$-in. I.D. column. A key to Figure 9 is presented in Table 1.

All control valves were stainless steel needle valves with Teflon packing. The centrifugal pump, P_1, supplies the constant head tank, E, with de-ionised water from the storage tank, A. Water flows from the constant head tank, E, through the control valve, J, and rotameter, G, to the Elgin head, M, of the column. Water flows down, as the continuous phase, through the column proper, R, leaving at the lower end of the column and passing through the interface control valve, X, and rotameter, Y, to the receiving tank, B. MIBK is supplied to the constant head tank, F, by the centrifugal pump, P_2, from the supply tank, D. From the constant head tank, F, MIBK flows through the control valve, K, and rotameter, H, to the dispersed phase nozzle, S, at the lower end of the column. MIBK rises, in the form of drops, through the descending water in the column and coalesces at the interface, Q. From the Elgin head MIBK flows directly to the receiving tank, C. It is possible to
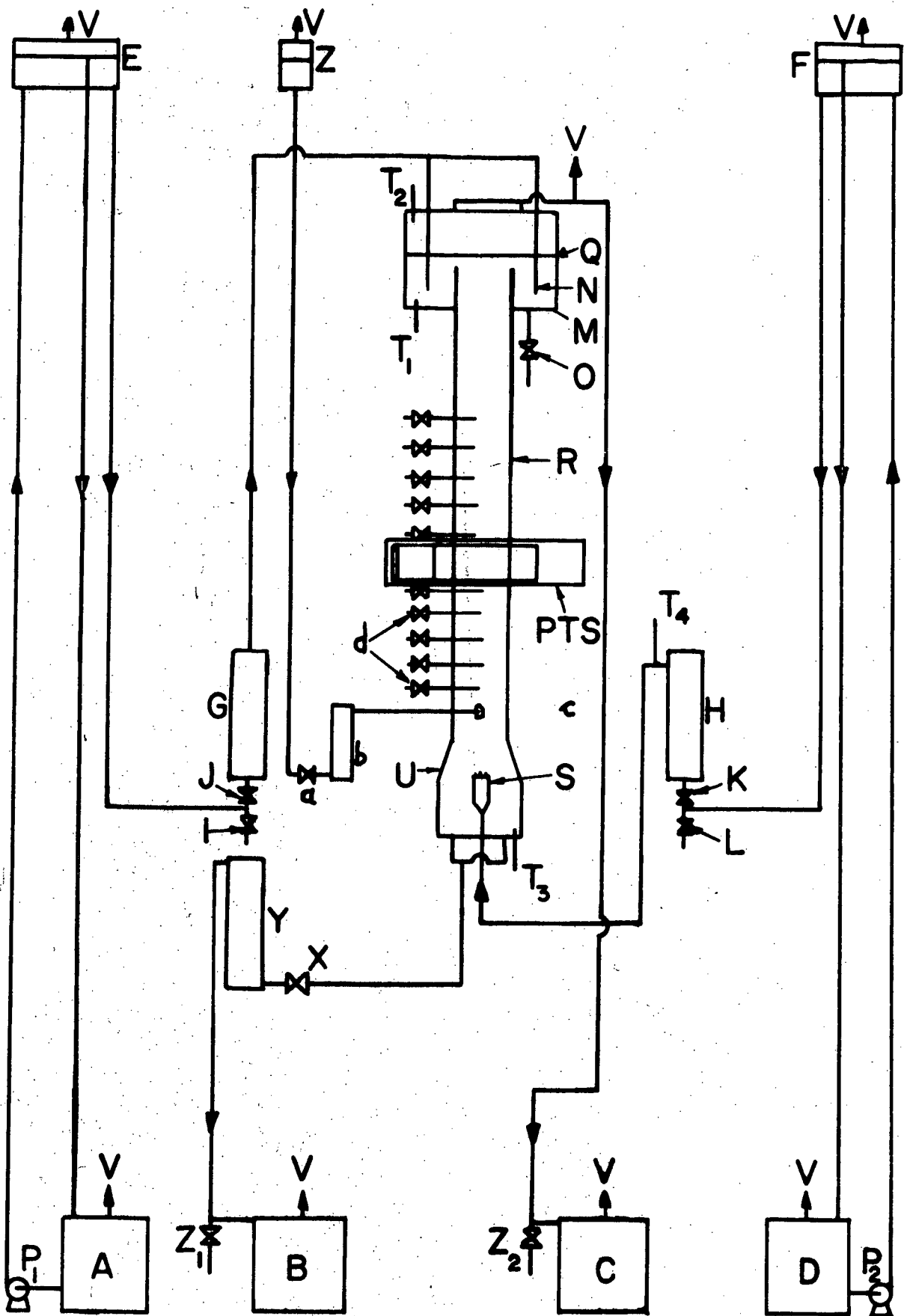
FIGURE 9. SCHEMATIC FLOW DIAGRAM FOR THE 1½-IN. I.D. COLUMN

TABLE 1

(Key to Figure 9)

A	Continuous phase feed tank.
B	Continuous phase receiver and storage tank.
C	Dispersed phase receiver and storage tank.
D	Dispersed phase feed tank.
E	Continuous phase constant head tank.
F	Dispersed phase constant head tank.
G	Continuous phase feed rotameter.
H	Dispersed phase feed rotameter.
I	Continuous phase inlet sample valve.
J	Continuous phase flowrate control valve.
K	Dispersed phase flowrate control valve.
L	Dispersed phase inlet sample valve.
M	Elgin head.
N	Continuous phase inlet pipes.
O	Elgin head drain valve.
P_1	Centrifugal pump for continuous phase.
P_2	Centrifugal pump for dispersed phase.
PTS	Piston-type sampler.
Q	Interface.
R	Column proper.
S	Dispersed phase nozzle.
T_1, T_2, T_3, T_4	Thermometers

U   Bottom conical section.

V   Vent to atmosphere.

X   Interface level control valve.

Y   Interface level control rotameter.

Z   Tracer constant head tank.

a   Tracer flowrate control valve.

b   Tracer feed rotameter.

c   Tracer distributor.

d   22-gauge hypodermic needle samplers.

take a bulk sample from the column with the piston sampler, PTS,
details of which are to be found elsewhere (37, 38). A drawing of
the piston sample collection vessel for dispersed phase hold-ups
greater than 12% is shown in Appendix V. The piston sample
collection vessel for dispersed phase hold-ups less than 12% is
similar and is described elsewhere (37). Both of the piston sample
collection flasks were calibrated by weighing them when they
contained various amounts of water.

Sodium chloride dissolved in MIBK-saturated water was used
as tracer. A concentrated solution of this flows from the constant
head tank, Z, through the control needle valve, a, and rotameter, b,
to the tracer distributor, c, in the column. Time average point
samples were taken from the column through 22-gauge, 3-in. long
hypodermic needles, d. The flowrate of these samples was
regulated by means of simple stainless steel-polyethylene stopcock
valves. The hypodermic needles were inserted through polyethylene
gaskets which were between 6-in. sections of the Pyrex glass column.
(See Appendix V for detailed drawings of the tracer distributor
and of the sample valves.) Samples containing tracer were analysed
for sodium with a Perkin - Elmer 303 atomic absorption spectro-
phometer.

The major part of the work was carried out with a Pyrex glass
column of $1\frac{1}{2}$-in. I.D. Details of the end sections of this column
are to be found elsewhere (118, 35). Its vertical dimensions
are shown in Figure 10. The arrangements shown in Figure 11 and 12

INTERFACE

6" LONG, 6" I.D. PYREX "DOUBLE TOUGH" PIPE

10" LONG, 1½" I.D. PYREX "DOUBLE TOUGH" PIPE WITH UNFLANGED UPPER END

3' LONG, 1½" I.D. PYREX "DOUBLE TOUGH" PIPE.

A   6" LONG, 1½" I.D. PYREX "DOUBLE TOUGH" PIPE (SEE TABLE VI-I FOR MEASURED DIMENSIONS)

B   1/16" THICK, 1½" I.D. POLYETHYLENE GASKET THROUGH WHICH SAMPLING NEEDLES PASSED (EACH SAMPLING POSITION IS INDICATED BY NUMBER)

D   STYLE 1-2 TEFLON GASKET (CORNING)

1/8" THICK, 1½" I.D. TEFLON GASKET THROUGH WHICH THE TRACER INJECTION NEEDLE PASSED

1' LONG, 1½" I.D. PYREX "DOUBLE TOUGH" PIPE

CUSTOM MADE PYREX "DOUBLE TOUGH" 3" TO 1½" REDUCER (30)

FIGURE 10.   1½-IN. I.D. COLUMN

were used together with that given in Figure 10 for investigating the effect of column length on the axial eddy diffusivity. Details of the column arragements used for the part of the work concerning sampling techniques are shown in Figures 13 and 14. Two sampling techniques for measuring concentration profiles were investigated. The first method was the use of the hook and bell-probes mentioned earlier. Both the hook-shaped probe and the bell-shaped probe were made from stainless steel. Details of these probes are to be found elsewhere (30, 118), and a diagram is shown in Figure 5. Samples were syphoned out of the column through these probes and through small needle valves and rotameters connected in series with them. The needle valves were used to control the flows, and the rotameters to measure them. The syphon was started by means of a water aspirator. The second sampling method made use of hypodermic needles as mentioned earlier. The piston sampler, mentioned in the Introduction, was employed in both sampling investigations.

The drops were produced at a nozzle similar in design to that of Kreager and Geankoplis (16). With this sort of nozzle drops are formed at the ends of jets extending from short tubes press-fitted into a plate forming the end of the spray nozzle. These tubes were chamfered to sharp edges at their delivery ends. The dispersed phase nozzle used with the $1\frac{1}{2}$-in. I.D. column was designed by Choudhury, and a detailed drawing is to be found in his thesis (35). The nozzle tips and nozzle tip support plate are described elsewhere (30, 35, 118). The average inside diameter of these nozzle tips was measured by the present author and was

FIGURE 11.   SHORT 1½-IN. I.D. COLUMN

INTERFACE

6" LONG, 6" I.D. PYREX "DOUBLE TOUGH" PIPE

10" LONG, 1½" I.D. PYREX "DOUBLE TOUGH" PIPE WITH UNFLANGED UPPER END

2' 6" LONG, 1½" I.D. PYREX "DOUBLE TOUGH" PIPE

3' LONG, 1½" I.D. PYREX "DOUBLE TOUGH" PIPE

A   6" LONG, 1½" I.D. PYREX "DOUBLE TOUGH" PIPE (SEE TABLE VI-I FOR MEASURED DIMENSIONS)

B   1/16" THICK, 1½" I.D. POLYETHYLENE GASKET THROUGH WHICH SAMPLING NEEDLES PASSED (EACH SAMPLING POSITION IS INDICATED BY NUMBER)

D   STYLE I-2 TEFLON GASKET (CORNING)

1/8" THICK, 1½" I.D. TEFLON GASKET THROUGH WHICH THE TRACER INJECTION NEEDLE PASSED

2' LONG, 1½" I.D. PYREX "DOUBLE TOUGH" PIPE

1' 6" LONG, 1½" I.D. PYREX "DOUBLE TOUGH" PIPE

CUSTOM MADE PYREX "DOUBLE TOUGH" 3" TO 1½" REDUCER

FIGURE 12.   LONG 1½-IN. I.D. COLUMN

INTERFACE

6" LONG, 6" I.D. PYREX "DOUBLE TOUGH" PIPE

10" LONG, $1\frac{1}{2}$" I.D. PYREX "DOUBLE TOUGH" WITH UNFLANGED UPPER END

3' LONG, $1\frac{1}{2}$" I.D. PYREX "DOUBLE TOUGH" PIPE

1' 6" LONG, $1\frac{1}{2}$" I.D. PYREX "DOUBLE TOUGH" PIPE

1' LONG, $1\frac{1}{2}$" I.D. PYREX "DOUBLE TOUGH" PIPE

CUSTOM MADE PYREX "DOUBLE TOUGH" 3" TO $1\frac{1}{2}$" REDUCER

D STYLE 1-2 TEFLON GASKET (CORNING)

FIGURE 13. $1\frac{1}{2}$-IN. I.D. COLUMN FOR COMPARING HOOK AND BELL-PROBES AND PISTON SAMPLER RESULTS

INTERFACE

6" LONG, 6" I.D. PYREX "DOUBLE TOUGH" PIPE

10" LONG, 1½" I.D. PYREX "DOUBLE TOUGH" PIPE WITH UNFLANGED UPPER END

3' LONG, 1½" I.D. PYREX "DOUBLE TOUGH" PIPE

1' LONG, 1½" I.D. PYREX "DOUBLE TOUGH" PIPE

A   1" LONG, 1½" PYREX "DOUBLE TOUGH" SPACER

B   1/16" THICK, 1½" I.D. POLYETHYLENE GASKET THROUGH WHICH SAMPLING NEEDLES PASSED

C   2½" LONG, 1½" I.D. PYREX "DOUBLE TOUGH" SPACER

D   STYLE 1-2 TEFLON GASKET (CORNING)

E   3" LONG, 1½" I.D. PYREX "DOUBLE TOUGH" SPACER

1' LONG, 1½" I.D. PYREX "DOUBLE TOUGH" PIPE

CUSTOM MADE PYREX "DOUBLE TOUGH" 3" TO 1½" REDUCER

FIGURE 14.   1½-IN. I.D. COLUMN FOR COMPARING HYPODERMIC NEEDLE, HOOK AND BELL-PROBES, AND PISTON SAMPLER RESULTS

found to be 0.103-in. (See Appendix V.) This nozzle and these nozzle tips were used for much of the work described in the present thesis including all the work involving mass transfer between phases. However, the end plate and nozzle tip assembly was replaced for certain runs so that the effect of drop size on the axial eddy diffusivity could be studied. Thus sets of nozzle tips of average inside diameter 0.126-in., 0.086-in., and 0.053-in. respectively were used in addition to those of 0.103-in. already mentioned. A dispersed phase nozzle was designed for use in a 3-in. I.D. Pyrex glass column used for part of the work and described later in this section of the thesis. Detailed drawings of the 0.126-in., 0.086-in., and 0.053-in. I.D. nozzle tips appear in Appendix V. The average velocity of MIBK in the dispersed phase distributor nozzle tips was maintained constant for each set of nozzle tips by blocking off nozzle tips with Teflon caps or plugs as the MIBK flowrate was reduced. Patterns of open nozzle tips used in this work are shown in Figures 15, 16, 17, and 18, one for each set of nozzle tips and for the various dispersed phase flowrates used.

Drop size distributions in the 1½-in. I.D. column were determined by photographing a 4-in. length of column situated between 7-in. and 11-in. above the top of the piston sampler block. The camera used was an Exacta VX II a) with a 1.6-in. extension ring and a Telemegor 5.5/250 telephoto lens. The camera aperature was set at f22 to give a depth of focus greater than the inside diameter of the column. Adox KB-14 (20 ASA) film was used.
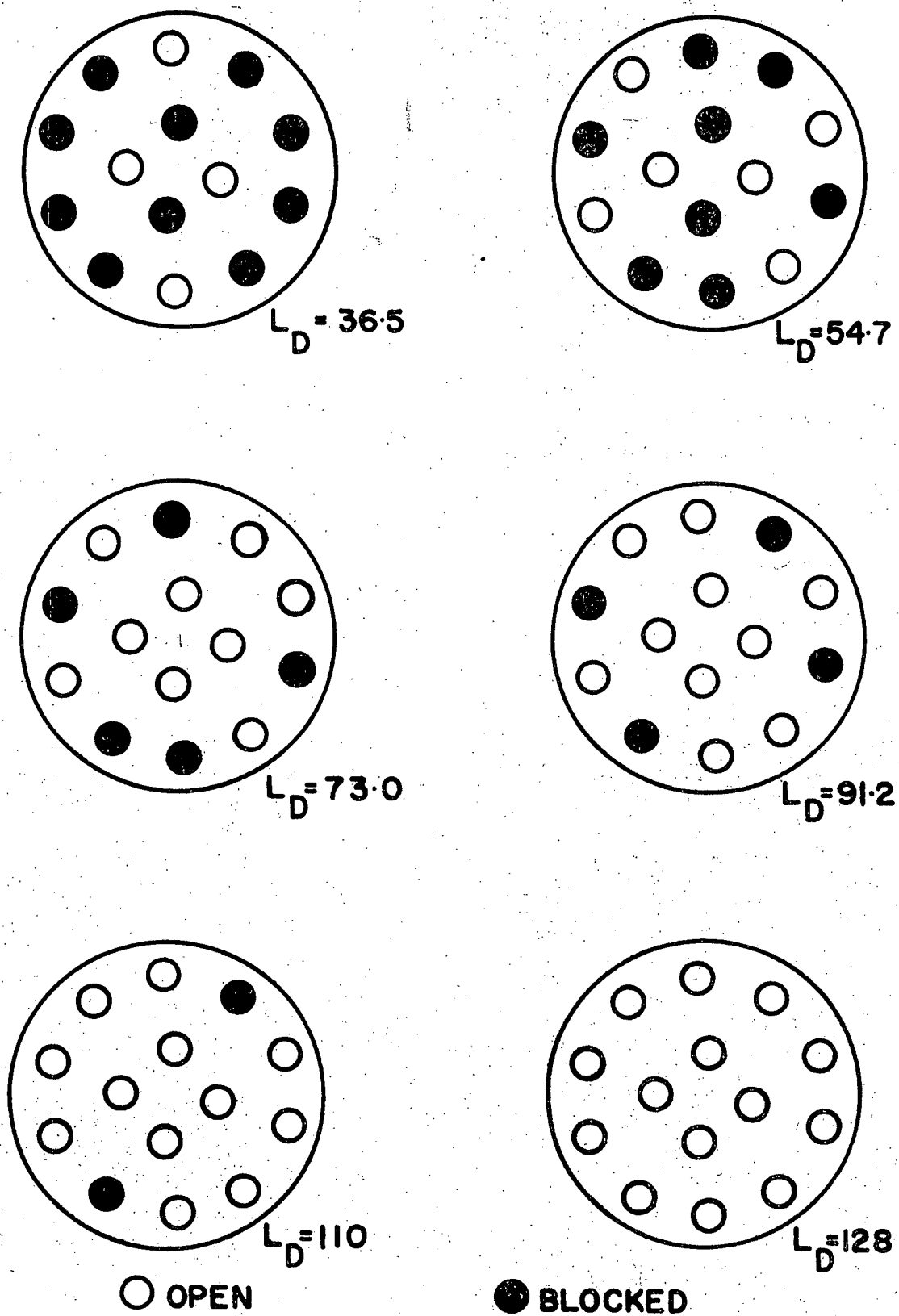
FIGURE 15. NOZZLE TIP PATTERNS. I.D. = 0.126-IN. (1½-IN. I.D. COLUMN)

$L_D = 30.4$

$L_D = 36.5$

$L_D = 54.7$

$L_D = 73.0$

$L_D = 91.2$

$L_D = 110$

$L_D = 128$

O OPEN   ● BLOCKED
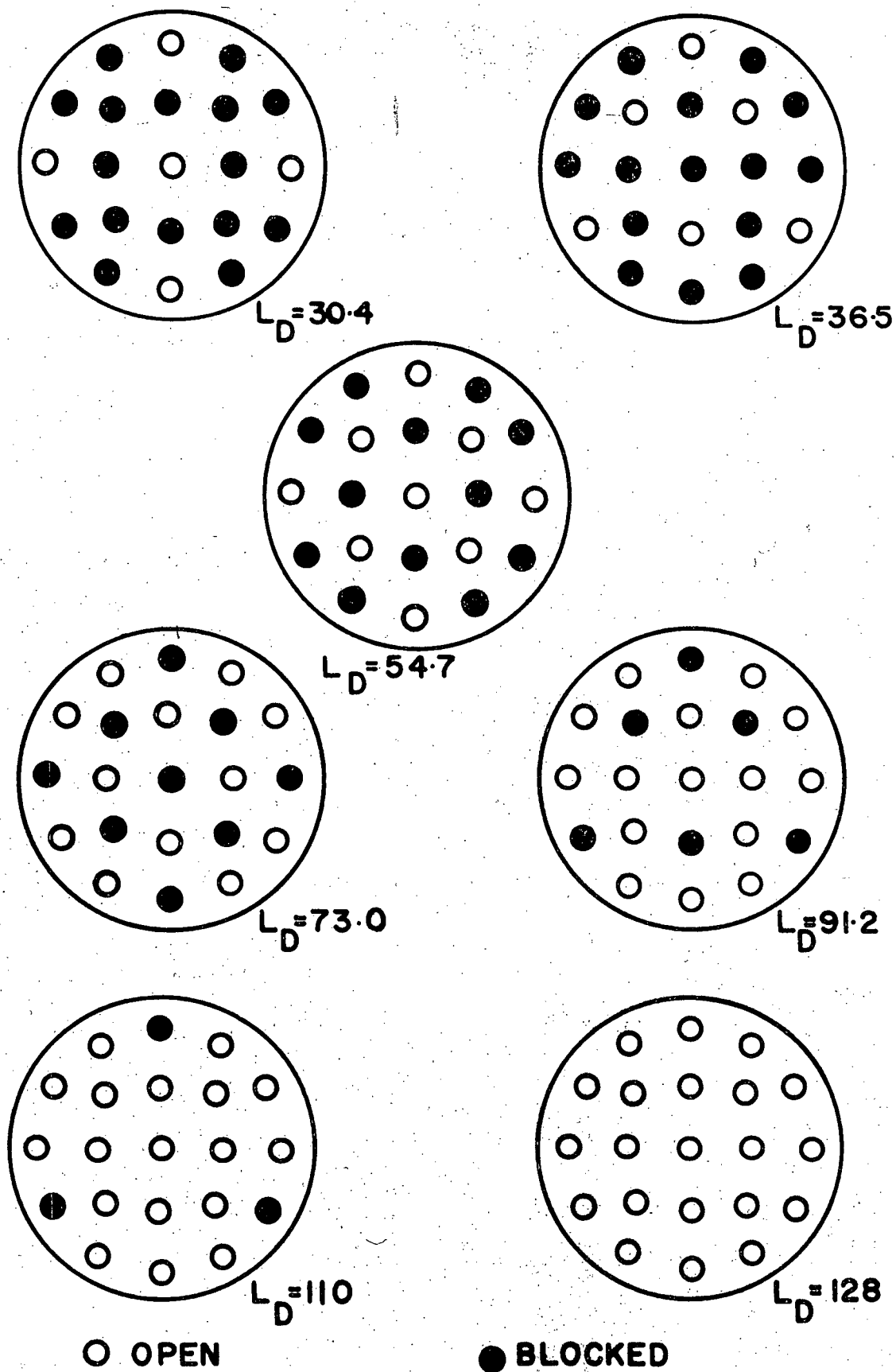
FIGURE 16. NOZZLE TIP PATTERNS. I.D. = 0.103-IN. ($1\frac{1}{2}$-IN. I.D. COLUMN)
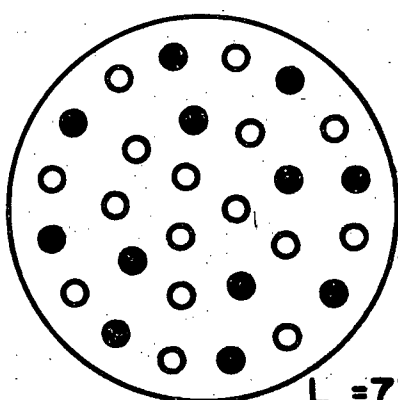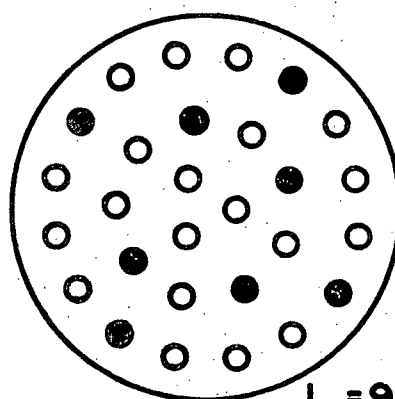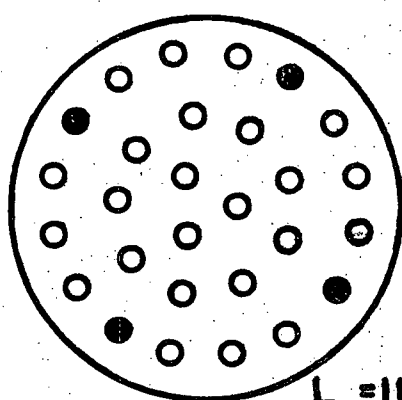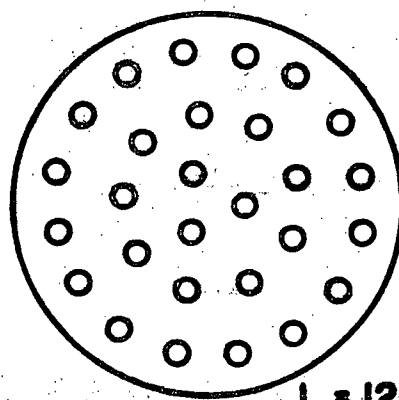
FIGURE 17. NOZZLE TIP PATTERNS. I.D. = 0.086-IN. (1½-IN. I.D. COLUMN)
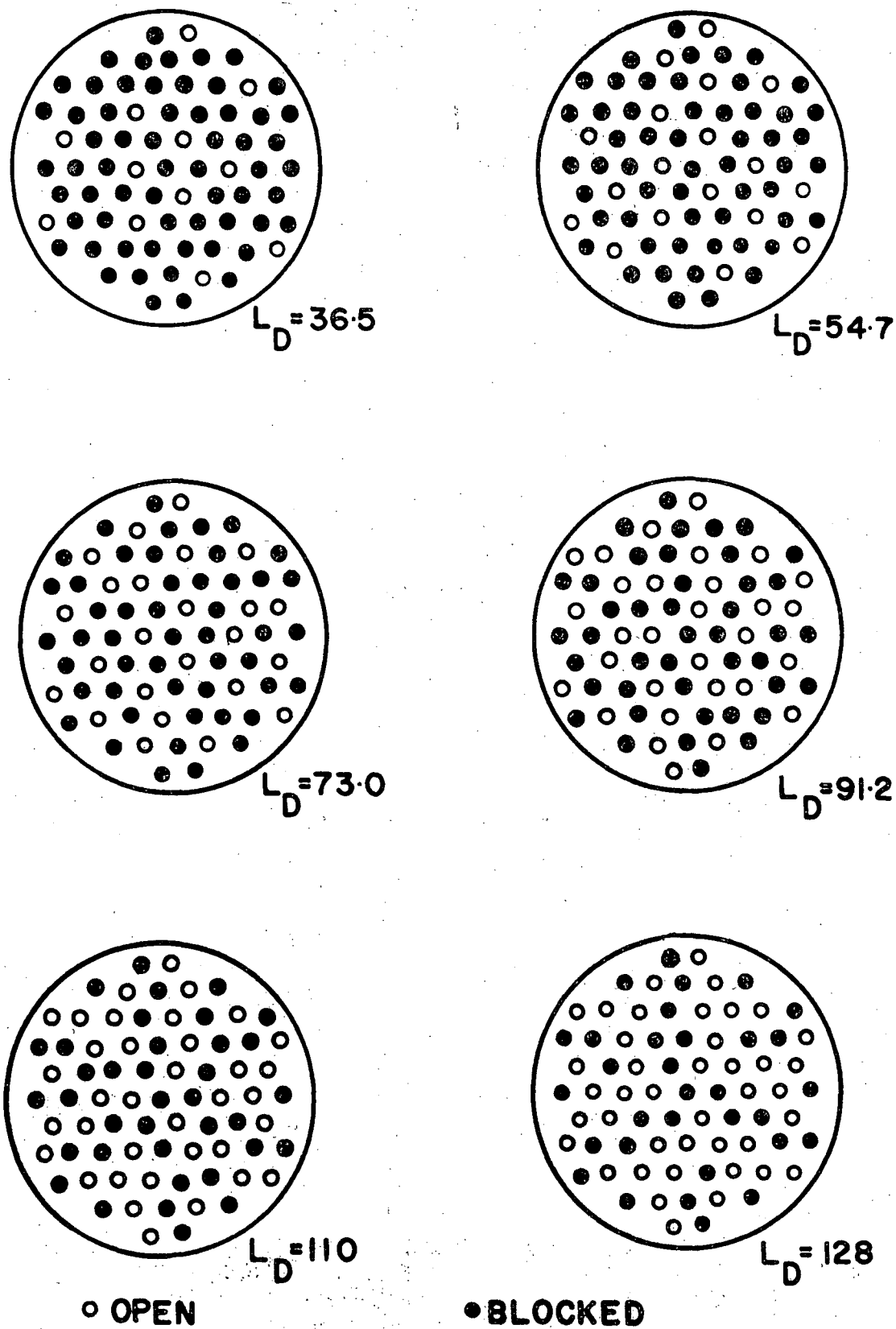
FIGURE 18. NOZZLE TIP PATTERNS. I.D. = 0.053-IN. (1½-IN. I.D. COLUMN)

The section of column photographed was surrounded by a parallel-sided Perspex box filled with distilled water to reduce the distorting effect of the round column. Back lighting was effected with a Braun Hobby F60 electronic flash unit with a one millisecond flash duration. The section of column photographed was shielded from extraneous light with a cardboard box which also supported the electronic flash head and a light-diffusing screen of eight sheets of tracing paper. Figure 19 shows the relative positions of flash, column, and camera. Detailed drawings of the Perspex box and the cardboard shield are given in Appendix V.

A few experimental runs were carried out with the 3-in. I.D. Pyrex glass column shown in Figure 20. In order to produce and maintain high continuous phase superficial velocities three continuous phase feed tanks, pressurized to about 15 p.s.i.g. with nitrogen, were used. A schematic flow diagram is presented in Figure 21. Detailed drawings of the end sections and dispersed phase distributor nozzle are given in Appendix V. Figure 22 shows the patterns of open and closed nozzle tips used for various dispersed phase flowrates. Sodium chloride tracer was injected into the column through the same tracer distributor as used in the $1\frac{1}{2}$-in. I.D. column. The tracer distributor was located on the centre line of the column and tracer flowed into it through a 3-in. long, 18-gauge hypodermic needle which passed through a 1/8-in. thick, 3-in. I.D., and 3 27/32-in. O.D. Teflon gasket. Samples were withdrawn as with the $1\frac{1}{2}$-in. I.D. column except that

BACK OF CAMERA

7⅞"

69⁵⁄₁₆"

1"

FLASH
UNIT

DIFFUSING
SCREEN

COLUMN

PERSPEX
BOX

LIGHT
SHIELD

CAMERA
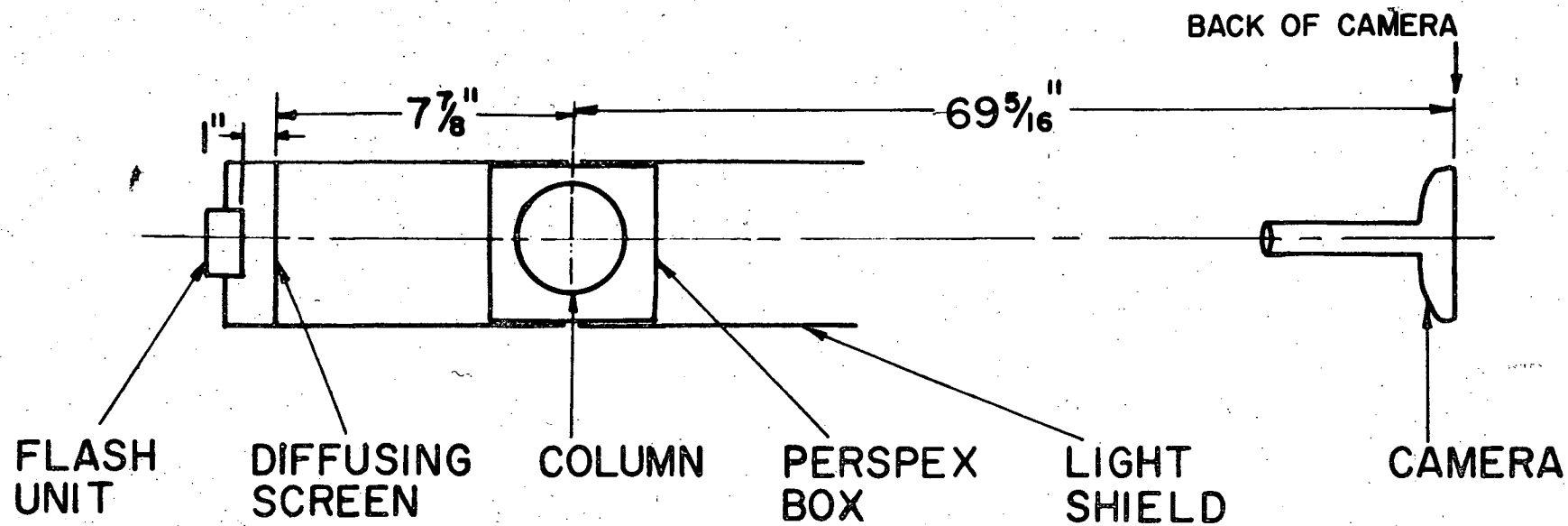
FIGURE 19.   PHOTOGRAPHIC CONDITIONS

53

INTERFACE

9" LONG, 9" I.D. Q.V.F. PIPE

10¾" LONG, 3" I.D. PYREX "DOUBLE TOUGH" PIPE

A 6" LONG, 3" I.D. PYREX "DOUBLE TOUGH" PIPE (SEE TABLE VI-I FOR MEASURED DIMENSIONS)

B 1/16" THICK, 3" I.D. POLYETHYLENE GASKET THROUGH WHICH SAMPLING NEEDLES PASSED (EACH SAMPLING POSITION IS INDICATED BY NUMBER)

6" LONG, 3" I.D. PYREX "DOUBLE TOUGH" PIPE WITH BOTH ENDS UNFLANGED (SEE TABLE VI-I FOR MEASURED DIMENSIONS)

1/8" THICK, 3" I.D. POLYETHYLENE GASKET THROUGH WHICH THE TRACER NEEDLE PASSED

CUSTOM MADE PYREX "DOUBLE TOUGH" 6" TO 3" REDUCER

FIGURE 20. 3-IN. I.D. COLUMN

FIGURE 21. SCHEMATIC FLOW DIAGRAM FOR THE 3-IN. I.D. COLUMN

TABLE 2

(Key to Figure 21)

A_1, A_2, A_3 Continuous phase feed tanks.

B   Dispersed phase feed and receiver tank.

C_1, C_2 Interface level control rotameters.

D_1, D_2 Interface level control valves.

G_1, G_2 Continuous phase feed rotameters.

H_1, H_2 Dispersed phase feed rotameters.

I   Continuous phase inlet sample valve.

J_1, J_2 Continuous phase flowrate control valves.

K_1, K_2 Dispersed phase flowrate control valves.

M   Elgin head.

N   Continuous phase inlet pipes.

NC   Nitrogen cylinder.

O   Elgin head drain valve.

P_1 Centrifugal pump for continuous phase feed.

P_2 Centrifugal pump for dispersed phase feed.

P_3 Centrifugal pump for continuous phase outlet.

PG   Pressure gauge.

PRV   Pressure relief valve.

Q   Interface.

R   Column proper.

S   Dispersed phase nozzle.

T_1, T_2 T_3, T_4	Thermometers
U^-	Bottom conical section.
V	Vent to atmosphere.
Z	Tracer constant head tank.
a	Tracer flowrate control valve.
b	Tracer feed rotameter.
c	Tracer distributor.
d	22-gauge hypodermic needle samplers.

$L_D = 36.5$ $L_D = 54.7$ $L_D = 73.0$ $L_D = 91.2$ $L_D = 109$ $L_D = 128$

o OPEN   • BLOCKED
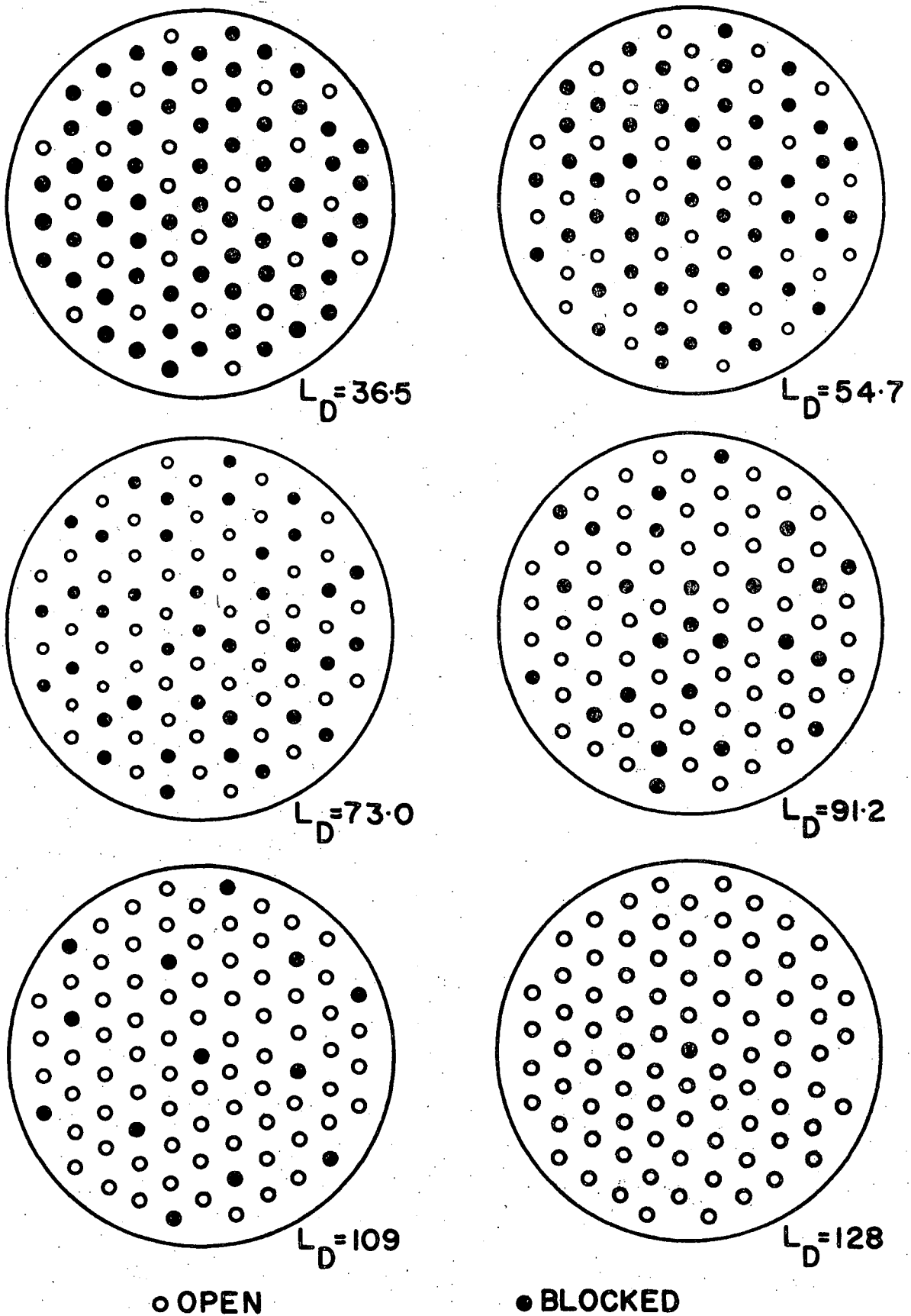
FIGURE 22.   NOZZLE TIP PATTERNS. I.D. = 0.102-IN. (3-IN. I.D. COLUMN)

the hypodermic needles passed through 1/16-in. thick, 3-in. I.D., and 3 27/32-in. O.D. polyethylene gaskets to the centre line of the column. The eighth 6-in. section of column above the tracer distributor was cut from a 1-ft. long piece of Pyrex glass pipe. The piece selected was remote from the ends so that its bore was reasonably uniform. This section of column was held in place by four aluminum tie rods between two large diameter aluminum flanges shown in Appendix V. A flat-sided Perspex box, also shown in Appendix V surrounded this 6-in. long piece of column. The space between the glass and the Perspex was filled with distilled water. Photographs were taken of the column through the Perspex box with the use of a cardboard light-shield, a tracing paper diffusing screen and an electronic flash as with the $1\frac{1}{2}$-in. column. Photographic conditions were the same as before except that lighting was by means of a Kakonet - II electronic flash unit with a flash duration of 0.5-millisecond.

EXPERIMENTAL PROCEDURE

1. COLUMN OPERATION

City water was passed through a Barnstead Bantam BD-1 mixed bed demineralizer to give better than 1 megohm-cm. resistivity water. In all experiments the continuous phase was demineralized water and the dispersed phase was technical grade methyl isobutyl ketone (MIBK) supplied by Chemcell Ltd. Each phase was kept saturated with the other by maintaining a layer of one phase in the feed tank of the other. The flowrates of both phases fed to the column were regulated with stainless steel needle valves and metered with rotameters. Four different drop size distributions were produced in the $1\frac{1}{2}$-in. I.D. column by means of four sets of nozzle tips of respective average inside diameters 0.126-in., 0.103-in., 0.086-in., and 0.053-in. Only one set of nozzle tips of average inside diameter 0.102-in. was used with the 3-in. I.D. column. The dispersed phase average velocity in the distributor nozzle tips was held at 0.36-ft./sec., 0.36-ft./sec., 0.38-ft./sec., 0.68-ft./sec., and 0.37-ft./sec. for the 0.126-in., 0.103-in., 0.086-in., 0.053-in., and 0.102-in. I.D. tips respectively by utilizing only a portion of the total nozzle tips available with the help of Teflon caps or plugs as described under the heading Apparatus. The higher nozzle tip

velocity of 0.68-ft./sec. in the 0.053-in. I. D. tips was found to be necessary in order to produce drops of a narrow range of sizes.

The interface in the Elgin head was maintained steady to within $\pm$ 1/16-in. by controlling the flow of continuous phase leaving the column by means of a stainless steel needle valve. A rotameter, in series with this valve, indicated the flowrate. The dispersed phase flow from the column head to the receiving tank was unrestricted.

2. SAMPLING TECHNIQUE STUDIES WITH MASS TRANSFER

An attempt was made to relate the samples taken by the bell and hook-probes to samples taken by means of the piston. Early in the work each of the sampling lines leading from the bell and hook-probes, respectively, used by earlier workers (38) was replaced by 27-ft. of smaller bore (3/32-in. I.D.) Nylon tubing. It was found that a conservative estimate of the minimum purge time for each of these new sampling lines was given by the following equation. (See Appendix VI)

$$\text{Purge time (min.)} = \frac{120}{\text{sampling rate (ml./min.)}}$$

In all of the work involving the hook or bell-probe described in this thesis these probes were positioned as closely as possible to the centre line of the column. The times for the column to reach steady state operating conditions at various flowrates of each phase was taken from the work of Bergeron (38).

In all experiments acetic acid was transferred from the continuous aqueous phase to the dispersed MIBK phase. At the end of an experiment the aqueous phase product was transferred to the aqueous phase feed tank and the aqueous phase product tank was filled with de-ionised water. This water was used to back-wash MIBK from the previous run in the column in order to prepare a feedstock of MIBK low in acetic acid concentration for the next run. The aqueous phase backwashing product was fed to the aqueous phase feed tank until the liquid level in that tank was about 6-in. from the top and then the remainder was fed to the drain.

Reagent grade glacial acetic acid, manufactured by Nichols Chemical Corporation Ltd., was used for preparing the aqueous acetic acid solution used as continuous phase feed in the follow-ing manner. If necessary the aqueous phase feed tank was filled to within about six inches from the top by adding de-ionised water. The contents of this tank were pumped up to the aqueous phase constant head tank and allowed to run back into the feed tank until the solution was homogeneous. Homogeneity was checked by periodically titrating the flow from the constant head tank with carbonate-free standard sodium hydroxide solution. (The sodium hydroxide solution was prepared as recommended by Swift (119) and was standardized by titrating against standard potassium hydrogen phthalate solution.) From a knowledge of the volume of liquid in the aqueous phase feed tank and the concentration of acetic acid in solution in that tank the amount of glacial

acetic acid to be added in order to produce a suitable acetic acid concentration in the aqueous phase feed was calculated. This amount of glacial acetic acid was poured into the aqueous phase feed tank. The contents of this tank then were circulated to give a homogeneous solution as before.

In this study the set of nozzle tips of average inside diameter 0.103-in. was used. In most of these experiments all of the dispersed phase distributor nozzle tips were kept open. Therefore a high ketone flowrate was obtained with the use of an average nozzle tip velocity of 0.36-ft./sec. A high ketone flowrate was required in order to produce a high dispersed phase hold-up so that the application of Equation 6 in connection with the piston sampler would result in a small error in the calculated value of c_D. A high aqueous phase flowrate was used so that the column was operating under conditions far from equilibrium in the vicinity of the piston sampler. Under these conditions solute concentration gradients which are substantially different from zero in both phases over the piston height are to be expected. Without this condition a comparison between the various sampling techniques would be meaningless.

a) Sampling with hook and bell-probes and piston

The apparatus was set up as shown in Figure 13. Each of the bell and hook-probes were positioned so that their respective

entrances were 3-in. below the centre line of the piston. The desired MIBK flowrate into the empty column was established, and aqueous-feed phase was pumped into the column at the maximum possible rate. When the interface reached the desired level the flowrate of the aqueous continuous phase was reduced to the operating value and the valve controlling the aqueous phase flowrate from the foot of the column was opened and adjusted to maintain the interface level. After allowing the column to reach steady state conditions sampling through the probes was commenced. Samples were collected in 50-ml. graduated cylinders which were closed with ground-glass stoppers immediately after the samples were taken. Samples were collected with each probe at the location mentioned above. The probes then were moved 1-in. up the column, and a second set of samples was taken. Sets of samples were collected at an additional four 1-in. intervals up the column. When the probe samples had been taken the probes were raised above the interface, and a piston sample was collected after a half-hour interval in the calibrated custom-made vessel shown in Figure V - 1, Appendix V. The volumes of each phase in samples taken with the bell-probe and with the piston were recorded. Sometime during the course of steady state operation column inlet and outlet samples of both phases were taken.

All of the samples containing two phases were shaken vigorously many times in order to bring the two phases to equilibrium. The concentration of acetic acid in each phase of

each sample was determined by titrating with standard sodium hydroxide solution using phenolphthalein as indicator. When titrating the MIBK phase SDAG-1K* was added to render the MIBK and aqueous phases miscible.

In addition to the experiments described above an experiment was performed with a modification of the hook-probe as shown in the sketch below.

GLASS TUBE

GLASS WOOL

POLYETHYLENE
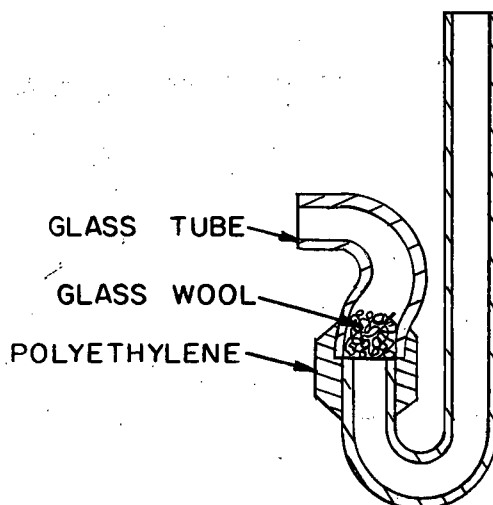
b) Sampling with hook and bell-probes, hypodermic needles, and piston

Short Pyrex spacers were included in the column above and below the piston block as shown in Figure 14. Hypodermic needles

---

* SDAG-1K is a mixture of 90% v/v ethanol and 10% v/v methanol.

were inserted through polyethylene gaskets between the spacers in a manner similar to that shown in Figure V - 2, Appendix V. The minimum purge time for these needles was found to be less than 45-sec. at a sampling rate of 3/4-ml./min. In all of the work involving hypodermic needles described in this thesis a needle was purged for at least $1\frac{1}{2}$-min. before taking a sample. A hypodermic needle sample was taken always with the open end of the needle on the centre line of the column unless otherwise indicated.

The column was brought to steady state operating conditions and probe samples were taken as before. Then the probes were raised above the interface and the column was allowed to attain steady state operating conditions. Samples were collected by means of the hypodermic needles in the following manner. Two needles, separated by not less than 10 inches, were used concurrently, the other needles being withdrawn to the column wall so as not to protrude into the column. The valves at the end of each of the two needles were opened so as to give sampling rates of about 1-ml./min. The samples were collected in 10-ml. graduated cylinders. After the final hypodermic needle sample was collected the column was allowed to reach steady state operating conditions and then a piston sample was taken. The concentration of acetic acid in each phase of each sample was determined by titrating with sodium hydroxide solution as before.

3. SEARCH FOR SUITABLE TRACER

An investigation and preliminary tests were made to find a tracer for use in the determination of axial eddy diffusivities with no mass transfer between the dispersed and the continuous phases. The necessary tracer properties are listed below:

a) high solubility in MIBK - saturated water,

b) insolubility in water - saturated MIBK,

c) concentration must be measurable at low values,

d) must not disturb the fluid flow patterns when injected into an operating column,

e) must not adsorb at MIBK - water interface or at any solid-liquid interface in the column,

f) must not react chemically with water, MIBK, or any solid surface in the column, and

g) the molecular diffusivity in MIBK - saturated water must be negligible compared with the axial eddy diffusivity.

The tracers considered, the method of quantitative analysis for their concentration, and their shortcomings, if any, are listed below.

a) Ferric nitrate. Analysis for this compound would be by the thiocyanate method making use of colorimetry. Ferric nitrate hydrolyses in MIBK-saturated water, ferric hydroxide precipitating.

b) Hydrochloric acid. Analysis would be by titration. Very low concentrations are not easily measurable.

c) Potassium chloride. Analysis would be carried out by means

of conductimetry. Very low concentrations are not easily measurable.

d) Water soluble dyes. Solutions of these compounds would be analysed colorimetrically. Even completely ionised dyes, such as crystal violet, dissolve in water-saturated MIBK.

e) Cupric sulphate. Analysis would be by the dithizone method making use of colorimetry. Dithizone is quite unstable.

f) Sodium chloride. Analysis would be for sodium by means of atomic absorption spectrophotometry. The molecular diffusivity of sodium chloride in water is 0.00005-ft^2/hr. at $65°$F for concentrations between 0 and 1-molar (128). No data is available for this diffusivity in MIBK-saturated water, but it is expected that the value would be closely similar to that for pure water and this value has been used. Axial eddy diffusivities in this work were found to be always greater than 7-ft^2/hr. Thus the condition that the molecular diffusivity is negligible compared with the axial eddy diffusivity is met.

A solution of sodium chloride in MIBK - saturated water was found to be a suitable tracer. The distribution coefficient* for sodium chloride between MIBK - saturated water and water - saturated MIBK was found to be 7060.

---

* The distribution coefficient is defined here as the concentration of sodium chloride in the aqueous layer divided by the concentration of that compound in the ketone layer where concentrations are expressed in the units of weight per unit volume of solution.

4. SAMPLING TECHNIQUE STUDIES WITH NO MASS TRANSFER

The apparatus was set up as shown in Figures 9 and 14 with the following modifications. The third polyethylene gasket below the piston was exchanged with the Teflon gasket further down the column. The hypodermic needle supporting the tracer distributor remained in this Teflon gasket so that there were only two hypodermic needle sampling positions between the tracer distributor and the piston. The MIBK leaving the Elgin head passed directly to the MIBK feed tank. The aqueous and MIBK feedstocks were free of acetic acid. The flows of MIBK and aqueous phases were started and the interface level was established as described in the present section of the thesis under the heading 1: Column Operation.

The experiments were performed under the following operating conditions

Continuous phase superficial velocity, $ft^3/hr. \ ft^2$	Dispersed phase superficial velocity, $ft^3/hr. \ ft^2$
36.5	128
36.5	30.4
27.7	128

A one molar sodium chloride tracer feed solution was prepared by dissolving a weighed amount of sodium chloride in MIBK - saturated water (119). This solution was started into the column as soon as the interface level had been established in the Elgin head. The column was run for one hour to allow steady state conditions to be attained. (Experiments for the study of steady state times are discussed later.) Five hook-

probe samples were taken from equally spaced positions throughout the height of the piston block. The hook-probe sampling rate was 5-ml./min. Four hypodermic needle samples were taken, one through each of the gaskets immediately above and below the piston block, and one through each of those approximately six inches above and below the piston block. Finally a piston sample was taken. Half hour time intervals were allowed between taking each probe sample, between taking the last probe sample and the first hypodermic needle sample, and between taking the last hypodermic needle sample and the piston sample. The aqueous phase of each sample was analysed for sodium by means of a Perkin-Elmer 303 atomic absorption spectrophotometer.

5. AXIAL EDDY DIFFUSIVITY AND DISPERSED PHASE HOLD-UP

a) Studies in the $1\frac{1}{2}$-in. I.D. column.

Initially a few experiments were performed in order to see whether or not the dispersion model would describe the experimental data adequately and, therefore, whether or not axial eddy diffusivities could be determined from this model. These experiments were carried out in a manner identical to that for the main bulk of experiments which is described below. It was found that a plot of the logarithm of the concentration of tracer versus height up the column was linear; accordingly the dispersion model was adopted.

In addition, before the main bulk of experimental data was collected some experiments were carried out to justify some of the experimental techniques used. Since these experi-

ments usually were carried out in conjunction with axial eddy diffusivity determinations their description will be given following that of the main experiments. The apparatus used for the subsidiary experiments described under ii) to viii) inclusive below was identical to that used for the main experiments.

i) Axial eddy diffusivity determinations.

The column was set up as shown in Figures 9 and 10 except that the MIBK line from the Elgin head led directly to the MIBK feed tank so that MIBK recycled through the apparatus. As required, some nozzle tips of the dispersed phase distributor were blocked off with Teflon caps or plugs according to the patterns shown in Figures 15 to 18 to ensure the desired average velocity of dispersed phase in the nozzle tips. The flow of MIBK into the column was started, and thereafter maintained at the desired rate. Water was pumped into the column at the maximum possible rate until the interface in the Elgin head reached a predetermined level. The flowrate of water was then reduced to the experimental value and water was allowed to leave the column at such a rate so as to maintain the desired constant interface level. The tracer (1-molar sodium chloride solution in MIBK - saturated water) was fed to the column at approximately 1% of the volumetric flowrate of the aqueous phase. After allowing the column to reach steady state operating conditions ten aqueous phase samples were taken by means of the hypodermic needles, one at a time. The first

sample was taken with the lowest needle in the column, the second sample from the next needle up the column, and so on. The samples were withdrawn from the centre of the column and at a rate less than 1.5% of the volumetric flowrate of aqueous phase though the column. The description of experiments performed to investigate radial concentration gradients and also the effect of sampling rate upon the column operation are discussed later. When a hypodermic needle was not being used it was withdrawn to the column wall. The flowrate of each phase from the column was determined by weighing a sample collected over a suitable time interval. The average of the temperatures of the fluids in the upper and lower sections of the Elgin head, of the fluid at the lower end of the column, and of the ketone phase entering the column was recorded. Finally three piston samples were taken at intervals of ten minutes and the volumes of the two phases in each sample recorded. The tracer concentration in each of the ten hypodermic needle samples and in the aqueous phase leaving the column were measured by means of an atomic absorption spectrophotometer. (Analysis was for sodium.) The calibration line for the atomic absorption spectrophotometer always was found to be a straight line. The equation for this line was calculated by the method of least squares. Samples whose concentrations were less than 0.05-microgm. sodium/ml. were discarded on the grounds of unreliability. The probable error in the concentration of a sample determined by this method was less than 2%.

Experiments were performed at all possible combinations of
the following operating conditions.

continuous phase superficial velocity, $ft^3/hr. \ ft^2$	dispersed phase superficial velocity, $ft^3/hr. \ ft^2$	nozzle tip average inside diameter, in.
9.0	36.5	0.053
18.2	54.7	0.086
27.7	73.0	0.103
36.5	91.2	0.126
48.4	110	
	128	

For each set of nozzle tips about 10 photographs of the
drops within the column were taken as described earlier under
the heading Apparatus at the operating conditions shown in each
line shown in the following table.

continuous phase superficial velocity, $ft^3/hr. \ ft^2$	dispersed phase superficial velocity, $ft^3/hr. \ ft^2$
9.0	36.5
27.7	36.5
48.4	36.5
27.7	54.7
27.7	91.2

Some, but not all, of the photographs were taken during runs
for determining axial eddy diffusivities. However, those
not taken during runs were taken under column operating con-
ditions identical to those which applied during runs. The
photographic negatives were examined by means of a Recordak
model M.P.E. microfilm reader. The drop size distributions were
determined by measuring the vertical and horizontal dimensions
of the projected images of the drops. With the photographic

conditions described earlier the depth of focus included the whole of the column cross-section. Only the drops lying within the central 46% of the column image, as projected on the screen, were examined, because as determined by experiments described below, the drops falling within these limits were not distorted optically. Five hundred drops were measured for each set of column operating conditions given in the last table.

ii) Optical distortion of drops.

As mentioned earlier optical distortion was reduced considerably by surrounding the round glass column with a flat-sided Perspex box. Details of the box are presented in Appendix V. The space between the box and the column was filled with distilled water. The same photographic conditions were used for the calibration photographs as for the photographs taken to determine drop size distributions as described under the heading Apparatus. The same 6-in. long section of column was used for the calibrations as was used for the actual drop size distribution measurements. The Perspex box was not shielded from extraneous light as in the drop size distribution studies since the photographs were taken in a darkroom. Photographs were taken of a 5/32-in. diameter ball bearing silver soldered to a stainless steel wire. The ball was photographed at positions shown in Figure 23 for each of the horizontal planes located $\frac{1}{2}$-in. above and $\frac{1}{2}$-in. below the centre of the Perspex box. Two sets

$1\frac{11}{32}"$ D.

$1\frac{5}{32}"$ D.

$\frac{3}{4}"$ D.

CAMERA
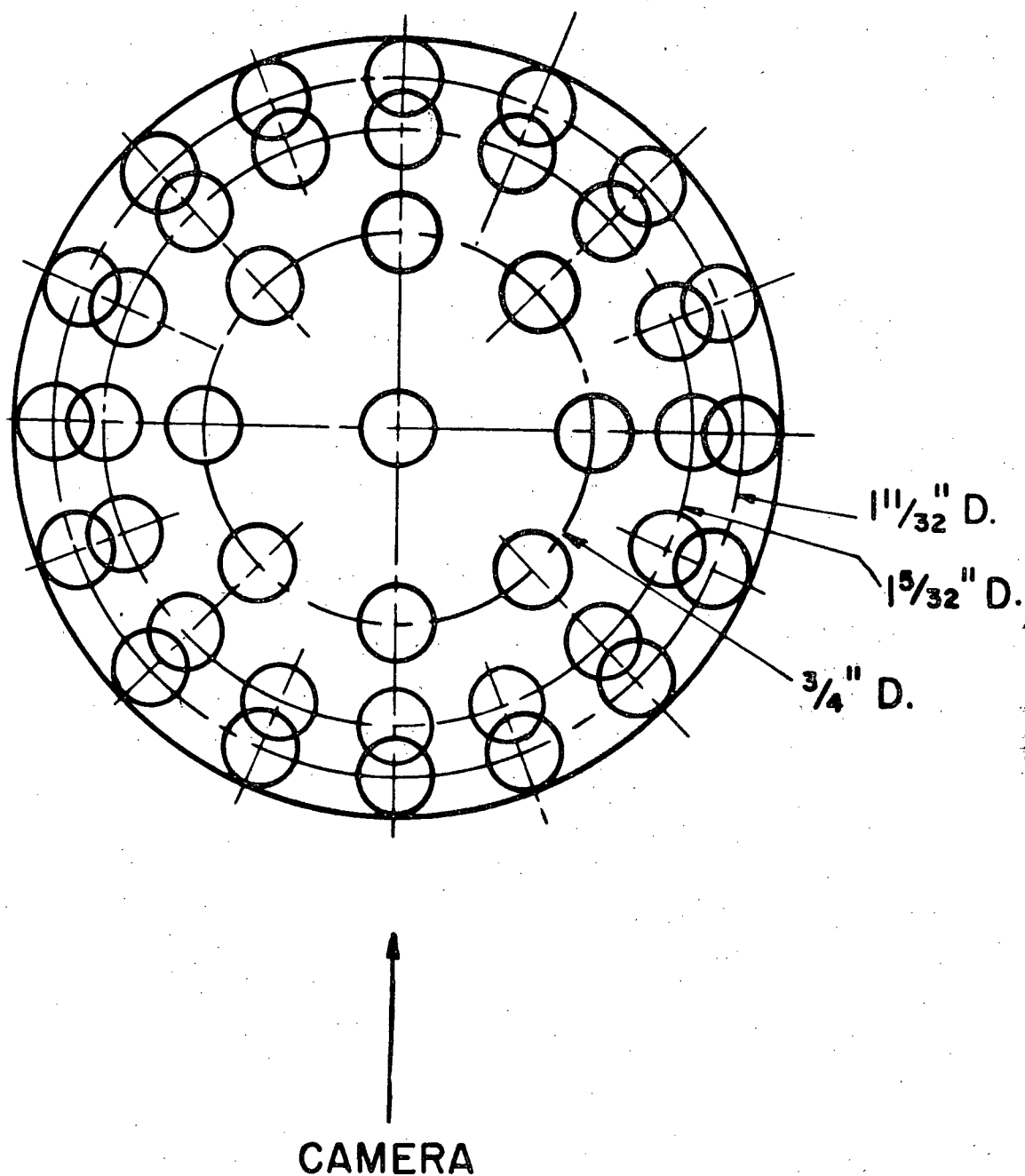
FIGURE 23. OPTICAL DISTORTION INVESTIGATION, $1\frac{1}{2}$-IN. I.D. COLUMN

of photographs were taken, one with MIBK - saturated water,
and one with a solution of sodium chloride in MIBK - saturated
water in the column. For this second solution the concentration
of sodium was 100-microgm./ml.

iii) Effect of tracer feed rate

The feed rate of tracer solution into the column should
be low enough so as not to disturb the fluid flow patterns
within the column. The effect of tracer feed rate was studied
using the superficial velocities of the two phases, and of the
tracer feed solution supplied to the column, given in each
line of the following table. Only the nozzle tips of 0.103-
in. I. D. were used for this study.

Continuous phase, $ft^3/hr.\ ft^2$	Dispersed phase, $ft^3/hr.\ ft^2$	Tracer solution, $ft^3/hr.\ ft^2$
27.7	30.4	0.16
27.7	30.4	0.31
27.7	30.4	0.62
18.2	73	0.10
18.2	73	0.20
18.2	73	0.40

iv) Steady-state time.

The experimental conditions for sections iv) to viii)
inclusive are shown in each line of the following table

Continuous phase superficial velocity, $ft^3/hr. ft^2$	Dispersed phase superficial velocity, $ft^3/hr. ft^2$
9	128
9	30.4
27.7	30.4

The time taken for the column to reach steady state operating conditions was estimated by taking samples by means of the first, fourth, seventh, and tenth hypodermic needles above the tracer distributor, and also by collecting aqueous phase leaving the column. One of each of these samples was taken between 3-min. and 21-min. after start-up and then at intervals varying between 5-min. and 30-min. until 2-hr. after start-up.

v) Reproducibility of results.

Several of the experiments for determining axial eddy diffusivity and hold-up were repeated under identical operating conditions in order to test the reproducibility of results.

vi) Cross-sectional homogeneity.

In addition to the sample taken from the centre of the column by means of the hypodermic needle immediately above the tracer distributor four samples were taken at the same elevation but at positions on a 1-in. circle concentric with the column. This experiment was carried out for each of the runs listed in section iv) above.

vii) Effect of sampling rate.

Samples of the continuous phase were taken at 0.25-ml./min., 0.75-ml./min., and 1.5-ml./min. for the continuous phase superficial velocity of 9-ft.^{3}/hr. ft.^{2} and at 0.5-ml./min., 1.0-ml./min., and 2.0-ml./min. for the continuous phase superficial velocity of 27.7-ft.^{3}/hr. ft.^{2} Only the first four sampling positions above the tracer distributor were studied.

viii) Effect of order of sampling.

Samples were taken consecutively from the lowest sampling position up to the highest one. A second set of samples was taken with this sampling order reversed. Both sampling orders were used in each of the experiments described in the table given in section iv).

ix) Effect of column length.

In addition to the standard experiments performed with the column of height 10-ft. 3 1/8-in., as shown in Figure 10, a single experiment was performed in each of two other columns, one of height 6-ft. 3$\frac{1}{2}$-in., and the other of height 16-ft. 4$\frac{1}{2}$-in. as shown in Figures 11 and 12 respectively. Each of these last two experiments was carried out with a continuous phase superficial velocity of 18.2-ft.^{3}/hr. ft.^{2}, and a dispersed phase superficial velocity of 54.7-ft.^{3}/hr. ft.^{2} The average I.D. of the

nozzle tips in both experiments was 0.103-in.

b) Studies in the 3-in. I.D. column.

Although the great bulk of the work described in this thesis was carried out in a $1\frac{1}{2}$-in. I.D. column, some tracer experiments were carried out in a 3-in. I.D. column. This column is shown in Figure 20 and a flowsheet is given in Figure 21. In order to produce a continuous phase superficial velocity in the column greater than 100-ft.^{3}/hr. ft.^{2} it was necessary to pressurize the aqueous phase feed tanks to 15 p.s.i.g. with nitrogen. Only one set of nozzle tips of 0.102-in. average I.D. was used. It was not possible to measure the dispersed phase hold-up because a piston sampler for this column was not available. As with the $1\frac{1}{2}$-in. I.D. column, experiments were carried out in conjunction with the axial eddy diffusivity experiments to justify some of the experimental techniques used for the 3-in. I.D. column. The experiments with this column are described below.

i) Optical distortion of drops.

The photographic test section was a 6-in. long, 3-in. I.D. length of Pyrex Double Tough glass pipe which was cut from a 1-ft. long flanged section as described earlier. This pipe was surrounded by a flat-sided Perspex box and the space between the pipe and the box was filled with distilled water. The

photographic conditions were similar to those used for the $1\frac{1}{2}$-in. I.D. column. A Kakonet - II electronic flash unit was used for lighting purposes. Photographs were taken of a 5/32-in. diameter ball bearing. The ball was photographed at positions shown in Figure 24 for each of the horizontal planes located $1\frac{1}{4}$-in. above and $1\frac{1}{4}$-in. below the centre of the Perspex box. Two sets of photographs were taken, one with MIBK - saturated water, and one with a solution of sodium chloride in MIBK - saturated water in the column. For this second solution the concentration of sodium was 100-microgm./ml.

ii) Steady-state time.

The experimental conditions for sections ii) and iii) are given in each line of the following table.

Column I.D. = 3-in.

Average nozzle tip I.D. = 0.102-in.

Continuous phase superficial velocity, $ft.^3/hr. ft.^2$	Dispersed phase superficial velocity, $ft.^3/hr. ft.^2$
18.2	36.5
100	36.5
18.2	109

Samples were taken by means of the first, fourth, seventh, and tenth hypodermic needles above the tracer distributor, and also by collecting aqueous phase leaving the column. One of each of

$2^{27}\!/_{32}$" D.

$2^{17}\!/_{32}$" D.

$1^{3}\!/_{4}$" D.

CAMERA
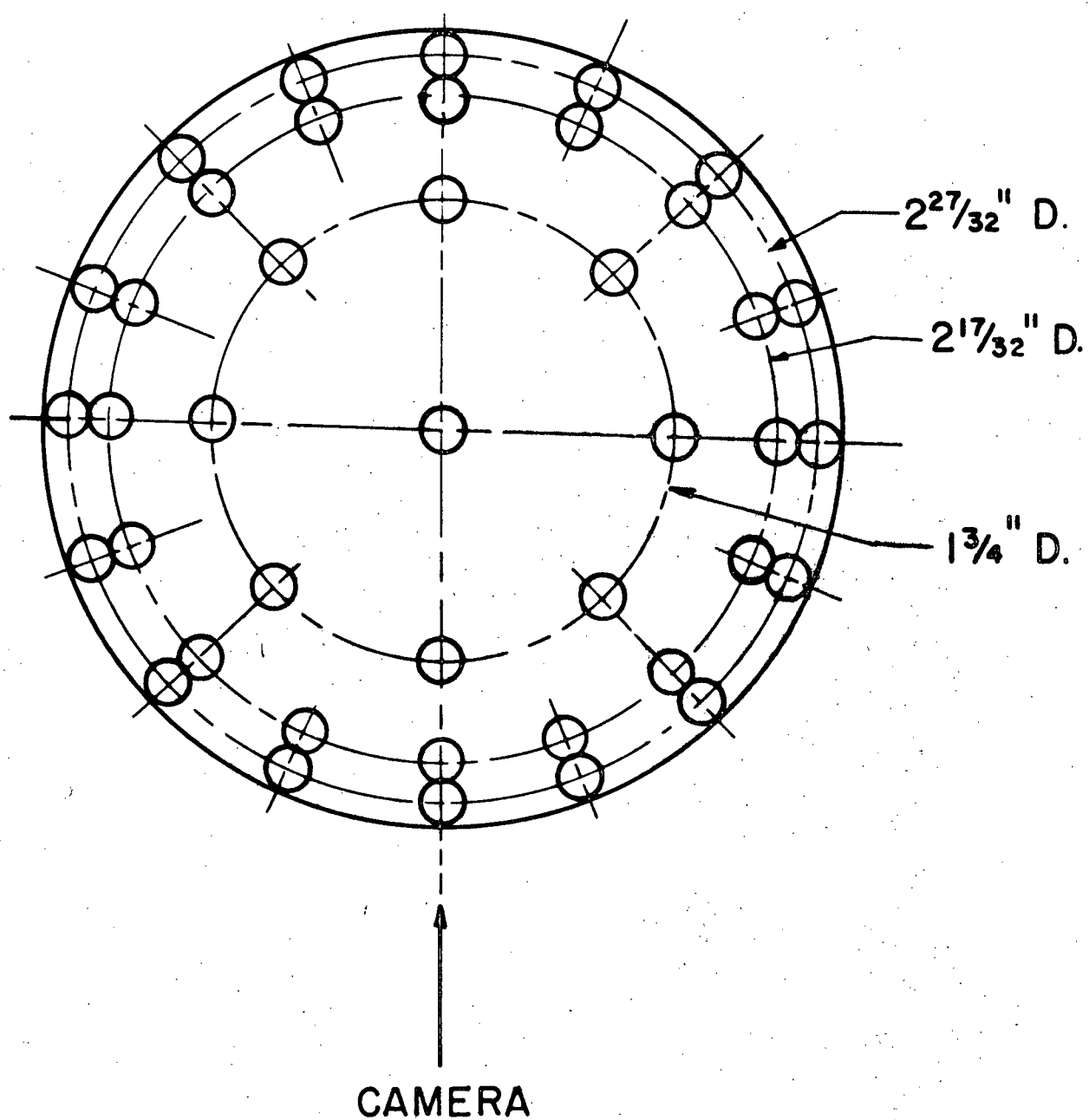
FIGURE 24. OPTICAL DISTORTION INVESTIGATION, 3-IN. I.D. COLUMN

these samples was taken between 2-min. and 10-min. after start-up and then at intervals varying between 5-min. and 30-min. until $1\frac{1}{2}$-hr. after start-up.

iii) Reproducibility of results.

Several of the experiments for determining axial eddy diffusivity were repeated under identical operating conditions in order to test the reproducibility of results.

iv) Cross-sectional homogeneity.

In addition to the samples taken from the centre of the column by means of the first and fifth hypodermic needles above the tracer distributor samples were taken from positions shown in the following sketch at each of the two above mentioned sampling elevations. These sets of samples were collected for each of the column operating conditions shown in the following table.

Continuous phase superficial velocity, $ft.^3/hr.\ ft.^2$	Dispersed phase superficial velocity, $ft.^3/hr.\ ft.^2$
18.2	36.5
100	36.5
18.2	73
100	73
18.2	109
100	109

2½" DIA.

1¼" DIA.

v) Axial eddy diffusivity determinations.

The experiments performed to determine axial eddy diffus-ivities were carried out in a manner similar to that for the $1\frac{1}{2}$-in. I.D. column. The experimental conditions are given in Table IV-5, Appendix IV. A sampling rate of 3-ml./min. was used in all experiments in the 3-in. I.D. column.

Photographs were taken of the fluids within the calibrated glass section described earlier which was installed as the eighth 6-in. section above the tracer distributor. This section of column was surrounded by a flat-sided Perspex box as shown in Appendix V. The photographic conditions were similar to those used for the $1\frac{1}{2}$-in. I.D. column. A Kakonet - II electronic flash unit was used for lighting purposes. The column operating

conditions for which photographs were taken are shown in each

line of the following table.

Continuous phase superficial velocity, $ft.^3/hr. ft.^2$	Dispersed phase superficial velocity, $ft.^3/hr. ft.^2$
18.2	36.5
36.5	36.5
75	36.5
220	36.5

6. CONCENTRATION PROFILES WITH MASS TRANSFER

The $1\frac{1}{2}$-in. I.D. column was set up as shown in Figures 9

and 10. The tracer distributor, and the Teflon gasket through

which the tracer supply hypodermic needle passed, were replaced

by a standard 1/16-in. thick Teflon gasket. Acetic acid was

transferred from the continuous phase to the dispersed phase.

The concentration profile in each phase was measured by means of

the bell-probe and hypodermic needles as described below.

The column was brought to the operating condition as

described under section 2 of Experimental Procedure. The times

at which steady state conditions were attained were determined

by taking samples by means of the lowest and the highest hypo-

dermic needles and of the aqueous phase leaving the column at

various times after start-up. All hypodermic needle samples

in this part of the work were taken at 3/4-ml./min. During

actual runs samples were taken with the bell-probe at the levels

of the first, third, fifth, seventh, ninth, and tenth hypo-
dermic needles up the column. A bell-probe sampling rate of
5.2-ml./min. was used for each sample taken. Samples were not
taken by means of the bell-probe at all levels of the needles
because of the lengthy procedure of sampling with the bell-
probe. The bell-probe was raised above the interface and after
a half-hour interval aqueous phase samples were taken with the
hypodermic needles consecutively starting with the lowest one.
Samples of the inlet and outlet streams of the column were taken
at the beginning of steady-state operation, after the bell-
probe samples had been taken, and after the hypodermic needle
samples had been taken. Finally a piston sample was taken in
order to measure the dispersed phase hold-up. Each bell-probe
sample was shaken vigorously many times to bring the two phases
to equilibrium. Each phase of each sample was analysed for
acetic acid by titrating with standard sodium hydroxide solution
as described earlier. The column operating conditions studied
are given in each line of the following table.

Run	Continuous phase superficial velocity, $ft.^3/hr.\ ft.^2$	Dispersed phase superficial velocity, $ft.^3/hr.\ ft.^2$
J1	36.5	54.7
J2	18.2	54.7
J3	36.5	91.2
J4	48.4	91.2
J5	48.4	128

RESULTS AND DISCUSSION

An initial investigation was undertaken to assess various methods of removing samples of either phase from the operating spray column. Previous measurements of concentration profiles within a liquid-liquid extraction spray column at The University of British Columbia involved the taking of samples by means of the hook and the bell-probes mentioned earlier (35, 37, 38, 39). As discussed under the heading Introduction some doubt existed as to whether the solute concentration in the continuous phase entering the hook-probe was the same as that in the continuous phase entering the bell-probe along with the drops. Accordingly various methods of sampling of the phases were investigated in this work.

A discussion of the results of the sampling technique studies is presented as a whole after all of these results are given. This procedure has been adopted in order that comparisons and contrasts between the results of various investigations can be seen more easily.

1. RESULTS OF SAMPLING TECHNIQUE STUDIES

a) Sampling with hook and bell-probes and piston with mass transfer between the phases.

Samples were taken from the operating spray column with the hook and the bell-probes at various locations shown for a

typical run in the abscissa of Figure 25. In each such run a piston sample also was taken. The concentration of acetic acid in the ketone phase of a bell-probe sample was calculated by means of equation 6 as described earlier.

$$c_D = c_D^a + \frac{V_C}{V_D} (c_C^a - c_C)$$

<div align="right">6</div>

The value of c_C was taken to be the concentration of acetic acid in the hook-probe sample taken from the same sampling elevation as the bell-probe sample. An average concentration in each phase over the piston height was determined from the results obtained with each probe by graphical integration of the respective concentration profiles of the sort shown in Figure 25. The average concentration of acetic acid in the ketone phase of the piston sample was calculated by means of Equation 6 where c_C was taken to be the average concentration in the aqueous phase over the piston height calculated from the hook-probe sample results.

It is assumed that backmixing of the continuous phase can be represented by "packets" of continuous phase rising with the dispersed phase drops. Presumably these "packets" are, in fact, mainly the wakes of rising drops*. On this basis it is shown in Appendix III that for a piston sample the average concentration of acetic acid in the continuous phase, excluding that in

---

* Note that the derivation of Equation III-8 in Appendix III is general in that wakes are not mentioned. In the model used there c_C is the average concentration of solute in the <u>descending</u> continuous phase at the elevation under consideration.

such wakes, is given by Equation III-8.

$$c_C = \left[\frac{\left(\frac{V_C}{V_D}\right) c_C^a + c_D^a - c_D^i + \left(\frac{L_C}{L_D}\right) c_C^o}{\frac{L_C}{L_D} + \frac{V_C}{V_D}} \right]$$

III-8

The average concentration of acetic acid in the dispersed

phase of each piston sample was calculated a second time

by means of Equation 6. However, instead of using c_C from the

hook-probe sample results as mentioned above, c_C was determined

from Equation III-8 applied to the piston sample.

The results of sampling the phases in the operating spray

column with the hook and the bell-probes and the piston for

each of several runs are given in Table 3. The results of a

typical experimental run are shown graphically in Figure 25.

b) Sampling with hook and bell-probes, hypodermic needles,

and piston with mass transfer between the phases.

Further runs were made in which samples were taken as

just described under a) but in which continuous phase samples

also were withdrawn by means of hypodermic needles in order

to provide an independent check on the hook-probe sample

results. In addition to the average concentrations over the

piston height calculated as described under a) all calculations

involving the hook-probe were repeated for the hypodermic

needle results.

TABLE 3. SAMPLING STUDIES WITH HOOK AND BELL PROBES AND PISTON

Run	Superficial flowrates ft³/hr.ft²	Concentration of acetic acid at the time of sampling, lb.-moles/ft³ x 10³							Average in piston by hook and piston	Average over piston height by hook and bell	Average in piston by Equations III-8 and 6	Hook-probe sampling rate, ml./min.	Bell-probe sampling rate, ml./min.
		Bell and hook probes at position[e]											
		1	2	3	4	5	6	7					
2[a]	92.5	46.8	48.0	48.8	49.4	50.0	50.7	50.7	49.4	49.4	49.5	8.6	20
	90.4	18.6	19.1	20.4	21.3	22.3	21.9	22.4	20.9	21.1	21.6		
4	93.7	55.1	54.6	57.3	58.0	58.6	59.6	60.1	58.0	58.0	55.8	8.6	20
	123.	21.6	23.5	23.4	23.9	24.0	24.2	25.0	10.6	23.8	21.6		
5[b]	69.0	-	60.7	62.3	63.7	64.5	65.1	65.6	63.2	63.2	62.3	8.6	17
	74.4	-	25.8	25.5	26.8	27.1	28.5	27.5	13.8	26.6	23.3		
6	87.5	43.9	45.2	45.9	46.3	46.5	47.2	46.8	46.1	46.1	45.5	4	17
	113.	18.2	18.7	19.5	19.7	19.4	20.1	20.7	16.0	19.3	19.0		
7	87.5	34.8	39.6	40.5	40.7	41.3	41.7	42.3	40.8	40.8	39.5	5	20
	113.	14.6	14.6	15.1	15.6	16.1	16.6	15.9	9.3	15.5	15.5		
8[c]	87.5	40.1	-	40.2	42.2	41.7	-	43.2	41.7	41.7	40.4	5	-
	113.	-	-	-	-	-	-	-	-	-	-		
9[d]	87.5	33.0	35.5	35.0	35.7	36.2	36.7	36.9	35.6	35.6	35.3	5	17
	113.	13.2	13.2	14.1	13.8	14.4	14.6	14.6	12.7	14.0	14.2		

[a] For each run the upper number in each column refers to the continuous phase, the lower number to the dispersed phase. Each run was carried out at room temperature.
[b] The hook-probe was 0.9 inches above the sampling position indicated. The values shown for the respective concentrations of acetic acid in the hook probe samples have been taken from a plot of the measured concentrations versus distance up the column.
[c] The bell-probe was above the interface throughout the run.
[d] The hook-probe was modified as shown in the sketch on page .
[e] The positions at which samples were taken are indicated by number in the abscissa of Figure 25.
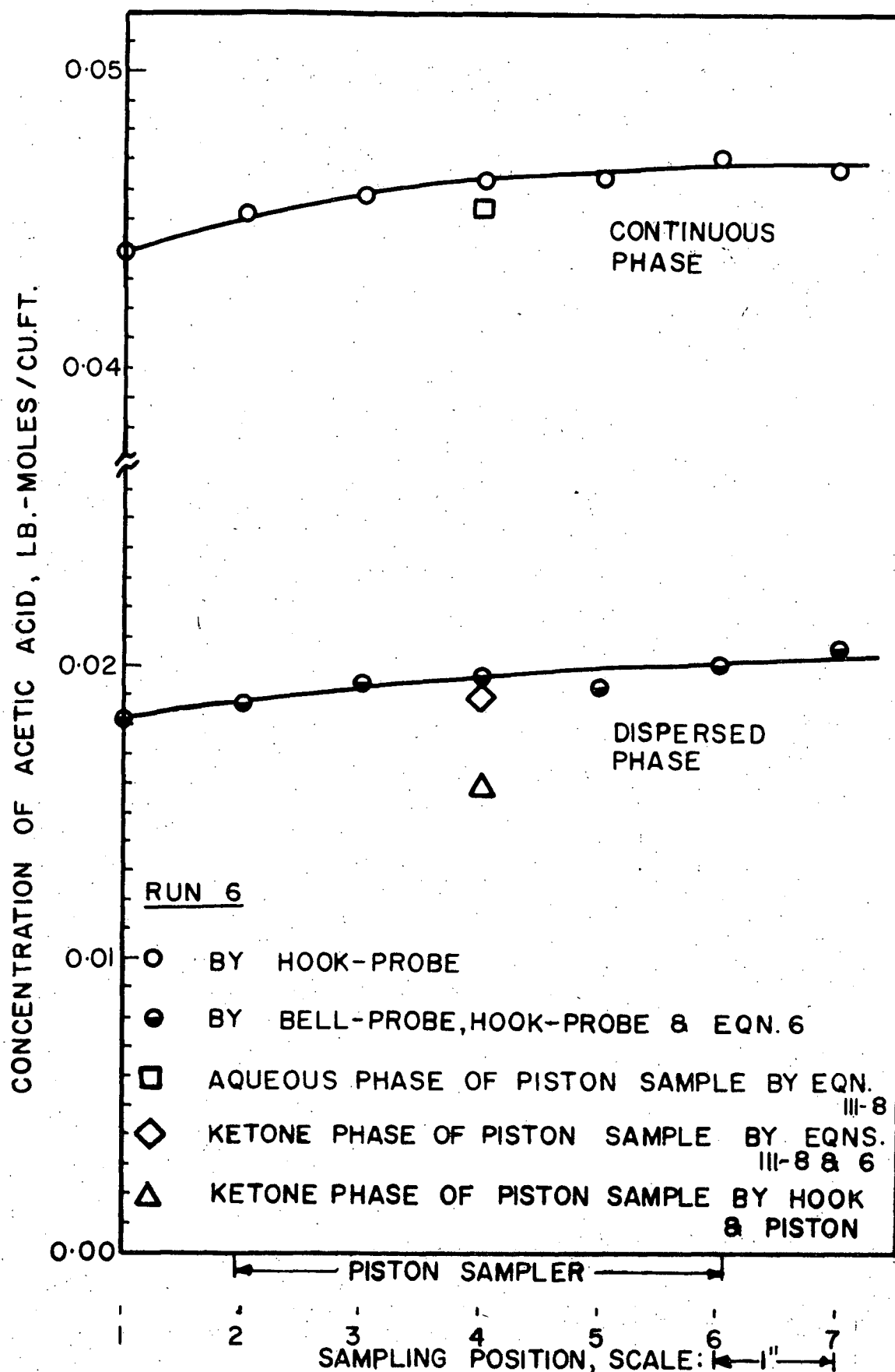
FIGURE 25. SAMPLING TECHNIQUE STUDIES WITH HOOK AND BELL-PROBES AND PISTON

Table 4 shows the results of sampling with the hypodermic needles, and further results obtained with the hook and the bell-probes and the piston. The results of a typical experimental run are shown graphically in Figure 26.

c) Sampling with hook-probes, hypodermic needles, and piston with no mass transfer between the phases.

For each run a straight line was fitted by the method of least squares to a plot of the natural logarithm of the solute concentration versus height up the column for the hook-probe results and the hypodermic needle results respectively. The equation for this straight line was transformed into the equation for the concentration versus height up the column. Integration of the transformed equation produced an average concentration over the piston height. The average concentration of solute in the continuous phase of a piston sample was determined directly by analysis for solute. This concentration included the contribution of the wakes.

The results of sampling technique studies under conditions of no mass transfer are presented in Table 5. The results of a typical run are shown graphically in Figure 27.

2. DISCUSSION OF SAMPLING TECHNIQUE STUDIES

In order to understand fully what material enters a sampling device it would be necessary to know exactly the concentration of solute at every point in the column and

TABLE 4. SAMPLING STUDIES WITH HOOK AND BELL-PROBES, HYPODERMIC NEEDLES, AND PISTON

Run	Superficial flowrate, ft.^{3}/hr.ft.^{2}	Concentration of acetic acid at the time of sampling, lb.-moles/ft.^{3} $\times 10^{-3}$ Bell and hook probes at position								Hook-probe sampling rate, ml./min.	Bell-probe sampling rate, ml./min.
		D	1	3	5	7	G	H			
13[a]	87.5	28.9	29.6	29.9	30.9	31.8	-	32.4		5	17
	113.	9.87	10.6	10.9	11.3	11.9	-	12.4			
15	87.5	26.8	27.3	28.2	28.9	29.2	-	-		5	17
	113.	9.83	10.2	10.5	10.8	11.2	-	-			
16	87.5	27.3	28.1[b]	29.7[b]	29.9[b]	-	31.0	-		5	17
	113.	9.6	10.2[b]	10.9[b]	10.8[b]	-	11.8	-			

	Concentration of acetic acid at the time of sampling, lb.-moles/ft.^{3} x 10^{-3}												average over piston height by means of		average in piston by means of		
Run	hypodermic needle at position[c]												hook and bell-probes	hypod-ermic needles and bell-probe	hypod-ermic needles and piston	hook-probe and piston	equations III-8 and 6
	A	B	C	D	E	F	G	H	I	J							
13[a]	26.5	27.6	27.3	28.4	28.8	30.9	31.8	31.8	32.3	33.3			30.5	29.9	29.9	30.5	30.1
	-	-	-	-	-	-	-	-	-	-			11.0	11.0	11.3	8.3	10.5
15	25.3	26.0	26.3	26.3	27.0	28.9	29.4	29.4	29.9	30.7			28.4	28.0	28.0	28.4	27.9
	-	-	-	-	-	-	-	-	-	-			10.7	10.7	10.4	8.3	10.3
16	25.3	26.3	27.0	27.3	27.0	29.9	30.4	30.4	31.4	32.3			29.1	28.9	28.9	29.1	28.9
	-	-	-	-	-	-	-	-	-	-			11.7	11.7	11.1	10.0	10.3

[a] For each run the upper number in each column refers to the continuous phase, the lower number to the dispersed phase. Each run was carried out at room temperature.

[b] Samples were taken 5/8-in. above the position indicated.

[c] The positions at which samples were taken are indicated by number or letter in the abscissa of Figure 26.
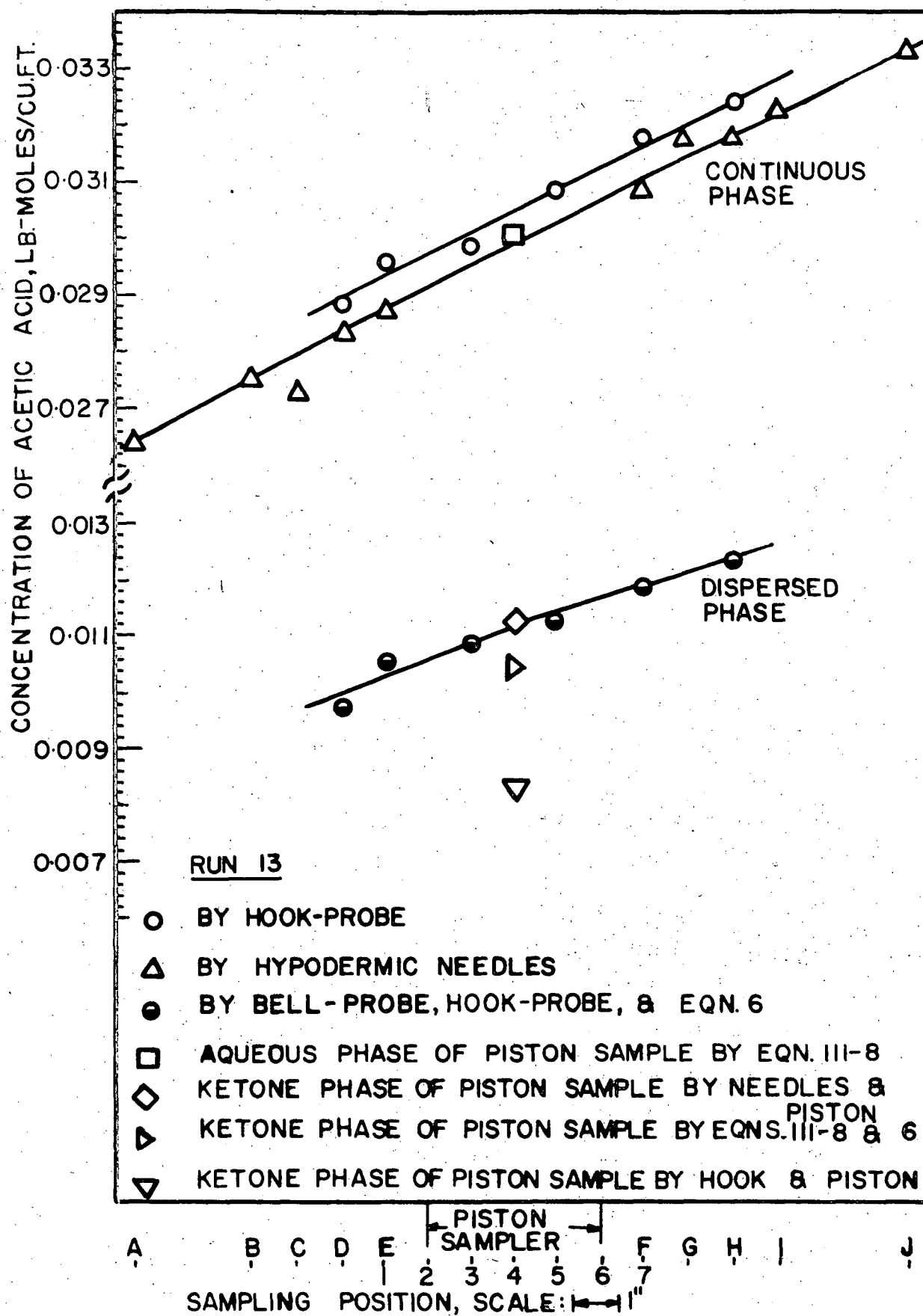
FIGURE 26. SAMPLING TECHNIQUE STUDIES WITH HOOK AND BELL-PROBES, HYPODERMIC NEEDLES AND PISTON

TABLE 5. SAMPLING TECHNIQUE STUDIES WITH NO MASS TRANSFER

Run	L_C, $ft.^3/hr.$ $ft.^2$	L_D, $ft.^3/hr.$ $ft.^2$	Sodium concentrations, microgm./ml.												Piston sample	Temp. $^{\circ}F$
			Hypodermic needle samples					Hook-probe samples							
			Height above piston centre, in.				Average over piston	Height above piston centre, in.					Average over piston		
			-8.96	-2.90	2.9	8.96		-2.88	-1.44	0.0	1.44	2.88			
43	36.5	128.	12.6	2.0	0.25	0.035	0.74	1.71	0.98	0.60	0.39	0.22	0.67	0.65	74
44	36.5	73.	35.2	8.0	1.5	0.33	3.6	7.0	4.7	3.5	2.6	1.7	3.62	3.6	73
44a	36.5	128	15.8	1.6	0.21	0.03	0.63	1.67	1.03	0.67	0.36	0.24	0.68	0.63	74
44b	27.7	128.	47.0	6.6	1.6	0.31	3.72	7.4	5.3	3.6	2.8	1.7	3.9	3.8	73
69	36.5	30.4	110.	61.3	34.9	19.8	46.8	60.2	54.6	46.0	39.8	34.2	46.3	46.1	72
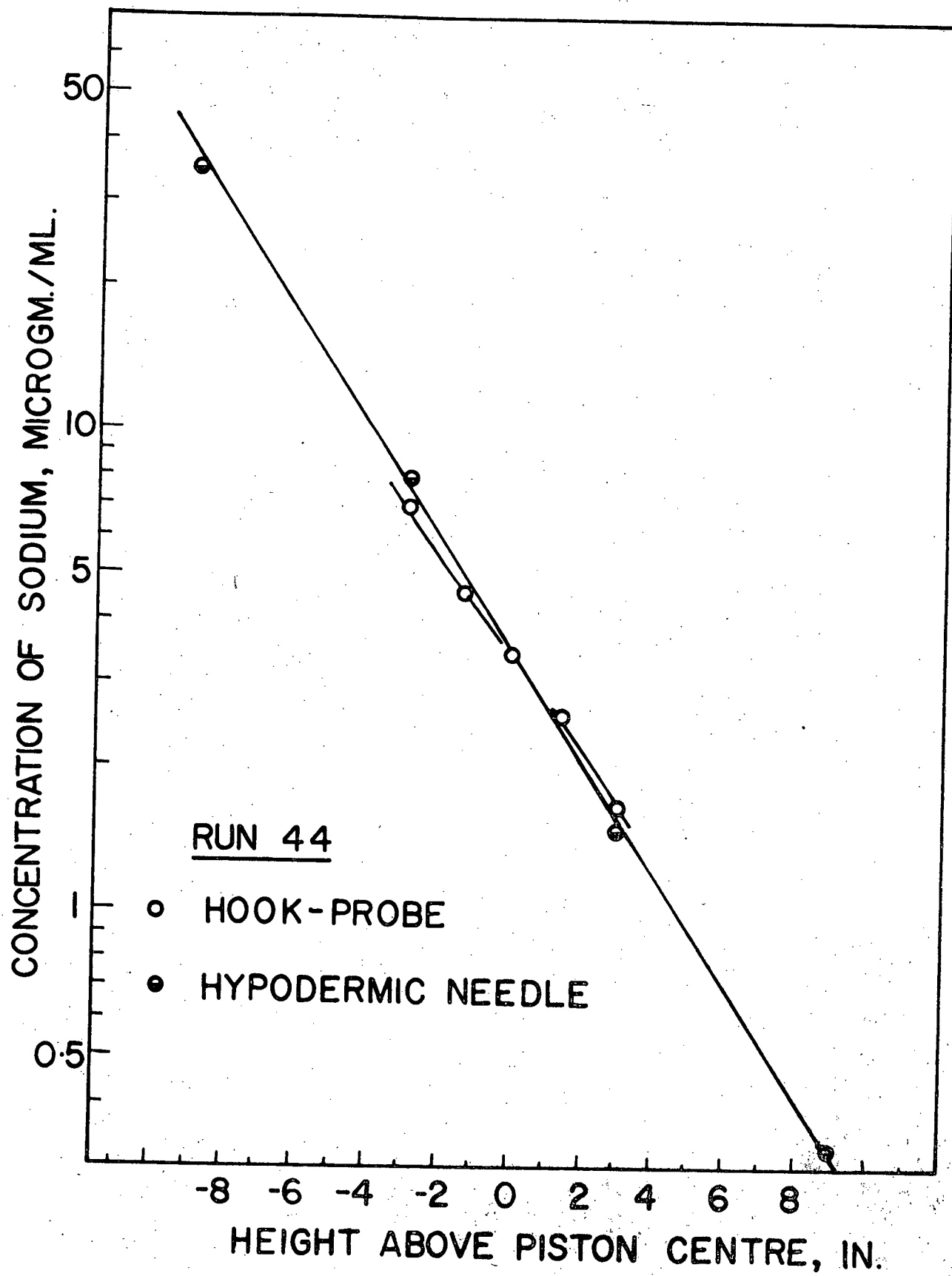
FIGURE 27. SAMPLING TECHNIQUE STUDIES WITH NO MASS TRANSFER

from which point every volume element of the sample originated. Although it turns out that some conclusions can be drawn for the case of no mass transfer between the phases, sufficient knowledge is not available to do so for the case of mass transfer. Fortunately the bulk of the work described in this thesis deals with the case where conclusions can be drawn: measurement of axial eddy diffusivities where no mass transfer between the phases occured. The comparative simplicity of the sampling techniques in the absence of mass transfer suggests that the results of these studies be discussed first.

Under conditions of no mass transfer the measured concentration of solute in the continuous phase of a piston sample is the average concentration in that phase over the piston height at the time of sampling. This average takes into account radial and axial variations in concentration, and includes the appropriate contributions from the descending continuous phase and from the rising aqueous phase in the wakes. It can be seen from Table 5 that the average solute concentration in a piston sample is found to be, to all intents and purposes, the same as the average solute concentration over the piston height calculated from the hook-probe or the hypodermic needle results. Therefore either the hook-probe or the hypodermic needles can be used to give the average concentration of solute in the continuous phase of a spray column under conditions applicable when tracer studies are being carried out.

Although, as mentioned under the heading Theory, the dispersion model envisages no radial concentration differences in the continuous phase, presumably such do occur in operating columns, for example in the wakes of rising drops. However, if the dispersion model is to be applied some average concentration must be used, and that obtained from a piston sample (and also, as shown in Table 5, by means of the hook-probe or the hypodermic needles) would seem to be a reasonable choice. Due to the many practical problems which would be encountered in incorporating several piston samplers along the length of the column and of the lengthy purge time needed in taking hook-probe samples hypodermic needles have been used for taking samples in the work involving tracer studies of axial eddy diffusivity.

With this rationale for the use of the hypodermic needles established, it is interesting to speculate on the mechanism lying behind the agreement noted in Table 5 between hypodermic needles, and hook-probe results under conditions of no mass transfer. Among the tenable postulates are the two alternatives that either the hook-probe and the hypodermic needles both sample the descending continuous phase and the rising wakes representatively, or the contribution of the wakes to the average solute concentration in a piston sample is negligible. The former explanation perhaps is possible. However, it seems unlikely that it is true because the physical natures of the hook-probe and of the hypodermic needles are different enough that these sampling devices would be expected to withdraw

continuous phase in different proportions from the wakes and from

the descending aqueous phase. The second alternative, then,

seems more likely to be valid than does the first and if this is

accepted two possibilities arise. Either the volume of the

wakes is small relative to the total volume of the continuous

phase, or the concentration of solute in the bulk of the

continuous phase is almost the same as that in the wakes. Letan

and Kehat (121) suggest that the wakes have almost the same

volume as the drops for heat transfer studies in a spray column.

The present studies of sampling techniques for conditions of

no mass transfer include conditions of dispersed phase hold-up

as high as 16%. Therefore, accepting the views of Letan and

Kehat, in tracer studies it would appear likely that the solute

concentration in the wakes is almost the same as in the bulk of

the continuous phase.

For continuous phase superficial velocities greater than

about 36-$ft.^3/hr.$ $ft.^2$ the rate of decrease of tracer concentration

with height up the column is so great that the tracer

concentration is measurable only in the samples taken at the

first two or three sampling points above the tracer distributor.

Because of this limitation the work of sampling under

conditions of no mass transfer was restricted to low continuous

phase superficial velocities. (The work includes both high

and low dispersed phase superficial velocities.)

When the studies of sampling techniques for runs in which

mass transfer took place between the two phases are considered,

it is found that definite conclusions can not be drawn as to

the exact significance of the results obtained. However, there

are indications that the hypodermic needles withdraw continuous

phase which is representative of the descending phase at the

sampling elevation. A comparison between the hook-probe and

the hypodermic needle results can be made with the help of

Figure 26. From this figure it can be seen that the solute

concentration profile in the continuous phase obtained by means

of the hypodermic needles lies below that obtained with the

hook-probe. The average solute concentration in the continuous

phase over the piston height calculated by graphical integration

of the hypodermic needle results lies very close to the average

solute concentration of the descending continuous phase (i.e.

wakes excluded) in the piston sample calculated by means of

Equation III-8. This agreement of the results of the hypodermic

needles with those calculated by means of Equation III-8 shows

that, if the model of Appendix III is correct, either the

hypodermic needle samples contain no continuous phase originating

in the wakes, or continuous phase from this source in hypodermic

needle samples does not contribute very much to the measured

hypodermic needle sample concentrations. Again this small

contribution could be the result of the wakes being of

similar solute concentration to that of the bulk of the

continuous phase, or the result of the inclusion of only

a small relative volume of wake fluid in the hypodermic needle

samples. The first of these last two alternatives seem much less

plausible than it did for sampling in tracer studies. In the

mass transfer case, for transfer out of the continuous phase,

the wake concentration would be low for two reasons: backmixing

of dilute material from the lower end of the column, and transfer

out of the wake into the dispersed phase. Only the first of

these two factors operates in the case of the tracer studies.

Unfortunately further information is needed to draw more

definite conclusions for the runs with mass transfer. As there

was no evidence which indicated that the needles gave erroneous

results their use as sampling devices was adopted in the five

mass transfer runs performed in order to investigate axial eddy

diffusivity. However, this procedure perhaps was no worse in

its effect than was the assumption (required for the dispersion

model) of constant radial concentration in the continuous phase

at a particular axial position which would not, of course, have

been completely valid.

The solute concentration profile in the dispersed phase is

substantially the same whether it is calculated from hook-probe

and bell-probe results by means of Equation 6 or from hypodermic

needles and bell-probe results by means of the same equation.

(See Table 5.) The reasons for this fact are that the values of

c_C from hypodermic needle results and from hook-probe results

differ by roughly two percent only, and $\dfrac{V_C}{V_D}$ for a bell-probe

sample is of the order of 1/7 only. With this ratio of V_C to V_D

a two percent change in c_C has only a negligible effect on the value of c_D calculated by means of Equation 6. Therefore no conclusions regarding c_C can be drawn from the fact that c_D from the bell-probe and the hypodermic needle results agrees with c_D obtained from the bell-probe and the hook-probe results. However, due to the calculated value of c_D for a bell-probe sample being insensitive to small errors in c_C it would be expected that this value of c_D is the true solute concentration in the dispersed phase entering the bell-probe if it can be assumed that the c_C used does involve only a small error. Now, as Table 4 shows, the average solute concentration in the dispersed phase of a piston sample calculated from hypodermic needle and piston results agrees with the average solute concentration in the dispersed phase over the piston height calculated from hypodermic needle and bell-probe results. Also, the average value of $\dfrac{V_C}{V_D}$ for a piston sample is about 5, and therefore the value of c_D obtained from Equation 6 applied to a piston sample is much more sensitive to the value of c_C used in Equation 6 than it is for a bell-probe sample. Hence the agreement of the values of c_D as noted above implies the correctness of the value of c_C used in the piston case: the concentration given by the hypodermic needles. All this relies, of course, on the assumption that only small errors apply to the concentrations given by the hypodermic needles. Thus one might complain that the argument given here involves an assumption of what is being proved. However, although this

complaint is justified to a degree, it should be realized that in

presenting the argument the very different $\frac{V_C}{V_D}$ ratio in the piston

sample from that in the bell-probe sample strenghtens the case for

the correctness of the hypodermic needle samples. If these are

correct, or even reasonably so, then the value of the dispersed

phase concentration from the bell-probe results also is correct.

One further comparison should be made. Table 4 shows that

c_D obtained from the piston results in conjunction with the hook-

probe results is lower than that obtained from the piston and

hypodermic needle results or the piston results and Equation III-8.

Table 3 shows similar low values of c_D when the hook-probe

analyses are used instead of continuous phase concentrations from

Equation III-8 in the calculation of c_D for the piston. These

last observations, of course, are consistent with the fact

mentioned earlier, that the value of c_C obtained from Equation III-8

agrees with the hypodermic needle results.

Now, a low value of c_D is obtained from a piston sample if a

high value of c_C is used in Equation 6. Recalling that c_C from

Equation III-8 assumes the inclusion of no wakes, and that if

wakes were included, the value of c_C would be reduced, and,

therefore the value of c_D calculated from piston results raised,

we can see that if it were postulated that the hook-probe sample

included an appreciable and effective contribution from the

wakes, the value of c_D calculated from piston and hook-probe

results would be increased in comparison to the value of c_D

calculated from needle and bell, hook and bell, and Equation III-8 and piston, all of which are in reasonable agreement. However, c_D from hook-probe and piston results are <u>lower</u> than the values of c_D obtained by the other methods. Hence it seems impossible that the low c_D results from hook and piston measurements are due to the hook-probe concentrations reflecting appreciable contributions from drop wakes. In other words c_C for the hook-probe is high, not low. Furthermore in Run 4 c_D from the piston sample based on hook-probe analyses is lower, indeed, than the dispersed phase concentration at the dispersed phase inlet nozzle. This result, of course, is impossible, and lends strong support to the hypothesis that c_C from the hook-probe results generally is too high.

It seems advantageous to compare hook-probe results with reference to the dispersed phase concentrations, as has been done above, instead of comparing directly the hook-probe and hypodermic needle results. There are two reasons for this approach. First, the difference obtained between the values of c_D is numerically much larger than is the difference between the values of c_C from the hook-probe and the hypodermic needles respectively. Second, the impossible result of c_D being calculated as even lower than that in the dispersed phase entering the column is missed when the direct comparison is made between c_C from the hook-probe and c_C from the hypodermic needles.

The postulate could be put forward that the hook-probe

tends to suck in material from some elevation higher up the column than its actual position. However, when an attempt was made to lessen such an effect by directing the end of the hook horizontally, as shown in the sketch on page 65, no change in the results were obtained. Perhaps the comparatively large size of the hook-probe disturbs the flow patterns in the column to produce high continuous phase concentrations at its inlet. For example, if the hook-probe deflects drops in such a way that extraction is less complete in the neighbourhood of the hook-probe inlet, then high continuous phase concentrations would be measured by this probe.

From plots such as that shown in Figure 26, and assuming that the hypodermic needle samples are representative of the continuous phase in the column at the sampling height, it can be seen that the continuous phase entering the hook-probe appears to be representative of that phase in the column approximately 1-in. above the probe entrance. As a result the continuous phase concentration profiles given by Ewanchyna (30, 31) appear to be somewhat in error. However, this error is only slight and his conclusions mentioned under the heading Introduction regarding the end effect at the continuous phase inlet of the column are still substantially valid.

3. AXIAL EDDY DIFFUSIVITY, DROP SIZE DISTRIBUTION, AND DISPERSED PHASE HOLD-UP STUDIES IN THE $1\frac{1}{2}$-IN. I.D. COLUMN

The axial eddy diffusivity, E, characterizes the extent to which solute is backmixed up the column, presumably through the

agency of wakes rising behind dispersed phase drops. In this work values of E have been determined by means of tracer studies with no mass transfer between the phases. If mass transfer were present some degree of turbulence at the surfaces of the drops would be expected due to interfacial phenomena such as the Marangoni effect. However, the effect of this interfacial turbulence on the size of the wakes and on the manner in which solute is transferred out of and into the wakes would be expected to be negligible compared with the effect of the oscillating motion of the drops. Consequently the values of E determined by tracer studies would be expected (subject to the limitations discussed on page 154.) to be applicable for the case of mass transfer.

A discussion of the results of the main bulk of experiments precedes that of the preliminary experiments performed in order to test the applicability of the dispersion model and the suitability of the experimental method.

a) Axial eddy diffusivity, drop size distribution, and hold-up studies.

i) Determination of axial eddy diffusivities and Peclet numbers.

The calculations to be described here were performed on an IBM 7040 electronic computer. A data sheet, a hand calculation, and a computer output for a typical run are given in Appendix IV.

These calculations produced the following quantities: superficial axial eddy diffusivities, axial eddy diffusivities,

Peclet numbers, reduced concentrations, and mass balances. The natural logarithms of the concentrations of the samples were plotted versus height down the column. The equation for the best straight line through these points was calculated by the method of least squares. The validity of this method for calculating the straight line involved the usual assumptions concerning the normality of the distribution of the natural logarithm of the concentration (125). The superficial velocity of the continuous phase was divided by the absolute magnitude of the slope of this line to give the superficial axial eddy diffusivity, (Ee). (See Equation 13.) The axial eddy diffusivity, E, was calculated by dividing the superficial axial eddy diffusivity by the volumetric fraction, e, of continuous phase in the column. The Peclet number, Pe, was calculated by means of the following equation.

$$Pe = \left(\frac{L_C}{e} + \frac{L_D}{1-e} \right) \left(\frac{d_p}{E} \right)$$

II-18

The interpretation to be placed on the drop diameter, d_p, is discussed below. In order that concentration profiles could be compared for various column operating conditions the reduced concentration at each sampling point was calculated by means of the following expression.

$$\text{reduced concentration} = \frac{\text{actual concentration x } 1000}{\text{concentration in the aqueous phase leaving the column}}$$

Mass balances were calculated for the aqueous phase, the ketone phase, and the tracer, respectively, over the column. A set of reduced concentration profiles for one superficial velocity of ketone phase and various superficial velocities of aqueous phase is shown in Figure 28. The linearity of each plot in Figure 28 indicates that Equation 13, and hence the dispersion model concept, describe the backmixing of the continuous phase. The reduced concentration profile, the dispersed phase hold-up, the axial eddy diffusivity, the Peclet number and the mass balance results for each run are given in Table IV-4, Appendix IV.

As this table shows at the level of accuracy possible in the present experiments there was no dependence of axial eddy diffusivity on the continuous phase superficial velocity, L_C. Continuous phase has been found (21, 22, 23) to move up the column in the wakes of rising dispersed phase drops. The velocity of the drops is negligibly affected by a small change in the low values of L_C used in the tracer studies. Correspondingly the flowrate of continuous phase up the column in the wakes of drops is substantially unaffected by such a change in the superficial velocity of the continuous phase. If the axial mixing of the continuous phase is caused by the drops and the associated wakes it is not surprising that the axial eddy diffusivity is independent of L_C for the narrow range of low values of L_C used in this work.
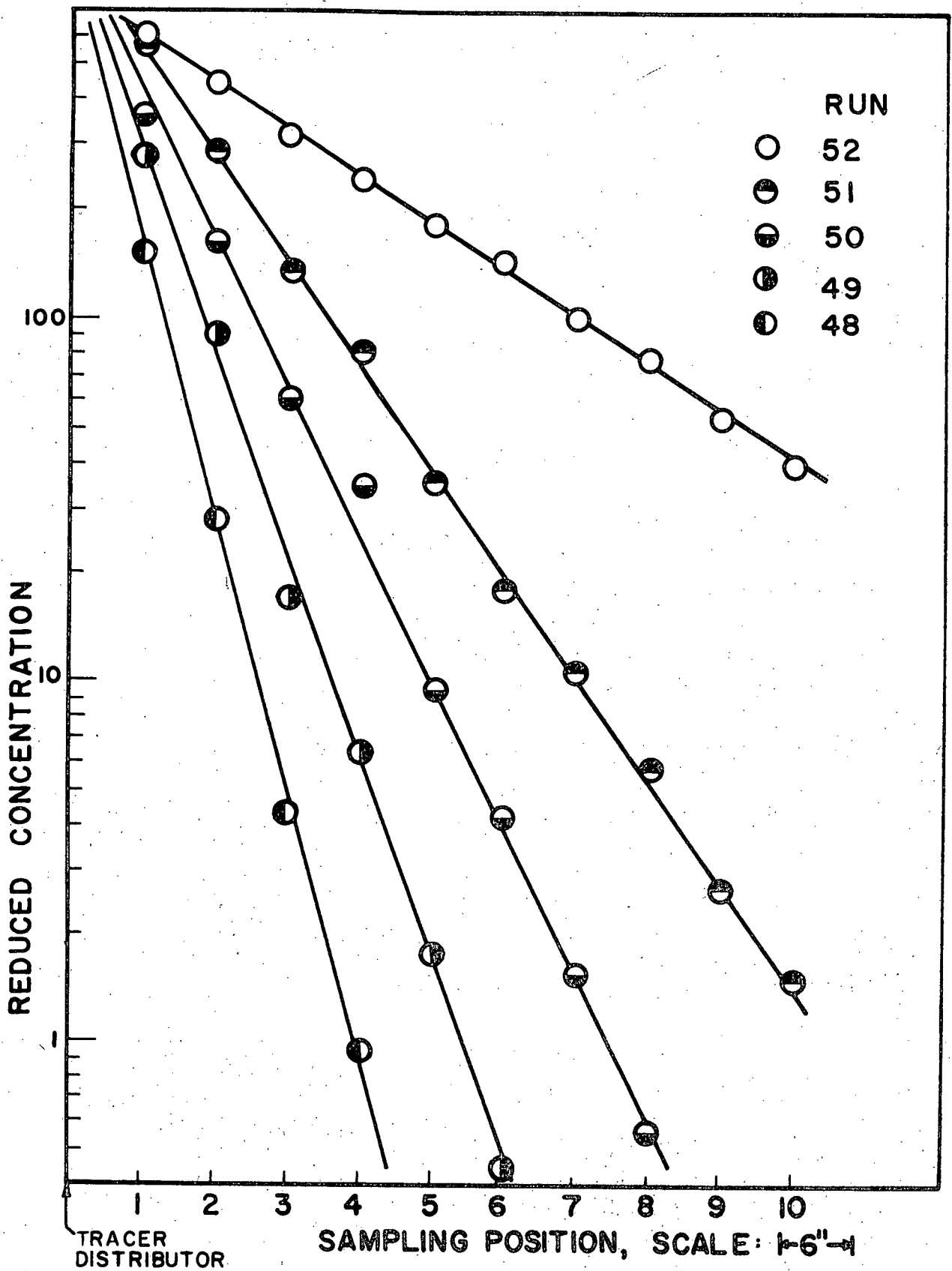
FIGURE 28.   REDUCED CONCENTRATION PROFILES

Figure 29 shows the dependence of axial eddy diffusivity on the dispersed phase flowrate for one continuous phase flowrate and various drop sizes. The axial eddy diffusivity remained approximately constant as the dispersed phase flowrate was decreased from high values but at low dispersed phase flowrates the axial eddy diffusivity increased rapidly. This effect is less pronounced at small drop sizes. The effect of increasing the drop size for a given dispersed phase superficial velocity was to increase the axial eddy diffusivity.

At first it was expected that an increase in the number of drops of a given size per unit volume of column would result in a larger volume of continuous phase being carried up the column in their wakes and hence an increase in the axial eddy diffusivity, E. However, as mentioned above, the opposite effect is observed at low superficial velocities, L_D, of dispersed phase. The reason for the decrease in E with an increase in the number of drops could be due to the increase in interference of the wakes of drops by neighbouring drops. This interference would tend to detach the wakes from the drops, resulting in a lower value of E. Apparently at low values of L_D the decrease in E due to interference of wakes predominates over the increase in E due to the larger number of drops. At high values of L_D the two effects on E counterbalance each other.

An increase in the drop size, d_p, for a given value of L_D would be expected to result in an increase in E due to an increase in the size of each wake and also due to less interference of wakes by neighbouring drops. However, the value of E would be expected to decrease due to a smaller
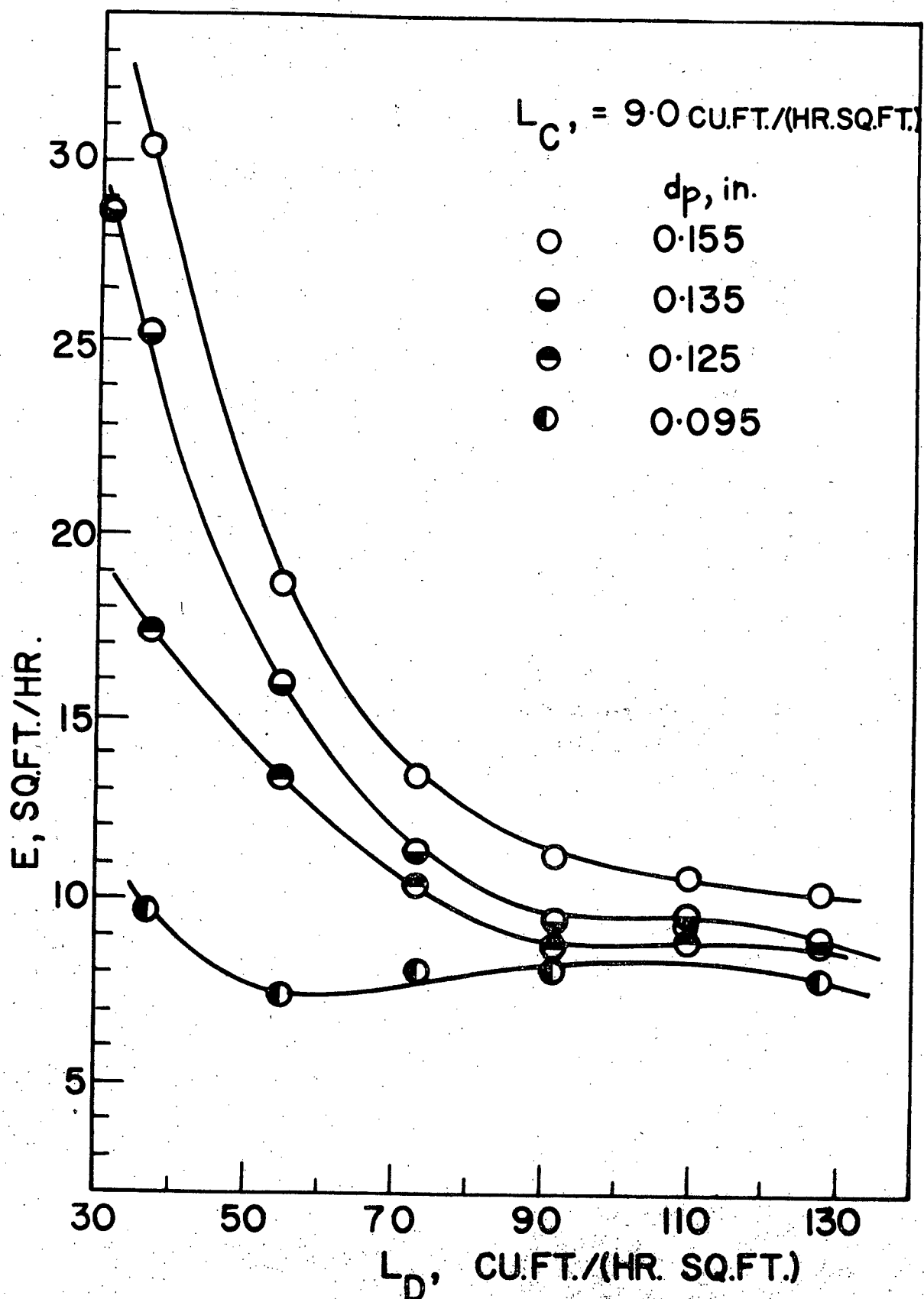
FIGURE 29. AXIAL EDDY DIFFUSIVITY IN THE $1\frac{1}{2}$-IN. I.D. COLUMN

number of drops and hence fewer wakes. Apparently the effects resulting in an increase in E when d_p is increased predominate over those which would tend to decrease E.

Figure 30 shows the axial eddy diffusivity, E, plotted against the superficial velocity of continuous phase, L_C, for four different values of the superficial velocity of dispersed phase, L_D. The drop size, d_p, was 0.135-in. As mentioned earlier E is independent of L_C and decreases with an increase in L_D. Also shown in Figure 30 are the results of Hazelbeck and Geankoplis (42). They used a 1.41-in. I.D. column, a drop size, d_p, of 0.134-in. and water and MIBK as the continuous and dispersed phases respectively. They used an aqueous solution of potassium chloride as tracer and the step function method. They found no dependence of E on L_D for values of L_D between 18.4-ft.^{3}/hr. ft.^{2} and 49.5-ft.^{3}/hr. ft.^{2}, but found that E increased linearly with L_C. As discussed on page 107 of this thesis it would be expected that E should be nearly independent of L_C for the narrow range of low values of L_C used for the experiments described in this thesis and also those described by Hazelbeck and Geankoplis. The fact that these workers (42) found a marked increase in E with in increase in L_C may have been due to problems associated with transient response techniques discussed under the heading Introduction.

Figure 30a is a plot of the dispersion number, $\frac{Ee}{Ud_p}$, against the Reynolds number, $\frac{d_p U \rho}{\mu}$. This figure shows a summary, prepared
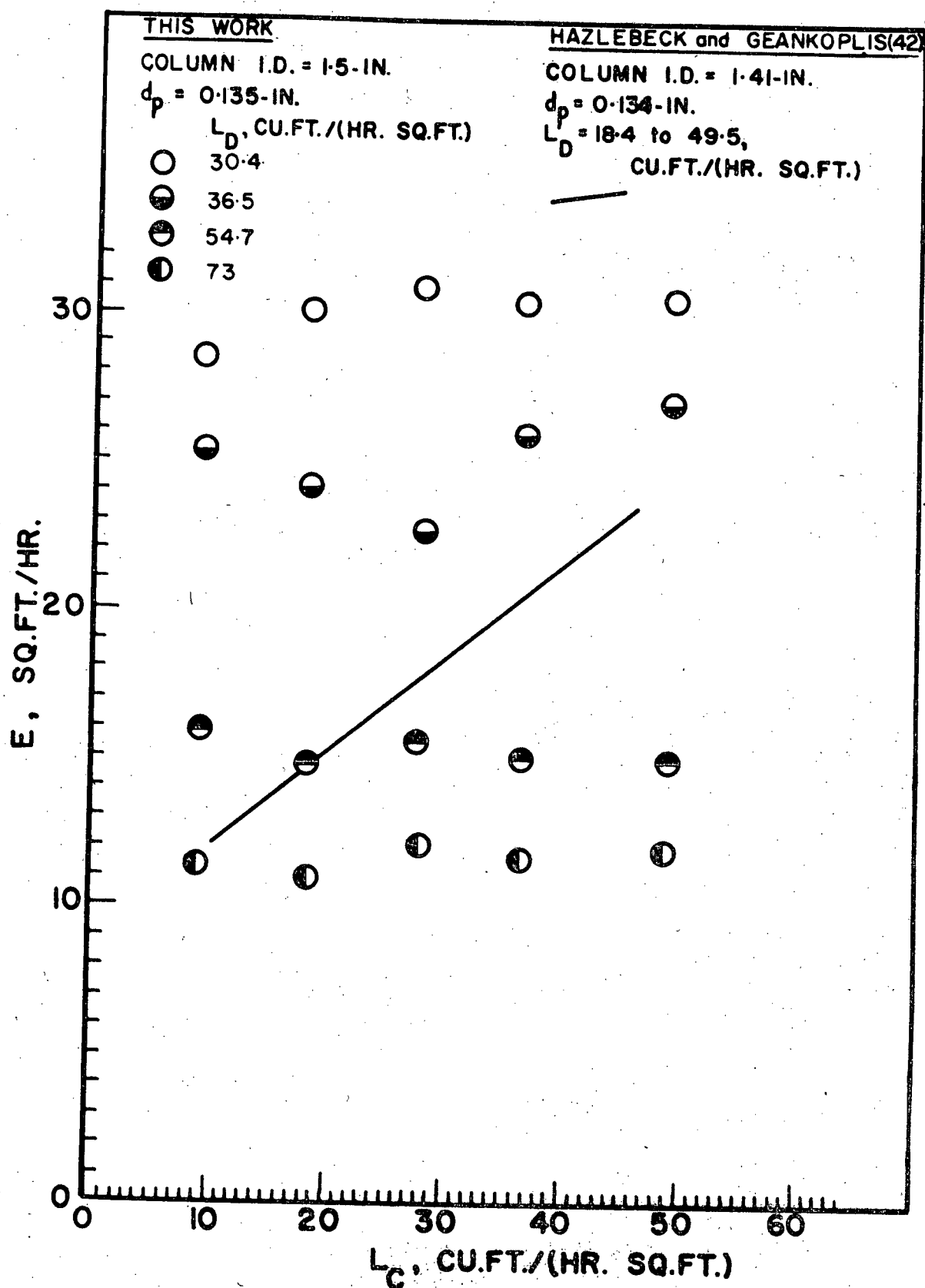
FIGURE 30. COMPARISON OF AXIAL EDDY DIFFUSIVITY AS DETERMINED IN THIS WORK WITH THAT OF OTHER WORKERS
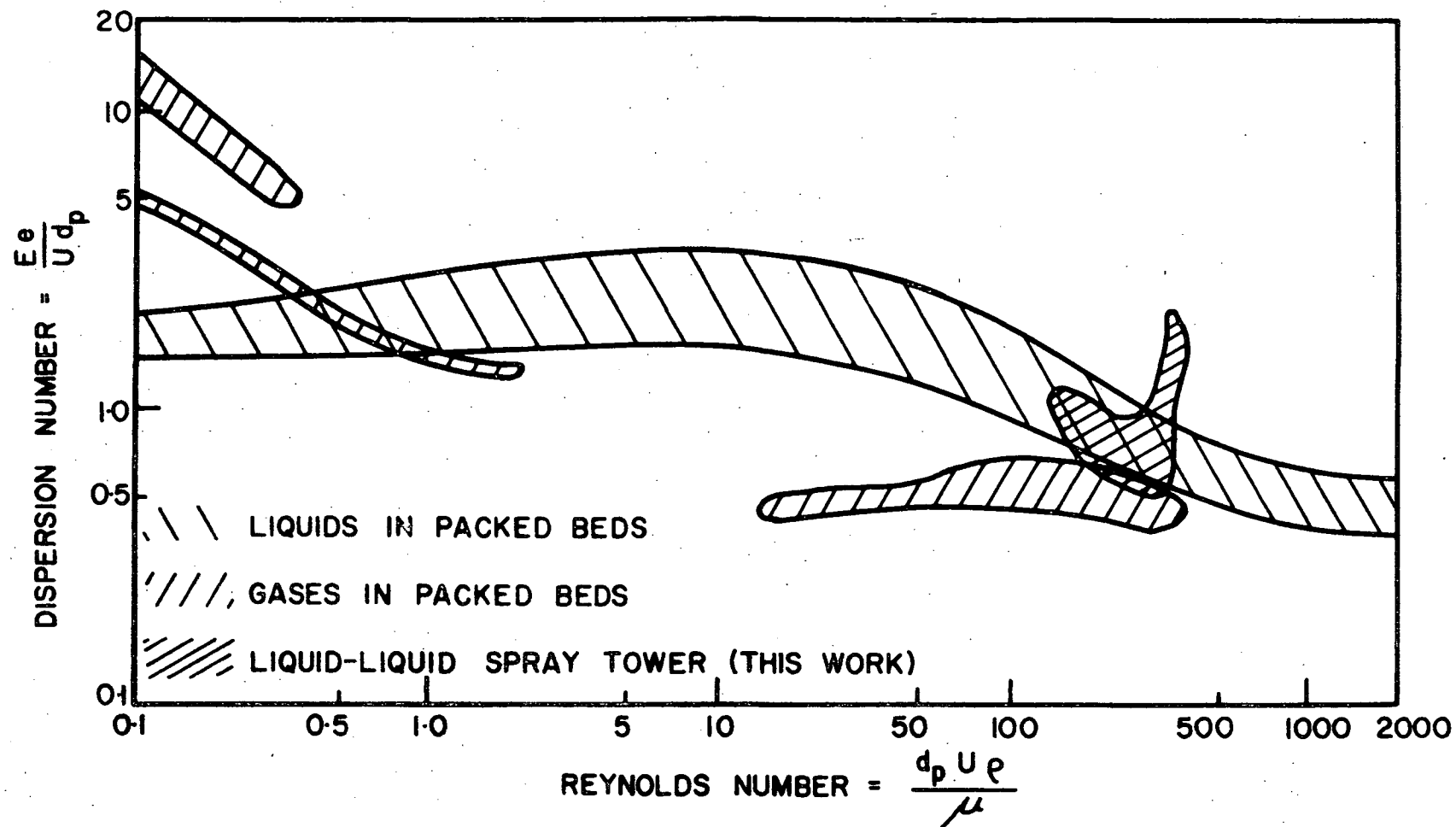
FIGURE 30a. COMPARISON OF DISPERSION NUMBER AS DETERMINED IN THIS WORK WITH THAT FOR PACKED BEDS

by Levenspiel and Bischoff (73), of the data in the literature for gas and liquid flow through packed beds. Also plotted are the results for liquid-liquid spray tower operation determined in this work. It can be seen from Figure 30a that the results for spray tower operation more or less coincide with those for liquid flow through packed beds, for the limited range of Reynolds number investigated. This agreement supports the correctness of the results of axial eddy diffusivity in a spray column presented in this thesis. In addition it lends support to the application of the mixing cell - packed bed analogy to spray column operation described below.

Plots of drop Peclet numbers versus dispersed phase hold-up for the four different drop size distributions studied are presented in Figures 31, 32, 33, and 34 respectively. Peclet numbers, predicted on the basis of the mixing cell - packed bed analogy (44, 64, 90, 92, 108, 109) were calculated for six lattice arrangements of drops as shown in Appendix II. All of the predicted Peclet numbers lie in the range between those for the lattice arrangements of orthorhombic - 2 and rhombohedral - 1 respectively. The values of the Peclet numbers for these two cases are plotted in each of Figures 31, 32, 33, and 34 in order that a comparison between the calculated and the predicted Peclet numbers can be made. The agreement between the experimental Pe and the predicted Pe is very good for large drops and becomes progressively worse
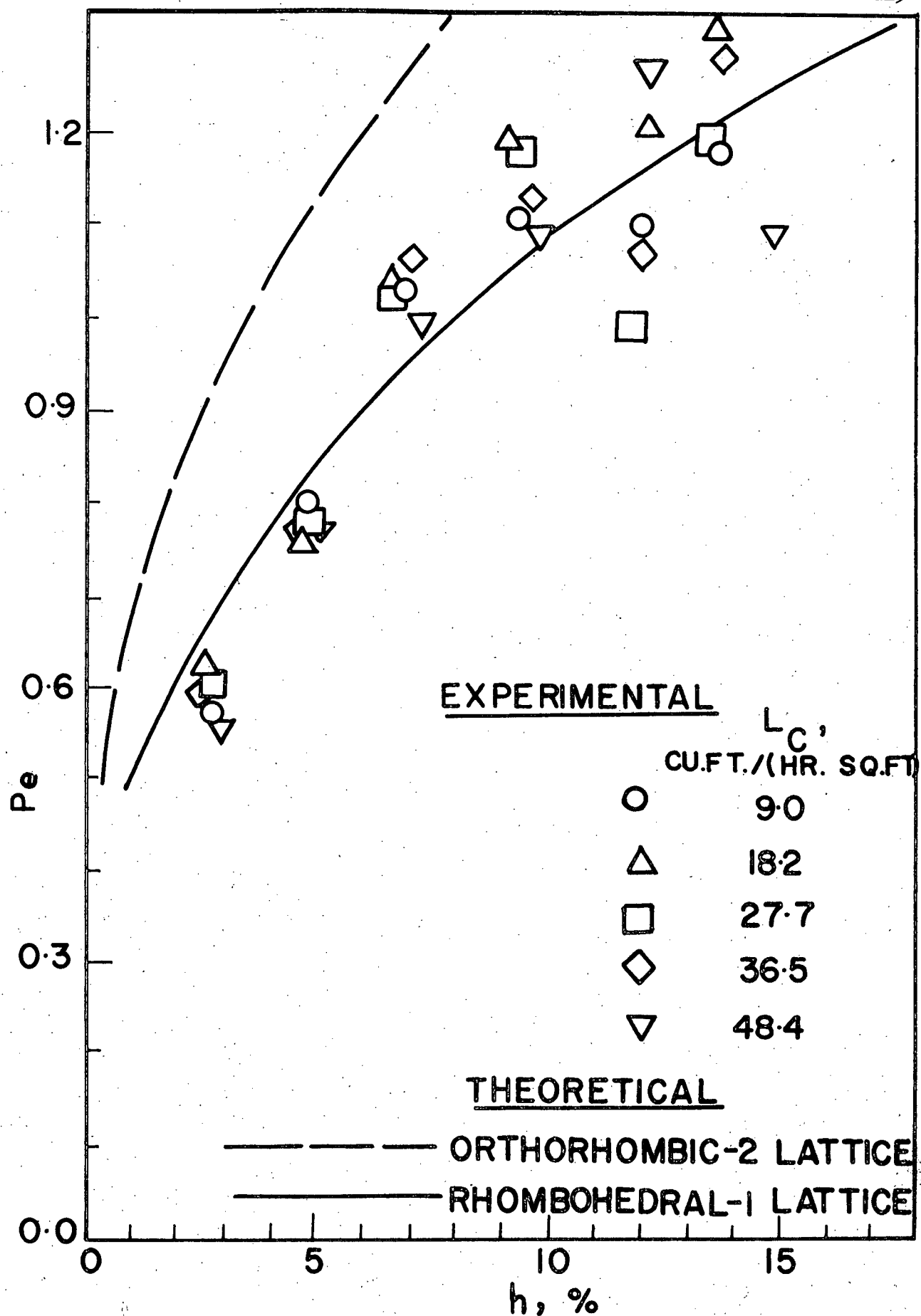
FIGURE 31. PREDICTED AND CALCULATED PECLET NUMBERS, d_p = 0.155-IN.
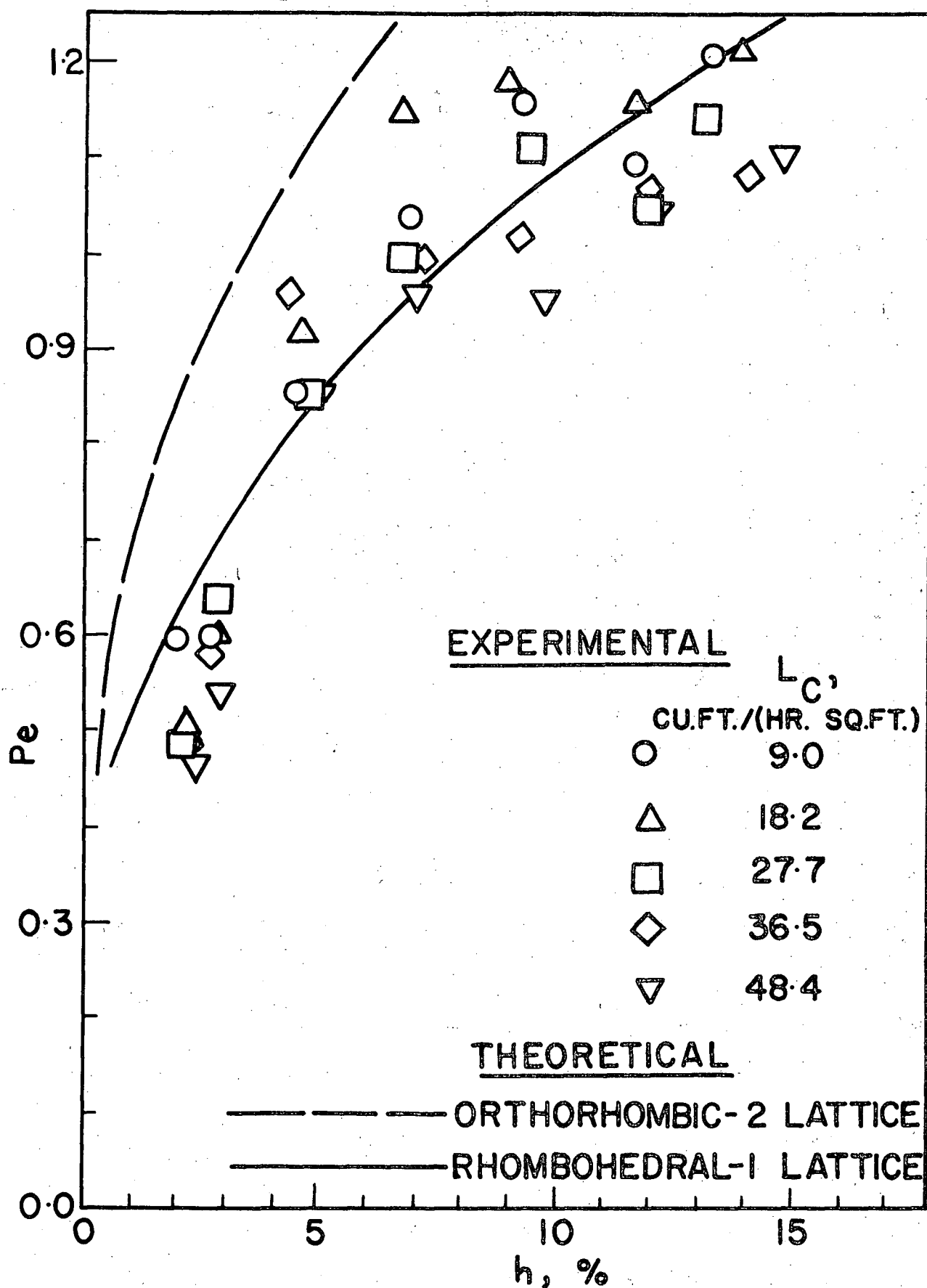
FIGURE 32. PREDICTED AND CALCULATED PECLET NUMBERS, d_p = 0.135-IN.
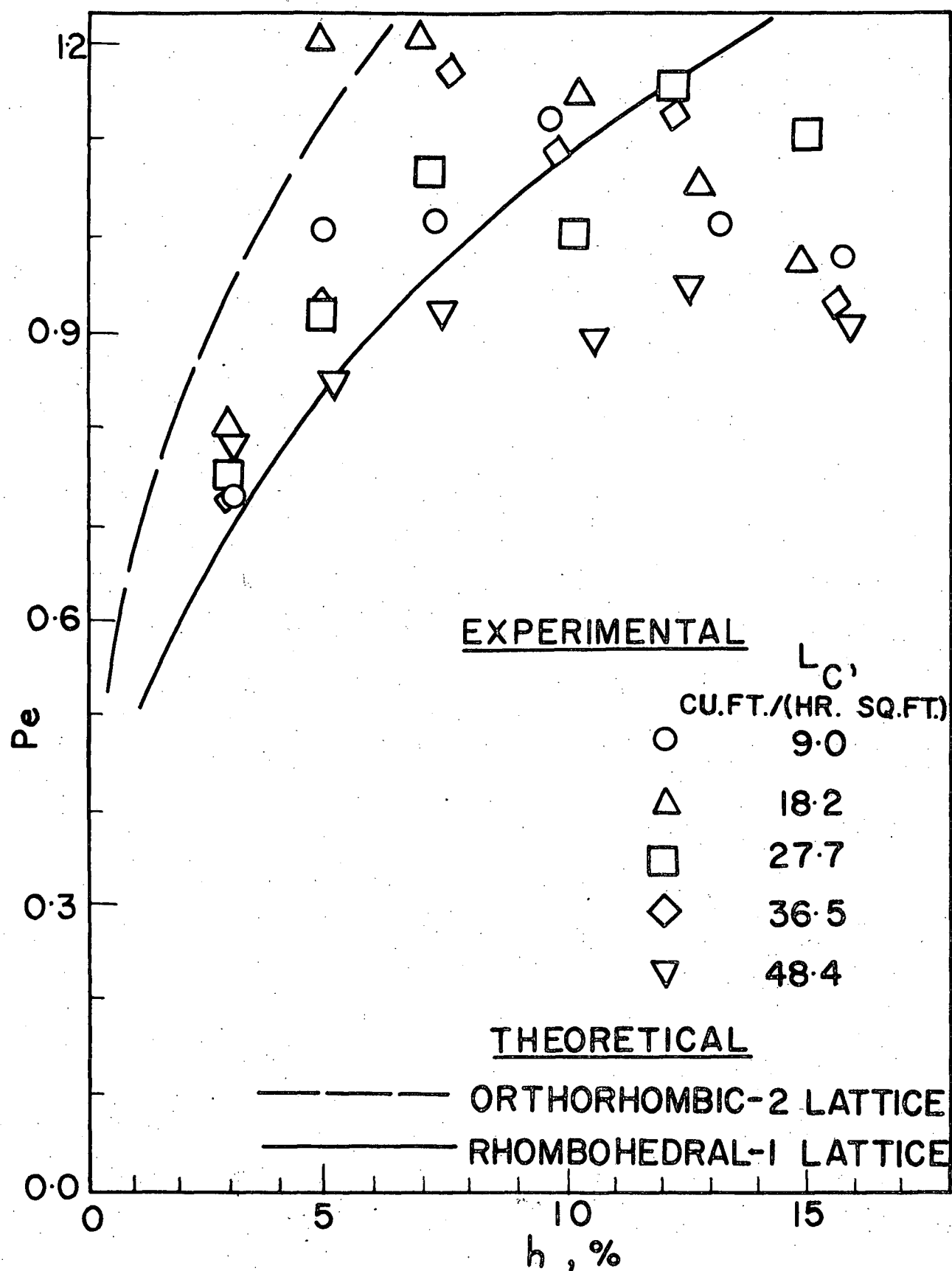
FIGURE 33. PREDICTED AND CALCULATED PECLET NUMBERS, d_p = 0.125-IN.
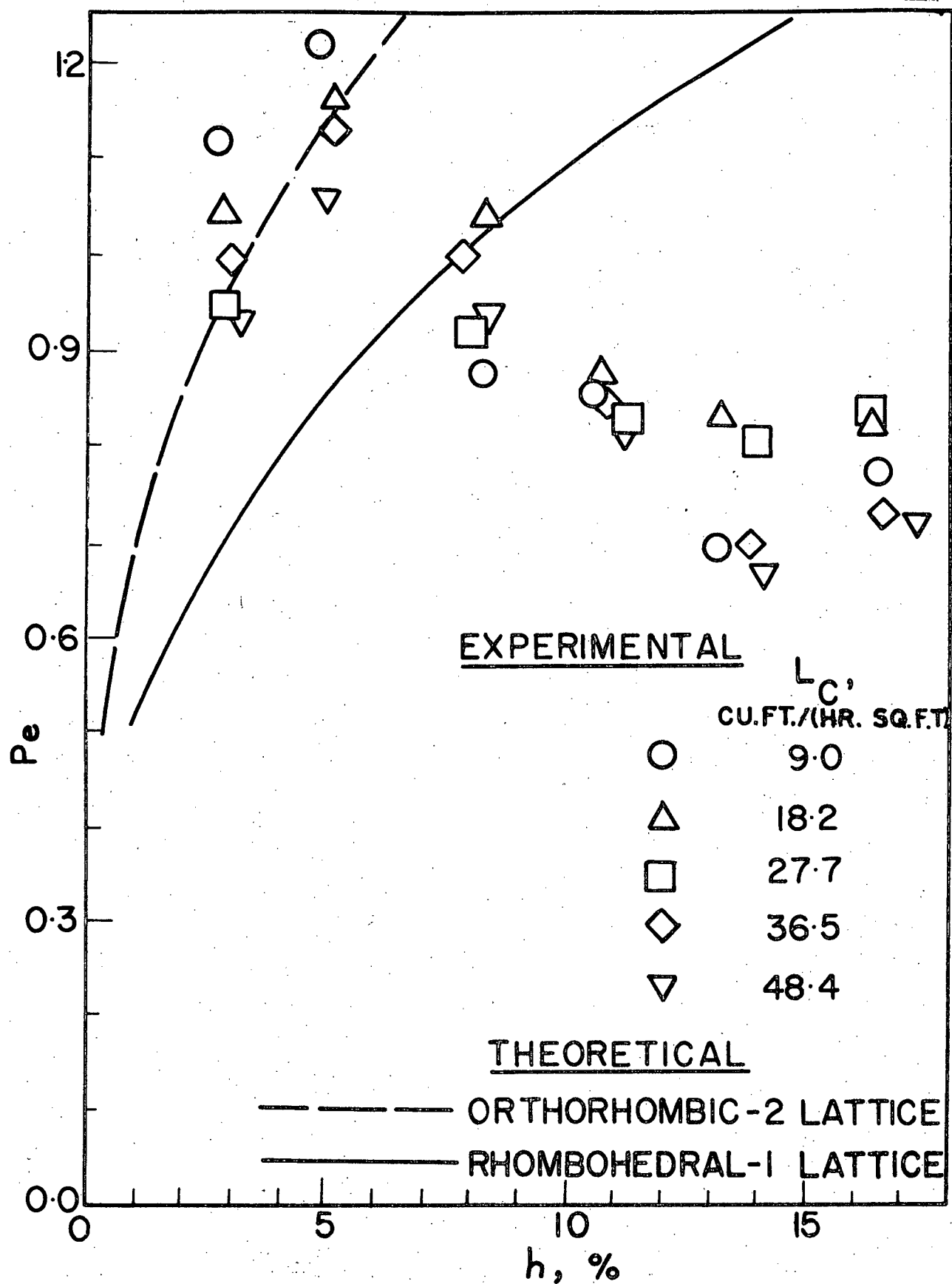
FIGURE 34.   PREDICTED AND CALCULATED PECLET NUMBERS, d_p = 0.095-IN.

as the drop size is reduced. A summary of the comparison is given in the table below. However, only by looking at Figures 31, 32, 33, and 34 can the trend of the experimental points away from the predicted values be seen clearly.

d_p , in.	0.155	0.135	0.125	0.095
Percentage number of experimental points in the predicted Pe range	47	46	53	17
Percentage number of experimental points within 10% of the predicted Pe range	87	63	70	43
Largest percentage difference between the experimental Pe and the nearest side of the predicted Pe range calculated along a line of constant h	20	28	30	45

The drops, of course, do not lie in an ordered lattice arrangement but are positioned in a random fashion relative to one another at any instant in time. However, the above results indicate that the assumption of a simple lattice arrangement of drops is of some limited use in applying the mixing cell - packed bed analogy in order to make a first estimate of the Peclet number.

The mixing cell - packed analogy predicts a decrease in E with a decrease in d_p at constant h and it predicts a decrease in E with an increase in h at constant d_p. The experimental results shown in Figure 29 bear out these predictions qualitatively.

ii) Calibration for optical distortion and drop size measurements.

Figure 23 presented earlier shows the positions of the 5/32-in. ball bearing placed in the column when the optical distortion was being measured. The camera, of course, viewed the column in elevation from the front. With the camera lens used the depth of focus was such that all the drops in the column were in focus. Distortions were small in almost all cases, and changed only slightly in most cases when the ball was moved from one position to another. Hence it seemed reasonable to divide the cross-section of the column into regions in each of which the optical distortion was taken to be constant. The boundaries between regions are shown in Figure 35. These boundaries were placed equidistant from adjacent positions occupied by the ball during the taking of the photographs for calibration for optical distortion. The optical distortion of the ball was found to be independent of the height of the ball in the photographic test section of the column and also independent of the concentration of tracer in the column. By considering only the drops which were located in the central portions of the photographs it was possible to avoid making distortion corrections, since the corrections applicable to such drops were only $\pm$ 1%. Accordingly only drops in the region shown as "drop size measurement field" in Figure 35 were measured for calculating drop size distributions.

The part of the column shown in Figure 35 which was used for drop size measurements contained the whole of the central
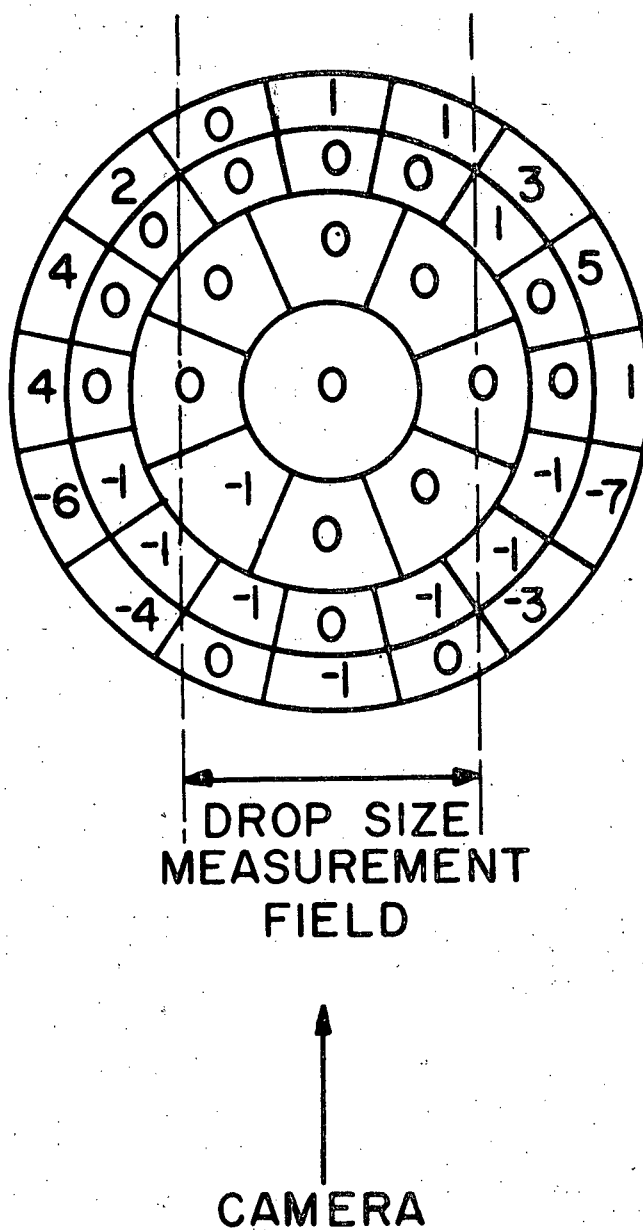
FIGURE 35. PERCENTAGE ERROR IN THE EQUIVALENT DIAMETER DUE TO OPTICAL DISTORTION IN THE 1½-IN. I.D. COLUMN

portion, but not all of the peripheral area of the column cross-section. As a result a disproportionate number of drops appearing in the central portion of the column cross-section, as opposed to those near the column wall, were considered for drop size distribution measurements. If there were any wall effect on drop size distributions it was not taken into account.

With no liquid in the photographic test section of the column the ball was positioned at the centre of this test section. The glass column and Perspex box were removed without disturbing the ball. A photograph of the ball in air then was taken in the usual way. The diameter of the projected image of the ball in this photograph was measured. The enlargement factor for calculating the apparent dimensions of the ball during calibration studies and of drops during drop size distribution measurements was determined by dividing the measured diameter of the projected image of the ball photographed in air by the actual diameter of the ball.

The vertical and horizontal dimensions of the images of 500 drops were measured for each run in which drop size distributions were determined. Each drop was assumed to be an oblate spheroid. This assumption has been found to be reasonably good for drops issuing from the 0.103-in. I.D. nozzle tips (39). The measured drop dimensions were corrected for optical magnification, but no correction for optical distortion was applied. The equivalent drop diameter, d_s, was calculated for each drop by

means of the following equation

$$d_s^3 = h_d p_d^2$$

where

h_d = the vertical dimension of the drop image,

and

p_d = the horizontal dimension of the drop image.

Out of 13,000 drops measured only one drop was found to have an equivalent drop diameter of greater than 0.25-in. This drop was not considered to be typical and was not considered in drop size distribution calculations.

The range of d_s from 0.00-in. to 0.25-in. was divided up into increments of 0.01-in. An IBM - 7040 electronic computer was used to calculate the percentage of the total number of drops, and the percentage of total drop volume found in each of these increments. These calculations were performed for the first 100 drops measured, the first 200 drops measured, the first 300, the first 400, and the first 500 drops measured in each set of data. It was found that the calculated drop size distributions for 400 and 500 drops respectively were almost the same for each of the sets of data. Evidently a sample size of 500 drops is sufficiently large to be representative of the whole population of drops in the column. Accordingly all subsequent discussion involving drop size is based on a total of 500 drops for each set of data. A typical set of results for the drop size distrib-

ution calculations is given in Table IV-6 and plotted in Figure 36.

A summary of all of the results is presented in Table IV-7. In

each case there was a peak between 0.01-in. and 0.03-in. in the

equivalent diameter on the drop size distribution plots. In

addition a second peak appeared at a higher drop diameter. The

mean of the two limits of the equivalent drop diameter range,

of width 0.01-in., in which the second peak occured was taken

to be the drop diameter, d_p, used in the Peclet number calcul-

ations. For example, from Figure 36 the drop diameter of 0.135-

in. was used to calculate Pe for Run 50. Rocchini (39) took

close-up photographs of a $1\frac{1}{2}$-in. I.D. spray column using the

0.103-in. I.D. nozzle tips and with the transfer of acetic acid

from the continuous phase to the dispersed phase. His photographic

conditions resulted in a very short depth of focus in which

drops were examined. Rocchini did not use any means for reducing

optical distortion but he corrected the drop size measurements

for optical distortion by means of a calibration graph. The

drop size distributions which he presents (39) have peaks at

exactly the same equivalent drop diameter as shown in Figure 36.

In the present work the second peak was very high and narrow for

drops produced from the 0.053-in. I.D. nozzle tips and very

low and broad for the 0.126-in. I.D. tips. Obviously the pro-

duction of irregularly sized drops at the nozzle tips would

result in a broad peak. However, it is felt that the main reason

for the change in the shape of the peaks is the invalidity of the

assumption that the larger drops are of oblate spheroid shape.
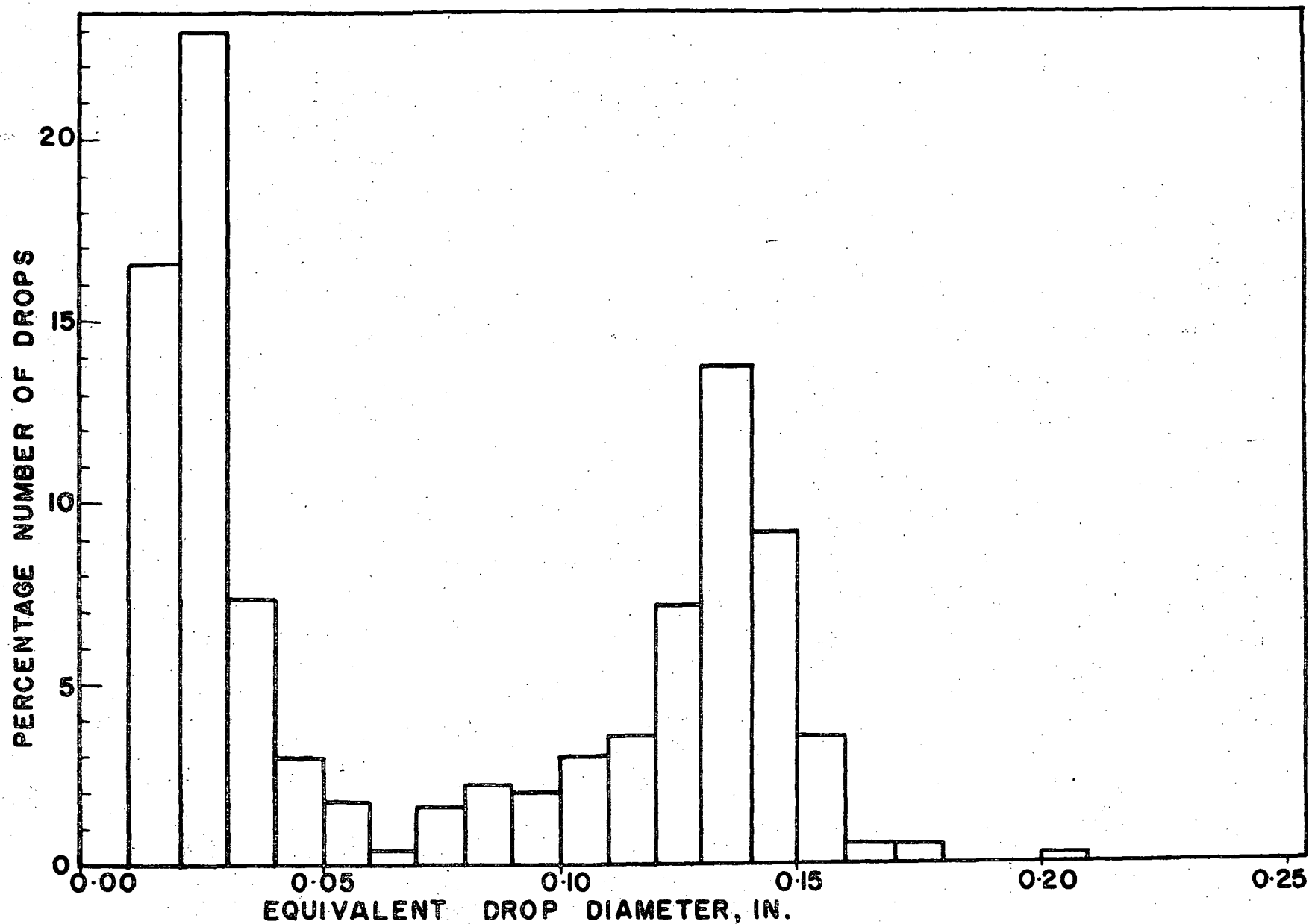
FIGURE 36.   DROP SIZE DISTRIBUTION FOR RUN 50, AVERAGE NOZZLE TIP DIAMETER = 0.103-IN.

Typical photographs of drops produced in the $1\frac{1}{2}$-in. I.D. column by the four different sizes of nozzle tips are shown in Figure 37. From photographs such as these it can be seen that larger drops are more irregular in shape than smaller drops. Typical drop size distribution histograms for the 0.103-in. I.D. and the 0.126-in. I.D. nozzle tips are presented in Figures 36 and 38 respectively.

For each of the three smallest nozzle tip diameters the second peak in the drop size distribution plot was not influenced by run conditions. In the case of the nozzle tips of average I.D. 0.126-in. the location of the peak was influenced slightly by run conditions. The drop diameter, d_p, for these nozzle tips was taken as 0.155-in. Garwin and Smith (43) report that the drop size is independent of the continuous phase flowrate. This conclusion is consistent with the above observations. Figure 39 is a typical example of plots made to show the percent of total drop volume versus equivalent drop diameter. There was no noticeable peak for the very small drops in this sort of plot since the contribution of these to the total volume was negligible.

iii) Hold-up studies.

Plots are given in Figures 40, 41, 42, and 43 for the dispersed phase hold-up (measured by means of the piston) versus the dispersed phase superficial velocity for each of the four nozzle tip sizes studied. Weaver, Lapidus, and Elgin (41)
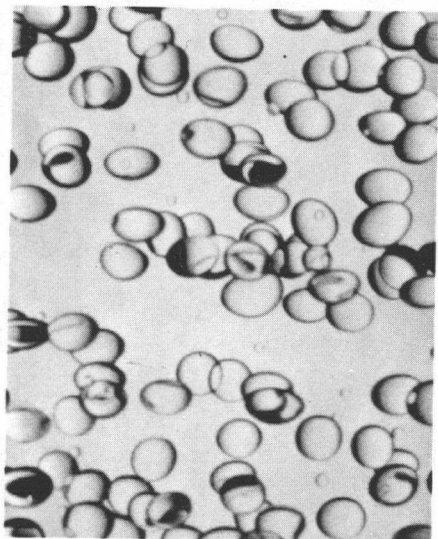
AVERAGE NOZZLE TIP DIA.
= 0.053-IN.
(RUN 148)
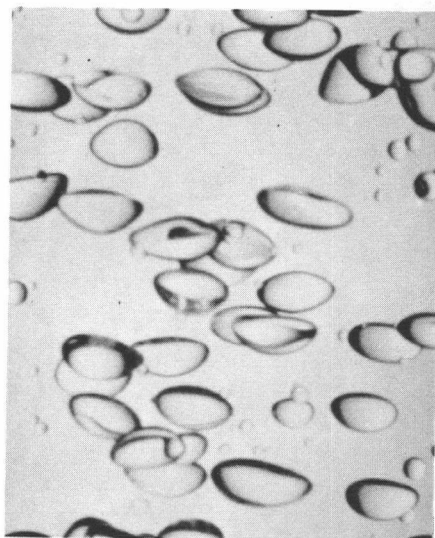
AVERAGE NOZZLE TIP DIA.
= 0.086-IN.
(RUN 96)
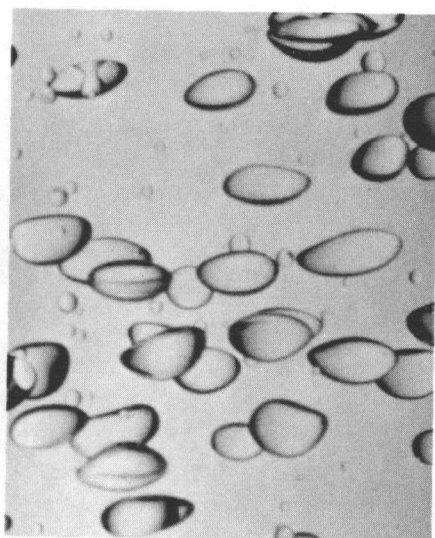
AVERAGE NOZZLE TIP DIA.
= 0.103-IN.
(RUN 65)
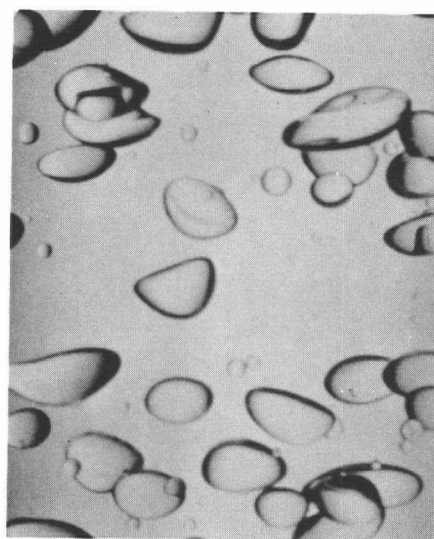
AVERAGE NOZZLE TIP DIA.
= 0.126-IN.
(RUN 126)

FIGURE 37. PHOTOGRAPHS OF DROPS AT OPERATING CONDITIONS CORRESPONDING TO RUNS INDICATED. MAGNIFICATION FACTOR = 3.
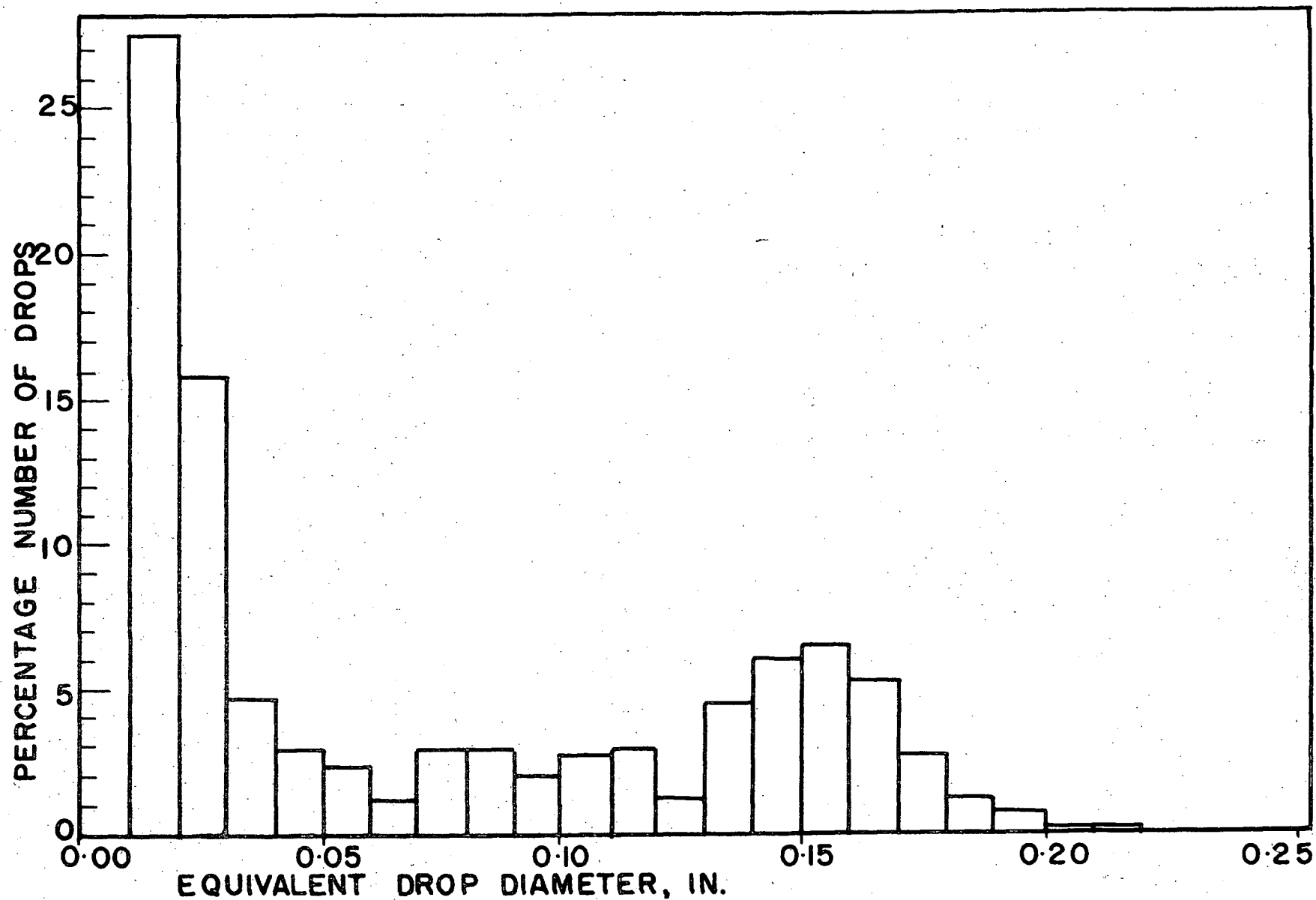
FIGURE 38. DROP SIZE DISTRIBUTION FOR RUN 130, AVERAGE NOZZLE TIP DIAMETER = 0.126-IN.
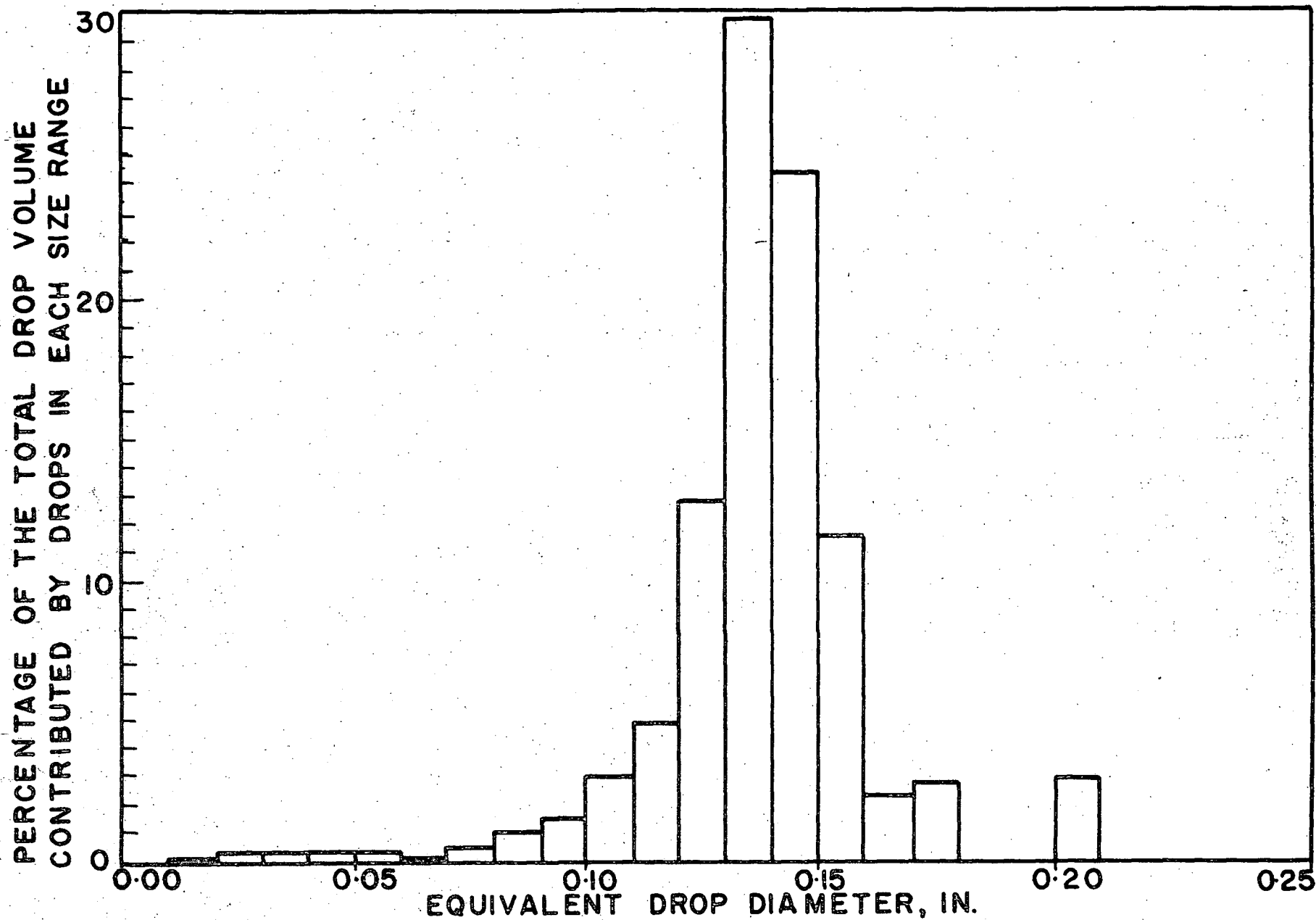
FIGURE 39.   DISTRIBUTION OF TOTAL PERCENT OF VOLUME OF DROPS FOR RUN 50, AVERAGE NOZZLE TIP DIAMETER = 0.103-IN.
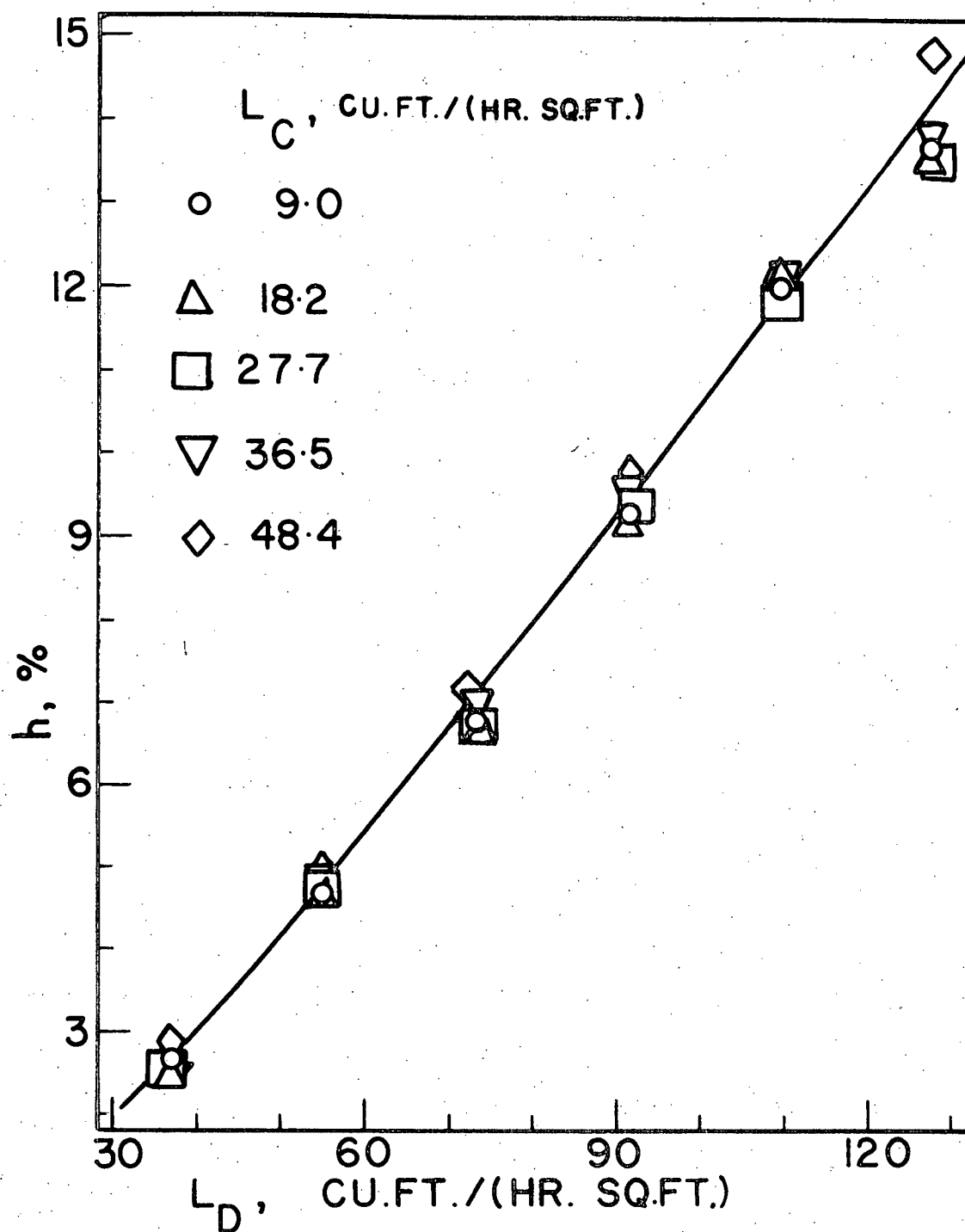
FIGURE 40. DISPERSED PHASE HOLD-UP, d_p = 0.155-IN.
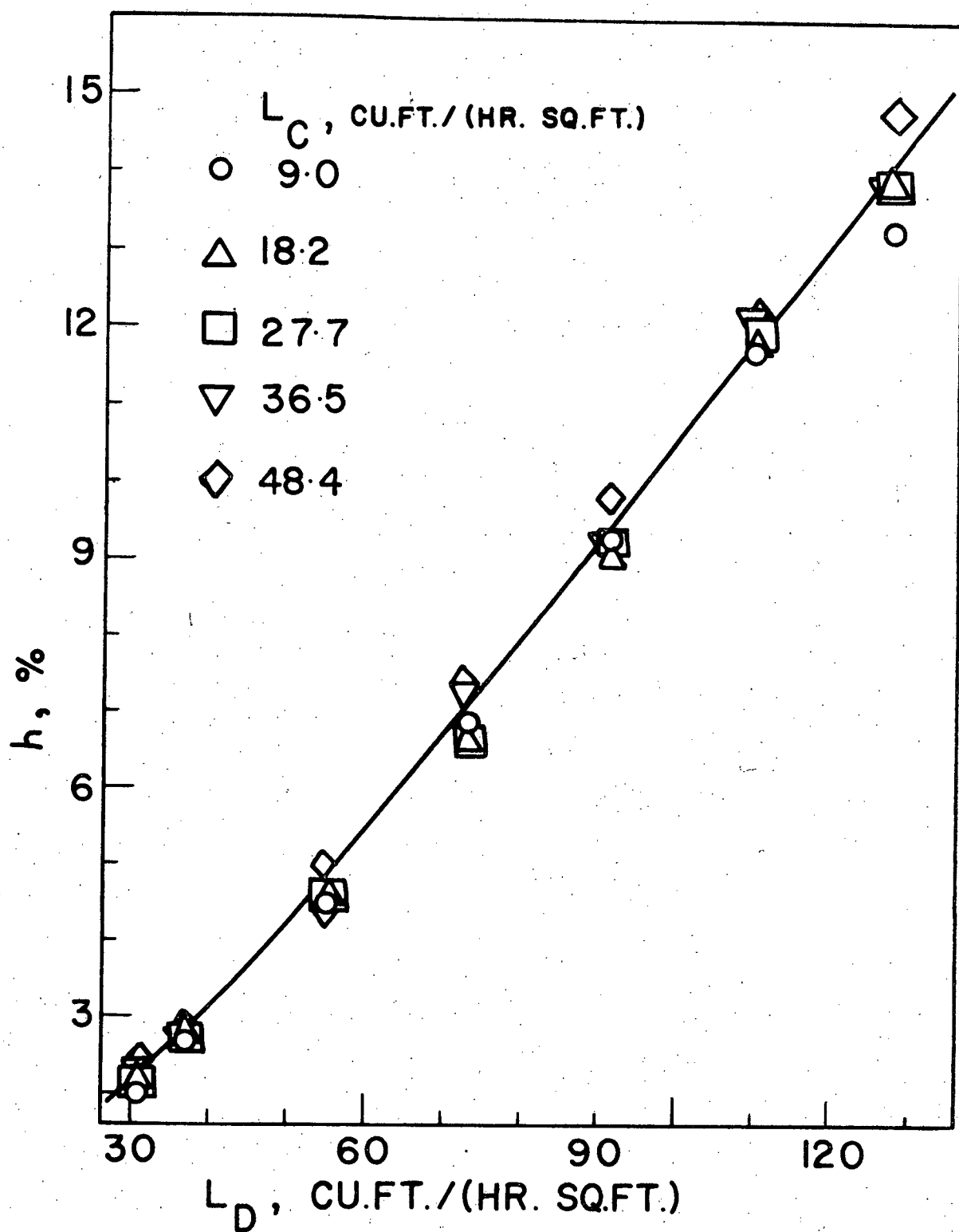
FIGURE 41. DISPERSED PHASE HOLD-UP, d_p = 0.135-IN.
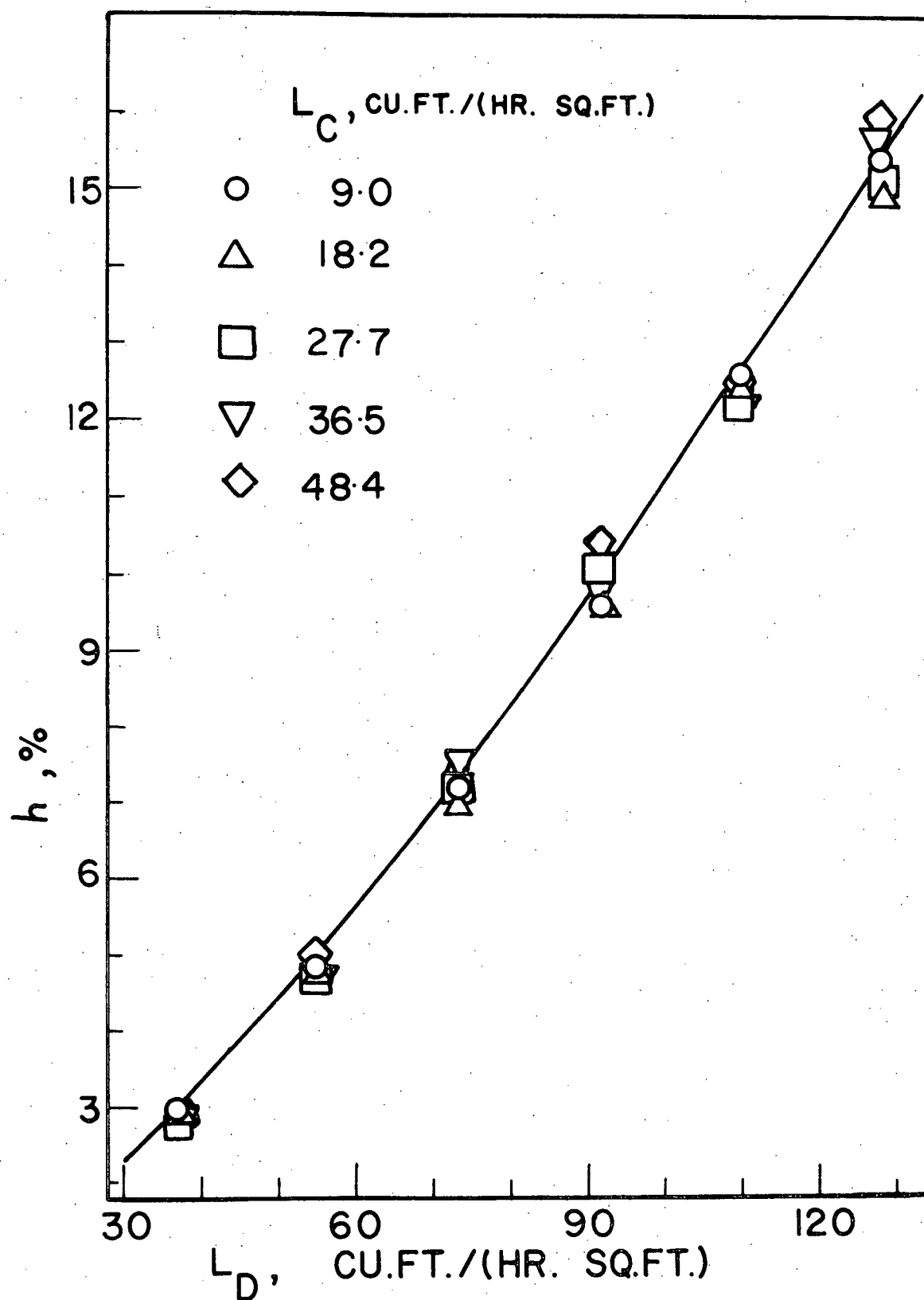
FIGURE 42.   DISPERSED PHASE HOLD-UP, d_p = 0.125-IN.
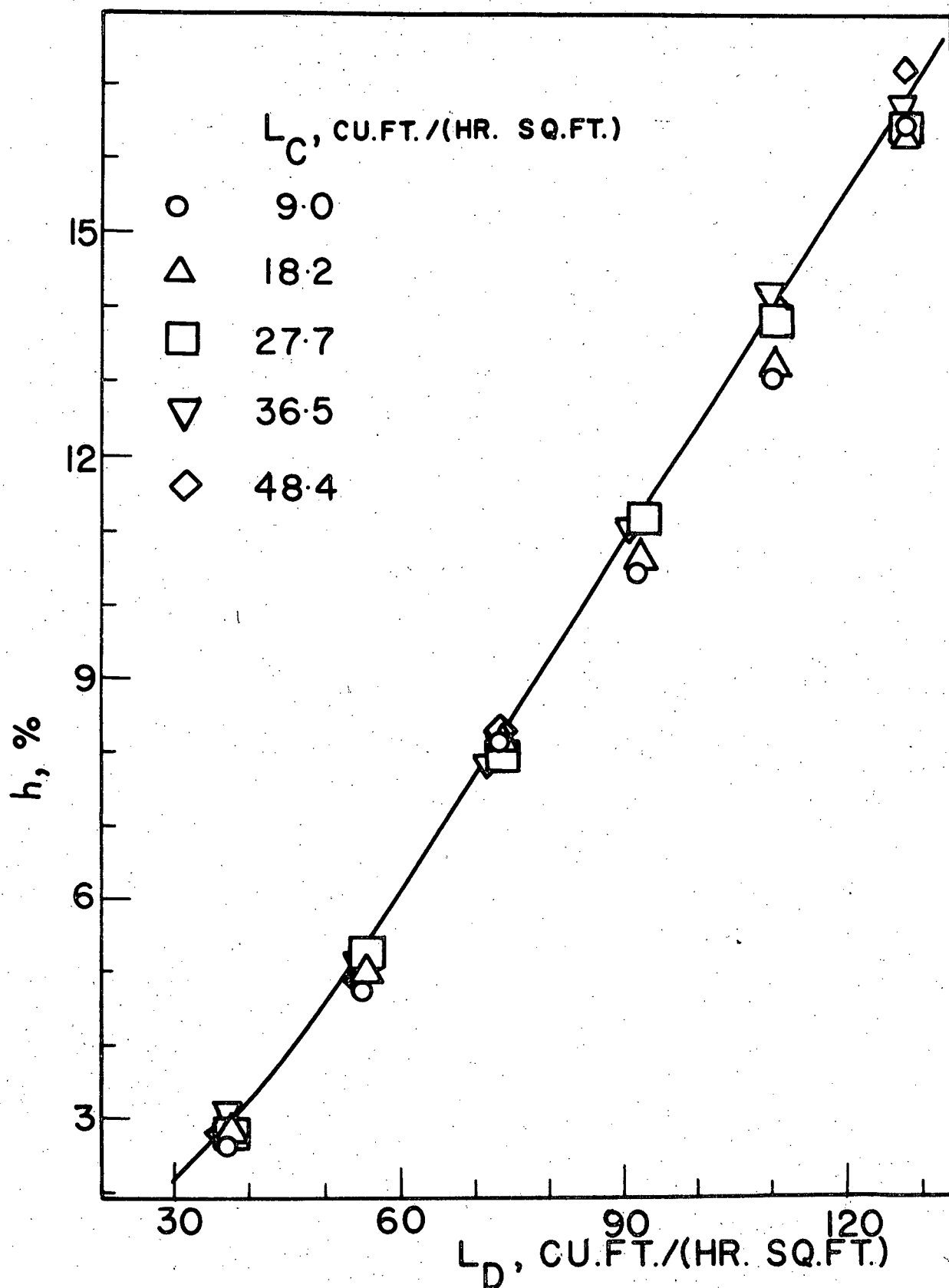
FIGURE 43. DISPERSED PHASE HOLD-UP, d_p = 0.095-IN.

extended the theory relating slip velocity and hold-up in fluidized

beds to spray column operation. They show that the slip velocity

is expected to decrease with increasing hold-up. As a result a

plot of hold-up versus dispersed phase superficial velocity, L_D,

is expected to be curved, concave upwards. Figures 40, 41, 42,

and 43 bear out this prediction for values of L_D less than

60-ft.^{3}/hr. ft.^{2} However, no explanation could be found for the

linearity of the hold-up curves for values of L_D greater than

60-ft.^{3}/hr. ft.^{2} The velocity, u, of rise of the dispersed phase

drops was of the order of 1000-ft./hr. and experiments were

carried out for continuous phase superficial velocities, L_C,

between 9-ft.^{3}/hr. ft.^{2} and 48.4-ft.^{3}/hr. ft.^{2} Increasing L_C

within this narrow range would be expected to result in only

a small decrease in u and therefore only a slight increase in

the hold-up. Although Figures 40, 41, 42, and 43 show no

regular dependence of the hold-up on L_C there is a slight

tendency for the hold-up to be somewhat higher at higher

continuous phase flowrates. For a given dispersed phase

flowrate decreasing the drop size should result in an in-

creased hold-up since usually smaller drops have a smaller

terminal velocity. However, no effect of this sort was noticed

in going from a drop diameter, d_p, of 0.155-in. to one of

0.135-in. as can be seen by comparing Figures 40 and 41. The

reason for this might be that drops of about 0.155-in.

equivalent diameter are so large that they are much distorted

from the oblate spheroid shape. The distortion usually results in

a large frontal area of each drop (114) which in turn increases the drag and lowers the terminal velocity. Comparison of Figures 41, 42, and 43, however, shows an increase in the hold-up as the drop size is decreased.

b) Results of the preliminary experiments.

The sampling positions 1 to 10 inclusive mentioned below are shown in the abscissa of Figure 28.

i) Time to reach steady-state.

The solute concentrations in samples taken by means of the first, fourth, seventh, and tenth hypodermic needles, shown in Figure 9, above the tracer distributor, and in the aqueous phase leaving the column were plotted versus time after start-up. Table 6 shows the time to reach steady-state at the last sampling position to do so.

TABLE 6. TIME TO REACH STEADY-STATE IN THE $1\frac{1}{2}$-IN. I.D. COLUMN UNDER CONDITIONS OF NO MASS TRANSFER.

Run	32	33	34
L_C, ft.^{3}/hr. ft.^{2}	9.0	9.0	27.7
L_D, ft.^{3}/hr. ft.^{2}	128	30.4	30.4
time to reach steady-state, min.	100	115	45
Temperature, $^\circ$F	71	68	69

Table 6 shows that the time to reach steady state varies little when L_D is varied over a wide range. Hence the effect of L_D on

the time to reach steady state was not taken into account. Table 6 also shows that the time to reach steady state decreases rapidly with an increase in L_C. Consideration of Table 6 suggested that 1-hr. would be a conservative estimate of the time required to reach steady state when L_C was greater than 30-ft.^{3}/hr. ft.^{2} and that 2-hr. would be a conservative estimate of this time for values of L_C between 9-ft.^{3}/hr. ft.^{2} and 30-ft.^{3}/hr. ft.^{2} These steady state times for various values of L_C were adopted for all the studies involving tracer in the 1½-in. column.

ii) Effect of tracer feed rate.

Table 7 shows the results of tests performed to investigate any effects of tracer feed rate on the reduced concentration profiles or on the axial eddy diffusivity values.

TABLE 7. EFFECT OF TRACER FEED RATE ON REDUCED CONCENTRATION PROFILES AND AXIAL EDDY DIFFUSIVITY IN THE 1½-IN. I.D. COLUMN.

Run	L_C, ft.^{3}/ hr. ft.^{2}	L_D, ft.^{3}/ hr. ft.^{2}	L_T, ft.^{3}/ hr. ft.^{2}	Reduced concentration at sampling positions										E. ft.^{2}/ hr.	Temp. °F
				1	2	3	4	5	6	7	8	9	10		
35	27.7	30.4	0.16	599	411	271	162	98	67	42	32	19	12	32.5	69
40	27.7	30.4	0.31	557	380	246	152	94	60	40	27	18	11	32.6	70
36	27.7	30.4	0.62	621	389	251	160	104	66	42	29	20	12	32.8	71
67	18.2	73	0.10	350	157	50	24	8	2.8	1.3	-	-	-	10.3	72
57	18.2	73	0.20	433	166	76	35	11	5	2.1	0.85	0.35	-	11.0	74
68	18.2	73	0.40	307	142	48	18	8	3.3	1.4	0.51	0.20	-	10.7	73

The reduced concentration at a given sampling point varies considerably for various tracer feed rates in many cases.

However, the resulting overall concentration profile and axial

eddy diffusivity are not affected appreciably by tracer-feed

rate. It is concluded that the effect of tracer feed rate on

the value of the axial eddy diffusivity is negligible for

tracer flowrates of less than 2% of the continuous phase

superficial velocity.

iii) Reproducibility of results.

Three runs were duplicated to provide a check on reproduci-

bility of results. The reduced concentration profiles and the

calculated values of the axial eddy diffusivity for these

experiments are given in Table 8.

TABLE 8. REPRODUCIBILITY OF RESULTS FOR AXIAL EDDY DIFFUSIVITY
IN THE $1\frac{1}{2}$-IN. I.D. COLUMN.

Run	L_C, ft.^{3}/ hr. ft.^{2}	L_D, ft.^{3}/ hr. ft.^{2}	Reduced concentration at sampling position										E, ft.^{2}/ hr.	Temp. $^\circ$F
			1	2	3	4	5	6	7	8	9	10		
32	9.0	128	575	256	155	79	48	28	14	9	3.8	2.0	8.6	71
47	9.0	128	529	308	157	86	46	28	14	7.8	5.3	2.9	8.9	71
33	9.0	30.4	755	644	566	487	391	330	297	259	223	179	29.3	68
42	9.0	30.4	754	668	571	492	397	252	288	250	221	179	28.7	73
34	27.7	30.4	523	408	257	166	93	58	38	28	19	12	33.0	69
40	27.7	30.4	557	380	246	152	94	60	40	27	18	11	32.6	70

The reproducibility of the calculated value of the axial eddy

diffusivity is good although point reduced concentrations are not

exactly the same in duplicate runs.

iv) Cross-sectional homogeneity.

The dispersion model requires that at any elevation in the

column the concentrations of solute in the continuous phase be

uniform. Accordingly it was necessary to check on whether or not cross-sectional homogeneity existed. Samples were withdrawn at the level of the first hypodermic needle above the tracer distributor (Figure 9) for each of the three runs listed in Table 9. This location was chosen because of all the sampling locations it would be the one most likely to exhibit non-uniformity of solute concentration. Samples were taken in each run at the positions shown in the sketch below:
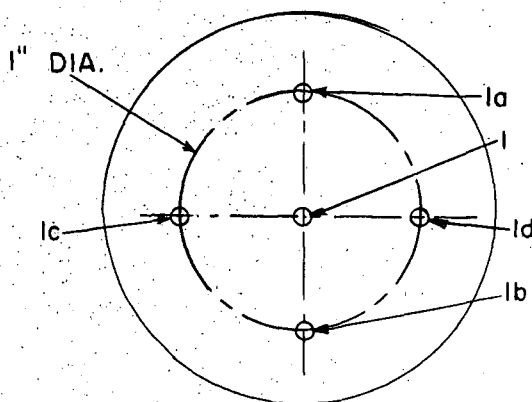
The corresponding reduced concentrations appear in Table 9. Also shown is the reduced concentration at position 1 for a sample taken in each run about 40 minutes before the five samples mentioned above. Although the concentration of solute is not exactly uniform over the cross-section of the column, the variation is not large compared with the variation of concentration with time at the centre of the cross-section. Position 1 was the first sampling position above the tracer distributor. The small variation in concentration over the cross-section at this

TABLE 9.   CROSS-SECTIONAL HOMOGENEITY IN THE $1\frac{1}{2}$-IN. I.D. COLUMN

Run	L_C, ft.^{3}/ hr.ft.^{2}	L_D, ft.^{3}/ hr.ft.^{2}	Reduced concentration at sampling position						Temp. $^\circ$F
			la	lb	l	lc	ld	l, sample taken earlier	
32	9.0	127.7	578	575	568	577	573	575	71
33	9.0	30.4	754	723	745	751	755	755	68
34	27.7	30.4	532	525	526	537	519	523	69

sampling elevation indicates that tracer leaving the distributor spreads over the cross-section in a small incremental column height. Hawrelak (37) studied a $1\frac{1}{2}$-in. I.D. spray column with the transfer of acetic acid from the continuous phase to the dispersed phase. He took samples from various positions at a given cross-section by means of hypodermic needles and found no radial concentration gradients.

v) Sampling rate.

Table 10 shows the reduced concentrations of solute in samples taken from the first four sampling positions above the tracer distributor at various sampling rates. Sampling rates of 1.0-ml./min. for superficial velocities of continuous phase greater than 27.7 ft.^{3}/hr. ft.^{2} and of 0.75 ml./min. for superficial velocities of continuous phase between 9.0-ft.^{3}/hr. ft.^{2} and 27.7-ft.^{3}/hr. ft.^{2} appear to be small enough so as not to disturb the operation of the column. Accordingly these sampling rates were used for all

TABLE 10. EFFECT OF SAMPLING RATE ON THE REDUCED CONCENTRATION PROFILE IN
THE $1\frac{1}{2}$-IN. I.D. COLUMN

Run	L_C $ft.^3/hr.ft.^2$	L_D $ft.^3/hr.ft.^2$	Reduced concentration at sampling position												Temp. $^\circ$F
			Sampling rate = 0.5 ml./min.				Sampling rate = 1.0 ml./min.				Sampling rate = 2.0 ml./min.				
			Position 1	Position 2	Position 3	Position 4	Position 1	Position 2	Position 3	Position 4	Position 1	Position 2	Position 3	Position 4	
34	27.7	30.4	523	388	255	158	523	408	257	166	522	387	254	155	69

Run	L_C $ft.^3/hr.ft.^2$	L_D $ft.^3/hr.ft.^2$	Reduced concentration at sampling position												Temp. $^\circ$F
			Sampling rate = 0.25 ml./min.				Sampling rate = 0.75 ml./min.				Sampling rate = 1.5 ml./min.				
			Position 1	Position 2	Position 3	Position 4	Position 1	Position 2	Position 3	Position 4	Position 1	Position 2	Position 3	Position 4	
33	9.0	30.4	749	642	566	485	755	644	566	487	751	644	568	488	68
32	9.0	128	575	257	155	80	575	256	155	79	573	255	155	79	71

of the tracer studies in the 1½-in. I.D. column.

vi) Order of sampling.

The usual order of sampling was to take a sample by means
of the first hypodermic needle above the tracer distributor,
then by means of the next higher needle, and so on. (See
Figures 9 and 10 for sampling positions.) For three runs samples
were taken in the reverse order, that is starting with the
highest hypodermic needle. As well in these same runs samples
were taken in the usual order. The results are given in Table 11.

It is evident from Table 11 that the order in which samples
are taken does not affect the measured concentration profile.

vii) Effect of column height.

For one set of column operating conditions three experiments
were performed with three different lengths of column. (See
Figures 10, 11, and 12.) Table 12 shows the reduced concentration
profile of solute in the test section and the calculated value of
the axial eddy diffusivity for each run.

The length of the column appears to have no significant
effect upon the axial eddy diffusivity.

TABLE 11. EFFECT OF THE ORDER OF SAMPLING ON THE MEASURED CONCENTRATION
PROFILE IN THE 1½-IN. I.D. COLUMN

Run	L_C ft³/hr.ft²	L_D ft³/hr.ft²	Order of sampling	Reduced concentration at sampling position										Temp. °F
				1	2	3	4	5	6	7	8	9	10	
33	9.0	30.4	usual (1 to 10)	755	644	566	487	391	330	297	259	223	179	68
			reverse (10 to 1)	747	642	564	485	389	327	297	258	215	178	
32	9.0	128	usual (1 to 10)	574	256	155	79	48	28	14	9.0	3.8	2.0	71
			reverse (10 to 1)	572	253	155	79	48	28	14	8.9	3.8	2.0	
34	27.7	30.4	usual (1 to 10)	523	408	257	166	93	58	38	28	19	12	69
			reverse (10 to 1)	526	374	254	153	97	61	40	27	18	11	

TABLE 12. EFFECT OF COLUMN HEIGHT ON THE MEASURED CONCENTRATION PROFILE
AND AXIAL EDDY DIFFUSIVITY IN THE 1½-IN. I.D. COLUMN

Run	Column length (nozzle tips to interface)	L_C ft³/hr.ft²	L_D ft³/hr.ft²	Reduced concentration at sampling positions										E ft²/hr.	Temp. °F
				1	2	3	4	5	6	7	8	9	10		
174	6-ft. 3 1/8-in.	18.2	54.7	426	286	136	81	39	20	9.9	5.7	3.0	1.4	14.9	68
51	10-ft. 3½-in.	18.2	54.7	561	298	138	83	37	18	11	5.8	2.7	1.5	14.5	71
175	16-ft. 4½-in.	18.2	54.7	562	299	146	73	45	23	9.9	5.2	2.7	1.5	14.5	68

4. AXIAL EDDY DIFFUSIVITY AND DROP SIZE DISTRIBUTION STUDIES
    IN THE 3-IN. I.D. COLUMN.

The results of the preliminary experiments concerning steady-state time, reproducibility of results, and cross-sectional homogeneity are discussed after those of the main experiments.

a) Main Experiments.

The value of the superficial axial eddy diffusivity, Ee, for each run was calculated in a manner similar to that already described for the $1\frac{1}{2}$-in. I.D. column. A summary of the results for the 3-in. I.D. column is given in Table IV-5. Figure 44 shows the superficial axial eddy diffusivity plotted against dispersed phase superficial velocity. The curve shown in this figure was drawn through the points by eye. As with the $1\frac{1}{2}$-in. I.D. column, the superficial axial eddy diffusivity decreases with increasing dispersed phase flowrate. However, there appears to be some tendency for higher superficial axial eddy diffusivity values for the 3-in. I.D. column to be associated with higher superficial velocities of the continuous phase. Comparison of the superficial axial eddy diffusivity results for the 3-in. I.D. column with those for the $1\frac{1}{2}$-in. I.D. column shows that at a drop size, d_p, of 0.135-in. and for a given superficial velocity of each phase the superficial axial eddy diffusivity in the 3-in. I.D. column was between 6.3 and 17.3 times that in the $1\frac{1}{2}$-in. I.D. column. It was evident that the continuous phase underwent channelling. (See later.) This fact, no doubt, resulted in an increase in axial mixing of the continuous phase in the 3-in. I.D.
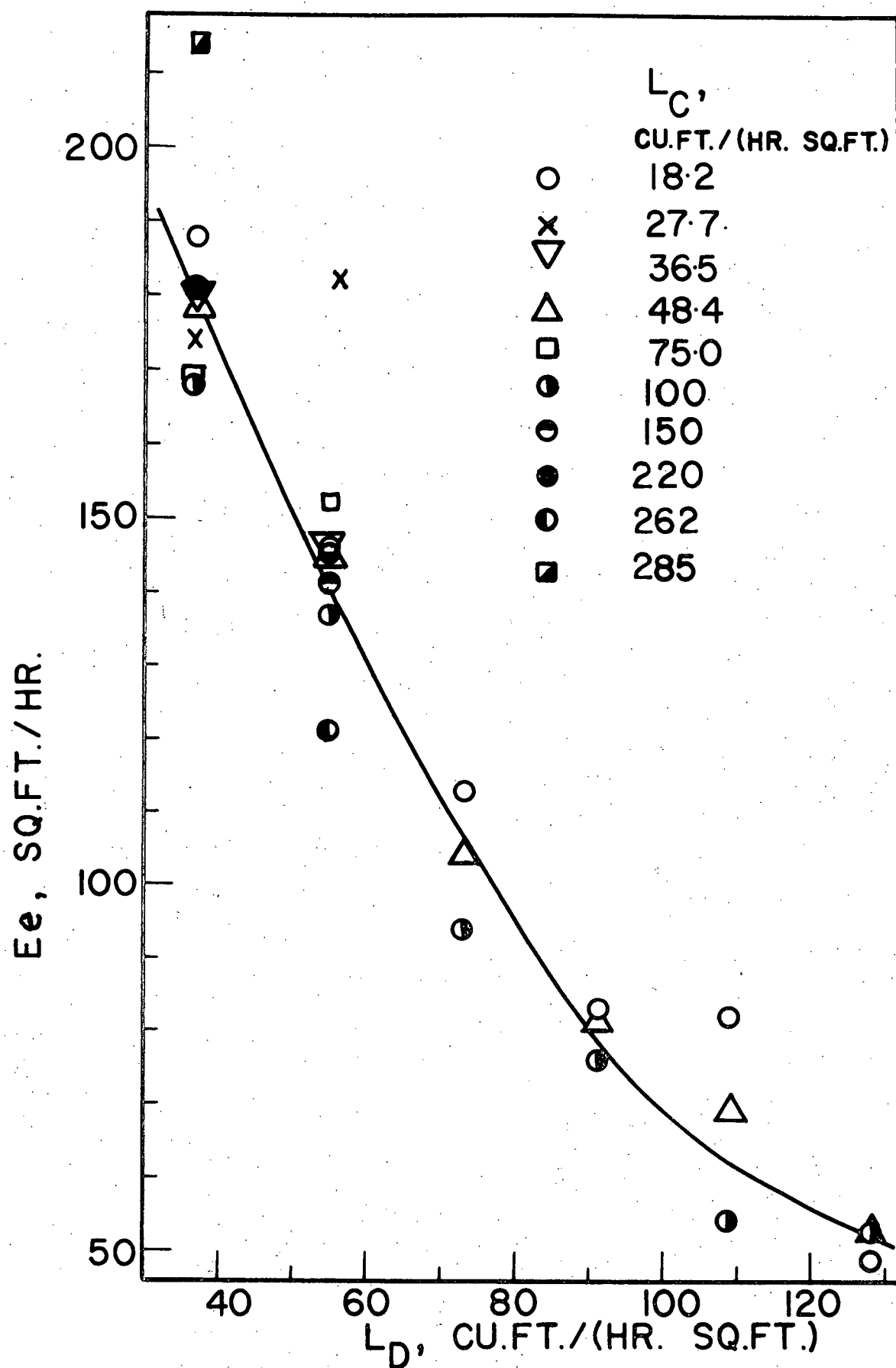
FIGURE 44.   SUPERFICIAL AXIAL EDDY DIFFUSIVITY IN THE 3-IN. I.D. COLUMN

column. Gier and Hougen (28)say that the "... bulk mixing effect would be expected to be most serious in spray columns of high diameter to height ratio." However, the results of the experiments described in this thesis show that the diameter, but not the height, of the column is important in assessing the extent of the axial mixing of the continuous phase. Actual eddy diffusivities were not calculated from the superficial axial eddy diffusivities because the dispersed phase hold-up, h, was not measured in the 3-in. I.D. column. Previous workers (3, 6, 30, 31, 43) have estimated the hold-up, h, by means of Equation 7.

$$h = \frac{100 \, L_D}{u}$$ 7

However, in the present work it was not possible to measure the velocity of rise of the dispersed phase drops with any accuracy due to the swirling motion of the drops (described later). As a result Equation 7 could not be used to estimate the hold-up, h.

The percentage error in the equivalent diameter of drops due to optical distortion was determined in a manner similar to that used for the $1\frac{1}{2}$-in. I.D. column. The optical distortion was independent of the vertical position of the ball and of the concentration of tracer in the column. Figure 45 shows this percentage error at various positions in the cross-section of the column. Also shown in Figure 45 is the portion of the cross-section in which drop size measurements were made. Just as for the $1\frac{1}{2}$-in. I.D. column restricting the drop size measurements to the field shown in this figure made it unnecessary to apply any correction for optical distortion. A summary of the drop

FIGURE 45. PERCENTAGE ERROR IN THE EQUIVALENT DIAMETER DUE TO OPTICAL DISTORTION IN THE 3-IN. I.D. COLUMN

size distributions measured appears in Table IV-8. The second

peak in each drop size distribution plot appeared between 0.13-in.

and 0.14-in. equivalent drop diameter.

b) Preliminary Experiments.

i) Steady-state time.

The concentration of tracer in samples taken by means of

the first, third, seventh, and tenth hypodermic needles above the

tracer distributor (Figures 20 and 21) and in the aqueous phase

leaving the column were plotted versus time after start-up. Table 13

shows the time to reach steady-state at the last sampling position

to do so.

TABLE 13. STEADY-STATE TIMES FOR THE 3-IN. I.D. COLUMN.

Run	177	180	203
L_C, ft.^{3}/hr. ft.^{2}	18.2	100	18.2
L_D, ft.^{3}/hr. ft.^{2}	36.5	36.5	109
time to reach steady-state, min.	55	25	57
Temperature, $^{\circ}$F	70	70	69

Although the time to reach steady-state varied little for a wide

range of dispersed phase superficial velocities it decreased

markedly for an increase in the superficial velocity of con-

tinuous phase. The time for the column to reach a steady-

state condition was taken to be 1-hr. for continuous phase

superficial velocities of less than 100-ft.^{3}/hr. ft.^{2} and 30-min.

for continuous phase superficial velocities of 100-ft.^{3}/hr. ft.^{2}

and greater.

ii) Reproducibility of results.

The reduced concentration profiles and the superficial axial eddy diffusivities for duplicate runs are presented in Table 14.

TABLE 14. REPRODUCIBILITY OF RESULTS FOR THE 3-IN. I.D. COLUMN

Run	L_C ft³/hr. ft²	L_D ft³/hr. ft²	Reduced concentration at sampling points										E ft²/hr.	Temp. °F
			1	2	3	4	5	6	7	8	9	10		
177	18.2	36.5	933	863	844	811	777	707	680	656	636	593	188	70
186	18.2	36.5	921	888	819	785	761	731	689	656	620	595	190	70
191	48.4	54.7	1080	933	780	701	546	457	395	317	273	257	145	70
207	48.4	54.7	1077	892	731	608	532	444	367	310	249	218	138	69
201	100	109	1118	613	167	101	40	18.8	6.03	1.09	-	-	53.6	67
208	100	109	1131	565	193	109	37	13.7	5.17	2.13	1.14	-	56.5	68

Table 14 shows that, although point concentrations are not exactly reproducible, the reduced concentration profiles and superficial axial eddy diffusivities for duplicate runs are quite similar.

iii) Cross-sectional homogeneity.

The reduced concentrations of solute at the positions shown in the following sketch are given in Table 15 for the levels of

the first and fifth hypodermic needles above the tracer distributor. (See Figures 20 and 21.)

Ia (5a)
Ib (5b)
If (5f)
Ie (5e)
I (5)
1¼" DIA.
Ig (5g)
2½" DIA.
Ih (5h)
Ic (5c)
Id (5d)
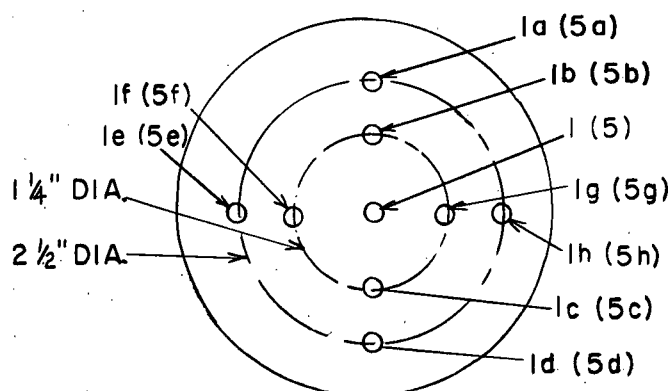
TABLE 15. CROSS-SECTIONAL HOMOGENEITY IN THE 3-IN. I.D. COLUMN

Run	L_C ft.^{3}/ hr.ft.^{2}	L_D ft.^{3}/ hr.ft.^{2}	Reduced concentration at sampling points									Temp. $^\circ$F
			1a	1b	1	1c	1d	1e	1f	1g	1h	
177	18.2	36.5	937	933	937	917	901	939	936	933	919	70
180	100	36.5	838	833	816	784	737	791	811	847	855	70
197	18.2	73	980	988	960	972	968	958	958	966	968	67
195	100	73	1290	1263	1097	947	889	913	1019	1021	1034	68
203	18.2	109	916	911	909	897	893	903	903	907	907	69
201	100	109	1277	1198	1120	990	895	893	920	1008	1034	67

Run	L_C ft.^{3}/ hr.ft.^{2}	L_D ft.^{3}/ hr.ft.^{2}	Reduced concentration at sampling points									Temp. $^\circ$F
			5a	5b	5	5c	5d	5e	5f	5g	5h	
177	18.2	36.5	807	798	733	773	762	776	760	751	742	70
180	100	36.5	230	225	218	206	196	223	225	220	208	70
197	18.2	73	664	682	694	672	724	696	684	698	708	67
195	100	73	194	184	169	151	144	161	163	170	176	68
203	18.2	109	611	599	603	576	553	591	601	609	611	69
201	100	109	41	40	40	39	38	41	41	40	39	67

Table 15 shows that the assumption of radial homogeneity is less

valid for the 3-in. I.D. column than for the 1½-in. I.D. column.

Visual observations of the very small dispersed phase drops during

experimental runs showed that large scale axial swirling motions

occurred in the continuous phase of the 3-in. I.D. column as

mentioned later. However, the plot of the natural logarithm

of the tracer concentration versus column height is straight for

the runs in the 3-in. I.D. column as required by the dispersion

model equation (Equation 13). Therefore a lack of cross-sectional

homogeneity in the 3-in. I.D. column seems not to be too serious

as far as the determination of superficial axial eddy diffusivities

is concerned.

5. VISUAL OBSERVATIONS OF THE MOTION OF THE DROPS

The motion of the drops in the 1½-in. I.D. column was very

erratic but always in an upwardly direction. There was no evidence

of drops ever taking a downward course. The very small drops of

about 0.02-in. diameter moved up the column very slowly. Due to

the small size of these drops their motion would have reflected

any large scale turbulence or channelling in the main bulk of the

continuous phase. However no such effects were observed. These

general flow characteristics were the same for the various flow-

rates of the two phases and for the four different drop size

distributions studied in the 1½-in. I.D. column. Evidently

the drops moved up the column in effective plug flow. Thus the

assumption of no axial eddy diffusion in the dispersed phase
(28, 31, 35) is valid.

In contrast to the observations of the drop motion in the
$1\frac{1}{2}$-in. I.D. column the drop behaviour in the 3-in. I.D. column
was quite different. Not only did the very small drops exhibit
an axial swirling motion but larger drops often took a downward
course for a short distance along the column. Obviously the
continuous phase underwent channelling. As discussed earlier this
phenomenon resulted in radial inhomogeneity of the continuous phase.
Due to the swirling motion of the drops the assumption of no
backmixing of the dispersed phase is invalid.

6. CONCENTRATION PROFILES WITH MASS TRANSFER

Five runs were performed with the transfer of acetic acid
from the continuous aqueous phase to the dispersed ketone phase in
the $1\frac{1}{2}$-in. I.D. column as described under Experimental Procedure.
Samples were taken from within the operating column by means of
the hypodermic needle samplers and also by means of the bell-
probe. The concentration, c_D, of acetic acid in the ketone phase
of each bell-probe sample at the time of sampling was calculated
by means of Equation 6 and the concentration, c_C, of acetic acid
in the hypodermic needle sample at the sampling elevation.

$$c_D = c_D^a + \frac{V_C}{V_D} (c_C^a - c_C)$$

6

For each run the concentration profiles of solute in both phases over the test section were plotted. Smoothed values of the concentrations of solute in each phase at the sampling positions were read from these plots. The value of the distribution coefficient, m, at each of the ten hypodermic needle sampling positions was calculated from the equilibrium curve for acetic acid distributed between MIBK - saturated water and water - saturated MIBK at 70°F. The arithmetic average of these ten values of m was calculated and used in subsequent calculations. The equilibrium curve is shown in Figure 46 and the equilibrium data used to prepare this plot appear in Table IV-13, Appendix IV. The capacity coefficient, $K_D a$, was calculated by means of the smoothed concentrations and Equation 20. Integration was carried out over the test section only.

$$K_D a = \frac{L_D}{H} \int \frac{dc_D}{\left(\dfrac{c_C}{m} - c_D \right)} \qquad\qquad 20$$

The experimental results are presented in Table IV-9, Appendix IV.

The dispersion model characterizes the extent of backmixing of the continuous phase. It is likely that the continuous phase which is backmixed enters the wakes of drops and is transported some distance up the column as wake material before passing back into the main bulk of the continuous phase. In the tracer experiments described earlier this backmixing was studied by measuring the extent to which a solute tracer, soluble only in the continuous phase, was carried up the column.
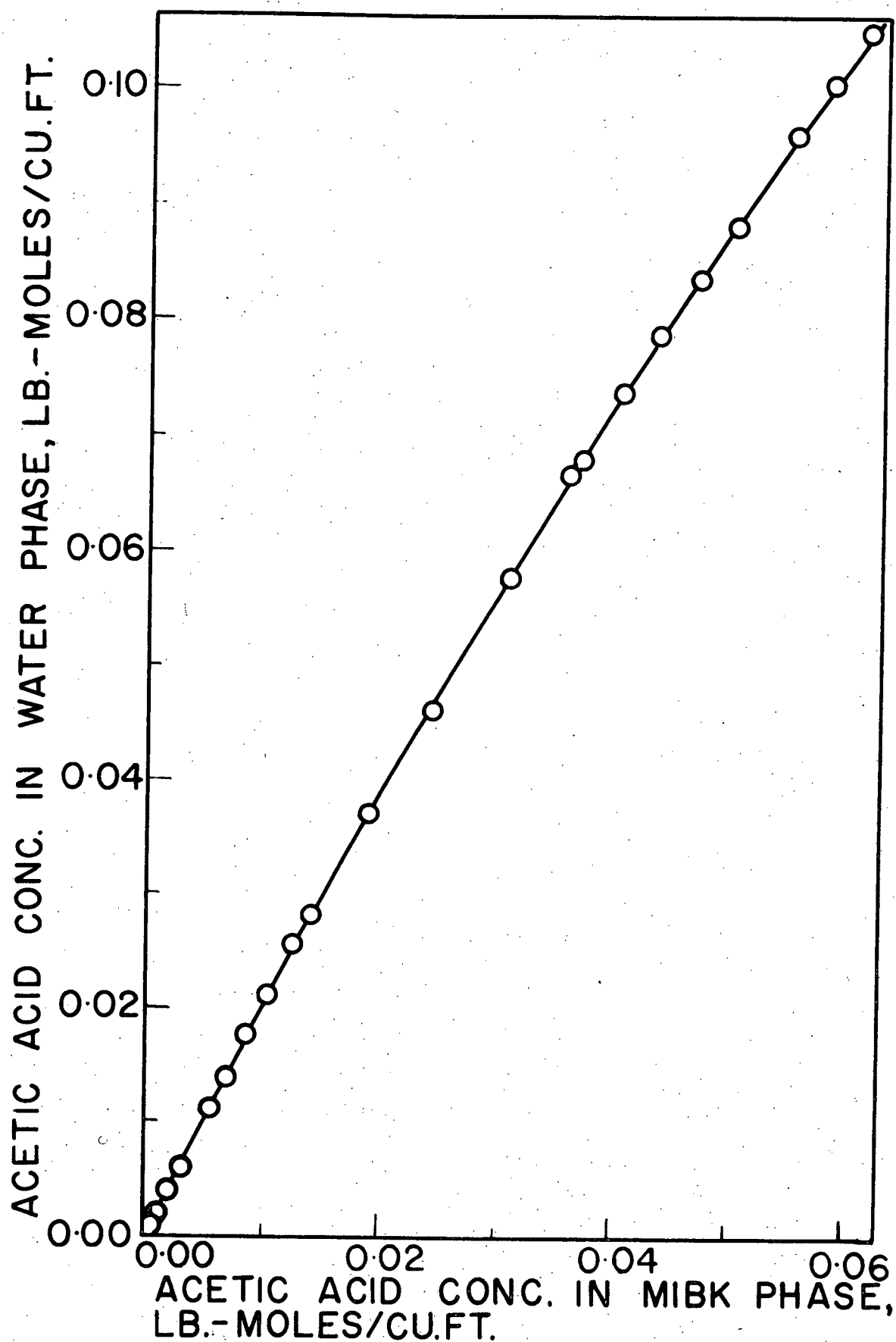
FIGURE 46.   EQUILIBRIUM CURVE FOR ACETIC ACID DISTRIBUTED BETWEEN
MIBK-SATURATED WATER AND WATER-SATURATED MIBK AT 70°F

When mass transfer can take place the simple conditions of the tracer work no longer obtain and caution must be exercised in using the tracer results and the dispersion model. The differences which can arise are that the wakes are no longer typical of the location from which they were drawn, and mass transfer can still occur from a wake while it is travelling with the drop.

In the case of mass transfer from the continuous to the dispersed phase, solute,in this case soluble in both phases, is transported along with continuous phase up the column in the wakes of the rising drops as was the case in the tracer studies. However, it is probable that the continuous phase, immediately prior to entering a wake, had been in the near vicinity of the associated drop. Consequently this continuous phase would be lower in solute concentration than the bulk of that phase at the same elevation. Therefore the amount of solute carried up the column in the rising wakes would be less than that predicted from the tracer studies wherein no such depletion of tracer could have taken place.

In addition to the above effect there is the dissimilarity of the diffusion pattern of solute between the wake and the surrounding continuous phase. In the case of the non-partitioned tracer diffusion must inevitably be from the wake to the continuous phase in which the concentration of tracer is less. However, in the case of mass transfer, as described in the present work, the wakes are moving towards a region of higher concentration of solute and therefore molecular diffusion of solute is from the continuous phase towards the wake. As has been discussed elsewhere in this thesis

molecular diffusion can be neglected with respect to eddy diffusion, and hence it is felt that this particular distortion of the wake composition can be neglected.

There is yet, however, one more factor to be considered. Mass transfer inevitably will occur between the wake and the drop itself by the transfer of the partitionable solute from the wake to the drop. For the moment our concern is with the wake itself and such mass transfer would still further deplete the solute in the wake and so when parts of this wake are cast off at higher levels the amount of solute transferred by the backmixing method will be lower than that had mass transfer not taken place. In passing one might mention that because part of the drop is exposed to the wake rather than to the surrounding continuous phase mass transfer to the drop will be lower than would have been true if the wake had not existed.

Evidently the dispersion model should be used with caution for the case of mass transfer between the phases. In spite of the above mentioned deficiences of the dispersion model it was used in this work to analyse the results of five runs involving mass transfer.

For each run Equation 14:

$$C_C = A\exp(\lambda_1 Z) + B\exp(\lambda_2 Z) - Q \qquad 14$$

was fitted to the measured concentration profile of acetic acid in the continuous phase over the test section for a value of $60\text{-ft}^2/\text{hr.}$ for the axial eddy diffusivity, E. Values of A and B were estimated by means of the least squares technique as

described under Theory. These calculations were performed on an IBM-7040 electronic computer. The flux of solute, J, down the column was calculated by means of Equation 21:

$$J = \tfrac{1}{2} \left[(L_C \, c_C^i - L_D \, c_D^o) + (L_C \, c_C^o - L_D \, c_D^i) \right]$$

21

The curve fitting was repeated for values of E decreased by one for each successive trial (i.e. 59, 58, 57, etc.) until either λ_1 or λ_2 reached a value of 10^{37}. Numbers greater than 10^{38} could not be handled by the IBM-7040 electronic computer. The lower limit of E was between 5 and 9. The value of E which resulted in the smallest sum of squares, Δ^2, of the deviations between the calculated and measured values of c_C, was taken to be the estimate of E. The values of E calculated by this method and the values of E calculated by means of tracer studies for similar column operating conditions are given in table 16.

TABLE 16. COMPARISON OF AXIAL EDDY DIFFUSIVITY BY MASS TRANSFER AND TRACER STUDIES.

Mass transfer studies				Tracer studies	
Run	L_C, $ft^3/hr.ft^2$	L_D, $ft^3/hr.ft^2$	E, $ft^2/hr.$	Run	E $ft^2/hr.$
J1	36.5	54.7	16	49	15
J2	18.2	54.7	42	51	15
J3	36.5	91.2	31	138	11
J4	48.4	91.2	39	139	11
J5	48.4	127	53	143	9

Table IV-10 shows the point values of Δ^2 and E for the estimation

of E in each of the five runs. In each run the value of the axial eddy diffusivity, E, determined from concentration profiles with mass transfer was less than E calculated from tracer studies for the same column operating conditions.

The estimation of E for each run was repeated several times. The first repetition involved the replacement in the calculations of J as given by Equation 21 by J as given by Equation 25:

$$J = (L_C \ c_C^i - L_D \ c_D^o)$$

25

The second repetition consisted of replacing the value of J used by that given by Equation 26:

$$J = (L_C \ c_C^o - L_D \ c_C^i)$$

26

Further repetitions involved the use of various arbitrarily chosen values of m and $K_D a$. Tables IV-11 and IV-12, Appendix IV show the values of E calculated for each of the three values of J used and also for the various values of m and $K_D a$ used for each run. Typical sets of results are shown graphically in Figures 47, 48, 49, and 50

Figure 47 shows how Δ^2 passes through a minimum value as E is varied arbitrarily. However, the minimum value of Δ is not pronounced enough to enable E to be estimated with any great accuracy. In addition, the true value of E in any case may not correspond exactly with the minimum value of Δ^2 because of
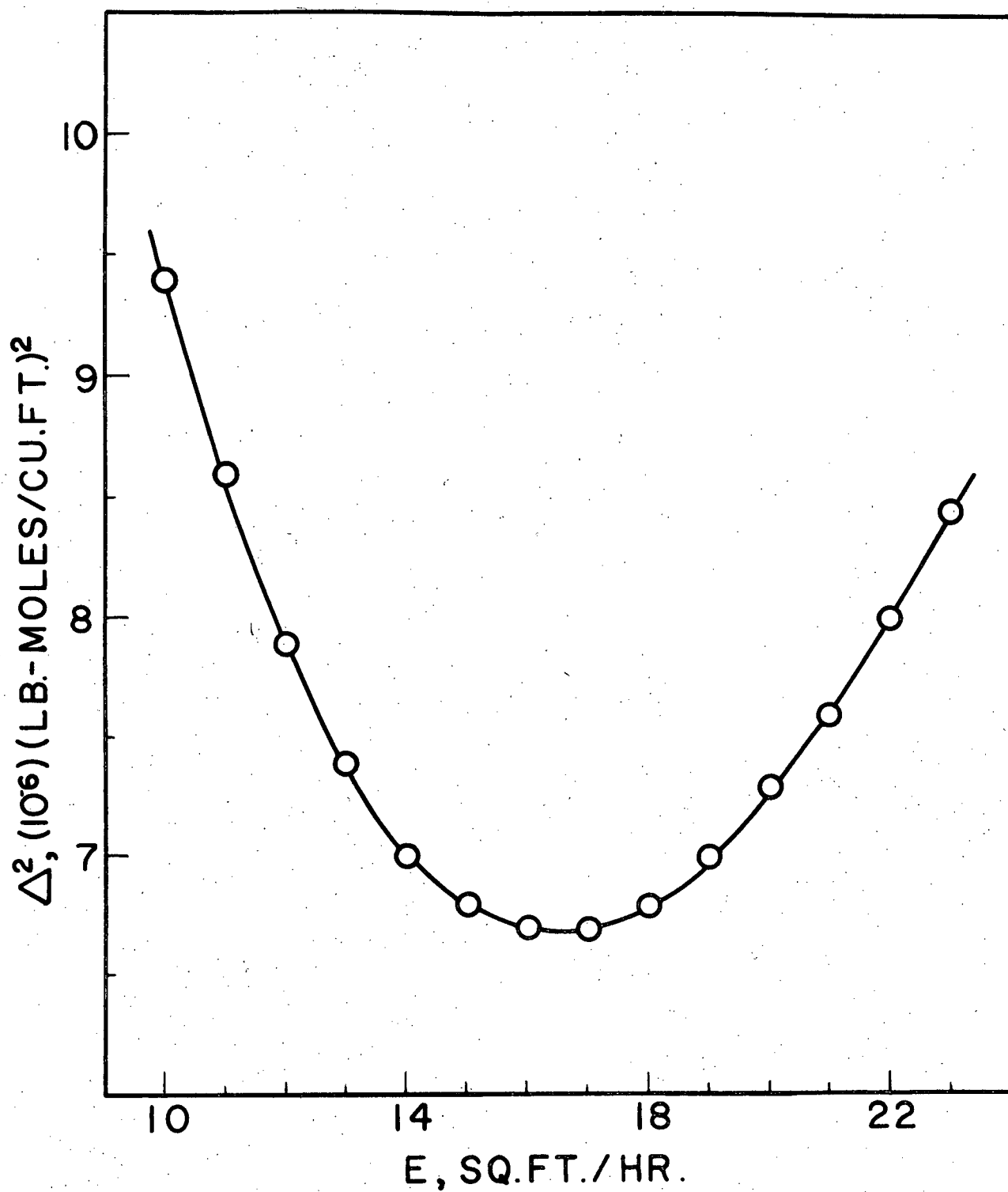
FIGURE 47. MINIMIZING Δ^2 FOR RUN J1
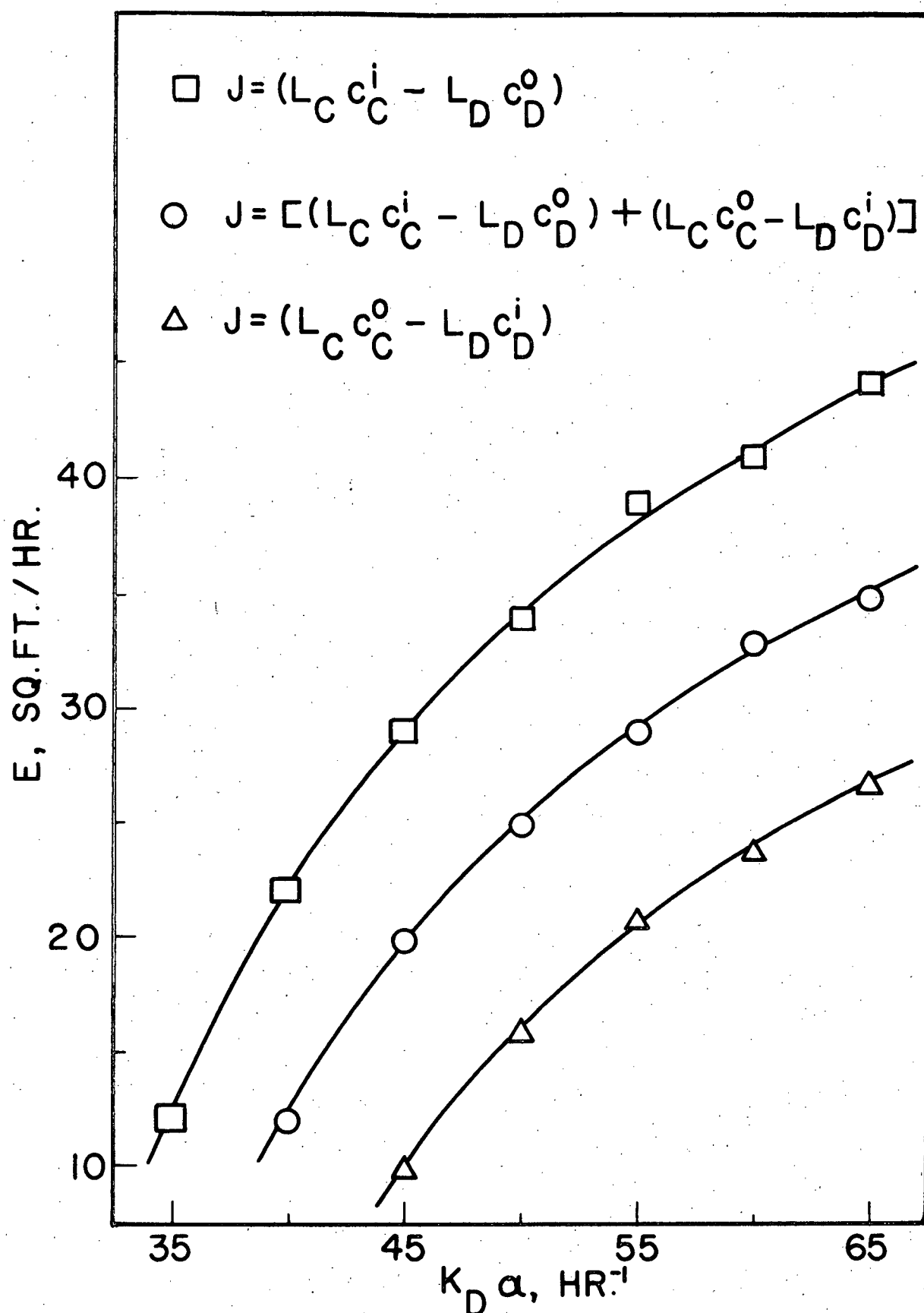
FIGURE 48. THE EFFECT ON E OF VARYING THE METHOD OF FLUX CALCULATION AND OF VARYING $K_D a$ FOR RUN J1
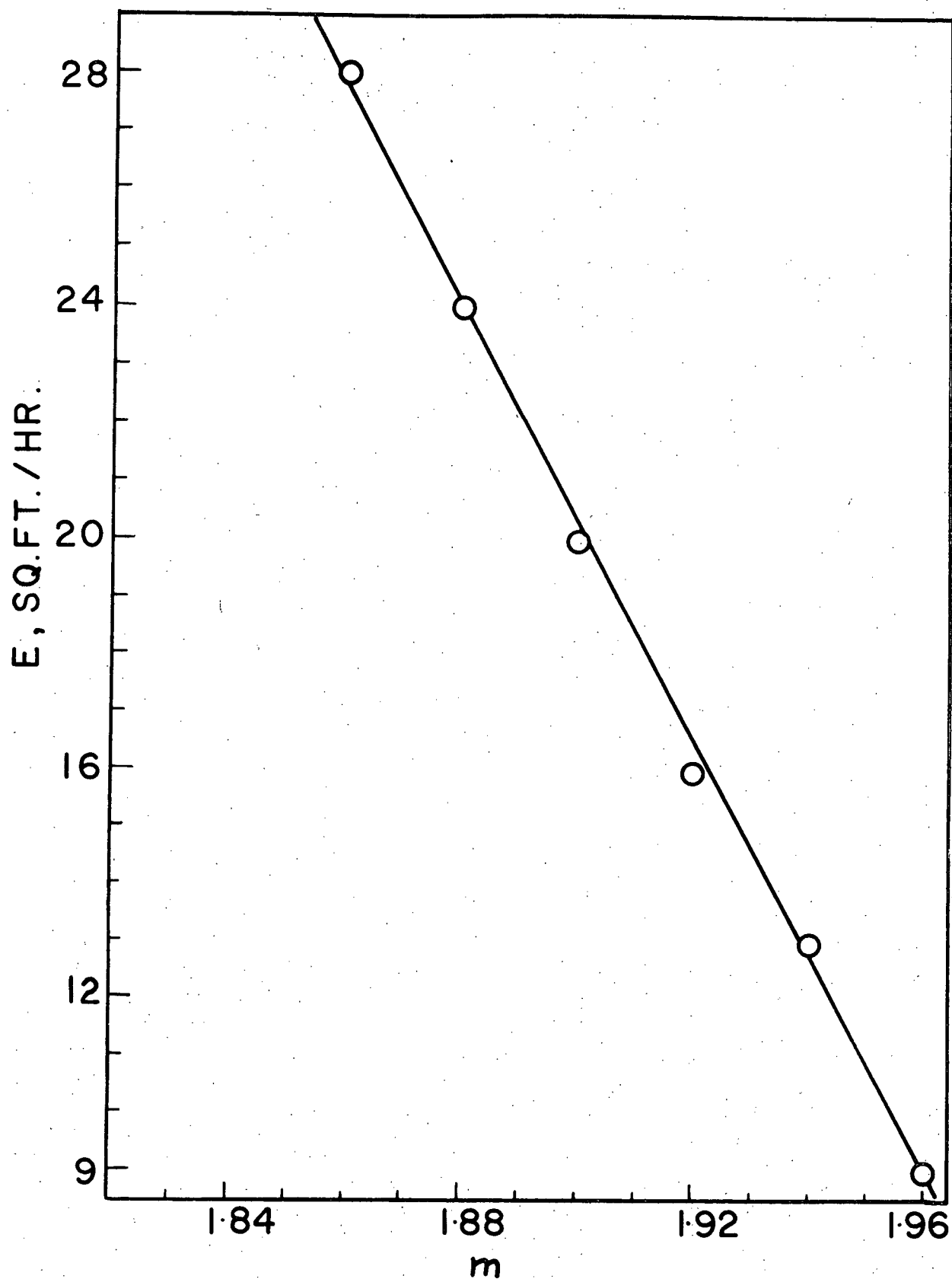
FIGURE 49. THE EFFECT ON E OF VARIATIONS IN m FOR RUN J1
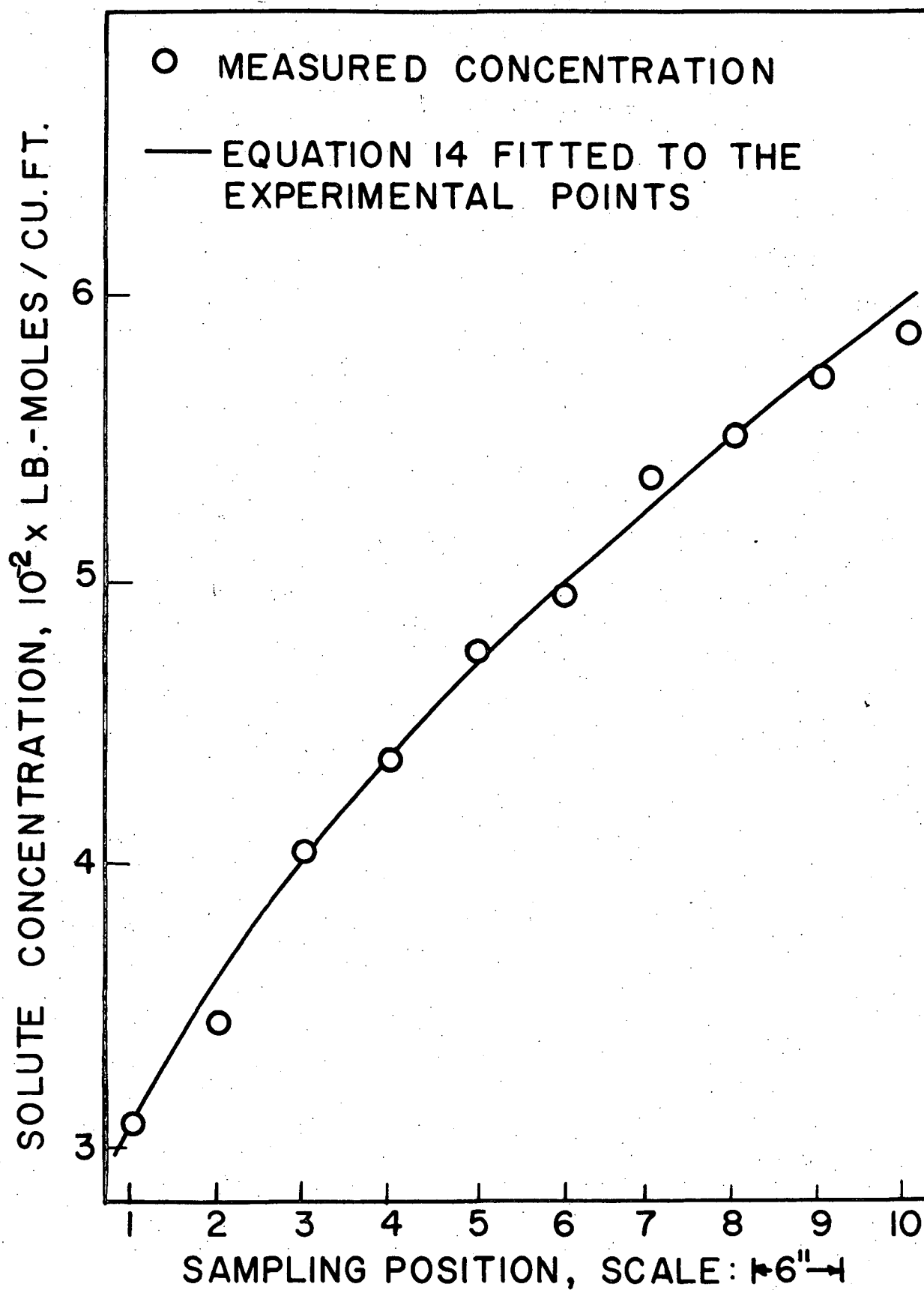
FIGURE 50. MEASURED AND FITTED CONCENTRATION PROFILES FOR RUN J1

the fact that the underlying assumptions on which the least
squares fitting technique is based have no sound basis as applied
in this case. These assumptions are that the concentration of
solute in the continuous phase at each sampling point comes from
a normal distribution and that each such distribution has the
same variance at all sampling points (125).

Figure 48 shows the effect on E of calculating J by the
various methods. This figure also shows the effect of arbitrary
changes in the value of $K_D a$ used in the calculation.

The differences in the values of J used arise because the
flux of solute down the column as calculated at the upper and
at the lower ends of the column are not equal. These differences
are due solely to experimental error. Large differences result
between the values of E calculated from the various values of
J. The error in the value of $K_D a$ calculated by means of Equation
20 may be quite large due to the difference $\left(\dfrac{c_C}{m} - c_D \right)$ being
small compared with $\left(\dfrac{c_C}{m} \right)$ or c_D. Figure 48 shows that the calculated
value of E is highly dependent upon the value of $K_D a$ used.
Hence small errors in c_C, m, or c_D result in a large error in E.

The effect on the calculated value of E of the value of m
used is shown in Figure 49. Evidently this effect is quite
substantial. As mentioned earlier the value of m used initially
(Table IV-9) was the arithmetic average of m at the ten hypodermic

needle sampling positions. The values of m at the highest and lowest hypodermic needles for Run J1 were 1.86 and 1.99 respectively. The assumption of constancy of m over the test section obviously is not valid. Furthermore there are no theoretical grounds for taking the arithmetic average of m as that value of m which should be used. In the light of Figure 49 and these facts the calculated value of E can be considerably in error.

Figure 50 shows the measured concentrations for Run J1. Superimposed is the curve calculated from Equation 14 using the value of $K_D a$ calculated by means of Equation 20, the value of J calculated from Equation 21, and the value of m calculated as the arithmetic mean of m at the ten hypodermic needle sampling positions. Although the value of E corresponding to this curve may be in error, the agreement between the curve and the experimental points is good.

CONCLUSIONS

A better understanding of sampling methods has resulted from the work described in this thesis. At low continuous phase flowrates a hook-probe sample is representative of the continuous phase in the column at the sampling elevation. However, at high flowrates of the phases such a sample appears to be representative of continuous phase in the column at some height above the sampling elevation. Hypodermic needles (22-gauge) do, however, withdraw continuous phase which is representative of that in the column at the sampling height. The dispersed phase solute concentration obtained from the bell-probe sample is representative of the dispersed phase in the column at the sampling elevation. Equation III-8 in conjunction with the results of a piston sample and the terminal conditions of the column gives the average solute concentration in the continuous phase, excluding the contribution from the wakes, of the piston sample at the time of sampling. This calculated value of the solute concentration in the continuous phase together with Equation 6 results in the average solute concentration in the dispersed phase of the piston sample at the time of sampling.

This work has tested the dispersion model as a means of describing axial mixing of the continuous phase of a spray column. The prediction by this model of an exponential decay of solute concentration upstream, with respect to continuous phase flow,

from the injection point of a tracer soluble only in the continuous phase, is in agreement with experimental results. The axial eddy diffusivity, which characterizes the axial mixing of the continuous phase, was calculated from such results. In addition the effects of column diameter, column height, drop size, and flowrates of the two phases have been measured experimentally. The axial eddy diffusivity of the continuous phase is independent of the superficial velocity of the continuous phase and of the column height and remains approximately constant as the dispersed phase superficial velocity is decreased from high values. However, the axial eddy diffusivity increases rapidly as the dispersed phase superficial velocity is decreased to low values. This effect is less pronounced at small drop sizes. The effect of increasing the drop size for a given dispersed phase superficial velocity is to increase the axial eddy diffusivity. The effect of increasing the column diameter is to increase the axial eddy diffusivity. For the same flowrates of respective phases in each of the two columns the superficial axial eddy diffusivity for the continuous phase is between 6.3 and 17.3 times greater in the 3-in. I.D. column than in the $1\frac{1}{2}$-in. I.D. column for the single value of d_p (0.135-in.) investigated.

The mixing cell-packed bed analogy, when applied to a spray column, predicts the Peclet number adequately for dispersed phase drops of about 0.155-in. d_p. For drops of smaller equivalent diameter the agreement between the predicted Peclet

number and the measured Peclet number becomes worse.

In the present work drop size distributions were measured in order to define the physical systems existing in the various backmixing studies. This was an auxilliary study and not a complete investigation of drop size distributions for various nozzle tip sizes, nozzle tip velocities, and the like. For the restricted conditions investigated drop size distribution plots show two peaks. For all the drop formation conditions investigated in this work the first peak occurs at an equivalent drop diameter of about 0.02-in. and indicates a large number of drops of this size. The second peak is high and narrow for drops of about 0.095-in. equivalent diameter (formed at 0.053-in. I.D. nozzle tips) and becomes progressively flatter and broader as the equivalent diameter is increased to about 0.155-in. (formed at 0.126-in. I.D. nozzle tips).

The piston sampler proved to be an excellent device for use in measuring the dispersed phase hold-up. This hold-up was found to be almost independent of the continuous phase superficial velocity as, indeed, would be expected. The hold-up increases approximately linearly with dispersed phase flowrates above 60-ft.^{3}/hr. ft.^{2} For a given dispersed phase flowrate the hold-up increases with decreasing drop size except when d_p is greater than about 0.14-in.

Axial eddy diffusivities can be calculated from runs involving mass transfer by fitting the dispersion model equation to experimental concentration profiles. However, the eddy diffusivity values obtained were very sensitive to small changes in the flux of solute down the column, the value of the mass transfer capacity coefficient, and the value of the distribution coefficient. The effect of small changes in other parameters such as superficial velocities and dispersed phase hold-up on the calculated values of the axial eddy diffusivity were not investigated. Investigations into the validity of the boundary conditions proposed by Danckwerts (60) as applied to an experimental column might lead to the accurate prediction of solute concentration profiles by means of the dispersion model equation and axial eddy diffusivity values measured in this work by tracer experiments with no mass transfer.

NOMENCLATURE

A   Constant of integration.

a   Interfacial area per unit volume of column, $ft.^2/ft.^3$

B   Constant of integration.

c_B Average solute concentration in the continuous phase backmixing stream, $lb.-moles/ft.^3$

$C_C = c_C/c_{CO}$ Reduced concentration in the continuous phase.

c_C Solute concentration in the continuous phase, $lb.-moles/ft.^3$ or microgm./ml.

c_C^a Solute concentration in the continuous phase of a bell-probe sample or a piston sample at the time of analysis, $lb.-moles/ft.^3$

c_{CO} Value of c_C when $z = 0$, microgm./ml.

$c_{C,j}$ Solute concentration in the continuous phase in the jth cell of a series of perfect mixers, $lb.-moles/ft.^3$ or microgm./ml.

c_C^i Solute concentration in the continuous phase inlet, $lb.-moles/ft.^3$

c_C^o Solute concentration in the continuous phase outlet, $lb.-moles/ft.^3$

c_D Solute concentration in the dispersed phase, $lb.-moles/ft.^3$

$c_{D,j}$ Solute concentration in the dispersed phase in the jth cell of a series of perfect mixers, lb.-moles/ft^3 or microgm./ml.

c_D^a Solute concentration in the dispersed phase of a bell-probe sample or a piston sample at the time of analysis, lb.-moles/ft^3

c_D^i Solute concentration in the dispersed phase inlet, lb.-moles/ft^3

c_D^o Solute concentration in the dispersed phase outlet, lb.-moles/ft^3

D Constant of integration.

d_i Height of a mixing cell, ft.

d_p Value of d_s at the second peak of a drop size distribution plot, in. or ft.

d_s Equivalent drop diameter = the diameter of a sphere whose volume is the same as that of the drop, ft.

E Continuous phase axial eddy diffusivity for the case of the dispersed phase moving relative to the co-ordinate axes, ft^2/hr.

E' Continuous phase axial eddy diffusivity for the case of the dispersed phase stationary relative to the co-ordinate axes, ft^2/hr.

$e = 1-\dfrac{h}{100}$ Volumetric fraction of continuous phase in the column.

H Test section height, ft.

h Volume percentage of dispersed phase in the column, %.

h_d — Vertical dimension of a drop image corrected for magnification, ft.

J — Net flux of solute down the column, lb.-moles/(hr.ft.^{2}).

K_D — Mass transfer coefficient based on $\left[\dfrac{c_C}{m} - c_D\right]$ driving force, $\dfrac{\text{lb.-moles}}{(\text{hr.})(\text{ft.}^2)(\text{lb.-moles/ft.}^3)}$.

L_B — Superficial velocity of the continuous phase back-mixing stream relative to the laboratory, ft.^{3}/(hr.ft.^{2}).

L_C — Superficial velocity of the continuous phase for the case of the dispersed phase moving relative to co-ordinate axes fixed with respect to the laboratory, ft.^{3}/(hr.ft.^{2}).

L_C' — Superficial velocity of the continuous phase for the case of the dispersed phase stationary relative to co-ordinate axes. These may be either fixed or moving relative to the laboratory, ft.^{3}/(hr.ft.^{2}).

L_D — Superficial velocity of the dispersed phase relative to the laboratory, ft.^{3}/(hr.ft.^{2}).

L_T — Superficial velocity of the tracer feed relative to the laboratory, ft.^{3}/(hr.ft.^{2}).

$m = \left(\dfrac{c_C}{c_D}\right)_{eq.}$ — Distribution coefficient for the solute between the continuous phase and the dispersed phase, (lb.-moles/ft.^{3})/(lb.-moles/ft.^{3}).

$Pe = \left(\dfrac{Ud_p}{E}\right)$ Peclet number for two phase flow.

$Pe' = \left(\dfrac{L_C' d_p}{E'}\right)$ Peclet number for single phase flow.

p_d Horizontal dimension of a drop image corrected for magnification, ft.

$Q = \dfrac{\gamma}{\beta}$

S Cross-sectional area of the column, ft.^{2}

t Time, hr.

$U = \left(\dfrac{L_C}{e} + \dfrac{L_D}{1-e}\right)$ Continuous phase interstitial velocity relative to the rising drops, ft./hr.

$u = \left(\dfrac{L_D}{1-e}\right)$ Average linear velocity of the dispersed phase drops relative to the laboratory, ft./hr.

V_B Volume of the continuous phase backmixing stream in a piston sample, ft.^{3}

V_C Volume of the continuous phase in a bell-probe sample or a piston sample, ft.^{3}

V_D Volume of the dispersed phase in a bell-probe sample or a piston sample, ft.^{3}

v_B Average volume of a continuous phase backmixing "packet" associated with each dispersed phase drop, ft.^{3}

v_D Average volume of a dispersed phase drop, ft.^{3}

y=z + ut   Distance along the column, in the direction of the
continuous phase flow, relative to co-ordinate axes
stationary with respect to the dispersed phase
drops, ft.

$Z = z/H$ Dimensionless distance along the column in the
direction of the continuous phase flow.

z   Distance along the column, in the direction of the
continuous phase flow, relative to co-ordinate axes
stationary with respect to the laboratory, ft.

$$\alpha = \frac{H}{2}\left[\frac{L_C}{Ee} + \frac{K_D a}{L_D}\right] \qquad ft.^{-1}$$

$$\beta = \frac{(L_D - mL_C)K_D a H^2}{mL_D Ee} \qquad ft.^{-1}$$

$$\gamma = \frac{JK_D a H^2}{L_D Ee c_{CO}}$$

$$\Delta^2 = \sum\left[C_C - A\exp(\lambda_1 Z) - B\exp(\lambda_2 Z) + Q\right]^2 \quad , \; (lb.\text{-}moles/ft.^3)^2$$

$$\lambda = \frac{d_i}{d_p}$$

$$\lambda_1 = \alpha + \sqrt{\alpha^2 + \beta} \quad , \quad ft.^{-1}$$

$$\lambda_2 = \alpha - \sqrt{\alpha^2 + \beta} \quad , \quad ft.^{-1}$$

ρ Density of the continuous phase, lb./ft.^{3}

μ Viscosity of the continuous phase, lb./hr.ft.

LITERATURE CITED

1. Geankoplis, C. J. and Hixson, A. N., Ind. Eng. Chem. 42, 1141 (1950)

2. Blanding, F. H. and Elgin, J.C., Trans. Am. Inst. Chem. Engrs. 38, 305 (1942)

3. Johnson, H.F. and Bliss, H., Trans. Am. Inst. Chem. Engrs. 42, 331 (1946)

4. Hayworth, C. B. and Treybal, R. E., Ind. Eng. Chem. 42, 1174 (1950)

5. Keith, F. W. and Hixson, A. N., Ind. Eng. Chem. 49, 1017 (1957)

6. Fleming, J. F. and Johnson, H. F., Chem. Eng. Progr. 49, 497 (1953)

7. Narasinga Rao, E. V. L., Kumar, R. and Kuloor, N. R., Chem. Eng. Sci. 21, 867 (1966)

8. Null, H. R. and Johnson, H. F., Am. Inst. Chem. Engrs. J. 4, 273 (1958)

9. Elgin, J. C. and Browning, F. M., Trans. Am. Inst. Chem. Engrs. 31, 639 (1935)

10. Sherwood, T. K., Evans, J. E. and Longcor, J. V. A., Trans. Am. Inst. Chem. Engrs. 35, 597 (1939)

11. Skryabin, A. K., Zhurnal Fizicheskoi Khimii <u>33</u>, No. 1, 74 (1959)

12. Elgin, J. C. and Foust, H. C., Ind. Eng. Chem. <u>42</u>, 1127 (1950)

13. Johnson, A. I., Minard, G. W., Huang, C. J., Hansuld, J. H. and McNamara, V. M., Am. Inst. Chem. Engrs. J. <u>3</u>, 101 (1957)

14. Licht, W. and Conway, J. B., Ind. Eng. Chem. <u>42</u>, 1151 (1950)

15. Geankoplis, C. J., Wells, P. L. and Hawk, E. L., Ind. Eng. Chem. <u>43</u>, 1848 (1951)

16. Kreager, R. M. and Geankoplis, C. J., Ind. Eng. Chem. <u>45</u>, 2156 (1953)

17. Vogt, H. J. and Geankoplis, C. J., Ind. Eng. Chem. <u>46</u>, 1763 (1954)

18. Morello, V. S. and Poffenberger, N., Ind. Eng. Chem. <u>42</u>, 1021 (1950)

19. Newman, M. L., Ind. Eng. Chem. <u>44</u>, 2457 (1952)

20. Campos, C. V., M. S. thesis, University of Tennessee, 1955

21. Garner, F. H. and Tayeban, M., Anales de Fisica Y Quimica, TOMO LVI-B, 479 (1960)

22. Garner, F. H. and Tayeban, M., Anales de Fisica Y Quimica, TOMO LVI-B, 491 (1960)

23. Hendrix, C. D., Shastikant, B. D. and Johnson, H. F., Am. Inst. Chem. Eng., 52nd Nat. Meeting (Feb. 1964), Memphis, Tennessee

24. Margarvey, R. H. and Bishop, R. L., Nature $\underline{188}$, 735 (1960)

25. Li, N. N. and Zeigler, E. N., Ind. Eng. Chem. $\underline{59}$, No. 3, 30 (1967)

26. Letan, R. and Kehat, E., Am. Inst. Chem. Engrs. J. $\underline{11}$, 804 (1965)

27. Letan, R. and Kehat, E., Am. Inst. Chem. Engrs. J. $\underline{13}$, 443 (1967)

28. Gier, T. E. and Hougen, J. O., Ind. Eng. Chem. $\underline{45}$, 1362 (1953)

29. Patton, J. L., M. S. thesis, University of Tennessee, 1955

30. Ewanchyna, J. E., M. Sc. thesis, University of Saskatchewan, 1955

31. Cavers, S. D. and Ewanchyna, J. E., Can. J. Chem. Eng. $\underline{35}$, 113 (1957)

32. Smith, A. R., Casswell, J. E., Larson, P. P. and Cavers, S. D., Can. J. Chem. Eng. $\underline{41}$, 150 (1963)

33. Groothuis, H. and Zuiderweg, F. J., Chem. Eng. Sci. $\underline{12}$, 288 (1960)

34. Smith, A. R., B. A. Sc. thesis, The University of British Columbia, 1958

35. Choudhury, P. R., M. A. Sc. thesis, The University of British Columbia, 1959

36. Gayler, R. and Pratt, H. R. C., Trans. Inst. Chem. Engrs. (London) $\underline{31}$, 78 (1953)

37. Hawrelak, R. A., M. A. Sc. thesis, The University of British Columbia, 1960

38. Bergeron, G., M. A. Sc. thesis, The University of British Columbia, 1963

39. Rocchini, R. J., M. A. Sc. thesis, The University of British Columbia, 1961

40. Cavers, S. D., Birmingham University Chemical Engineer 14, 8 (1963)

41. Weaver, R. E., Lapidus, L. and Elgin, J. C., Am. Inst. Chem. Engrs. J. 5, 533 (1959)

42. Hazlebeck, D. E. and Geankoplis, C. J., Ind. Eng. Chem. Fundamentals 2, 310 (1963)

43. Garwin, L. and Smith, B. D., Chem. Eng. Progr. 49, 591 (1953)

44. Miyauchi, T. and Vermeulen, T., Ind. Eng. Chem. Fundamentals 2, 304 (1963)

45. Hartland, S. and Mecklenburgh, J. C., Chem. Eng. Sci. 21, 1209 (1966)

46. Jacques, G. L. and Vermeulen, T., U. S. Atomic Energy Comm., U. C. R. L.-8029 (1957)

47. Wilson, H. A., Proc. Cambridge Phil. Soc. 12, 406 (1904)

48. Towle, W. L. and Sherwood, T. K., Ind. Eng. Chem. 31, 457 (1939)

49. Woertz, B. B. and Sherwood, T. K., Trans. Am. Inst. Chem. Engrs. 35, 517 (1939)

50. Kalinske, A. A. and Pien, C. L., Ind. Eng. Chem. 36, 220 (1944)

51. Bernard, R. A. and Wilhel,, R. H., Chem. Eng. Progr. 46, 233 (1950)

52. Gilliland, E. R. and Mason, E. A., Ind. Eng. Chem. 41, 1191 (1949)

53. Gilliland, E. R. and Mason, E. A., Ind. Eng. Chem. 44, 218 (1952)

54. Mar, B. W. and Babb, A. L., Ind. Eng. Chem. 51, 1011 (1959)

55. Mar, B. W., Ph. D. thesis, University of Washington, 1958

56. Argo, W. B. and Cova, D. R., Ind. Eng. Chem. Process Design Develop. 4 , 352 (1965)

57. Westerterp, K. R. and Meyberg, W. H., Chem. Eng. Sci. 17, 373 (1962)

58. Smoot, L. D., Ph. D. thesis, University of Washington, 1960

59. Askins, J. W., Hinds, G. P. and Kunreuther, F., Chem. Eng. Progr. 47, 401 (1951)

60. Danckwerts, P. V., Chem. Eng. Sci. 2, 1 (1953)

61. Levenspiel, D. and Smith, W. K., Chem. Eng. Sci. 6, 227 (1957)

62. Evans, E. V. and Kenney, C. N., Trans. Inst. Chem. Engrs. (London) 44, T189 (1966)

63. Ebach, E. A. and White, R. R., Am. Inst. Chem. Engrs. J. 4, 161 (1958)

64. Carberry, J. J. and Bretton, R. H., Am. Inst. Chem. Engrs. J. 4, 367 (1958)

65. Miyauchi, T. and Oya, H., Am. Inst. Chem. Engrs. J. 11, 395 (1965)

66. Rippel, G. R., Eidt, C. M., Jr. and Jordon, H. B., Jr., Ind. Eng. Chem. Process Design Develop. 5, 32 (1966)

67. Shemilt, L. W. and Krishnaswamy, P. R., 16th Canadian Chemical Engineering Conference, Windsor, Ontario (Oct. 1966)

68. Van der Laan, E. T., Chem. Eng. Sci. 7, 187 (1958)

69. Wehner, J. F. and Wilhelm, R. H., Chem. Eng. Sci. 6, 89 (1956)

70. Aris, R., Chem. Eng. Sci. 9, 266 (1959)

71. Bischoff, K. B., Chem. Eng. Sci. 12, 69 (1960)

72. Bischoff, K. B. and Levenspiel, O., Chem. Eng. Sci. 17, 245 (1962)

73. Levenspiel, O. and Bischoff, K. B., Advan. Chem. Eng. 4, 95 (1963)

74. Mixson, F. O., Whitaker, D. R. and Orcutt, J. C., Am. Inst. Chem. Engrs. J. 13, 21 (1967)

75. Sater, V. E. and Levenspiel, O., Ind. Eng. Chem. Fundamentals 5, 86 (1966)

76. Bischoff, K. B. and Phillipps, J. B., Ind. Eng. Chem. Process Design Develop. 5, 416 (1966)

77. Babcock, R. E., Green, D. W. and Perry, R. H., Am. Inst. Chem. Engrs. J. 12, 922 (1966)

78. Pellet, G. L., TAPPI 49, No. 2, 75 (1966)

79. Moon, J. S., Ph. D. thesis, University of California, Berkeley, 1963

80. Von Rosenberg, D. U., Am. Inst. Chem. Engrs. J. $\underline{2}$, 55 (1956)

81. DeMaria, F. and White, R. R., Am. Inst. Chem. Engrs. J. $\underline{6}$, 473 (1960)

82. Klinkenberg, A. and Sjenitzer, F., Chem. Eng. Sci. $\underline{5}$, 258 (1956)

83. Westerterp, K. R. and Landsman, P., Chem. Eng. Sci. $\underline{17}$, 363 (1962)

84. Brutvan, D. R., Ph. D. thesis, Rensselaer Polytechnic Institute, Troy, New York, 1958

85. Klinkenberg, I. A., Trans. Inst. Chem. Engrs. (London) $\underline{43}$, T141 (1965)

86. Miller, S. F. and King, C. J., Am. Inst. Chem. Engrs. J. $\underline{12}$, 767 (1966)

87. Rothfeld, L. B. and Ralf, J. L., Am. Inst. Chem. Engrs. J. $\underline{9}$, 852 (1963)

88. Sinclair, R. J. and Potter, O.E., Trans. Inst. Chem. Engrs. (London) $\underline{43}$, T3 (1965)

89. Deisler, P. F. and Wilhelm, R. H., Ind. Eng. Chem. $\underline{45}$, 219 (1953)

90. Kramers, H. and Alberda, A. G., Chem. Eng. Sci. $\underline{2}$, 173 (1953)

91. Strang, D. A. and Geankoplis, C. J., Chem. Eng. Sci. 50, 1305 (1958)

92. McHenry, K. W. and Wilhelm, R. H., Am. Inst. Chem. Engrs. J. 3, 83 (1957)

93. Stahel, E. P. and Geankoplis, C. J., Am. Inst. Chem. Engrs. J. 10, 174 (1964)

94. Gray, R. I. and Prados, J. W., Am. Inst. Chem. Engrs. J. 9, 211 (1963)

95. Miyauchi, T., U. S. Atomic Energy Comm., U. C. R. L. - 3911 (1957)

96. Sleicher, C. A., Jr., Am. Inst. Chem. Engrs. J. 5, 145 (1959)

97. Tichacek, L. J., Am. Inst. Chem. Engrs. J. 9, 394 (1963)

98. Levenspiel, O. and Bischoff, K. B., Ind. Eng. Chem. 51, 1431 (1959)

99. McMullen, A. K., Miyauchi, T. and Vermeulen, T., U. S. Atomic Energy Comm., U. C. R. L.-3911 Supplement (1958)

100. Miyauchi, T. and Vermeulen, T., Ind. Eng. Chem. Fundamentals 2, 113 (1963)

101. Wilburn, N. P., Ind. Eng. Chem. Fundamentals 3, 189 (1964)

102. Smoot, L. D. and Babb, A. L., Ind. Eng. Chem. Fundamentals 1, 93 (1962)

103. Jambheker, A. D., M. S. thesis, University of Tennessee, 1955

104. Liles, A. W. and Geankoplis, C. J., Am. Inst. Chem. Engrs. J. $\underline{6}$, 591 (1960)

105. Brittan, M. I. and Woodburn, E. T., Am. Inst. Chem. Engrs. 58th Ann. Meeting, Philadelphia (Dec. 1965)

106. Gottschlich, C. F., Am. Inst. Chem. Engrs. J. $\underline{9}$, 88 (1963)

107. Van Deemter, J. J., Zuiderweg, F. J. and Klinkenberg, A., Chem. Eng. Sci. $\underline{5}$, 271 (1956)

108. Aris, R. and Amundson, N. R., Am. Inst. Chem. Engrs. J. $\underline{3}$, 280 (1957)

109. Sleicher, C. A., Jr., Am. Inst. Chem. Engrs. J. $\underline{6}$, 529 (1960)

110. Epstein, N., Can. J. Chem. Eng. $\underline{36}$, 210 (1958)

111. Baldwin, J. T. and Durbin, L. D., Can. J. Chem. Eng. $\underline{44}$, 151 (1966)

112. Roemer, M. H. and Durbin, L. D., Ind. Eng. Chem. Fundamentals $\underline{6}$, 120 (1967)

113. Vermeulen, T., Moon, J. S., Hennico, A. and Miyauchi, T., Chem. Eng. Progr. $\underline{62}$, No. 9, 95 (1966)

114. Treybal, R. E., Liquid Extraction, p. 183, 2nd Ed., McGraw-Hill Book Co., Inc., New York, 1963

115. Einstein, H. A., Ph. D. Dissertation, Eidg. Techn. Hochshule, Zürich, 1937

116. Jacques, G. L., Cotter, J. E. and Vermeulen, T., U. S. Atomic Energy Comm. U. C. R. L.-8658 (1959)

117. Cairns, E. J. and Prausnitz, J. M., Chem. Eng. Sci. $\underline{12}$, 20 (1960)

118. LePage, N. A. W., B. A. Sc. thesis, The University of British Columbia, 1956

119. Swift, E. H., A System of Chemical Analysis for the Common Elements, pp. 100-103, 557, W. H. Freeman and Co., San Francisco, 1939

120. Wellek, R. M., Agrawal, A. K. and Skelland, A. H. P., Am. Inst. Chem. Engrs. J. $\underline{12}$,854 (1966)

121. Letan, R. and Kehat, E., submitted for publication to Am. Inst. Chem. Engrs. J., 1967, referred to by permission.

122. Carberry, J. J., Am. Inst. Chem. Engrs. J. $\underline{4}$, No. 1, 13M (1958)

123. Prausnitz, J. M., Am. Inst. Chem. Engrs. J. $\underline{4}$, No. 1, 14M (1958)

124. Mickley, H. S., Sherwood, T. K. and Reed, C. E,, Applied Mathematics in Chemical Engineering, 2nd Ed., p. 210, McGraw-Hill Book Co., New York, 1957

125. Bennett, C. A. and Franklin, N. L., Statistical Analysis in Chemistry and the Chemical Industry, pp. 214-243, John Wiley and Sons, Inc., New York, 1963

126. Geankoplis, C. J., Ind. Eng. Chem. $\underline{44}$, 2458 (1952)

127. Gerster, J. A., Chem. Eng. Progr. $\underline{59}$, 79 (1963)

128. Jost, W., Diffusion, p. 477, Academic Press Inc., New York, 1960

APPENDIX I

DISPERSION MODEL THEORY

The assumptions upon which the mathematical model is based are given under the heading of Theory.

Consider the control zone in the C-phase, shown in Figure I-1, during the incremental time dt. The case considered is one in which mass transfer is taking place between the continuous phase and the dispersed phase. A solute mass balance over the control zone gives the following terms.

i) Solute out due to mass transfer.

$$K_D\left(\frac{c_C}{m} - c_D\right)Sa(dz)(dt)$$

ii) Solute out due to C-phase flow.

$$L_C S\left(c_C + \left(\frac{\partial c_C}{\partial z}\right)(dz)\right)(dt)$$

iii) Solute in due to C-phase flow.

$$L_C S c_C(dt)$$

iv) Solute in due to eddy diffusion.

$$E\left(\frac{\partial}{\partial z}\left(c_C + \left(\frac{\partial c_C}{\partial z}\right)(dz)\right)\right)Se(dt) = EeS\left(\frac{\partial c_C}{\partial z}\right)(dz)(dt) + EeS\left(\frac{\partial^2 c_C}{\partial z^2}\right)(dz)(dt)$$
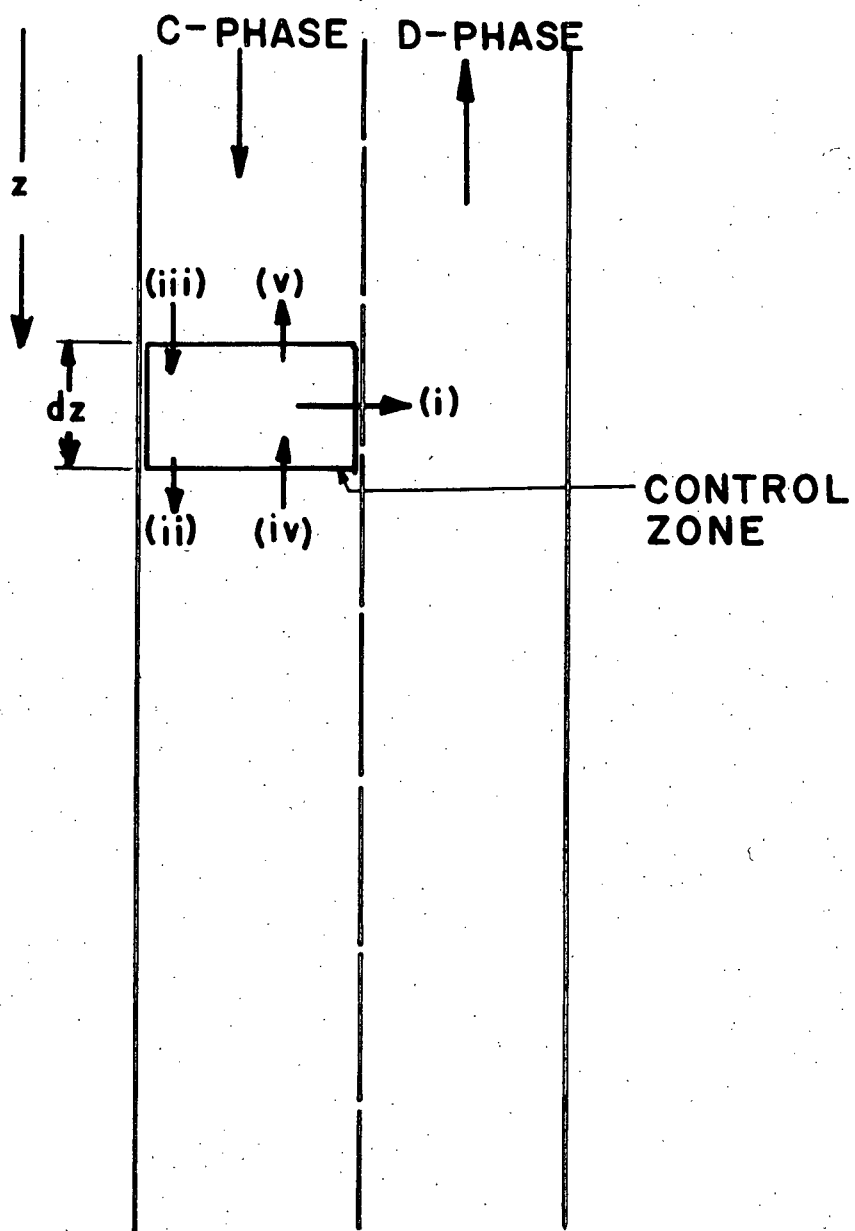
FIGURE I-1. SOLUTE MASS BALANCE IN THE CONTINUOUS PHASE

v) Solute out due to eddy diffusion.

$$E\left(\frac{\partial c_C}{\partial z}\right)(dz)eS(dt)$$

Terms i) to v̄) inclusive have been shown on Figure I-1 as arrows with the corresponding numbers as given here indicated beside them.

vi) Accumulation of solute.

$$\left(\frac{\partial c_C}{\partial t}\right)Se(dz)(dt)$$

These terms combine into the following mass balance.

$$K_D\left(\frac{c_C-c_D}{m}\right)Sa(dz)(dt)+L_CSc_C(dt)+L_CS\left(\frac{\partial c_C}{\partial z}\right)(dz)(dt)+E\left(\frac{\partial c_C}{\partial z}\right)Se(dz)(dt)$$

$$+\left(\frac{\partial c_C}{\partial t}\right)Se(dz)(dt)=L_CSc_C(dt)+E\left(\frac{\partial c_C}{\partial z}\right)Se(dz)(dt)+E\left(\frac{\partial^2 c_C}{\partial z^2}\right)(dz)Se(dt)$$

The above equation can be rearranged to give

$$Ee\left(\frac{\partial^2 c_C}{\partial z^2}\right) - L_C\left(\frac{\partial c_C}{\partial z}\right) - K_Da\left(\frac{c_C}{m} - c_D\right) = e\left(\frac{\partial c_C}{\partial t}\right)$$

I-1

At steady state Equation I-1 reduces to

$$Ee\left(\frac{d^2 c_C}{dz^2}\right) - L_C\left(\frac{dc_C}{dz}\right) - K_Da\left(\frac{c_C}{m} - c_D\right) = 0$$

I-2

Equation I-2 can be rearranged to give

$$c_D = \frac{-Ee}{K_D a}\left(\frac{d^2 c_C}{dz^2}\right) + \frac{L_C}{K_D a}\left(\frac{dc_C}{dz}\right) + \frac{c_C}{m}$$

I-3

The net flux, J, of solute down the column at the elevation z is given by Equation I-4.

$$J = L_C c_C - E\left(\frac{dc_C}{dz}\right)e - L_D c_D$$

I-4

The substitution of c_D from Equation I-3 into Equation I-4 yields

$$J = L_C c_C - Ee\left(\frac{dc_C}{dz}\right) + \frac{L_D Ee}{K_D a}\left(\frac{d^2 c_C}{dz^2}\right) - \frac{L_D L_C}{K_D a}\left(\frac{dc_C}{dz}\right) - \left(\frac{L_D c_C}{m}\right)$$

I-5

Equation I-5 can be rearranged to give

$$\left(\frac{d^2 c_C}{dz^2}\right) - \left(\frac{K_D a}{L_D}\right)\left(\frac{dc_C}{dz}\right) - \left(\frac{L_C}{Ee}\right)\left(\frac{dc_C}{dz}\right) + \left(\frac{L_C c_C K_D a}{L_D Ee}\right) - \left(\frac{c_C K_D a}{mEe}\right) = \left(\frac{JK_D a}{L_D Ee}\right)$$

I-6

Concentrations and distances can be put on a dimensionless basis by means of Equations I-7 and I-8.

$$c_C = c_{CO} C_C$$

I-7

$$z = ZH$$

I-8

These two equations now can be used to transform Equation I-6 into Equation I-9.

$$\left(\frac{d^2 C_C}{dZ^2}\right) - 2\alpha\left(\frac{dC_C}{dZ}\right) - \beta C_C = \gamma,$$

I-9

where $\alpha, \beta,$ and γ are given by Equation I-10, I-11, and I-12.

$$2\alpha = \left(\frac{L_C H}{Ee}\right) + \left(\frac{K_D aH}{L_D}\right)$$

I-10

$$\beta = \frac{(L_D - mL_C)K_D aH^2}{mL_D Ee}$$

I-11

$$\gamma = \frac{JK_D aH^2}{L_D Ee c_{CO}}$$

I-12

If

$$\beta \neq 0$$

I-12a)

and

$$(\alpha^2 + \beta) \geqslant 0$$

I-12b)

the solution of Equation I-9 is given by Equation I-13.

$$C_C = A\exp(\lambda_1 Z) + B\exp(\lambda_2 Z) - Q$$

I-13

A and B are constants of integration and $\lambda_1, \lambda_2,$ and Q are given by Equations I-14, I-15, and I-16 respectively.

$$\lambda_1 = \alpha + \sqrt{\alpha^2 + \beta}$$

I-14

$$\lambda_2 = \alpha - \sqrt{\alpha^2 + \beta}$$

I-15

$$Q = \frac{\gamma}{\beta} = \frac{Jm}{c_{CO}(L_D - mL_C)}$$

I-16

Other solutions of Equation I-9 are appropriate when the conditions given by Equation I-12a) and I-12b) are not met. However, the applicability of these other solutions is more limited than that of Equation I-13 and no extra information can be obtained by their use. When the condition given by Equation I-12b) is not satisfied problems involving instability may arise.

For a solute which dissolves only in the continuous phase $c_D = 0,$

and Equation I-4 reduces to

$$J = L_C c_C - Ee\left(\frac{dc_c}{dz}\right)$$

I-17

If, in addition, continuous phase samples are withdrawn from the portion of the column which, for the continuous phase, is upstream from the feed point of tracer then

$$J = 0.$$

Then Equation I-17 becomes

$$L_C c_C = Ee\left(\frac{dc_C}{dz}\right)$$

I-18

The solution of Equation I-18 is

$$c_C = Dexp\left(\frac{L_C z}{Ee}\right),$$

I-19

where D is a constant of integration. But

$$c_C = c_{CO} \qquad\qquad when \qquad z = 0.$$

Therefore,

$$c_C = c_{CO}exp\left(\frac{L_C z}{Ee}\right)$$

I-20

Equation I-20 can be rearranged to give

$$\frac{L_C z}{Ee} = \ln\left(\frac{c_C}{c_{CO}}\right)$$

I-21

APPENDIX II

A. MIXING CELL - PACKED BED ANALOGY (44, 64, 90, 92, 108, 109)

Consider a series of perfect mixers as shown in the sketch below. Suppose that a solute is extracted from a moving continuous phase by a stationary dispersed phase. Let the inter-

stage superficial velocity of the continuous phase be L_C', the solute concentration for the continuous phase in the jth mixer be $c_{C,j}$, and the solute concentration for the dispersed phase in the jth mixer be $c_{D,j}$. Let the mass transfer coefficient, K_D; the interfacial area per unit volume of mixer, a; and the height of a mixing cell, d_i, be the same for each mixer. At steady state a solute mass balance for the continuous phase of the jth mixer results in the following equation.
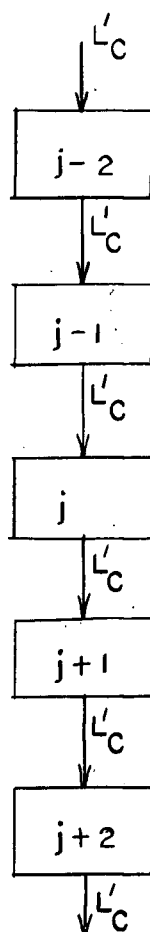
$$(L_C')(c_{C,j-1}) = (L_C')(c_{C,j}) + K_D a \left(\frac{c_{C,j}}{m} - c_{D,j} \right) d_i$$

II-1

Equation II-1 can be rearranged to give

$$(c_{C,j-1} - c_{C,j}) - \frac{d_i K_D a}{L_C'} \left(\frac{c_{C,j}}{m} - c_{D,j} \right) = 0$$

II-2

If E is replaced by E' and L_C is replaced by L_C' Equation I-2 becomes Equation II-3 which is applicable to the continuous phase of a packed bed with solute transferred from the fluid phase to the packing.

$$E' e \left(\frac{d^2 c_C}{dz^2} \right) - L_C' \left(\frac{dc_C}{dz} \right) - K_D a \left(\frac{c_C}{m} - c_D \right) = 0$$

II-3

It is assumed that the solute concentration in each packing piece is uniform throughout the piece at the value c_D. Substitution of the central difference equivalents of differentials, as given in Equations II-4 and II-5, into Equation II-3 leads to Equation II-6 (8).

$$\left(\frac{dc_C}{dz}\right) = \frac{(c_{C,j+1} - c_{C,j-1})}{2d_i}$$

<div align="right">II-4</div>

$$\left(\frac{d^2c_C}{dz^2}\right) = \frac{(c_{C,j+1} - 2c_{C,j} + c_{C,j-1})}{d_i^2}$$

<div align="right">II-5</div>

$$(c_{C,j-1} - c_{C,j})\left(\frac{E'e}{d_iL_C'} + \frac{1}{2}\right) + (c_{C,j+1} - c_{C,j})\left(\frac{E'e}{d_iL_C'} - \frac{1}{2}\right) - \frac{K_D a d_i}{L_C'}\left(\frac{c_{C,j}}{m} - c_{D,j}\right) = 0$$

<div align="right">II-6</div>

By considering the interstices between the packing pieces of a packed bed as perfect mixing cells' an analogy can be drawn between a series of perfect mixers and a packed bed. For Equations II-2 and II-6 to be consistent the following equality must be satisfied.

$$\frac{2}{\lambda} = \left(\frac{L_C'}{e}\right)\left(\frac{d_p}{E'}\right),$$

<div align="right">II-7</div>

where

$$\lambda = \frac{d_i}{d_p} .$$

<div align="right">II-8</div>

The right hand side of Equation II-7 defines the Peclet number Pe':

$$Pe' = \left(\frac{L_C'}{e}\right)\left(\frac{d_p}{E'}\right)$$

<div align="right">II-9</div>

The mixing cell length, d_i, is supposed (112) to be the vertical centre-to-centre distance between the layers of packing pieces in an ordered packing system. Although exact values for d_i can be calculated for ordered packings, it would be expected that only an average value for d_i could be calculated for random packings. For a packed bed the value of λ is approximately one. Thus for this case Equations II-7 and II-9 yield the following well known relationship (44, 64, 92, 108, 109, 122, 123).

$$Pe' = 2$$

B. SPRAY COLUMN - PACKED BED ANALOGY.

For a spray column operating at steady state and with a solute which dissolves only in the continuous phase Equation I-2 reduces to

$$Ee\left(\frac{d^2 c_C}{dz^2}\right) = L_C\left(\frac{dc_c}{dz}\right)$$

II-10

Consider a spray column operating at steady state with axes of reference moving at the same velocity, u, as the rising dispersed phase drops. The drops appear stationary, on a time-average basis, relative to the co-ordinate system. That is, the system appears as a packed bed with the packing pieces not touching each other. Let y be the axial position relative to the moving co-ordinate axes. Thus,

$$y = z + ut$$

II-11

Let the axial mixing of the continuous phase be characterized by
an axial eddy diffusivity, E', relative to the moving co-ordinate
axes. Consider the control zone in the continuous phase as shown
in the following sketch. Let the control zone be fixed relative
to the moving co-ordinate system and be of incremental height (dy).
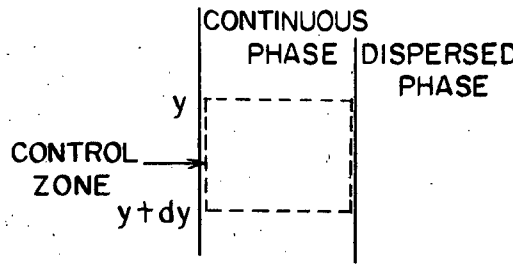
A solute mass balance over the control zone for unit area of
column and for an incremental time interval (dt) gives

$$\left[(L_C + ue)c_C + E'\frac{e\partial}{\partial y}\left(c_C + \left(\frac{\partial c_C}{\partial y}\right)(dy)\right)\right](dt) = \left[(L_C + ue)\left(c_C + \left(\frac{\partial c_C}{\partial y}\right)(dy) + E'e\left(\frac{\partial c_C}{\partial y}\right)\right](dt)$$

$$+ \left[uec_C - ue\left(c_C + \left(\frac{\partial c_C}{\partial y}\right)(dy)\right](dt)$$

II-12

The left-hand side of Equation II-12 represents the amount of
solute entering the control zone. The terms in the first set of
square brackets on the right-hand side of Equation II-12 represent
the amount of solute leaving the control zone. The terms in the
second set of square brackets on the right-hand side of Equation
II-12 represent the accumulation of solute in the control zone.

Equation II-12 simplifies to

$$E'e\left(\frac{\partial^2 c_C}{\partial y^2}\right) = L_C\left(\frac{\partial c_C}{\partial y}\right)$$

II-13

But

$$\left(\frac{\partial c_C}{\partial y}\right) = \left(\frac{dc_c}{dz}\right)$$

(124)

and

$$\left(\frac{\partial^2 c_C}{\partial y^2}\right) = \left(\frac{d^2 c_C}{dz^2}\right)$$

(124)

Therefore Equation II-13 becomes

$$E'e\left(\frac{d^2 c_C}{dz^2}\right) = L_C\left(\frac{dc_C}{dz}\right)$$

II-14

A comparison of Equations II-10 and II-14 shows that

$$E' = E$$

II-15

The identities given in Equations II-15 above, and in II-16, and II-17 below:

$$u = \frac{L_D}{1-e}$$

II-16

$$L_C' = L_C + ue$$

II-17

can be used with the following definition of Pe :

$$Pe = \left(\frac{L_C'}{e}\right)\left(\frac{d_p}{E}\right) = \left[\left(\frac{L_C}{e}\right) + \left(\frac{L_D}{1-e}\right)\right]\left(\frac{d_p}{E}\right)$$

II-18

and with Equation II-7 to produce Equation II-19.
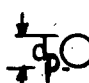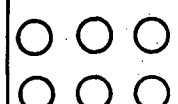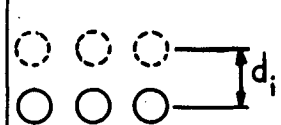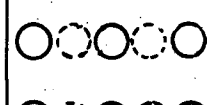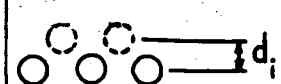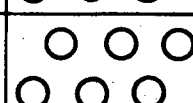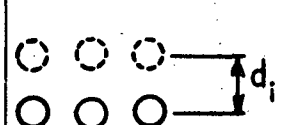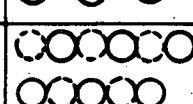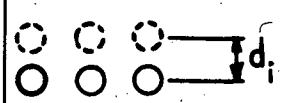
$$Pe = \frac{2}{\lambda}$$

II-19

For simple ordered lattice arragements of uniform spherical drops the vertical distance between layers of drops, d_i, is a function of the hold-up, h, and the drop diameter, d_p. The Peclet number, Pe, calculated from Equation II-19, is a function of h only. The function giving d_i and Pe are presented in the following table for six simple lattice arrangements of drops.

Each drop is supposed to be concentric with an imaginary larger sphere whose diameter is equal to the centre - to - centre distance between neighbouring drops. In the six lattice arrangements considered each imaginary sphere touches each of its nearest neighbours. These lattice arrangements represent the stable systems for beds of packed spheres and it is suggested by the author of this thesis that they are the ones most likely to be applicable for use in applying the mixing cell - packed bed analogy to a spray column.

It can be seen from the following table that for a given value of h all of the predicted Pe values lie in the range between the Pe values for the lattice arrangements of orthorhombic - 2 and rhombohedral - 1.

LATTICE	d_i	Pe	NUMBER OF NEAREST NEIGHBOURS	DIAGRAM
				⊙ LAYERS 1,3,5 ◌ LAYERS 2,4,6 (ONLY 2 LAYERS SHOWN)
CUBIC	$\sqrt[3]{\dfrac{\pi d_p^3}{6h}}$	$\sqrt[3]{\dfrac{48h}{\pi}}$	6	PLAN VIEW / FRONT VIEW d_i
ORTHO-RHOMBIC-1	$\sqrt[3]{\dfrac{\pi d_p^3}{8h}}$	$\sqrt[3]{\dfrac{64h}{\pi}}$	8	PLAN VIEW / FRONT VIEW d_i
RHOMBO-HEDRAL-1	$\sqrt[3]{\dfrac{\pi d_p^3}{12h}}$	$\sqrt[3]{\dfrac{96h}{\pi}}$	12	PLAN VIEW / FRONT VIEW d_i
ORTHO-RHOMBIC-2	$\sqrt[3]{\dfrac{\pi d_p^3}{3\sqrt{3}\,h}}$	$\sqrt[3]{\dfrac{24\sqrt{3}\,h}{\pi}}$	8	PLAN VIEW / FRONT VIEW d_i
TETRAGONAL	$\sqrt[3]{\dfrac{\pi\sqrt{3}\,d_p^3}{12h}}$	$\sqrt[3]{\dfrac{32\sqrt{3}\,h}{\pi}}$	10	PLAN VIEW / FRONT VIEW d_i
RHOMBO-HEDRAL-2	$\sqrt[3]{\dfrac{2\pi d_p^3}{9\sqrt{3}\,h}}$	$\sqrt[3]{\dfrac{36\sqrt{3}\,h}{\pi}}$	12	PLAN VIEW / FRONT VIEW d_i

APPENDIX III

ANALYSIS OF PISTON SAMPLE RESULTS TO PRODUCE THE AVERAGE CONTIN-
UOUS PHASE CONCENTRATION, EXCLUDING THE CONTRIBUTION FROM THE
WAKES, IN THE PISTON SAMPLE AT THE TIME OF SAMPLING

The analysis of piston sample results to produce the average
continuous phase concentration, excluding the contribution from
the wakes, in the piston at the time of sampling is based on a
model in which it is pictured that each drop carries some
continuous phase with it, for example in its wake (21, 22, 23,
24, 26, 121). It is assumed that on the average a volume v_B of
continuous phase of average solute concentration c_B is carried
up the column past a given elevation by each rising dispersed
phase drop. Thus the frequency, $\dfrac{L_D}{v_D}$, of drops passing through
unit area at a given elevation is equal to the frequency, $\dfrac{L_B}{v_B}$,
of passage of volumes, v_B, of continuous phase in the form of
a backmixing stream.

i.e.
$$\frac{L_D}{v_D} = \frac{L_B}{v_B}$$

Thus

$$\frac{v_D}{v_B} = \frac{L_D}{L_B}$$

III-1

The number of dispersed phase drops in a piston sample is

$$\frac{V_D}{v_D} ,$$

and the number of packets of backmixed continuous phase in a piston sample is

$$\frac{V_B}{v_B} .$$

Therefore,

$$\frac{V_D}{v_D} = \frac{V_B}{v_B}$$

or

$$\frac{v_D}{v_B} = \frac{V_D}{V_B}$$

III-2

From Equations III-1 and III-2,

$$\frac{V_D}{V_B} = \frac{L_D}{L_B}$$

or

$$V_B = \frac{L_B V_D}{L_D}$$

III-3

Consider the lower portion of a spray column as shown in Figure III-1. It is assumed that the descending continuous phase is fully mixed at any given elevation. A mass balance on solute over the section of column shown in Figure III-1 yields

$$L_B c_B + L_D c_D + L_C c_C^o = L_C c_C + L_B c_C + L_D c_D^i$$

The above equation can be rearranged to give

$$\frac{L_B V_D}{L_D}(c_B - c_C) = \frac{L_C V_D}{L_D}(c_C - c_C^o) + V_D(c_D^i - c_D)$$

III-4

Now consider a piston sample. Figure III-2a represents this sample at the instant of sampling. Figure III-2b represents the same sample but later in time: when the sample is analysed. A mass balance on solute in the piston sample over the time between sampling and analysis yields

$$V_D c_D + V_B c_B + (V_C - V_B)c_C = V_D c_D^a + V_C c_C^a$$

III-5

Substituting for V_B from Equation III-3 in Equation III-5 and then rearranging gives

$$\frac{L_B V_D}{L_D}(c_B - c_C) = V_D(c_D^a - c_D) + V_C(c_C^a - c_C)$$

III-6

Equating

$$\frac{L_B V_D}{L_D}(c_B - c_C)$$

as given by each of Equations III-4 and III-6 results in:

$$\frac{V_D L_C}{L_D}(c_C - c_C^o) + V_D(c_D^i - c_D) = V_D(c_D^a - c_D) + V_C(c_C^a - c_C)$$

III-7

Equation III-7 can be rearranged to give

$$
c_C = \left[\frac{\left(\dfrac{V_C}{V_D}\right) c_C^a + c_D^a - c_D^i + \left(\dfrac{L_C}{L_D}\right) c_C^o}{\dfrac{L_C}{L_D} + \dfrac{V_C}{V_D}} \right]
$$

<div align="right">III-8</div>

The concentration, c_C, given by Equation III-8 is the average

solute concentration in a piston sample, excluding the

contribution from the wakes, at the time of sampling.
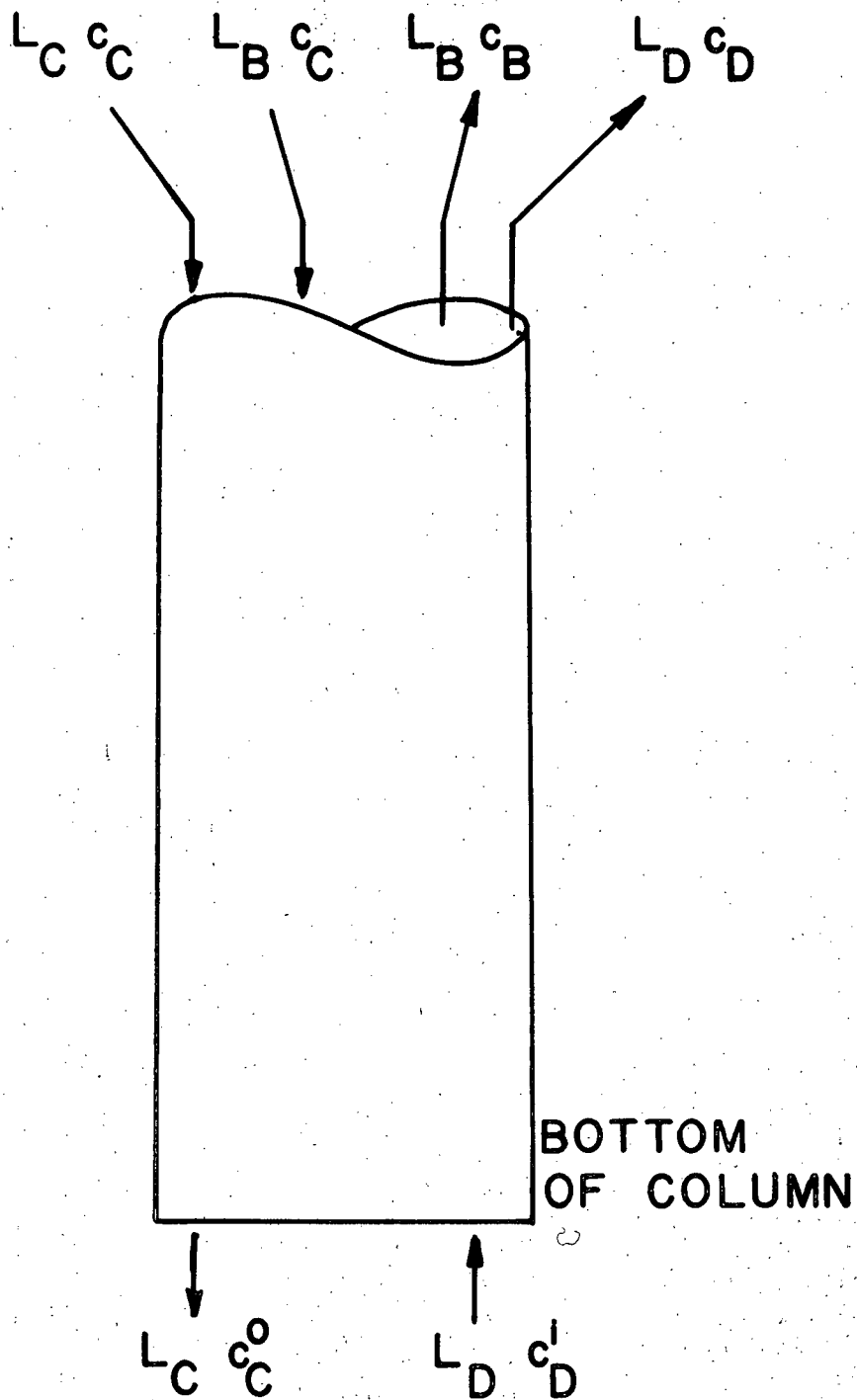
FIGURE III-1. LOWER PORTION OF A SPRAY COLUMN

V_D c_D

V_B c_B

$(V_C - V_B) c_C$
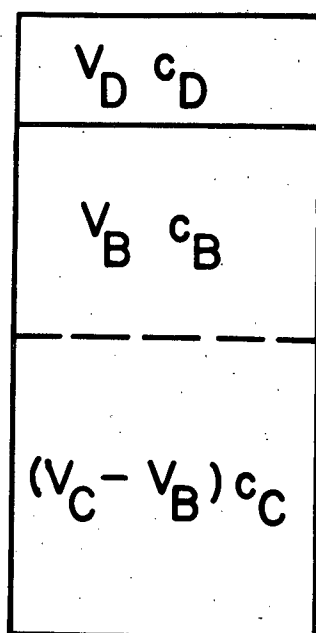
PISTON SAMPLE
AT THE TIME
OF SAMPLING

(a)

V_D c_D^a

V_C c_C^a
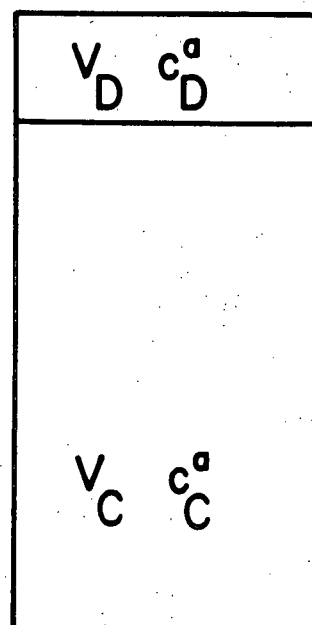
PISTON SAMPLE
AT THE TIME
OF ANALYSIS

(b)

FIGURE III-2.   THE EFFECT OF TIME ON A PISTON SAMPLE

APPENDIX IV

CALCULATIONS AND TABULATED RESULTS FOR AXIAL EDDY DIFFUSIVITY

DETERMINATIONS AND DROP SIZE DISTRIBUTIONS

a) CALCULATIONS.

A specimen hand calculation is presented starting from a data sheet shown in Table IV-1. (Actual data sheets were more abbreviated than the one shown in Table IV-1.)

RUN 50

Water flowrate = 27.7 $ft.^3/hr. ft.^2$

Ketone flowrate = 54.7 $ft.^3/hr. ft.^2$

Tracer flowrate = 0.310 $ft.^3/hr. ft.^2$

Column I.D. = 1.5 in. Cross-sectional area of column $\doteq$ 0.01227 $ft.^2$

Sampling rate = 1 ml./min. = 0.002119 $ft.^3/hr.$ = 0.1727 $ft.^3/hr. ft.^2$

Ketone hold-up = 4.7%

TABLE IV-1.   DATA SHEET.

RUN NO. 50   DATE: 25 AUG. 1966

Column I.D. = 1.5-in.   Tracer feed conc.=23,000-microgm./ml.
Nozzle tip average I.D.=0.103-in.   9 open nozzle tips
Water rotameter reading = 86-mm. L_C=27.7-ft.^{3}/hr.ft.^{2}
Ketone rotameter reading=108-mm. L_D=54.74-ft.^{3}/hr.ft.^{2}
Tracer rotameter reading=7.5-mm. L_T=0.310-ft.^{3}/hr.ft.^{2}
Average temperature of the fluids in the column = 72°F
Sampling rate = 1-ml./min.   Steady state time=1-hr.

ANALYSIS OF SAMPLES (See figure 10 for sampling positions)

Sampling position	Sample collection tube	Dilution factor	Absorption reading on spectrophometer, %
1	G1	25	54.7
2	G2	10	58.0
3	G3	5	48.3
4	G4	5	31.8
5	G5	1	40.6
6	G6	1	20.6
7	G7	1	8.1
8	G8	1	3.4
9	G9	1	1.6
10	G10	1	0.9
aqueous phase leaving column	G11	100	41.7

CALIBRATION OF ATOMIC ABSORPTION SPECTROPHOTOMETER

Sample conc., microgr. /ml.	Absorption, %
0	0.0
1	18.7
3	46.7
5	64.3
7	76.2
9	84.3

PISTON SAMPLE

Trial	A	B	C	D	E	F	G
1	0.95	6.45	0.95	6.25	116.4	5.3	4.55
2	0.95	6.85	0.95	6.65	116.4	5.7	4.90
3	1.0	6.60	1.0	6.40	116.4	5.4	4.64

A=reading of ketone/air interface level, ml.
B=reading of water/ketone interface level, ml.
C=corrected A from calibration curve, ml.
D=corrected B from calibration curve, ml.
E=total volume in sample, ml.
F=volume of ketone in sample, ml.
G=hold-up of dispersed phase, %

AQUEOUS PHASE OUTLET SAMPLE

Collection time=40-min.
Weight of collection flask=
   1-lb. 15-oz.
Weight of flask + sample=
   16-lb. 2-oz.
Weight of sample=14-lb.3-oz.

KETONE PHASE OUTLET SAMPLE

Collection time=10-min.
Weight of coll. flask=1-lb.5-oz.
Weight of flask + sample=6-lb.14-oz.
Weight of sample=5-lb.9-oz.

Calibration of atomic absorption spectrophotometer

Sodium conc.	Absorption %	Absorbance	$(Absorbance)^2$	(Conc.) (Absorbance)
0	0.0	0.0000	0.0000	0.0000
1	18.7	0.0899	0.0081	0.0899
3	46.7	0.2733	0.0747	0.8199
5	64.3	0.4473	0.2001	2.2365
7	76.2	0.6234	0.3886	4.3638
9	84.3	0.8041	0.6466	7.2369
Total 25		2.2380	1.3181	14.7470

Let the calibration line be

$$conc. = (m_1)(absorbance) + k_1$$

By least squares fit

$$m_1 = \frac{(2.2380)(25) - (6)(14.7470)}{(2.2380)^2 - (6)(1.3180)} = 11.22$$

and

$$k_1 = \frac{(25)(1.3181) - (2.2380)(14.7470)}{(6)(1.3181) - (2.2380)^2} = -0.018$$

Therefore,

$$conc. = (11.22)(absorbance) - 0.018$$

Table IV-2 shows the calculation of the solute concentration at the sampling positions in the column. Also shown in Table IV-2 are quantities required for further computations. The dimensions of each piece of Pyrex pipe in the test section of the column are given in Table VI-1, Appendix VI.

Water balance

Density of MIBK-saturated water = 0.996 gm./ml. (Measured by means
of specific gravity bottle)

Aqueous phase leaving the lower end of the column =

14 lb. 3 oz. in 40 min. = 27.897 $ft.^3/hr.ft.^2$

Sampling rate = 1 ml./min. = 0.1727 $ft.^3/hr.ft.^2$

Tracer feed rate = 0.310 $ft.^3/hr.ft.^2$

Aqueous phase fed to the column = 27.7 $ft.^3/hr.ft.^2$

Apparent loss = $\left[\dfrac{27.7 + 0.310 - 0.1727 - 27.897}{27.7} \right] (100)\% = -0.22\%$

Ketone balance

Density of water-saturated MIBK = 0.806 gm./ml. (Measured by means
of specific gravity bottle)

Ketone phase leaving the Elgin head of the column =

5 lb. 9 oz. in 10 min. = 54.07 $ft.^3/hr.ft.^2$

Ketone phase fed to the column = 54.74 $ft.^3/hr.ft.^2$

Apparent loss = $\left[\dfrac{54.74 - 54.07}{54.74} \right] (100)\% = 1.22\%$

Tracer balance

The amount of tracer leaving the column due to sampling is

neglected.

TABLE IV-2. CALCULATION OF QUANTITIES USED FOR THE CALCULATION OF E.

Sampling position (Figs. 9 and 10)	Height above tracer distributor =w,ft.	Dilution factor	Absorption %	Absorbance	Measured conc., microgm. per ml.	Sample conc. =C_C, microgm. per ml.	$Log_e(C_C)$ = q	w^2	wq	q^2
1	0.5115	25	54.7	0.3439	3.8406	96.015	4.564	0.2616	2.3345	20.8301
2	1.014	10	58.0	0.3768	4.2097	42.097	3.740	1.0282	3.7924	13.9876
3	1.517	5	48.3	0.2865	3.1965	15.9825	2.771	2.3013	4.2036	7.6784
4	2.020	5	31.8	0.1662	1.8468	9.2340	2.223	4.0804	4.4905	4.9417
5	2.527	1	40.6	0.2262	2.5200	2.2500	0.9423	6.3857	2.3812	0.8543
6	3.015	1	20.6	0.1002	1.1062	1.1062	0.1008	9.0902	0.3039	0.0102
7	3.518	1	8.1	0.0367	0.3938	0.3938	-0.9319	12.3763	-3.2784	0.8684
8	4.028	1	3.4	0.0150	0.1503	0.1503	-1.895	16.2248	-7.6331	3.5910
9	4.537	1	1.6	0.0070	0.0605	0.0605	-2.805	20.5844	-12.7263	7.8680
10	5.045	1	0.9	0.0039	0.0258	0.0258				
11**		100	41.7	0.2343	2.6108	261.08				
Total*	22.6875					167.559	8.709	72.3329	-6.1317	60.6297

* For positions 1 to 9 (incl.) only. (Sample conc. at position 10 is less than 0.05 microgm./ml.)

**Position 11 refers to the aqueous phase leaving the column.

Tracer leaving the lower end of the column =

$(27.897)(261.08)=7,283$ (microgm./ml.)(ft.^{3})/(hr.)(ft.^{2} of column)

Tracer fed to the column = $(0.310)(23,000) = 7,130$ (microgm./ml.)

(ft.^{3})/(hr.)(ft.^{2} of column)

Apparent loss $=\left[\dfrac{7,130 - 7,283}{7,130}\right] (100) \% = -2.15\%$

Axial eddy diffusivity

The following statistical computations are based on the methods

described by Bennett and Franklin (125).

n = the number of sample concentrations less than 0.05-microgm./

   ml. = 9

$S(q,w)= \sum(q)(w) - \dfrac{\sum(q)\sum(w)}{n} = -6.1317 - \dfrac{(22.6875)(8.709)}{9} = -28.0856$

$S(q^2) = \sum(q^2) - \dfrac{(\sum q)^2}{n} = 60.6297 - \dfrac{8.709^2}{9} = 52.2023$

$S(w^2) = \sum(w^2) - \dfrac{(\sum w)^2}{n} = 72.3329 - \dfrac{22.6875^2}{9} = 15.1415$

$\sqrt{S(w^2)} = 3.8912$

$S^2_{q,w} = \dfrac{(S(q^2))(S(w^2)-(S(q,w))^2}{(n-2)(S(w^2))} = \dfrac{(52.2023)(15.1415)-(-28.0856)^2}{(7)(15.1415)} = 0.01529$

$S_{q,w} = 0.1236$

A least squares fit (125) of the data to the equation

   $q = (M)(w) + K$

yields

$K = \dfrac{(\sum q)(\sum w^2) - \sum((q)(w))\sum w}{(n)(\sum(w^2)) - (\sum w)^2} = \dfrac{(8.709)(72.3329)-(-6.1317)(22.6875)}{(9)(72.3329) - (22.6875)^2}$

$= 5.640$

and

$$M = \frac{S(q,w)}{S(w^2)} = \frac{-1.8549}{15.1415} = -1.8549$$

95% confidence limits on M are (125)

$$M \pm \frac{(t_{n-2,\alpha})\,(S_{q,w})}{\sqrt{S(w^2)}}$$

where

$t_{n-2,\alpha}$ = the value of the t-distribution for (n-2) degrees

of freedom and $(100)(1-\alpha)$ % confidence limits.

$$t_{7,0.05} = 2.3646 \qquad (125)$$

95% confidence limits on M are

$$-1.8549 \pm \frac{(2.3646)(0.1236)}{3.8912} = -1.8549 \pm 0.07511$$
$$= -1.9300 \text{ to } -1.7798$$

(It should be noted that for runs where n = 2 no statistical test regarding the confidence of results can be performed. For runs where n = 3 the 95% confidence limits on M are likely to be wide since

$$t_{1,0.05} = 12.71.$$

In fact the 95% confidence limits calculated for runs where n = 3 are not likely to represent the true situation because it is not possible to include non-statistical reasoning in the statistical analysis. For example, there is no reason to doubt the linearity of the relationship between q and ω for runs where n is greater than 3.)

The superficial axial eddy diffusivity, (Ee), is given by the following equation.

$$(Ee) = \frac{-L_C}{M}$$

$$(Ee) = \frac{-27.7}{-1.8549} = 14.93 \text{ ft.}^2/\text{hr.}$$

The flowrate, L_C, of aqueous phase fed to the column can be measured and kept constant to within approximately 1% of L_C. On the assumption that the recorded value of L_C comes from a normal distribution an estimate of the standard deviation, σ_{LC}, of L_C is given by (125)

$$\sigma_{LC} = \frac{(L_C/100)}{3} \cdot$$

Therefore

$$\sigma_{LC} = \frac{27.7}{300} = 0.09233$$

An estimate of the variance, σ_M^2, of M is given by

$$\sigma_M^2 = \frac{S_{q,w}^2}{S(w^2)} = \frac{0.01529}{15.1415} = 0.001010$$

The variance, σ_{Ee}^2, of (Ee) is given by the following equation (125)

$$\sigma_{Ee}^2 = (Ee)^2 \left[\left(\frac{\sigma_{LC}}{L_C} \right)^2 + \left(\frac{\sigma_M}{M} \right)^2 \right]$$

$$= (14.93)^2 \left[\left(\frac{0.09233}{27.7} \right)^2 + \left(\frac{0.00101}{3.4407} \right) \right] = 0.06791$$

Therefore

$$\sigma_{Ee} = 0.2606$$

In calculating 95% confidence limits for (Ee) it must be remembered that M was determined from n data points. A reasonable approximation is to assume that (Ee) comes from a t-distribution

with (n-2) degrees of freedom. Therefore the 95% confidence limits on (Ee) are

$$(Ee) \pm (t_{n-2, \ 0.05})(\sigma_{\overline{Ee}})$$

$$= 14.93 \pm (2.3646)(0.2606) = 14.93 \pm 0.62$$

$$= 14.31 \text{ to } 15.55$$

Now

$$e = \left(1 - \frac{hold\text{-}up}{100}\right)$$

The three values of e calculated from hold-up measurements are

$$e = 1 - \frac{4.55}{100} = 0.9545$$

$$e = 1 - \frac{4.90}{100} = 0.9510$$

$$e = 1 - \frac{4.64}{100} = 0.9536$$

The arithmetic average of $e = \frac{0.9545 + 0.9510 + 0.9536}{3} = 0.9530$

The best estimate, σ_e^2, of the variance of e is given by

$$\sigma_e^2 = \frac{(n)(\sum e^2) - (\sum e)^2}{(n)(n-1)} = \frac{(3)(2.72482421) - (2.8591)^2}{(3)(2)}$$

$$= 0.000003303$$

The axial eddy diffusivity, E, is given by

$$E = \frac{(Ee)}{e} = \frac{14.93}{0.9530} = 15.67$$

The variance, σ_E^2, of E is given by

$$\sigma_E^2 = (E^2)\left[\left(\frac{\sigma_{\overline{Ee}}}{Ee}\right)^2 + \left(\frac{\sigma_e}{e}\right)^2\right]$$

$$= (15.67^2)\left[\left(\frac{0.2606}{14.93}\right)^2 + \frac{0.000003303}{(0.9530)^2}\right] = 0.0748$$

Therefore

$$\sigma_E = 0.2735$$

On the assumption that E comes from a t-distribution with (n-2) degrees of freedom the 95% confidence limits for E are taken to be

$$E \pm (t_{n-2,0.05})(\sigma_E) = 15.67 \pm (2.3646)(0.2735)$$
$$= 15.67 \pm 0.65 = 15.02 \text{ to } 16.32$$

The Peclet number, Pe, is calculated from the following equation.

$$Pe = \frac{(d_p)\left(\dfrac{L_D}{1-e} + \dfrac{L_C}{e}\right)}{E}$$

II-18

where d_p is the dispersed phase drop diameter.

$$Pe = \frac{\left(\dfrac{0.135}{12}\right)\left(\dfrac{54.74}{0.047} + \dfrac{27.7}{0.953}\right)}{15.67} = 0.857$$

Table IV-3 shows the results of the above calculations as carried out on an IBM-7040 electronic computer.

b) TABULATED RESULTS

Table IV-4 gives the reduced concentration profiles, the dispersed phase hold-up, the number of experimental points used for the estimation of the axial eddy diffusivity, the axial eddy diffusivity, and the Peclet number for each run carried out with the $1\frac{1}{2}$-in. I.D. column. The reduced concentration profile, the number of experimental points used for the estimation of the

TABLE IV-3. TYPICAL COMPUTER RESULTS

RUN 50

WATER FLOWRATE = 27.70 CU.FT./(HR. SQ.FT.)
KETONE FLOWRATE = 54.74 CU.FT./(HR. SQ.FT.)
TRACER FLOWRATE = 0.310 CU.FT./(HR. SQ.FT.)
NOZZLE TIP AVERAGE DIA. = 0.103 IN.   EQUIVALENT DROP DIA. = 0.135 IN.
AVERAGE VELOCITY OF DISPERSED PHASE IN NOZZLE TIPS = 0.36 FT./SEC.
COLUMN I.D. = 1.5 IN.   COLUMN HEIGHT (NOZZLE TIPS TO INTERFACE) = 10-FT. 3 1/8-IN.
TEMPERATURE = 72 °F

CALIBRATION OF ATOMIC ABSORPTION SPECTROPHOTOMETER

SOD.CONC.	PER CENT ABSORPTION	ABSORBANCE	CONCENTRATIONS ARE IN MICROGM./ML.
0	0.0	0.000	
1	18.7	0.090	
3	46.7	0.273	
5	64.3	0.447	
7	76.2	0.623	
9	84.3	0.804	

CONCENTRATION = 11.219*ABSORBANCE-0.018

POSITION (SEE FIG. 10)	DILUTION FACTOR	PER CENT ABSORPTION	ABSORBANCE	MEASURED CONC.	SAMPLE CONC.	LOG.E CONC.	REDUCED CONC.
1	25	54.7	0.344	3.840	96.004	4.564	367.705
2	10	58.0	0.377	4.209	42.087	3.740	161.197
3	5	48.3	0.287	3.196	15.981	2.771	61.210
4	5	31.8	0.166	1.847	9.233	2.223	35.365
5	1	40.6	0.226	2.520	2.520	0.924	9.651
6	1	20.6	0.100	1.106	1.106	0.101	4.236
7	1	8.1	0.037	0.393	0.393	-0.933	1.507
8	1	3.4	0.015	0.150	0.150	-1.894	0.576
9	1	1.6	0.007	0.061	0.061	-2.805	0.232
10	1	0.9	0.004	0.026	0.026	-3.650	0.100
11	100	41.7	0.234	2.611	261.089	5.565	1000.000

(POSITION 11 REFERS TO THE AQUEOUS PHASE LEAVING THE COLUMN)

WATER MASS BALANCE APPARENT LOSS = -0.201 PER CENT
KETONE MASS BALANCE APPARENT LOSS = 1.257 PER CENT
TRACER MASS BALANCE APPARENT LOSS = -2.139 PER CENT
KETONE HOLD-UP = 4.70 PER CENT

LOG.E(CONC)= -1.8549*(HEIGHT ABOVE TRACER INJECTION)+5.6414   95 PC CONFIDENCE LIMITS ON SLOPE ARE   -1.9404 TO -1.7693
LOG.10(CONC)= -4.2718*(HEIGHT ABOVE TRACER INJECTION)+LOG.10(281.86)

NUMBER OF POINTS FOR ESTIMATION OF EDDY DIFFUSIVITY = 9

SUPERFICIAL AXIAL EDDY DIFFUSIVITY =14.93 SQ.FT./HR.   95 PC CONFIDENCE LIMITS ARE 14.23 SQ.FT./HR. TO 15.63 SQ.FT./HR.

AXIAL EDDY DIFFUSIVITY =15.67 SQ.FT./HR.   95 PC CONFIDENCE LIMITS ARE 14.93 SQ.FT./HR. TO 16.41 SQ.FT./HR.

PECLET NUMBER = 0.858

TABLE IV-4. AXIAL EDDY DIFFUSIVITY RESULTS FOR THE 1½-IN. I.D. COLUMN

AVERAGE INSIDE DIAMETER OF NOZZLE TIPS = 0.126 IN.
DISPERSED PHASE EQUIVALENT DROP DIAMETER = 0.155 IN.
AVERAGE VELOCITY OF DISPERSED PHASE IN NOZZLE TIPS = 0.36 FT./SEC.
COLUMN INSIDE DIAMETER = 1.5 IN.
COLUMN HEIGHT (NOZZLE TIPS TO INTERFACE) = 10-FT. 3 1/8-IN. (SEE FIG. 10 FOR DIAG. OF APPARATUS)
LW = CONTINUOUS PHASE SUPERFICIAL VELOCITY, CU.FT./(HR. SQ.FT.)
LK = DISPERSED PHASE SUPERFICIAL VELOCITY, CU.FT./(HR. SQ.FT.)
LT = TRACER FEED SUPERFICIAL VELOCITY, CU.FT./(HR. SQ.FT.)
HOLD-UP = VOLUMETRIC PERCENTAGE OF DISPERSED PHASE IN COLUMN
PP = NUMBER OF SAMPLE CONCENTRATIONS USED FOR ESTIMATION OF AXIAL EDDY DIFFUSIVITY
E = AXIAL EDDY DIFFUSIVITY WITH 95 PER CENT CONFIDENCE LIMITS, SQ.FT./HR.
PE = PECLET NUMBER BASED ON DISPERSED PHASE DROP DIAMETER
ER1 = WATER BALANCE APPARENT LOSS, PER CENT
ER2 = KETONE BALANCE APPARENT LOSS, PER CENT
ER3 = TRACER BALANCE APPARENT LOSS, PER CENT

RUN	LW	LK	LT	TEMP °F	REDUCED CONCENTRATION AT SAMPLING POINTS (SEE FIG. 10) 1	2	3	4	5	6	7	8	9	10	HOLD-UP	PP	E	PE	ER1	ER2	ER3
126	9.0	36.5	0.112	71	837.39	720.74	631.46	530.62	405.09	359.35	318.52	282.61	254.87	215.17	2.7	10	30.49±2.66	0.59	1.08	-1.05	2.55
127	18.2	36.5	0.200	71	760.53	576.77	417.22	304.01	198.41	147.83	105.04	76.49	60.75	46.53	2.5	10	29.63±1.73	0.64	2.65	0.14	-1.35
128	27.7	36.5	0.310	70	694.03	532.74	328.25	184.81	89.88	56.47	34.84	20.22	19.74	11.59	7.6	10	30.26±2.73	0.62	1.23	-1.05	6.11
129	36.5	36.5	0.350	72	612.47	357.07	200.93	108.89	47.00	24.43	14.15	7.92	5.27	2.46	2.6	10	30.46±1.46	0.62	1.45	0.14	5.02
130	48.4	36.5	0.680	72	520.28	206.90	93.93	32.37	12.59	5.74	3.11	1.37	0.62	0.27	2.9	10	30.04±1.34	0.56	-1.45	1.33	-0.45
77	9.0	54.7	0.112	72	707.79	549.90	439.74	342.22	238.22	201.20	146.76	124.30	93.92	73.79	4.7	10	18.77±0.76	0.82	-1.77	-0.96	-5.91
76	18.2	54.7	0.200	72	624.01	415.69	142.03	169.91	87.35	52.99	31.38	22.71	14.38	8.29	4.7	10	19.85±0.86	0.77	1.37	1.26	-3.62
75	27.7	54.7	0.310	70	407.72	188.50	102.32	40.93	16.77	10.24	4.91	2.47	0.92	0.45	4.7	10	19.47±0.69	0.79	-1.21	1.26	3.38
79	36.5	54.7	0.350	71	355.61	168.54	47.38	22.79	9.55	3.18	1.36	0.46	0.18	0.08	4.6	8	20.27±0.96	0.78	1.29	1.26	1.25
78	48.4	54.7	0.682	71	312.21	85.19	25.34	7.08	1.73	0.49	0.14	0.05	0.03	0.03	4.8	6	19.74±0.57	0.78	0.54	1.26	0.44
82	9.0	73.0	0.112	71	742.70	584.97	386.07	280.12	165.41	133.78	83.59	61.69	49.10	28.76	6.8	10	13.44±0.73	1.05	2.28	1.71	9.13
81	18.2	73.0	0.200	70	469.37	200.41	102.20	48.95	22.06	11.41	6.13	2.86	1.23	0.61	6.7	10	13.48±0.29	1.06	1.37	0.15	4.04
80	27.7	73.0	0.310	71	247.88	88.00	26.40	11.08	3.51	1.10	0.41	0.16	0.04	0.00	6.7	7	13.88±0.51	1.04	-1.13	-0.37	3.43
131	36.5	73.0	0.350	71	400.42	123.95	27.75	4.28	0.94	0.27	0.11	0.02	0.00	0.00	7.0	6	13.00±1.10	1.07	-1.41	0.67	-3.64
132	48.4	73.0	0.680	70	235.96	98.01	7.16	0.64	0.20	0.03	0.01	0.02	0.01	0.01	7.2	5	13.73±4.03	1.00	1.94	1.19	0.96
83	9.0	91.2	0.112	71	643.46	442.38	263.43	190.87	108.02	77.57	52.92	33.13	20.43	11.54	9.3	10	11.39±0.46	1.13	-0.56	0.56	0.29
84	18.2	91.2	0.200	70	322.17	127.69	55.90	16.60	7.49	3.24	1.31	0.45	0.09	0.00	9.2	8	10.80±0.42	1.21	1.37	0.98	-1.99
86	27.7	91.2	0.310	72	169.15	49.23	8.32	2.39	0.64	0.16	0.06	0.02	0.00	0.01	9.4	5	10.87±1.23	1.19	-1.04	0.14	-11.01
85	36.5	91.2	0.350	72	111.50	18.66	2.28	0.52	0.16	0.13	0.04	0.00	0.00	0.00	9.6	4	11.15±2.18	1.14	1.17	1.39	1.40
133	48.4	91.2	0.680	70	101.15	11.64	0.95	0.09	0.02	0.01	0.00	0.00	0.01	0.00	9.8	3	11.55±6.27	1.10	0.48	1.39	0.34
88	9.0	109.5	0.112	71	477.46	321.85	182.33	116.59	64.74	51.73	26.18	18.38	10.31	6.24	12.0	10	10.71±0.44	1.11	0.91	1.00	1.71
87	18.2	109.5	0.200	73	293.75	123.06	36.80	12.68	3.74	2.13	0.46	0.14	0.00	0.00	12.1	7	9.75±0.82	1.23	-0.74	1.00	1.46
90	27.7	109.5	0.310	74	155.20	38.37	6.12	2.92	0.82	0.24	0.10	0.05	0.03	0.03	11.8	6	12.34±1.74	1.00	-1.53	1.43	0.20
89	36.5	109.5	0.350	73	101.39	13.85	1.69	0.43	0.16	0.07	0.05	0.03	0.03	0.05	12.1	4	11.27±2.98	1.09	-0.06	0.57	-1.05
134	48.4	109.5	0.680	70	86.18	7.53	0.27	0.02	0.01	0.00	0.00	0.01	0.00	0.02	12.1	3	9.63±10.7	1.29	-0.48	1.00	-3.24
94	9.0	127.7	0.112	75	595.54	354.25	189.80	121.78	60.06	45.56	23.91	15.67	10.33	5.57	13.7	10	10.25±0.46	1.19	1.96	0.13	-3.93
93	18.2	127.7	0.200	75	304.16	145.78	29.33	9.84	3.26	1.28	0.37	0.13	0.11	0.11	13.6	7	9.31±0.71	1.33	-0.88	-1.17	1.83
92	27.7	127.7	0.310	75	136.22	31.81	4.30	1.10	0.31	0.15	0.11	0.09	0.11	0.09	13.7	5	10.43±1.61	1.19	-1.98	-0.31	-0.39
91	36.5	127.7	0.350	75	80.62	8.82	0.94	0.10	0.06	0.06	0.04	0.04	0.08	0.04	13.8	3	9.56±0.62	1.31	1.01	0.99	3.67
135	48.4	127.7	0.680	71	73.37	6.30	0.36	0.04	0.01	0.02	0.00	0.01	0.00	0.00	14.8	3	10.74±6.04	1.10	1.04	-1.17	-1.69

TABLE IV - 4. CONTINUED (1)

AVERAGE INSIDE DIAMETER OF NOZZLE TIPS = 0.103 IN.
DISPERSED PHASE EQUIVALENT DROP DIAMETER = 0.135 IN.
AVERAGE VELOCITY OF DISPERSED PHASE IN NOZZLE TIPS = 0.36 FT./SEC.
COLUMN INSIDE DIAMETER = 1.5 IN.
COLUMN HEIGHT (NOZZLE TIPS TO INTERFACE) = 10-FT. 3 1/8-IN. (SEE FIG. 10 FOR DIAG. OF APPARATUS)
LM = CONTINUOUS PHASE SUPERFICIAL VELOCITY, CU.FT./(HR. SQ.FT.)
LK = DISPERSED PHASE SUPERFICIAL VELOCITY, CU.FT./(HR. SQ.FT.)
LT = TRACER FEED SUPERFICIAL VELOCITY, CU.FT./(HR. SQ.FT.)
HOLD-UP = VOLUMETRIC PERCENTAGE OF DISPERSED PHASE IN COLUMN
PP = NUMBER OF SAMPLE CONCENTRATIONS USED FOR ESTIMATION OF AXIAL EDDY DIFFUSIVITY
E = AXIAL EDDY DIFFUSIVITY WITH 95 PER CENT CONFIDENCE LIMITS, SQ.FT./HR.
PE = PECLET NUMBER BASED ON DISPERSED PHASE DROP DIAMETER
ER1 = WATER BALANCE APPARENT LOSS, PER CENT
ER2 = KETONE BALANCE APPARENT LOSS, PER CENT
ER3 = TRACER BALANCE APPARENT LOSS, PER CENT

RUN	LM	LK	LT	TEMP °F	REDUCED CONCENTRATION AT SAMPLING POINTS (SEE FIG. 10)										HOLD-UP	PP	E	PE	ER1	ER2	ER3
					1	2	3	4	5	6	7	8	9	10							
42	9.0	30.4	0.112	73	753.80	667.83	570.77	491.85	397.31	352.38	287.87	243.90	220.82	179.30	2.0	10	28.75±1.14	0.59	-1.45	1.36	-0.58
41	18.2	30.4	0.200	72	707.53	553.41	394.93	296.47	216.56	154.04	116.61	86.90	62.63	43.73	2.2	10	30.28±0.70	0.52	1.56	0.11	1.08
40	27.7	30.4	0.310	70	557.18	379.70	245.61	152.31	94.03	59.91	39.94	26.89	14.25	11.05	2.1	10	32.61±0.88	0.50	0.93	-1.00	-4.32
39	36.5	30.4	0.350	71	530.33	313.13	156.83	89.60	45.57	24.26	14.02	8.51	4.74	2.44	2.3	10	31.46±0.88	0.49	-0.96	-0.11	2.61
38	48.4	30.4	0.680	72	321.45	157.78	75.85	34.72	13.26	5.85	2.84	1.39	0.73	0.27	2.4	10	31.77±1.01	0.46	-0.48	1.22	1.38
65	9.0	36.5	0.112	72	785.37	674.85	535.94	456.83	362.18	308.49	263.29	220.44	185.25	150.64	2.7	10	25.46±0.81	0.59	-1.45	1.25	0.22
64	18.2	36.5	0.310	73	474.64	421.40	273.44	183.72	122.93	80.36	51.39	36.77	28.33	18.32	2.8	10	24.27±0.87	0.61	-1.78	1.25	-5.51
63	27.7	36.5	0.310	73	468.70	298.94	154.47	79.92	39.52	20.37	12.03	6.25	3.52	1.65	2.8	10	22.69±0.65	0.65	-1.30	-0.97	1.01
62	36.5	36.5	0.350	72	468.71	218.69	93.48	55.69	23.24	11.61	5.91	2.83	1.38	0.69	2.8	10	26.19±0.62	0.57	-0.96	-0.99	0.94
66	48.4	36.5	0.680	72	252.25	125.44	37.92	19.80	7.38	2.51	1.28	0.42	0.15	0.04	2.9	8	27.31±1.48	0.54	1.04	-0.97	1.28
52	9.0	54.7	0.112	69	606.70	445.86	321.65	247.82	186.34	148.54	100.96	78.02	54.98	41.13	4.5	10	16.00±0.48	0.86	-0.80	1.26	-4.05
51	18.2	54.7	0.200	71	561.34	298.12	138.22	82.65	36.99	18.09	10.89	5.77	2.66	1.50	4.6	10	14.51±0.42	0.74	0.17	1.26	-1.41
50	27.7	54.7	0.310	71	367.71	161.20	61.21	35.37	9.65	4.24	1.51	0.58	0.23	0.10	4.7	6	15.67±0.74	0.86	-0.20	1.26	-2.14
49	36.5	54.7	0.350	72	282.28	91.35	17.18	6.58	1.73	0.45	0.14	0.05	0.01	0.01	4.7	6	14.92±1.17	0.71	-0.06	2.37	-2.16
48	48.4	54.7	0.680	70	152.55	28.19	4.41	0.96	0.16	0.03	0.02		0.00	0.00	5.0	5	14.97±0.73	0.86	1.55	2.37	0.69
58	9.0	73.0	0.112	72	476.43	306.56	205.75	129.59	90.42	60.62	35.92	75.68	13.60	10.15	6.9	10	11.43±0.27	1.06	-1.62	-0.67	-4.19
57	18.2	73.0	0.200	74	433.47	165.92	76.12	34.61	10.63	4.98	2.09	0.85	0.35	0.70	6.7	8	11.01±0.32	1.13	-1.28	1.19	-0.06
56	27.7	73.0	0.310	71	207.05	48.11	16.38	5.81	1.57	0.37	0.12	0.03	0.01	0.03	6.8	6	12.18±1.02	1.01	-0.69	1.19	-2.34
136	36.5	73.0	0.150	69	244.16	40.81	6.76	1.48	0.26	0.05	0.01	0.00	0.00	0.03	7.3	5	11.68±0.66	1.00	-1.86	0.15	-2.97
137	48.4	73.0	0.680	70	227.60	33.31	2.99	0.34	0.06	0.05	0.03	0.05	0.05	0.03	7.4	4	11.97±1.54	0.98	1.55	1.19	-2.12
54	9.0	91.2	0.112	72	649.60	371.42	209.44	132.97	69.61	49.36	28.13	16.28	9.24	5.80	9.3	10	9.57±0.25	1.16	-0.32	-0.27	3.45
53	18.2	91.2	0.200	72	285.81	110.45	35.22	14.38	4.35	1.38	0.57	0.20	0.12	0.03	9.1	7	9.54±0.33	1.20	0.98	0.98	0.45
55	27.7	91.2	0.310	71	165.85	32.54	8.02	1.95	0.32	0.15	0.03	0.01	0.00	0.00	9.4	5	10.05±0.84	1.12	1.13	1.81	1.85
138	36.5	91.2	0.350	71	131.13	23.91	3.40	0.57	0.11	0.05	0.05	0.03	0.03	0.03	9.3	3	11.07±0.85	1.04	0.58	0.14	-0.76
139	48.4	91.2	0.680	70	83.18	8.34	0.65	0.08	0.03	0.02		0.03	0.02	0.02	9.8	3	11.11±4.35	1.00	0.53	1.81	1.42
61	9.0	109.5	0.112	72	401.08	255.86	163.06	93.11	46.32	29.79	14.98	11.12	6.46	3.32	11.7	10	9.63±0.36	1.11	-1.62	1.00	-0.54
60	18.2	109.5	0.200	72	276.62	93.68	28.69	10.74	7.42	0.84	0.35	0.09	0.03	0.00	11.8	7	9.17±0.48	1.17	1.59	1.00	-1.82
59	27.7	109.5	0.310	74	131.87	32.72	4.72	1.27	0.24	0.07	0.03	0.02	0.00	0.00	12.0	5	9.99±0.99	1.06	0.75	-1.43	-0.94
140	36.5	109.5	0.350	70	109.34	13.57	1.55	0.19	0.09	0.07	0.05	0.03	0.07	0.07	12.1	3	9.81±1.52	1.09	1.45	0.57	-1.05
141	48.4	109.5	0.680	71	53.59	2.23	0.23	0.06	0.05	0.05	0.03	0.03	0.03	0.05	12.1	3	10.13±12.2	1.07	0.53	0.57	1.04
47	9.0	127.7	0.112	71	529.47	308.22	156.84	86.04	46.19	27.85	14.28	7.78	5.27	2.88	13.3	10	8.94±0.31	1.22	-1.45	0.99	-1.68
46	18.2	127.7	0.200	75	249.59	98.12	21.64	6.94	1.70	0.47	0.15	0.07	0.09	0.07	14.0	6	8.32±0.60	1.26	-1.25	0.99	-2.87
45	27.7	127.7	0.310	74	116.15	22.72	3.73	0.12	0.12	0.08	0.06	0.08	0.08	0.06	14.1	4	9.14±0.87	1.15	-0.64	-0.31	-4.18
142	36.5	127.7	0.350	70	81.06	7.73	0.97	0.11	0.05	0.03	0.03	0.05	0.05	0.07	14.1	3	9.65±0.40	1.10	-1.86	-0.99	-2.86
143	48.4	127.7	0.680	70	36.21	1.66	0.11	0.03	0.02		0.03		0.02		14.8	2	9.25	1.12	0.53	1.42	0.34

TABLE IV-4. CONTINUED (2)

AVERAGE INSIDE DIAMETER OF NOZZLE TIPS = 0.086 IN.
DISPERSED PHASE EQUIVALENT DROP DIAMETER = 0.125 IN.
AVERAGE VELOCITY OF DISPERSED PHASE IN NOZZLE TIPS = 0.38 FT./SEC.
COLUMN INSIDE DIAMETER = 1.5 IN.
COLUMN HEIGHT (NOZZLE TIPS TO INTERFACE) = 10-FT. 3 1/8-IN. (SEE FIG. 10 FOR DIAG. OF APPARATUS)

LW = CONTINUOUS PHASE SUPERFICIAL VELOCITY, CU.FT./(HR. SQ.FT.)
LK = DISPERSED PHASE SUPERFICIAL VELOCITY, CU.FT./(HR. SQ.FT.)
LT = TRACER FEED SUPERFICIAL VELOCITY, CU.FT./(HR. SQ.FT.)
HOLD-UP = VOLUMETRIC PERCENTAGE OF DISPERSED PHASE IN COLUMN
PP = NUMBER OF SAMPLE CONCENTRATIONS USED FOR ESTIMATION OF AXIAL EDDY DIFFUSIVITY
E = AXIAL EDDY DIFFUSIVITY WITH 95 PER CENT CONFIDENCE LIMITS, SQ.FT./HR.
PE = PECLET NUMBER BASED ON DISPERSED PHASE DROP DIAMETER
ER1 = WATER BALANCE APPARENT LOSS, PER CENT
ER2 = KETONE BALANCE APPARENT LOSS, PER CENT
ER3 = TRACER BALANCE APPARENT LOSS, PER CENT

RUN	LW	LK	LT	TEMP F	REDUCED CONCENTRATION AT SAMPLING POINTS (SEE FIG. 10)										HOLD -UP	PP	E	PE	ER1	ER2	ER3
					1	2	3	4	5	6	7	8	9	10							
96	9.0	36.5	0.112	70	896.39	662.35	496.47	433.99	282.18	254.82	186.14	147.35	94.63	77.43	3.0	10	17.35±1.16	0.74	-1.62	1.25	-0.71
97	18.2	36.5	0.200	69	561.82	271.11	147.93	98.41	45.02	30.50	17.67	7.94	5.15	2.75	2.9	10	16.23±0.66	0.83	-0.88	0.14	-1.82
98	27.7	36.5	0.310	70	314.14	149.25	80.05	31.96	10.11	5.45	2.00	1.20	0.66	0.31	2.8	10	18.17±1.17	0.76	0.62	1.25	2.85
99	36.5	36.5	0.350	70	235.63	74.26	20.27	10.93	2.09	1.38	0.44	0.18	0.10	0.07	2.9	7	18.11±2.14	0.75	1.45	0.14	4.95
100	48.4	36.5	0.680	69	97.50	42.26	7.46	2.11	0.29	0.07	0.05	0.00	0.03	0.00	2.9	5	17.14±3.91	0.80	-0.97	1.25	-0.97
101	9.0	54.7	0.112	72	561.61	453.17	260.53	181.61	120.17	81.66	46.47	36.83	23.38	13.65	4.9	10	11.47±0.56	1.03	-0.80	1.26	3.71
102	18.2	54.7	0.200	73	389.16	177.99	58.66	34.56	8.83	5.19	1.95	0.67	0.21	0.00	4.8	9	10.37±0.63	1.16	1.59	1.26	0.77
103	27.7	54.7	0.310	73	146.91	67.11	12.25	5.92	2.80	0.47	0.00	0.00	0.00	0.00	4.8	6	13.11±2.61	0.93	0.79	1.26	0.05
104	36.5	54.7	0.350	73	93.48	23.63	4.12	1.51	0.39	0.04	0.00	0.00	0.00	0.00	4.8	5	14.11±2.06	0.87	0.19	2.37	3.25
105	48.4	54.7	0.680	73	34.45	6.92	0.72	0.15	0.00	0.00	0.00	0.00	0.00	0.00	5.0	4	13.77±3.03	0.87	0.84	2.37	-4.54
106	9.0	73.0	0.112	73	410.67	285.08	161.50	107.92	57.52	42.32	24.20	16.80	10.63	5.83	7.7	10	10.39±0.39	1.03	-0.85	0.67	1.67
107	18.2	73.0	0.200	73	305.57	129.34	36.06	16.59	4.53	1.65	0.45	0.20	0.00	0.00	7.0	7	9.06±0.60	1.23	0.92	1.19	2.69
108	27.7	73.0	0.310	74	136.85	35.29	6.15	1.67	0.35	0.11	0.07	0.07	0.09	0.14	7.2	5	10.02±0.74	1.08	-0.64	-0.89	1.44
109	36.5	73.0	0.350	74	80.32	13.16	0.94	0.00	0.00	0.00	0.00	0.00	0.00	0.00	7.5	3	8.92±12.2	1.19	-0.51	1.19	3.57
110	48.4	73.0	0.680	74	22.19	2.29	0.00	0.00	0.00	0.00	0.01	0.00	0.00	0.00	7.3	2	11.56	0.95	2.48	0.67	2.78
111	9.0	91.2	0.112	72	422.19	256.99	125.99	74.49	36.49	24.99	14.94	7.85	4.25	2.57	9.6	10	8.82±0.30	1.13	0.41	0.56	1.39
112	18.2	91.2	0.200	72	225.76	78.04	21.44	7.87	2.30	0.66	0.20	0.03	0.00	0.00	9.6	7	8.61±0.29	1.18	-0.71	0.56	-2.49
113	27.7	91.2	0.310	71	128.84	28.08	5.16	0.90	0.22	0.00	0.00	0.00	0.00	0.00	10.1	5	9.59±0.61	1.01	-0.64	0.98	2.80
114	36.5	91.2	0.350	71	59.68	8.57	0.70	0.13	0.08	0.06	0.03	0.03	0.06	0.06	9.8	3	9.15±8.49	1.11	0.96	0.14	-0.13
115	48.4	91.2	0.680	70	36.61	2.42	0.21	0.04	-0.02	0.02	0.04	0.06	0.04	0.02	10.5	3	10.51±4.03	0.92	-0.02	0.56	4.14
116	9.0	109.5	0.112	69	574.28	343.98	168.56	96.93	46.44	31.44	17.23	10.07	5.64	2.89	12.6	10	8.90±0.31	1.03	0.22	1.43	-3.16
117	18.2	109.5	0.200	70	287.24	97.25	25.51	9.15	2.29	0.76	0.22	0.00	0.00	0.00	12.3	7	8.66±0.32	1.09	1.12	1.00	6.34
118	27.7	109.5	0.310	70	117.37	24.99	2.56	0.40	0.00	0.00	0.00	0.00	0.00	0.00	12.2	4	8.22±1.74	1.18	-0.79	1.00	2.81
119	36.5	109.5	0.350	70	65.88	6.72	0.48	0.00	0.00	0.00	0.00	0.00	0.00	0.00	12.7	3	8.51±4.42	1.15	0.16	1.43	3.42
120	48.4	109.5	0.680	70	27.62	1.75	0.00	0.00	0.00	0.00	0.00	0.00	0.00	0.00	12.5	2	10.08	0.96	1.04	1.43	1.89
121	9.0	127.7	0.112	70	463.18	246.69	128.48	73.25	37.99	21.43	10.57	6.40	3.57	2.07	15.4	10	8.85±0.24	0.99	2.57	-0.31	-1.36
122	18.2	127.7	0.200	70	243.02	74.94	17.54	6.75	1.93	0.70	0.12	0.00	0.00	0.00	15.1	6	9.12±0.65	1.00	1.76	0.13	3.06
123	27.7	127.7	0.310	69	107.13	18.12	1.98	0.28	0.00	0.00	0.00	0.00	0.00	0.00	15.0	4	8.18±1.00	1.13	0.24	-1.17	4.04
124	36.5	127.7	0.350	71	41.59	4.13	0.17	0.00	0.00	0.00	0.00	0.00	0.00	0.00	15.6	2	9.40	0.96	1.17	-0.31	3.98
125	48.4	127.7	0.680	71	22.83	1.16	0.00	0.00	0.00	0.00	0.00	0.00	0.00	0.00	15.8	2	9.71	0.93	0.53	1.42	4.26

TABLE IV-4. CONTINUED (3)

AVERAGE INSIDE DIAMETER OF NOZZLE TIPS = 0.053 IN.
DISPERSED PHASE EQUIVALENT DROP DIAMETER = 0.095 IN.
AVERAGE VELOCITY OF DISPERSED PHASE IN NOZZLE TIPS = 0.68 FT./SEC.
COLUMN INSIDE DIAMETER = 1.5 IN.
COLUMN HEIGHT (NOZZLE TIPS TO INTERFACE) = 10-FT. 3 1/8-IN. (SEE FIG. 10 FOR DIAG. OF APPARATUS)
LW = CONTINUOUS PHASE SUPERFICIAL VELOCITY, CU.FT./(HR. SQ.FT.)
LK = DISPERSED PHASE SUPERFICIAL VELOCITY, CU.FT./(HR. SQ.FT.)
LT = TRACER FEED SUPERFICIAL VELOCITY, CU.FT./(HR. SQ.FT.)
HOLD-UP = VOLUMETRIC PERCENTAGE OF DISPERSED PHASE IN COLUMN
PP = NUMBER OF SAMPLE CONCENTRATIONS USED FOR ESTIMATION OF AXIAL EDDY DIFFUSIVITY
E = AXIAL EDDY DIFFUSIVITY WITH 95 PER CENT CONFIDENCE LIMITS, SC.FT./HR.
PE = PECLET NUMBER BASED ON DISPERSED PHASE DROP DIAMETER
ER1 = WATER BALANCE APPARENT LOSS, PER CENT
ER2 = KETONE BALANCE APPARENT LOSS, PER CENT
ER3 = TRACER BALANCE APPARENT LOSS, PER CENT

RUN	LW	LK	LT	TEMP °F	REDUCED CONCENTRATION AT SAMPLING POINTS (SEE FIG. 10) 1	2	3	4	5	6	7	8	9	10	HOLD -UP	PP	E	PE	ER1	ER2	ER3
148	9.0	36.5	0.112	68	498.46	400.76	231.73	146.04	71.48	59.88	34.34	22.98	13.47	6.03	2.7	10	9.66±0.73	1.10	1.96	-0.97	4.34
147	18.2	36.5	0.200	68	285.99	107.67	48.81	12.74	5.25	2.27	0.90	0.41	0.15	0.09	2.8	8	9.89±0.58	1.05	0.92	1.25	1.42
146	27.7	36.5	0.310	68	161.17	48.48	6.57	1.82	0.62	0.25	0.09	0.05	0.05	0.07	2.9	6	10.70±1.74	0.95	0.62	1.25	2.01
145	36.5	36.5	0.350	68	89.06	16.72	1.67	0.31	0.08	0.06	0.06	0.08	0.11	0.06	3.0	4	9.82±1.97	1.02	1.12	2.36	2.73
144	48.4	36.5	0.680	68	21.28	1.94	0.20	0.08	0.07	0.05	0.05	0.02	0.05	0.07	3.0	3	10.78±2.35	0.92	1.04	1.25	1.68
153	9.0	54.7	0.112	68	560.75	392.12	213.61	125.96	54.30	31.41	17.16	3.57	4.17	1.97	4.8	10	7.45±0.38	1.21	-1.62	2.37	0.51
152	18.2	54.7	0.200	68	287.15	122.05	24.83	7.81	1.84	0.48	0.13	0.04	0.02	0.01	5.1	6	7.37±0.66	1.17	-0.27	2.37	1.24
151	27.7	54.7	0.310	68	118.93	25.34	3.44	0.23	0.03	0.01	0.01	0.00	0.00	0.01	5.3	4	7.07±2.73	1.18	1.13	-0.96	2.89
150	36.5	54.7	0.350	68	70.68	5.54	0.43	0.04	0.04	0.02	0.02	0.04	0.02	0.02	5.2	3	7.57±0.32	1.15	-0.06	1.26	0.31
149	48.4	54.7	0.680	68	24.65	1.30	0.03	0.01	0.00	0.00	0.01	0.00	0.00	0.01	4.9	2	8.69	1.07	1.04	1.26	1.36
158	9.0	73.0	0.112	68	765.71	465.25	245.89	161.00	67.10	43.98	19.29	12.76	6.73	3.27	8.2	10	8.11±0.34	0.69	-0.80	0.69	3.45
157	18.2	73.0	0.200	67	327.39	113.56	21.42	5.31	1.22	0.24	0.05	0.01	0.01	0.01	8.1	6	6.82±0.51	1.00	2.65	1.21	5.39
156	27.7	73.0	0.310	67	104.00	26.37	2.34	0.44	0.05	0.03	0.03	0.02	0.02	0.03	8.0	4	8.04±2.49	0.93	0.12	1.21	6.16
155	36.5	73.0	0.350	68	72.49	5.80	0.38	0.04	0.04	0.02	0.02	0.04	0.02	0.02	7.9	3	7.59±2.15	1.01	-1.41	1.21	4.26
154	48.4	73.0	0.680	68	28.74	0.97	0.06	0.05	0.05	0.04	0.04	0.05	0.06	0.04	8.3	2	7.84	0.94	0.03	0.69	-0.51
163	9.0	91.2	0.112	69	474.10	297.44	173.87	97.69	44.40	21.90	15.58	6.31	3.52	1.91	10.4	10	8.06±0.38	0.87	-1.45	-1.14	3.62
162	18.2	91.2	0.200	68	329.94	109.41	28.55	8.85	1.84	0.47	0.15	0.07	0.03	0.03	10.7	6	7.75±0.57	0.89	-0.74	0.53	0.66
161	27.7	91.2	0.310	68	127.40	25.41	2.30	0.42	0.06	0.02	0.04	0.02	0.02	0.02	11.2	4	8.01±1.88	0.54	-1.53	0.53	0.48
160	36.5	91.2	0.350	68	83.24	8.55	0.54	0.03	0.00	0.00	0.00	0.00	0.00	0.00	10.9	3	8.17±5.80	0.85	0.61	1.78	1.57
159	48.4	91.2	0.680	69	18.66	0.71	0.02	0.00	0.01	0.01	0.01	0.00	0.01	0.00	11.2	2	8.38	0.82	0.48	1.36	0.07
168	9.0	109.5	0.112	68	453.70	329.33	173.77	104.22	51.12	31.65	17.00	10.74	6.60	3.81	13.1	10	9.59±0.37	0.70	0.91	0.59	3.75
167	18.2	109.5	0.200	68	244.59	77.40	19.36	4.87	1.13	0.37	0.16	0.09	0.09	0.07	13.2	6	7.91±0.38	0.85	-0.88	1.45	1.66
166	27.7	109.5	0.310	68	119.48	20.52	1.88	0.32	0.11	0.09	0.09	0.09	0.11	0.11	13.9	4	8.00±1.50	0.81	-1.09	1.02	1.29
165	36.5	109.5	0.350	69	55.97	6.71	0.57	0.11	0.09	0.09	0.11	0.11	0.09	0.11	13.8	3	9.29±5.04	0.71	0.65	1.02	3.08
164	48.4	109.5	0.680	67	12.70	0.69	0.07	0.07	0.05	0.05	0.05	0.07	0.05	0.07	14.1	2	9.74	0.68	1.04	1.45	1.26
173	9.0	127.7	0.112	68	482.44	343.44	138.97	76.34	29.43	20.21	9.51	5.48	2.57	1.11	16.2	10	7.98±0.45	0.74	-1.62	-0.74	1.73
172	18.2	127.7	0.200	69	352.27	94.93	17.96	4.83	1.25	0.28	0.12	0.05	0.05	0.05	16.4	6	7.66±0.34	0.83	-1.33	1.42	1.33
171	27.7	127.7	0.310	69	97.27	16.67	1.19	0.18	0.05	0.03	0.03	0.05	0.05	0.08	16.4	3	7.56±1.10	0.85	-1.09	0.13	-1.75
170	36.5	127.7	0.350	69	41.43	2.79	0.25	0.07	0.07	0.07	0.04	0.04	0.07	0.03	16.6	3	8.53±3.49	0.75	1.01	-1.17	1.34
169	48.4	127.7	0.680	68	18.71	0.65	0.05	0.03	0.03	0.03	0.05	0.05	0.03	0.03	17.2	2	8.75	0.72	0.53	-2.04	0.41

217

superficial axial eddy diffusivity, and the superficial axial

eddy diffusivity for each run with the 3-in. I.D. column are

given in Table IV-5. Dispersed phase hold-ups in the 3-in. I.D.

column were not measured. Consequently it was not possible to

reduce superficial axial eddy diffusivities to true axial eddy

diffusivities or to calculate Peclet numbers.

Measurements of the dispersed phase drop sizes were analysed

on an IBM-7040 electronic computer. No hand calculations are

presented due to their voluminous nature. However, the algebraic

equation used to process the data is given below.

Let r = the vertical dimension of the drop image as measured

by means of the microfilm reader, mm.,

x = the horizontal dimension of the drop image as

measured by means of the microfilm reader, mm.

f_1 = the conversion factor for mm. to in. = 0.03937,

f_2 = the enlargement factor = a linear dimension of the

observed image divided by the same linear dimension

of the actual object = 4.309,

and d_s = the equivalent diameter of the drop = the diameter

of a sphere having the same volume as the drop.

Then

$$d_s = \frac{(f_1)(\sqrt[3]{(r)(x^2)})}{f_2}$$

The range of d_s between 0.00 and 0.25-in. was divided up into

TABLE IV-5. SUPERFICIAL AXIAL EDDY DIFFUSIVITY RESULTS FOR THE 3-IN. I.D. COLUMN

AVERAGE INSIDE DIAMETER OF NOZZLE TIPS = 0.102 IN.
DISPERSED PHASE EQUIVALENT DROP DIAMETER = 0.135 IN.
AVERAGE VELOCITY OF DISPERSED PHASE IN NOZZLE TIPS = 0.37 FT./SEC.
COLUMN INSIDE DIAMETER = 3.0 IN.
COLUMN HEIGHT (NOZZLE TIPS TO INTERFACE) = 10-FT. 9 7/8-IN. (SEE FIG. 20 FOR DIAG. OF APPARATUS)
LW = CONTINUOUS PHASE SUPERFICIAL VELOCITY, CU.FT./(HR. SQ.FT.)
LK = DISPERSED PHASE SUPERFICIAL VELOCITY CU.FT./(HR. SQ.FT.)
LT = TRACER FEED SUPERFICIAL VELOCITY, CU.FT./(HR. SQ.FT.)
PP = NUMBER OF SAMPLE CONCENTRATIONS USED FOR ESTIMATION OF SUPERFICIAL AXIAL EDDY DIFFUSIVITY
SE = SUPERFICIAL AXIAL EDDY DIFFUSIVITY WITH 95 PER CENT CONFIDENCE LIMITS, SQ.FT./HR.
ER1 = WATER BALANCE APPARENT LOSS, PER CENT
ER2 = TRACER BALANCE APPARENT LOSS, PER CENT

RUN	LW	LK	LT	TEMP °F	REDUCED CONCENTRATION AT SAMPLING POINTS (SEE FIG. 20)										PP	SE	ER1	ER2
					1	2	3	4	5	6	7	8	9	10				
177	18.2	36.5	0.050	70	933.27	863.08	843.83	810.94	776.76	707.25	680.23	655.87	635.98	593.46	10	187.9±16.4	-1.28	-0.29
181	27.7	36.5	0.100	69	939.04	877.36	842.38	759.66	693.78	676.66	604.44	568.84	471.59	470.11	10	174.7±20.1	-1.83	-0.48
182	36.5	36.5	0.150	68	972.18	945.34	846.65	741.07	625.71	598.60	583.77	525.69	435.07	389.08	10	181.3±21.8	0.75	2.06
183	48.4	36.5	0.150	66	923.97	799.06	718.67	602.38	516.67	490.81	433.57	327.94	312.99	273.32	10	179.8±14.6	1.40	0.19
184	75.0	36.5	0.200	69	938.87	717.45	606.97	451.64	330.10	283.24	236.75	192.38	150.23	123.07	10	169.0± 9.5	-0.03	-3.00
180	100.0	36.5	0.250	70	816.45	644.68	440.35	337.54	218.34	171.58	153.89	97.49	75.67	53.16	10	168.0±10.3	-0.94	-1.09
179	220.0	36.5	0.410	67	591.95	282.48	142.48	49.30	35.00	21.28	11.30	6.10	3.75	2.19	10	181.4±14.5	-0.78	3.53
185	285.0	36.5	0.410	70	487.74	274.18	109.02	53.78	28.72	16.72	9.16	4.14	1.88	0.87	8	214.0±13.6	0.76	-1.26
194	18.2	54.7	0.050	68	1028.76	974.63	936.07	864.67	816.58	767.73	711.99	672.35	634.91	583.14	10	146.1± 6.5	-1.70	3.52
193	27.7	54.7	0.100	69	1022.09	973.11	909.10	853.88	784.30	735.85	662.86	620.22	577.73	502.74	10	181.2±14.5	-1.24	-6.18
192	36.5	54.7	0.150	71	1011.09	938.87	782.22	724.39	635.31	574.52	499.13	422.79	368.37	334.76	10	146.7± 8.0	1.59	1.68
191	48.4	54.7	0.150	70	1079.57	933.14	780.05	700.88	545.95	456.55	394.57	317.39	272.97	257.38	10	144.9± 9.5	-0.72	-0.65
178	75.0	54.7	0.200	71	955.69	756.42	593.65	428.57	319.98	273.73	210.35	170.16	134.21	96.94	10	152.0± 6.9	-0.25	-4.12
190	100.0	54.7	0.250	71	1123.63	748.57	549.14	366.41	234.51	179.48	149.88	80.05	54.91	40.04	10	137.2± 8.1	-1.75	-2.62
189	150.0	54.7	0.410	70	1163.87	731.16	451.55	259.36	145.42	76.33	47.72	27.65	17.87	9.48	10	140.9± 4.1	-0.16	-4.76
188	220.0	54.7	0.410	70	1081.40	623.83	320.26	149.96	72.90	32.54	11.63	5.67	2.76	1.32	9	144.8± 8.2	0.04	3.94
187	262.0	54.7	0.410	70	1195.62	540.40	166.24	46.87	12.57	5.44	2.31	1.12	0.17	0.00	7	121.6±10.7	-0.44	-0.93
197	18.2	73.0	0.050	67	956.95	882.90	785.93	730.68	692.97	623.84	608.65	541.26	486.45	455.21	10	113.7± 7.7	-0.58	4.73
196	48.4	73.0	0.150	70	1089.17	896.39	700.69	514.75	400.69	356.02	287.76	211.93	161.29	132.63	10	104.2± 5.4	0.61	-2.20
195	100.0	73.0	0.250	68	1286.97	1071.40	634.73	400.65	166.85	122.51	61.29	37.89	23.20	12.09	10	94.0± 6.4	-1.05	0.39
200	18.2	91.2	0.050	70	894.06	768.91	692.25	610.54	537.10	486.32	452.12	385.60	360.91	323.60	10	82.8± 4.5	1.00	2.78
199	48.4	91.2	0.150	67	1036.04	748.89	606.34	412.92	288.35	220.73	181.26	114.90	87.42	74.25	10	81.2± 4.4	-1.51	-1.55
198	100.0	91.2	0.250	69	1155.97	683.49	276.73	160.04	85.52	38.56	19.68	10.34	5.35	3.54	10	76.2± 3.2	-1.46	1.01
203	18.2	109.0	0.050	69	905.74	822.91	798.86	718.11	603.11	528.61	491.67	428.69	387.63	336.02	10	81.9± 6.8	1.00	3.64
202	48.4	109.0	0.150	68	1064.79	851.97	630.45	439.27	272.23	202.34	138.32	94.93	65.80	52.66	10	69.5± 3.4	0.43	4.58
201	100.0	109.0	0.250	67	1117.61	613.37	167.42	100.85	40.26	18.75	6.03	1.09	0.18	0.00	8	53.7± 7.4	-0.91	-0.50
206	18.2	128.0	0.040	69	996.85	875.33	744.95	592.89	471.32	408.91	325.84	275.32	234.48	190.85	10	49.0± 2.0	0.12	7.27
205	48.4	128.0	0.150	69	954.09	700.15	471.77	289.27	157.78	115.89	64.79	38.37	24.82	18.17	10	52.9± 2.6	1.46	-0.35
204	100.0	128.0	0.250	70	580.25	291.22	83.51	31.47	17.03	4.63	2.06	0.72	0.57	0.28	7	52.9± 4.4	-0.64	-1.48

0.01-in. increments. The number of drops, and the total drop volume associated with the drops, appearing in each of these increments were calculated. For each increment the number of drops was converted into the percentage of the total number of drops measured. Similarly the sum of the volumes of the drops in each increment was converted into a percentage of the total drop volume associated with all of the drops. These calculations were performed for the first 100 drops examined and were extended to the first 200, 300, 400, and 500 drops examined. A typical set of results appears in Table IV-6. The results for the 500 drops examined for each run in which drop sizes were measured appear in Table IV-7 for the $1\frac{1}{2}$-in. I.D. column and in Table IV-8 for the 3-in. I.D. column. Due to the overlapping of the drops in the photographs it was not possible to measure the drop sizes for runs when L_D was large. Therefore it was assumed that the drop size distributions were the same at high and low values of L_D.

Table IV-9 shows the superficial flowrates, the measured concentrations, the calculated capacity coefficient, the hold-up, and the error in the mass balance for each run involving mass transfer. Table IV-10 shows the relation between Δ^2 and E for the estimation of E. The values of $K_D a$ and m were taken from Table IV-9 and the values of J were calculated by means of Equation 21. Tables IV-11 and IV-12 show the effect on E of varying $K_D a$, m, and the method of calculation of J. Table IV-13 gives the equilibrium concentration of acetic acid in MIBK - saturated water and water - saturated MIBK at 70°F as determined in this work.

TABLE IV-6.   TYPICAL DROP SIZE DISTRIBUTION RESULTS

WATER SUPERFICIAL VELOCITY = 27.70 CU.FT./(HR. SQ.FT.)
KETONE SUPERFICIAL VELOCITY = 54.74 CU.FT./(HR. SQ.FT.)
NOZZLE TIP AVERAGE DIAMETER = 0.103 IN.
COLUMN DIAMETER = 1.5 IN.
CONDITIONS CORRESPOND TO RUN   50

RANGE OF EQUIVALENT DROP DIA. IN INCHES	PERCENTAGE OF DROPS IN GIVEN SIZE RANGE FOR TOTAL NUMBER OF DROPS SHOWN AT HEAD OF LIST					PERCENTAGE OF TOTAL DROP VOLUME CONTRIBUTED BY DROPS IN GIVEN SIZE RANGE FOR TOTAL NUMBER OF DROPS SHOWN AT HEAD OF LIST				
	100	200	300	400	500	100	200	300	400	500
0.00-0.01	0.0	0.0	0.0	0.0	0.0	0.0	0.0	0.0	0.0	0.0
0.01-0.02	15.0	15.5	15.7	16.0	16.6	0.1	0.1	0.1	0.1	0.1
0.02-0.03	25.0	24.5	25.0	24.2	23.0	0.4	0.4	0.4	0.4	0.3
0.03-0.04	6.0	7.0	5.3	6.3	7.4	0.2	0.3	0.2	0.2	0.3
0.04-0.05	5.0	4.0	3.3	3.5	3.0	0.4	0.4	0.3	0.3	0.3
0.05-0.06	3.0	3.0	2.7	2.2	1.8	0.5	0.5	0.4	0.3	0.3
0.06-0.07	0.0	0.5	0.7	0.5	0.4	0.0	0.1	0.2	0.1	0.1
0.07-0.08	1.0	2.0	1.7	1.2	1.6	0.4	0.8	0.7	0.5	0.6
0.08-0.09	0.0	2.0	2.3	2.2	2.2	0.0	1.1	1.2	1.2	1.1
0.09-0.10	2.0	2.0	2.3	2.0	2.0	1.6	1.7	1.9	1.6	1.6
0.10-0.11	3.0	3.5	4.3	3.7	3.0	3.1	3.9	4.6	4.0	3.1
0.11-0.12	4.0	2.5	3.0	3.0	3.6	5.4	3.6	4.3	4.2	5.0
0.12-0.13	3.0	5.0	6.3	7.0	7.2	5.0	9.4	11.6	12.7	12.8
0.13-0.14	16.0	13.5	12.3	13.2	13.8	33.7	31.0	27.8	29.5	30.0
0.14-0.15	9.0	9.5	10.0	10.0	9.2	23.2	26.9	27.7	27.3	24.5
0.15-0.16	6.0	4.0	3.7	3.5	3.6	18.3	13.3	11.8	11.3	11.6
0.16-0.17	2.0	1.5	1.0	0.7	0.6	7.7	6.4	4.1	3.1	2.4
0.17-0.18	0.0	0.0	0.0	0.2	0.6	0.0	0.0	0.0	1.3	2.8
0.18-0.19	0.0	0.0	0.0	0.0	0.0	0.0	0.0	0.0	0.0	0.0
0.19-0.20	0.0	0.0	0.0	0.0	0.0	0.0	0.0	0.0	0.0	0.0
0.20-0.21	0.0	0.0	0.3	0.2	0.4	0.0	0.0	2.7	2.0	3.0
0.21-0.22	0.0	0.0	0.0	0.0	0.0	0.0	0.0	0.0	0.0	0.0
0.22-0.23	0.0	0.0	0.0	0.0	0.0	0.0	0.0	0.0	0.0	0.0
0.23-0.24	0.0	0.0	0.0	0.0	0.0	0.0	0.0	0.0	0.0	0.0
0.24-0.25	0.0	0.0	0.0	0.0	0.0	0.0	0.0	0.0	0.0	0.0

TABLE IV-7. DROP SIZE DISTRIBUTIONS IN THE 1½-IN. I.D. COLUMN

RANGE OF EQUIVALENT DROP DIA. IN INCHES	PERCENTAGE OF DROPS IN GIVEN SIZE RANGE FOR A TOTAL OF 500 DROPS. CONDITIONS CORRESPOND TO RUN AT HEAD OF LIST																					
	AVERAGE NOZZLE TIP I.D. = 0.126-IN.						AVERAGE NOZZLE TIP I.D. = 0.103-IN.						AVERAGE NOZZLE TIP I.D. = 0.086-IN.					AVERAGE NOZZLE TIP I.D. = 0.053-IN.				
	126	128	130	75	86	92	65	63	66	50	55	45	96	98	100	103	113	148	146	144	151	149
0.00-0.01	0.2	0.0	0.0	0.4	0.2	0.0	1.0	0.0	0.0	0.0	0.0	0.0	0.0	0.0	0.2	0.2	0.0	0.0	0.8	0.2	0.2	0.2
0.01-0.02	22.4	29.4	28.2	21.6	21.6	19.0	9.6	18.6	22.0	16.6	9.0	6.4	19.8	20.0	25.4	18.4	10.8	11.4	10.4	13.2	13.2	7.0
0.02-0.03	16.6	17.4	16.2	16.0	17.8	19.4	16.0	20.0	23.4	23.0	16.8	12.2	22.0	23.4	19.6	20.2	20.0	9.6	10.0	8.6	10.2	13.0
0.03-0.04	6.0	5.4	4.8	8.2	5.6	8.2	10.0	6.6	6.2	7.4	11.4	7.8	6.8	8.2	5.4	8.8	8.2	1.2	2.4	1.6	1.2	0.6
0.04-0.05	1.6	2.0	3.0	5.0	3.0	2.0	4.6	4.0	3.4	3.0	4.0	4.4	1.8	2.6	3.0	2.4	2.4	0.4	0.6	0.4	0.0	0.2
0.05-0.06	0.6	3.2	2.4	1.8	3.2	2.2	2.2	2.2	0.6	1.8	1.8	3.0	0.8	1.2	1.4	0.0	2.2	0.2	0.4	0.4	0.2	0.2
0.06-0.07	2.0	2.4	1.2	1.6	2.8	2.2	1.0	1.6	0.8	0.4	1.6	0.8	1.8	1.0	1.2	0.8	0.6	1.0	0.4	0.8	0.0	0.0
0.07-0.08	1.6	2.2	3.0	2.4	1.8	1.0	1.4	2.2	1.0	1.6	1.4	1.4	0.6	1.8	1.2	0.8	1.0	1.2	2.0	1.2	1.0	3.8
0.08-0.09	2.8	2.2	3.0	2.4	2.0	1.6	3.2	1.8	1.2	2.2	1.0	1.4	0.8	0.4	1.6	2.2	1.8	18.4	17.8	14.0	18.0	16.4
0.09-0.10	3.2	2.2	2.0	2.2	2.4	2.0	3.2	1.8	2.4	2.0	2.2	2.4	2.8	2.2	1.4	2.0	4.0	44.2	42.8	43.4	45.0	47.4
0.10-0.11	3.6	3.0	2.8	3.0	2.4	3.0	4.0	2.4	2.4	3.0	2.4	3.8	3.0	3.0	4.6	3.8	4.8	9.4	7.6	11.4	7.4	8.6
0.11-0.12	3.4	2.6	3.0	2.0	3.4	3.4	5.4	5.2	3.6	3.6	4.6	5.6	8.4	8.2	9.6	11.4	15.0	2.4	4.4	3.2	2.6	4.4
0.12-0.13	6.0	3.4	2.4	2.6	3.2	4.0	8.2	10.0	6.0	7.2	6.4	11.2	21.4	13.8	14.8	17.8	16.6	0.6	0.4	1.2	0.8	1.0
0.13-0.14	5.2	3.4	4.6	4.2	3.4	4.0	15.0	11.8	14.0	13.8	16.4	15.2	8.2	11.0	9.0	7.4	8.6	0.0	0.0	0.4	0.2	0.0
0.14-0.15	6.4	6.2	6.2	5.8	6.0	7.0	10.9	7.8	8.4	9.2	12.0	13.8	1.6	2.2	1.2	3.6	2.2	0.0	0.0	0.0	0.0	0.0
0.15-0.16	8.2	5.2	6.6	8.6	5.6	5.6	2.2	3.6	4.2	3.6	5.8	6.0	0.2	1.0	0.4	0.2	1.4	0.0	0.0	0.0	0.0	0.0
0.16-0.17	5.6	2.6	5.4	5.8	6.4	7.6	1.4	0.2	0.2	0.6	1.8	3.0	0.0	0.0	0.0	0.0	0.2	0.0	0.0	0.0	0.0	0.2
0.17-0.18	2.4	4.2	2.8	2.8	4.6	2.8	0.2	0.2	0.2	0.6	0.2	0.6	0.0	0.0	0.0	0.0	0.2	0.0	0.0	0.0	0.0	0.0
0.18-0.19	0.6	0.8	1.2	1.2	1.8	3.2	0.2	0.0	0.0	0.0	0.6	0.8	0.0	0.0	0.0	0.0	0.0	0.0	0.0	0.0	0.0	0.0
0.19-0.20	1.2	1.0	0.8	0.6	1.8	0.4	0.2	0.0	0.0	0.0	0.4	0.2	0.0	0.0	0.0	0.0	0.0	0.0	0.0	0.0	0.0	0.0
0.20-0.21	0.4	0.8	0.2	1.2	0.4	0.4	0.2	0.0	0.0	0.0	0.4	0.0	0.0	0.0	0.0	0.0	0.0	0.0	0.0	0.0	0.0	0.0
0.21-0.22	0.0	0.2	0.2	0.2	0.4	0.6	0.0	0.0	0.0	0.0	0.2	0.0	0.0	0.0	0.0	0.0	0.0	0.0	0.0	0.0	0.0	0.0
0.22-0.23	0.0	0.0	0.0	0.2	0.0	0.2	0.0	0.0	0.0	0.0	0.0	0.0	0.0	0.0	0.0	0.0	0.0	0.0	0.0	0.0	0.0	0.0
0.23-0.24	0.0	0.2	0.0	0.2	0.2	0.0	0.0	0.0	0.0	0.0	0.0	0.0	0.0	0.0	0.0	0.0	0.0	0.0	0.0	0.0	0.0	0.0
0.24-0.25	0.0	0.0	0.0	0.0	0.0	0.2	0.0	0.0	0.0	0.0	0.0	0.0	0.0	0.0	0.0	0.0	0.0	0.0	0.0	0.0	0.0	0.0

TABLE IV-7. CONTINUED

RANGE OF EQUIVALENT DROP DIA. IN INCHES	PERCENTAGE OF TOTAL DROP VOLUME CONTRIBUTED BY DROPS IN GIVEN SIZE RANGE FOR A TOTAL OF 500 DROPS. CONDITIONS CORRESPOND TO RUN AT HEAD OF LIST																					
	AVERAGE NOZZLE TIP I.D. = 0.126-IN.						AVERAGE NOZZLE TIP I.D. = 0.103-IN.						AVERAGE NOZZLE TIP I.D. = 0.086-IN.					AVERAGE NOZZLE TIP I.D. = 0.053-IN.				
	126	128	130	75	86	92	65	63	66	50	55	45	96	98	100	103	113	148	146	144	151	149
0.00-0.01	0.0	0.0	0.0	0.0	0.0	0.0	0.0	0.0	0.0	0.0	0.0	0.0	0.0	0.0	0.0	0.0	0.0	0.0	0.0	0.0	0.0	0.0
0.01-0.02	0.1	0.1	0.1	0.1	0.1	0.1	0.0	0.1	0.1	0.1	0.0	0.0	0.1	0.1	0.2	0.1	0.1	0.1	0.1	0.1	0.1	0.1
0.02-0.03	0.2	0.2	0.2	0.2	0.2	0.2	0.2	0.3	0.4	0.3	0.2	0.1	0.4	0.4	0.4	0.4	0.3	0.2	0.2	0.2	0.2	0.3
0.03-0.04	0.2	0.2	0.2	0.2	0.2	0.2	0.4	0.3	0.3	0.3	0.4	0.2	0.4	0.4	0.3	0.4	0.4	0.1	0.2	0.1	0.1	0.0
0.04-0.05	0.1	0.1	0.2	0.3	0.2	0.1	0.3	0.4	0.3	0.3	0.3	0.3	0.2	0.3	0.4	0.3	0.2	0.0	0.1	0.1	0.0	0.0
0.05-0.06	0.1	0.4	0.3	0.2	0.3	0.2	0.3	0.3	0.1	0.3	0.2	0.3	0.1	0.2	0.3	0.0	0.4	0.1	0.1	0.1	0.1	0.0
0.06-0.07	0.4	0.6	0.3	0.3	0.5	0.4	0.2	0.4	0.2	0.1	0.3	0.1	0.6	0.3	0.3	0.2	0.2	0.4	0.2	0.4	0.0	0.0
0.07-0.08	0.4	0.7	1.0	0.7	0.5	0.3	0.5	0.9	0.4	0.6	0.4	0.4	0.3	1.0	0.6	0.4	0.4	0.8	1.5	0.7	0.7	0.5
0.08-0.09	1.2	1.1	1.5	1.0	0.8	0.6	1.6	1.1	0.7	1.1	0.4	0.5	0.6	0.3	1.2	1.6	1.1	18.8	18.3	13.8	18.5	15.7
0.09-0.10	1.9	1.6	1.2	1.3	1.3	1.1	2.2	1.5	2.1	1.6	1.3	1.2	2.7	2.3	1.5	2.0	3.4	56.2	54.9	54.8	58.3	56.8
0.10-0.11	2.8	2.9	2.5	2.4	1.8	2.1	3.6	2.8	2.7	3.1	1.9	2.7	4.1	4.2	6.8	5.0	5.5	16.3	13.0	18.3	12.7	13.5
0.11-0.12	3.6	3.2	3.6	2.1	3.4	3.3	6.6	7.8	5.4	5.0	4.9	5.2	14.8	15.1	18.9	19.3	22.9	5.3	10.3	6.9	6.3	9.1
0.12-0.13	8.2	5.3	3.5	3.5	4.2	4.9	12.9	19.0	11.5	12.8	8.8	13.2	47.2	31.9	35.9	38.4	31.7	1.8	1.2	3.4	2.3	2.7
0.13-0.14	8.9	6.6	8.6	7.0	5.5	6.2	29.5	27.6	34.0	30.0	28.3	23.0	22.1	31.3	26.8	19.4	20.2	0.0	0.0	1.3	0.7	0.0
0.14-0.15	13.6	15.3	14.6	12.0	11.8	13.3	25.8	22.6	24.8	24.5	25.2	25.2	5.5	7.9	4.5	11.7	6.5	0.0	0.0	0.0	0.0	0.0
0.15-0.16	21.2	15.7	18.9	21.5	13.3	12.9	6.4	13.0	15.1	11.6	14.8	13.5	0.8	4.2	1.7	0.8	4.9	0.0	0.0	0.0	0.0	0.0
0.16-0.17	17.2	9.2	18.6	17.4	18.4	21.3	5.1	0.8	0.8	2.4	5.8	8.2	0.0	0.0	0.0	0.0	0.8	0.0	0.0	0.0	0.0	1.3
0.17-0.18	8.9	17.9	11.3	10.2	15.4	9.2	0.8	1.1	1.0	2.8	0.7	1.9	0.0	0.0	0.0	0.0	1.0	0.0	0.0	0.0	0.0	0.0
0.18-0.19	2.7	4.0	5.9	5.2	7.3	12.5	1.0	0.0	0.0	0.0	2.6	3.0	0.0	0.0	0.0	0.0	0.0	0.0	0.0	0.0	0.0	0.0
0.19-0.20	6.0	6.0	4.7	3.0	8.5	1.9	1.1	0.0	0.0	0.0	2.1	0.9	0.0	0.0	0.0	0.0	0.0	0.0	0.0	0.0	0.0	0.0
0.20-0.21	2.2	5.5	1.3	6.8	2.2	2.2	1.4	0.0	0.0	3.0	0.0	0.0	0.0	0.0	0.0	0.0	0.0	0.0	0.0	0.0	0.0	0.0
0.21-0.22	0.0	1.5	1.6	1.4	2.4	3.8	0.0	0.0	0.0	0.0	1.3	0.0	0.0	0.0	0.0	0.0	0.0	0.0	0.0	0.0	0.0	0.0
0.22-0.23	0.0	0.0	0.0	1.5	0.0	1.4	0.0	0.0	0.0	0.0	0.0	0.0	0.0	0.0	0.0	0.0	0.0	0.0	0.0	0.0	0.0	0.0
0.23-0.24	0.0	2.0	0.0	1.7	1.8	0.0	0.0	0.0	0.0	0.0	0.0	0.0	0.0	0.0	0.0	0.0	0.0	0.0	0.0	0.0	0.0	0.0
0.24-0.25	0.0	0.0	0.0	0.0	0.0	1.9	0.0	0.0	0.0	0.0	0.0	0.0	0.0	0.0	0.0	0.0	0.0	0.0	0.0	0.0	0.0	0.0

TABLE IV-8.   DROP SIZE DISTRIBUTIONS IN THE 3-IN. I.D. COLUMN

RANGE OF EQUIVALENT DROP DIA. IN INCHES	AVERAGE NOZZLE TIP I.D. = 0.102-IN. CONDITIONS CORRESPOND TO RUN AT HEAD OF LIST							
	PERCENTAGE OF THE DROPS IN GIVEN SIZE RANGE				PERCENTAGE OF THE TOTAL DROP VOLUME CONTRIBUTED BY DROPS IN GIVEN SIZE RANGE			
	177	182	184	179	177	182	184	179
0.00-0.01	8.4	2.4	1.0	0.6	0.0	0.0	0.0	0.0
0.01-0.02	29.8	32.8	32.2	13.0	0.1	0.1	0.1	0.0
0.02-0.03	5.6	12.4	10.8	13.6	0.1	0.2	0.2	0.2
0.03-0.04	3.6	2.2	2.8	4.8	0.2	0.1	0.1	0.2
0.04-0.05	1.8	1.0	1.6	4.0	0.2	0.1	0.1	0.3
0.05-0.06	1.2	1.4	1.8	1.0	0.2	0.2	0.3	0.1
0.06-0.07	1.4	2.4	0.8	2.0	0.4	0.7	0.2	0.4
0.07-0.08	1.6	0.8	0.8	2.4	0.6	0.3	0.4	0.9
0.08-0.09	3.2	2.8	1.4	2.6	2.1	1.7	0.8	1.3
0.09-0.10	2.8	2.6	1.8	3.8	2.6	2.3	1.5	2.7
0.10-0.11	2.8	1.4	4.0	4.2	3.2	1.7	4.4	4.1
0.11-0.12	5.4	4.0	5.8	8.6	8.5	6.2	8.5	10.8
0.12-0.13	11.2	10.0	10.2	12.4	22.4	19.4	19.2	19.4
0.13-0.14	12.2	13.2	16.6	16.4	30.5	32.5	38.4	32.1
0.14-0.15	7.4	7.8	6.6	7.0	22.3	23.3	19.0	16.7
0.15-0.16	0.8	2.0	0.8	3.2	2.9	7.2	2.8	9.3
0.16-0.17	0.6	0.6	1.0	0.4	2.7	2.6	4.1	1.4
0.17-0.18	0.2	0.0	0.0	0.0	1.0	0.0	0.0	0.0
0.18-0.19	0.0	0.2	0.0	0.0	0.0	1.3	0.0	0.0
0.19-0.20	0.0	0.0	0.0	0.0	0.0	0.0	0.0	0.0
0.20-0.21	0.0	0.0	0.0	0.0	0.0	0.0	0.0	0.0
0.21-0.22	0.0	0.0	0.0	0.0	0.0	0.0	0.0	0.0
0.22-0.23	0.0	0.0	0.0	0.0	0.0	0.0	0.0	0.0
0.23-0.24	0.0	0.0	0.0	0.0	0.0	0.0	0.0	0.0
0.24-0.25	0.0	0.0	0.0	0.0	0.0	0.0	0.0	0.0

TABLE IV-9.   CONCENTRATION STUDIES WITH MASS TRANSFER IN THE $1\frac{1}{2}$-IN. I.D. COLUMN

Run	L_C	L_D	Concentration at sampling points.[1] (See Figure 10), $10^3 \times$ lb.-moles/ft.^{3}										c_C^i and c_D^i	c_C^o and c_D^o	$K_D a$	Average m	h %	M.B.[2]	Time to reach steady state min.	Temp °F
			1	2	3	4	5	6	7	8	9	10								
J1	36.5	54.7	30.66	34.30	40.37	43.70	47.71	49.47	53.72	55.24	57.21	58.82	81.37	19.28	42.54	1.92	4.6	3.3	65	71
			9.11		15.2		19.88		23.3		25.95	27.2	0.00	40.06						
J2	18.2	54.7	9.04	10.05	11.84	13.96	15.33	17.00	19.43	22.31	24.25	27.32	83.32	54.63	56.24	2.04	4.5	2.75	122	71
			2.91		4.21		5.72		7.50		9.82	11.1	0.00	25.19						
J3	36.5	91.2	15.48	16.69	18.27	19.73	21.43	23.07	25.50	27.59	30.41	32.54	80.75	11.53	79.03	2.02	9.3	0.39	90	69
			6.1		7.4		8.76		10.81		12.40	13.55	3.64	31.23						
J4	48.4	91.2	25.25	27.71	30.35	32.78	35.42	37.51	40.06	42.49	45.25	48.02	80.43	16.39	94.63	1.96	9.8	3.22	101	72
			9.16		12.2		15.0		17.9		20.9	22.7	4.02	37.03						
J5	48.4	127.7	14.63	15.48	16.39	17.36	18.85	20.21	21.73	23.43	25.40	27.59	82.93	13.72	141.1	2.04	14.8	-3.42	85	70
			6.1		7.04		8.1		9.70		11.1	12.2	4.74	31.87						

[1] The upper number refers to the continuous phase, the lower number to the dispersed phase.

[2] M.B. is the error in the mass balance. This mass balance was calculated according to the following equation.

$$M.B. = \left[\frac{L_C(c_C^i - c_C^o) - L_D(c_D^o - c_D^i)}{L_C(c_C^i - c_C^o)} \right] 100 \%$$

TABLE IV-10. THE RELATION BETWEEN E AND Δ^2. (The values of K_Da, and m were taken from Table IV-9. The values of J were calculated from Equation 21.)

The numbers listed under the various values of E tested $= 10^8 \Delta^2$.

Run	J	K_Da	m	E	60	59	58	57	56	55	54	53	52	51	50	49	48	47
J1	0.743	42.54	1.92		2800	2800	2700	2700	2600	2600	2500	2500	2400	2400	2300	2300	2200	2200
J2	0.119	56.24	2.04		820	760	690	630	570	510	460	400	350	300	250	210	170	140
J3	0.0943	79.03	2.02		1300	1200	1200	1100	1000	990	930	880	820	770	720	660	610	560
J4	0.477	94.63	1.96		920	860	800	740	680	620	560	500	450	400	350	300	260	210
J5	0.0017	141.1	2.04		58	47	38	31	25	20	18	18	19	23	29	38	50	65

Run	J	K_Da	m	E	46	45	44	43	42	41	40	39	38	37	36	35	34	33
J1	0.743	42.54	1.92		2100	2100	2000	2000	1900	1800	1800	1700	1700	1600	1600	1500	1400	1400
J2	0.119	56.24	2.04		110	89	73	64	63	71	89	120	160	220	290	380	490	620
J3	0.0943	79.03	2.02		510	460	410	370	320	280	240	200	170	140	110	85	65	51
J4	0.477	94.63	1.96		180	140	110	88	68	53	44	41	45	57	78	110	150	200
J5	0.0017	141.1	2.04		83	100	130	160	190	230	270	320	370	430	500	570	650	740

Run	J	K_Da	m	E	32	31	30	29	28	27	26	25	24	23	22	21	20	19
J1	0.743	42.54	1.92		1300	1300	1200	1100	1100	1000	970	920	870	840	790	750	720	690
J2	0.119	56.24	2.04		770	960	1200	1400	1700	2000	2400	2900	3400	4000	4600	5400	6300	7300
J3	0.0943	79.03	2.02		42	39	43	55	76	110	150	200	270	350	440	560	700	850
J4	0.477	94.63	1.96		260	330	420	530	650	790	950	1100	1300	1600	1800	2100	2400	2800
J5	0.0017	141.1	2.04		840	940	1100	1200	1300	1500	1600	1800	2000	2200	2500	2700	3000	3300

Run	J	K_Da	m	E	18	17	16	15	14	13	12	11	10	9	8	7	6	5
J1	0.743	42.54	1.92		670	660	660	660	680	720	770	840	920	1000	1200	1300	1500	
J2	0.119	56.24	2.04		8500	9800	11000	13000	15000	17000	20000	23000	27000	31000	36000	42000	49000	57000
J3	0.0943	79.03	2.02		1000	1300	1500	1800	2100	2500	2900	3300	3800	4400	5100	5800	6600	
J4	0.477	94.63	1.96		3200	3600	4100	4700	5200	5900	6600	7400	8200	9100	10000			
J5	0.0017	141.1	2.04		3600	4000	4300	4800	5200	5700	6200	6800	7400	8000				

TABLE IV-11. CALCULATED VALUES OF E FOR VARIOUS VALUES OF $K_D a$ AND J. (The values of m were taken from Table IV-9)

Run	J	m	$K_D a$	25	30	35	40	42.54	45	50	55	60	65
	0.743[a]	1.92	E	60	5	5	12	16	20	25	29	33	35
J1	0.782[b]	1.92	E	60	5	12	22	26	29	34	38	41	43
	0.704[c]	1.92	E	60	60	5	6	6	10	16	21	24	27

Run	J	m	$K_D a$	35	40	45	50	55	56.24	60	65	70	75	80
	0.119[a]	2.04	E	30	34	37	40	42	42	44	45	47	48	49
J2	0.138[b]	2.04	E	34	38	41	44	46	47	48	50	51	53	54
	0.0994[c]	2.04	E	26	30	33	35	38	38	39	41	42	44	45

Run	J	m	$K_D a$	65	70	75	79.03	80	85	90	95	100	105
	0.0943[a]	2.02	E	22	26	29	31	32	34	37	39	41	42
J3	0.0992[b]	2.02	E	23	27	30	32	33	35	38	40	42	44
	0.0893[c]	2.02	E	21	24	28	30	30	33	35	37	39	41

Run	J	m	$K_D a$	70	75	80	85	90	94.63	95	100	105	110	115
	0.477[a]	1.96	E	21	26	30	33	36	39	39	42	44	46	48
J4	0.527[b]	1.96	E	32	37	41	44	48	50	50	53	55	57	59
	0.427[c]	1.96	E	10	14	19	22	25	28	28	31	33	35	37

Run	J	m	$K_D a$	120	125	130	135	140	141.1	145	150	155	160	165
	0.0017[a]	2.04	E	44	47	49	51	53	53	55	56	58	60	60
J5	-0.0560[b]	2.04	E	26	28	30	32	34	34	35	37	38	40	41
	0.0594[c]	2.04	E	60	60	60	60	60	60	60	60	60	60	60

[a] The flux of solute down the column, $J = \frac{1}{2}(L_C c_C^i - L_D c_D^o) + (L_C c_C^o - L_D c_D^i)$

[b] The flux of solute down the column, $J = (L_C c_C^i - L_D c_D^o)$

[c] The flux of solute down the column, $J = (L_C c_C^o - L_D c_D^i)$

TABLE IV-12. CALCULATED VALUES OF E FOR VARIOUS VALUES OF m. (The values of J and $K_D a$ were taken from Table IV-9.)

Run	J	$K_D a$	m	1.82	1.84	1.86	1.88	1.90	1.92	1.94	1.96	1.98	2.00	2.02
J1	0.743	42.54	E	36	32	28	24	20	16	12	9	6	6	6

Run	J	$K_D a$	m	1.94	1.96	1.98	2.00	2.02	2.04	2.06	2.08	2.10	2.12
J2	0.119	56.24	E	48	46	45	44	43	42	41	40	40	39

Run	J	$K_D a$	m	1.92	1.94	1.96	1.98	2.00	2.02	2.04	2.06	2.08	2.10	2.12
J3	0.0943	79.03	E	44	41	39	36	34	31	29	26	24	22	19

Run	J	$K_D a$	m	1.86	1.88	1.90	1.92	1.94	1.96	1.98	2.00	2.02	2.04	2.06
J4	0.477	94.63	E	59	55	51	47	43	39	35	32	28	24	21

Run	J	$K_D a$	m	1.94	1.96	1.98	2.00	2.02	2.04	2.06	2.08	2.10	2.12	2.14
J5	0.0017	141.1	E	60	60	60	60	58	53	49	45	41	37	34

TABLE IV-13. EQUILIBRIUM DATA FOR ACETIC ACID DISTRIBUTED

BETWEEN MIBK-SATURATED WATER AND WATER-SATURATED MIBK

AT 70°F. (MEASURED IN THIS WORK.)

Concentration of acetic acid, lb.-moles/ft.^{3}		Distribution coefficient, m
Water phase	MIBK phase	
0.001010	0.0005545	1.8214
0.002218	0.001099	2.0180
0.004089	0.001990	2.0547
0.006307	0.003079	2.0482
0.006743	0.003287	2.0512
0.01127	0.005485	2.0542
0.01385	0.006772	2.0453
0.01763	0.008619	2.0460
0.02564	0.01262	2.0314
0.02109	0.01040	2.0286
0.02802	0.01412	1.9846
0.03728	0.01901	1.9609
0.04663	0.02446	1.9069
0.05794	0.03111	1.8622
0.06683	0.03614	1.8493
0.06802	0.03738	1.8199
0.07376	0.04059	1.8171
0.07891	0.04368	1.8064
0.08381	0.04733	1.7709
0.08807	0.05050	1.7441
0.09625	0.05564	1.7297
0.1008	0.05881	1.7146
0.1051	0.06188	1.6978
0.1104	0.06569	1.6812
0.1150	0.06901	1.6671

APPENDIX V

DETAILS OF THE APPARATUS

Figures V-1 to V-23 inclusive show the details of various portions of the $1\frac{1}{2}$-in. I.D. and 3-in. I.D. spray columns and their accessories. All stainless steel parts were made from Type 304 stainless steel.

The piston sample collection flask shown in Figure V-1 was used for dispersed phase hold-ups greater than 12%. The collection flask for hold-ups less than 12% is described elsewhere (37). Figure V-2 is a diagram of the hypodermic needle sampling system and Figure V-3 gives details of the sampling valve. The tracer injection arrangement is given in Figure V-4 and details of the tracer distributor are shown in Figure V-5.

Figures V-6, V-7, and V-8 show the 0.126-in. I.D., 0.086-in. I.D., and the 0.053-in. I.D. nozzle tips together with the respective nozzle tip support plates and nozzle tip caps or plugs for use in the $1\frac{1}{2}$-in. I.D. spray column. The nozzle tip support plates were press fitted into the nozzle designed by Choudhury (35). The flow straightener in the nozzle designed by Choudhury was not used in the present work. The 0.103-in. I.D. nozzle tips, the corresponding nozzle tip support plate and nozzle tip caps are described elsewhere (30, 35). The inside diameter of

each nozzle tip in each set of nozzles was measured by means of a travelling microscope. Two such diameters at right angles to each other were measured for each nozzle tip. The arithmetic average of the nozzle tip inside diameter was calculated for each set of tips.

The Perspex box used to reduce optical distortion in the $1\frac{1}{2}$-in. I.D. column is shown in Figure V-9. An O-ring was press fitted in each of the top and bottom of the box to prevent the loss of water from between the box and the column. The cardboard light shield, which fitted over the Perspex box, is shown in Figure V-10. The inside surfaces of the light shield were painted with black ink to reduce unwanted light reflections. The eight sheets of tracing paper in the light shield served as a diffusing screen for the light.

Figure V-11 shows the nozzle and nozzle tips assembled in the lower portion of the 3-in. I.D. column. Details of the various parts of the assembly are given in Figures V-12 to V-17 inclusive. The diametrically opposite holes labelled B in Figure V-17 were outlets for the aqueous phase. The third hole labelled B was for a thermometer well. The nozzle support fitted into E. C was for a drain valve.

Figure V-18 shows the Elgin head for the 3-in. I.D. column and Figures V-19, V-20, and V-21 give details of various component parts. The aqueous phase inlet pipes, shown as A in Figure V-18,

were screwed into the holes marked C in Figure V-19. The two holes labelled B in Figure V-19 were the dispersed phase exits and E in the same Figure accommodated a thermometer well. F in Figure V-20 accommodated another thermometer well. The six holes, C, in Figure V-20 were for bolts which held a standard flange. This flange compressed the polyethylene packing shown in Figure V-21. E in Figure V-20 was for a drain valve.

Figure V-22 shows the Perspex box used to reduce optical distortion in the 3-in. I.D. column. O-rings were press fitted into the top and the bottom of the box to prevent the escape of water from between the box and the column. Drop photographs were taken through a 6-in. long section of 3-in. I.D. glass pipe cut from a longer piece. This 6-in. piece used for photography therefore had unflanged ends. It was held in place, concentric with the rest of the column, by means of two flanges, one of which is shown in Figure V-23. Four 9-in. long aluminum tie-rods held the flanges in position. Each end of these was threaded and carried a nut for tightening purposes.

§14-35 FULL LENGTH PYREX GROUND GLASS JOINT

0·2 ml. DIVISIONS (APPROX. 2 mls./cm.)

25 mm. DIA.

0·2 ml. DIVISIONS (APPROX. 2 mls./cm.)

HOOKS FOR SPRINGS

40 mm. DIA.

TEFLON STOPCOCK (WITH LARGE DIA. HOLE FOR FAST DELIVERY)

118·0 mls.

102·0 mls.

¼"
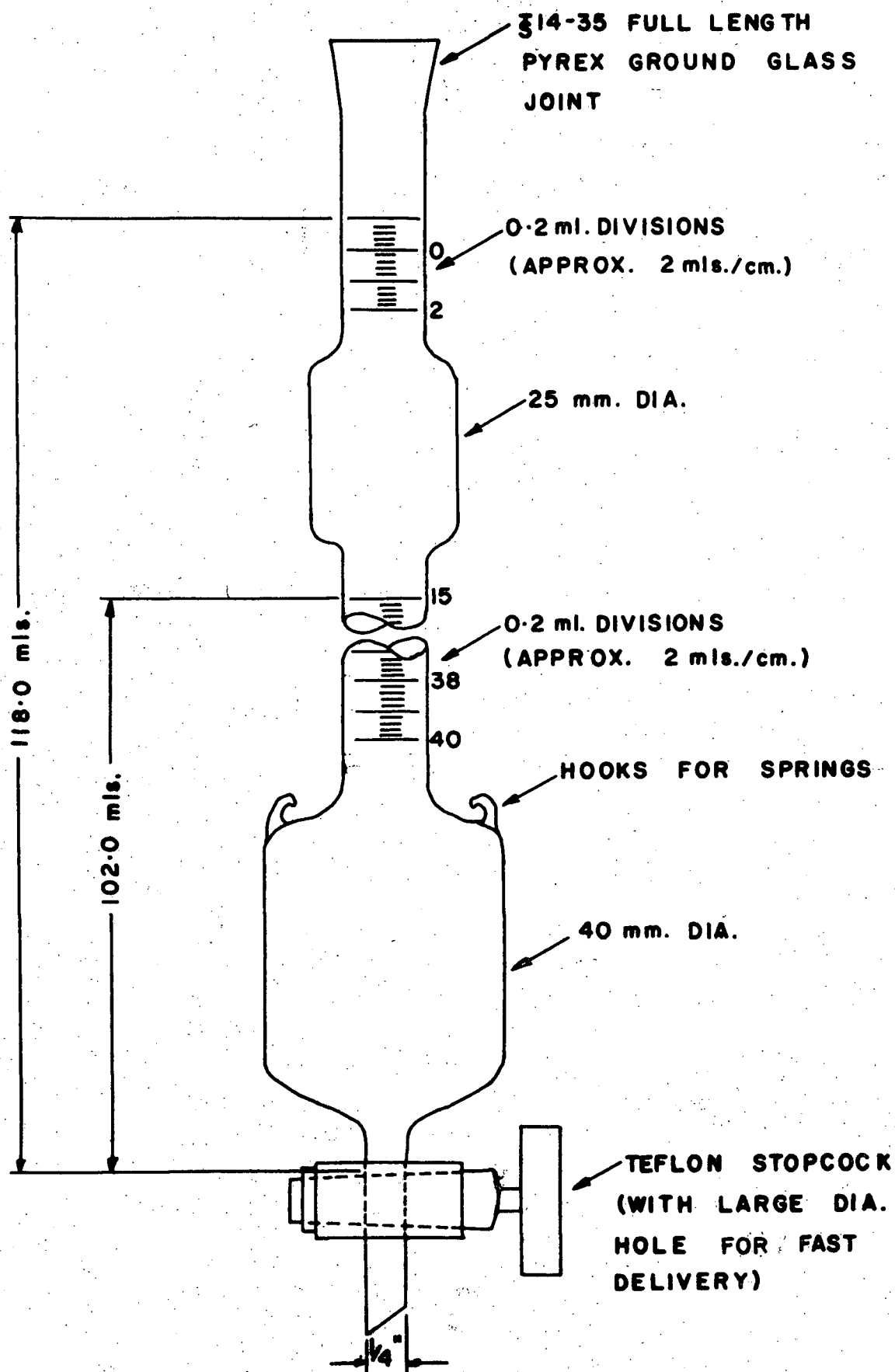
FIGURE V-1. PISTON SAMPLE COLLECTION FLASK FOR LARGE HOLD-UPS

3" LONG 22 GAUGE HYPODERMIC NEEDLE

$\frac{1}{16}$" THICK, $1\frac{1}{2}$" I.D., $2\frac{5}{32}$" O.D. POLYETHYLENE GASKET WITH 0.025" DIA. HOLE FOR NEEDLE

SAMPLING VALVE

COLUMN WALL
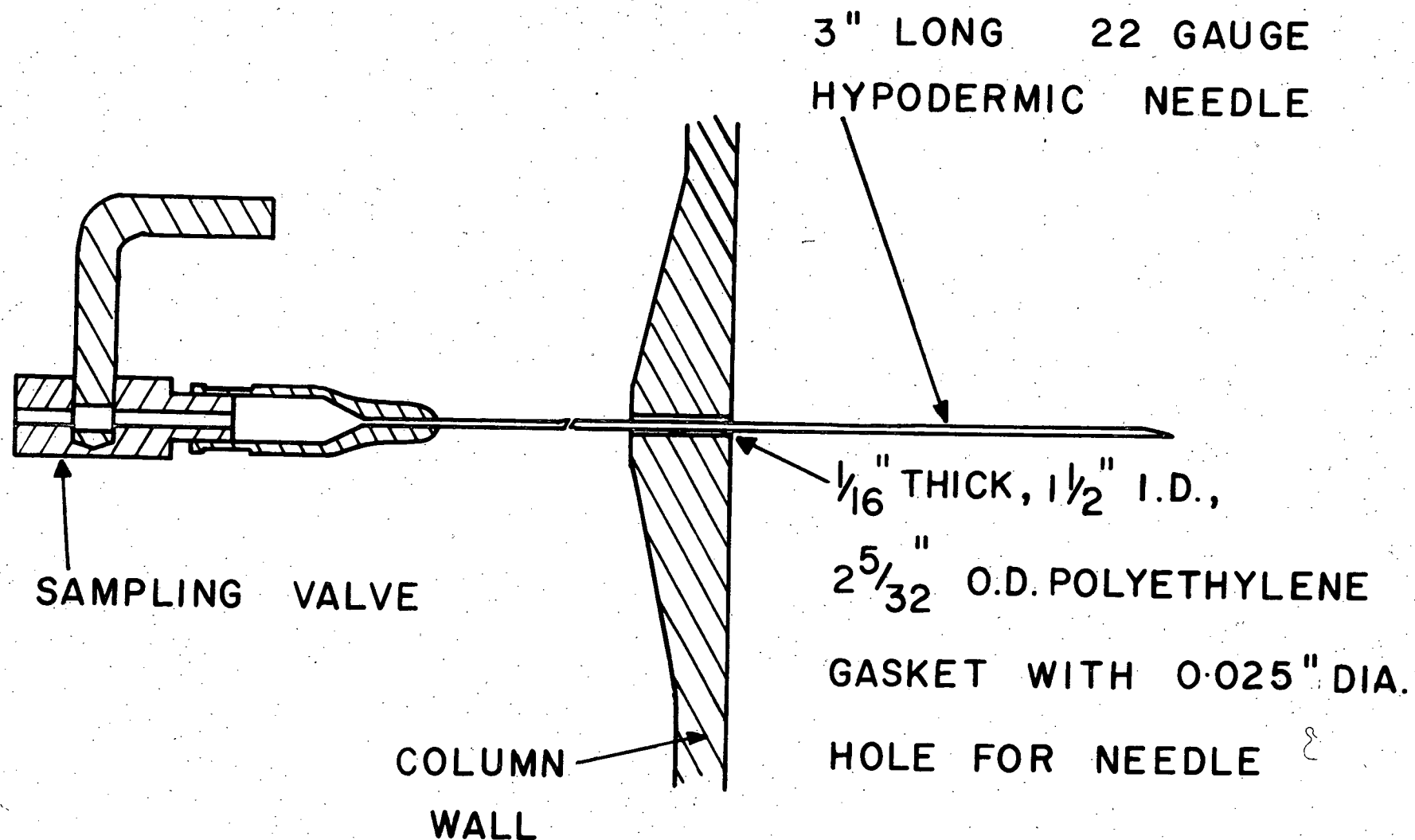
FIGURE V-2. HYPODERMIC NEEDLE INSTALLED FOR SAMPLING

0.7"

0.5"

0.25"

0.125" D.

A

A

0.055" D.

0.225"

0.25" D.

0.165" D.

SECTION ON A-A

BODY MATERIAL: POLYETHYLENE

0.4"

0.0625" R.

0.125" D.

0.089" D.

0.64"

30°

0.1"
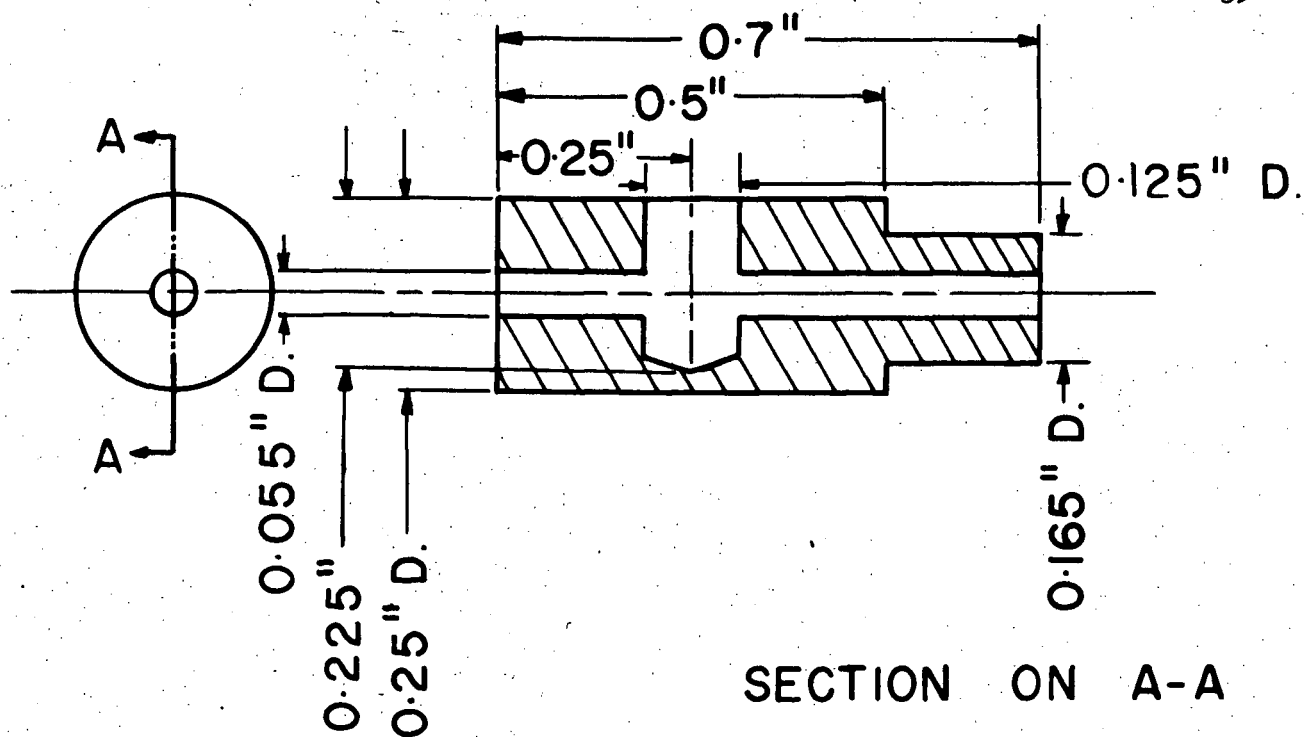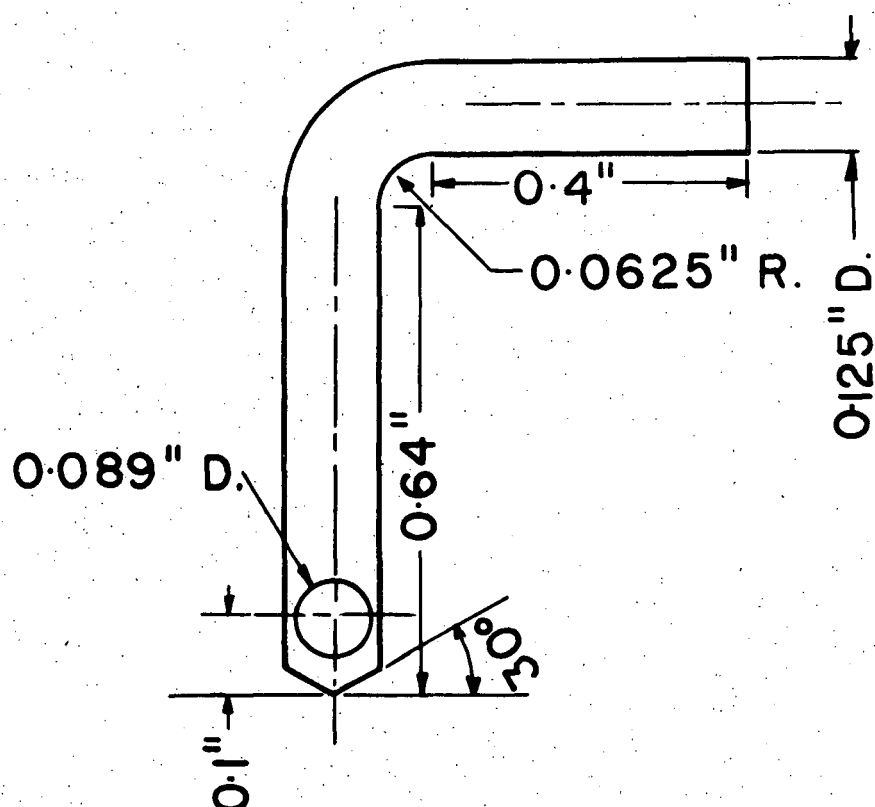
STEM MATERIAL: STAINLESS STEEL

FIGURE V-3. SAMPLING VALVE FOR HYPODERMIC NEEDLE

¼" NYLON COMPRESSION NUT

¼" NYLON UNION

2" LONG 18 GAUGE HYPODERMIC NEEDLE

TRACER DISTRIBUTOR

⅛" THICK, 1½" I.D., 2⁵⁄₃₂" O.D. TEFLON GASKET WITH 0·057" DIA. HOLE FOR NEEDLE

½" LONG, ¼"O.D. 0·057" I.D. POLYETHYLENE

COLUMN WALL

¼" O.D., ⅛" I.D. POLYETHYLENE TUBE
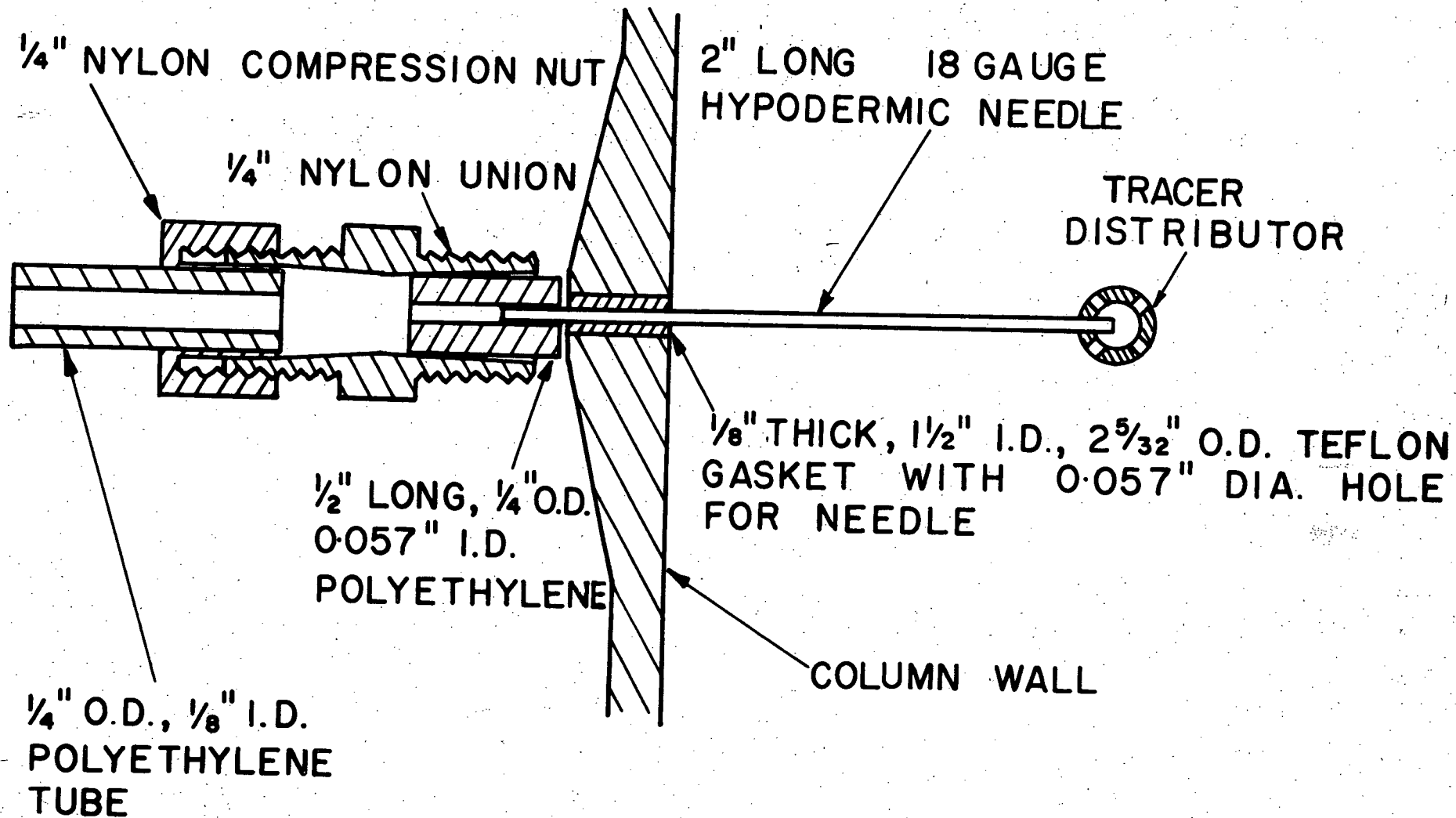
FIGURE V-4. TRACER INJECTION SYSTEM

SECTION ON A-A

GLASS

POLYETHYLENE

I HOLE 0.043" D.

4 HOLES 0.063" D.

0.157" D.
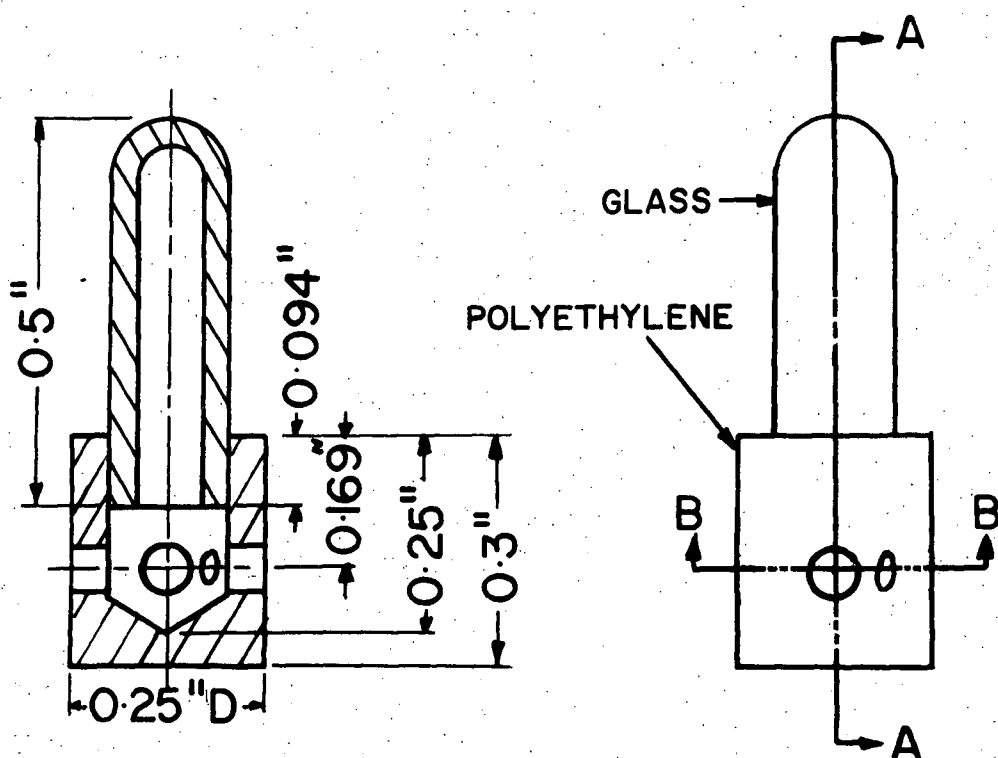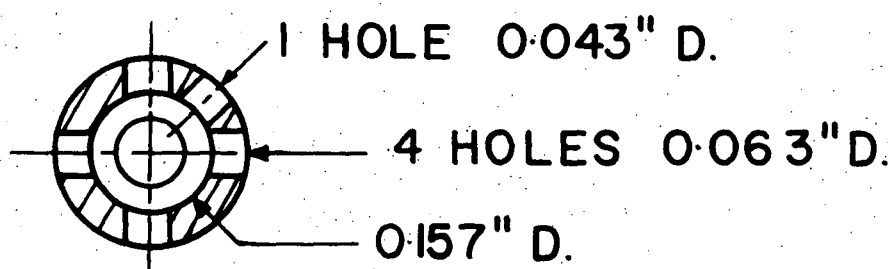
SECTION ON B-B

FIGURE V-5. TRACER DISTRIBUTOR

10 HOLES ³⁄₁₆ " D.
ON ¹⁵⁄₁₆ " P.C.D.

4 HOLES ³⁄₁₆ " D.
ON ³⁄₈ " P.C.D.

⅛ " X 1¼ " D.

9°

STAINLESS STEEL NOZZLE TIP SUPPORT

A   A

⅛ " D.
³⁄₁₆ " D.
45°
CHAMFER

¼ "

SECTION ON A-A

STAINLESS STEEL NOZZLE TIP

A'   A'

¼ " D.

3⁄16 " D.

0.1"

0.2"

SECTION ON A-A'
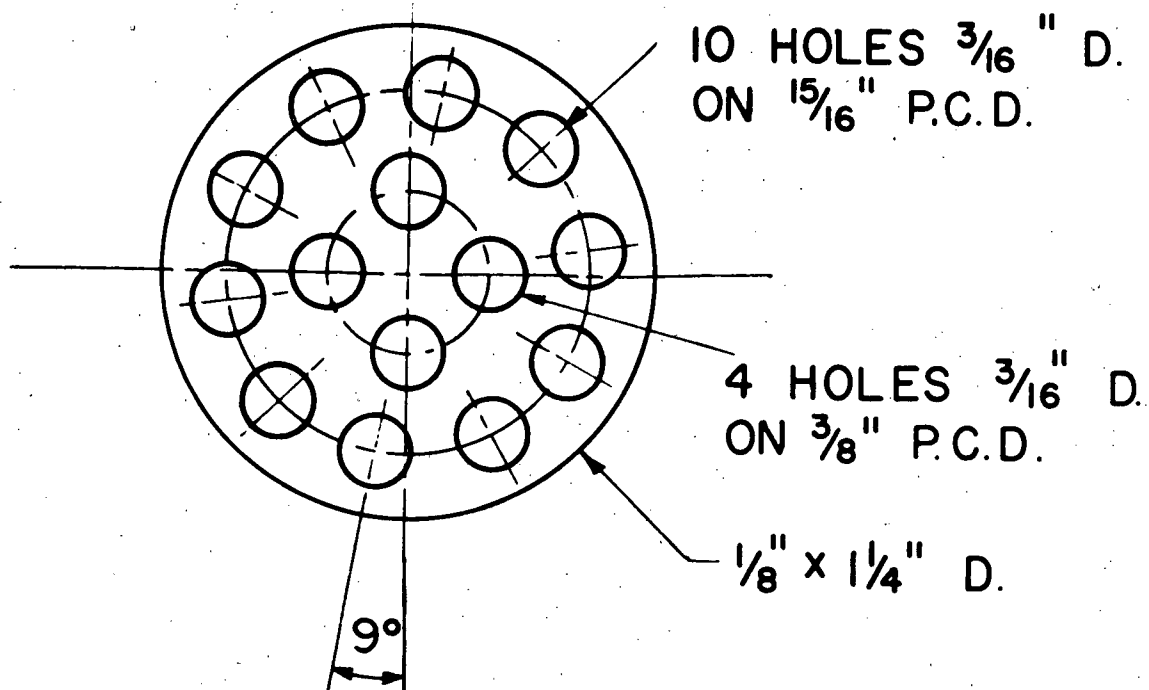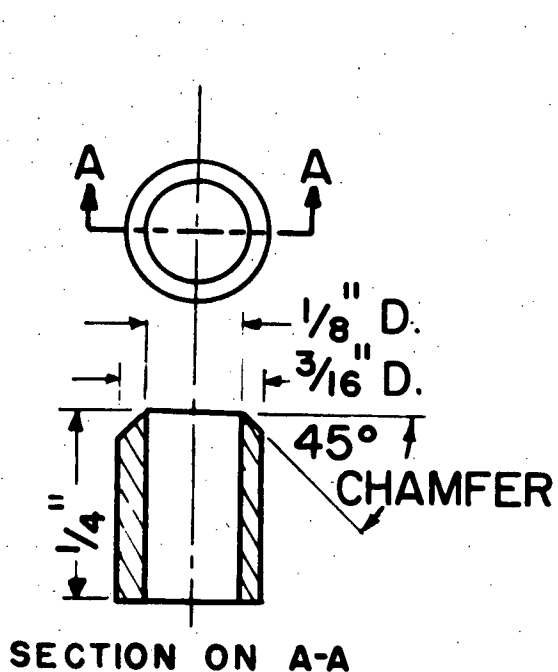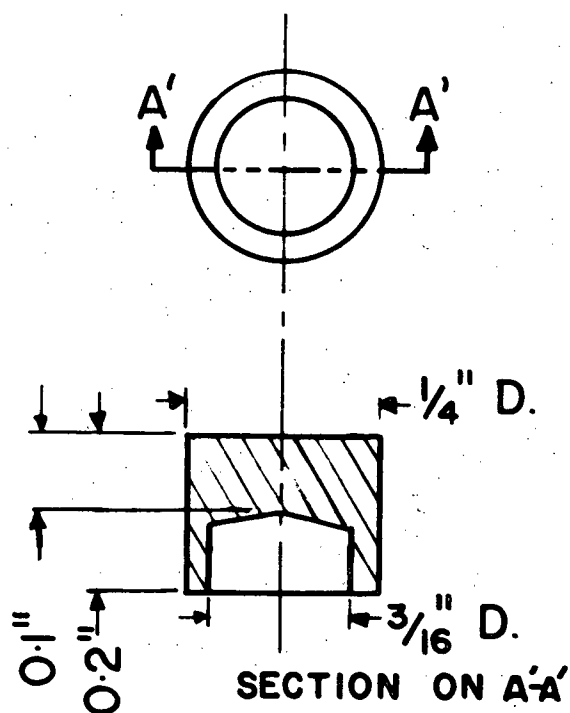
TEFLON NOZZLE CAP

FIGURE V-6. 0.126-IN. I.D. NOZZLE TIPS, NOZZLE TIP SUPPORT PLATE, AND NOZZLE TIP CAPS
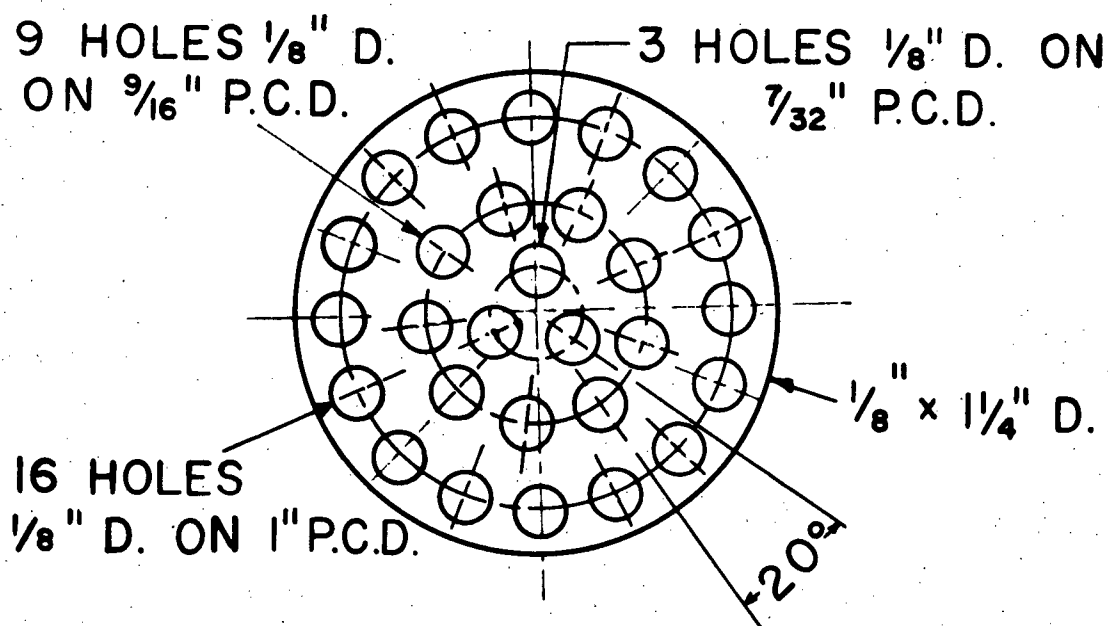
9 HOLES ⅛" D.
ON ⁹⁄₁₆" P.C.D.

3 HOLES ⅛" D. ON
⁷⁄₃₂" P.C.D.

⅛" × 1¼" D.

16 HOLES
⅛" D. ON 1" P.C.D.

20°

STAINLESS STEEL NOZZLE TIP SUPPORT

A   A

45°
CHAMFER

¼"

⅛" D.

0.086" D.

SECTION ON A-A

STAINLESS STEEL
NOZZLE TIP

⅛"

0.086" D.
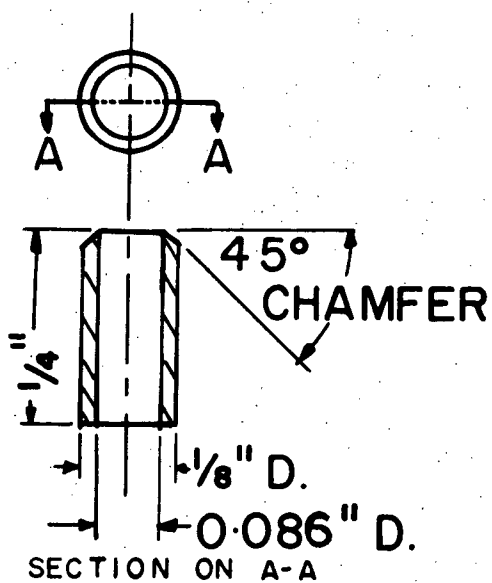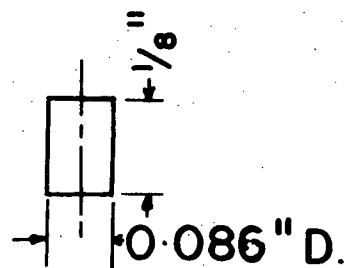
TEFLON NOZZLE
TIP PLUG

FIGURE V-7. 0.086-IN. I.D. NOZZLE TIPS, NOZZLE TIP SUPPORT PLATE, AND
NOZZLE TIP PLUGS
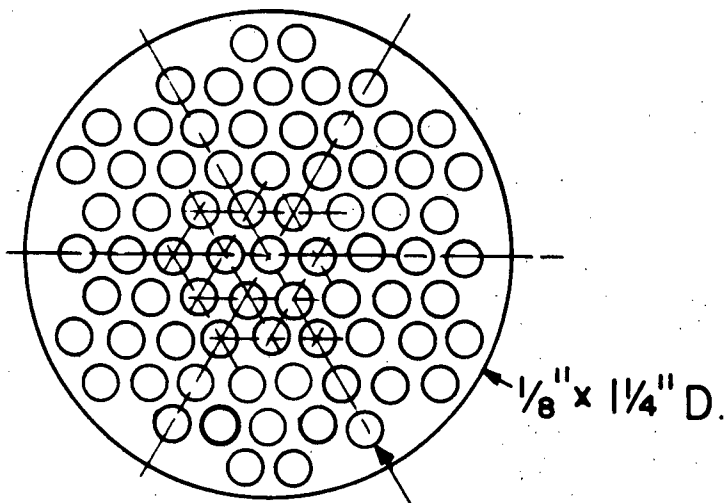
¹⁄₈" x 1¼" D.

73 HOLES ³⁄₃₂" D. ON ⅛"
TRIANGULAR PITCH
STAINLESS STEEL NOZZLE TIP SUPPORT

45° CHAMFER

³⁄₃₂" D.
0.052" D.
SECTION ON A-A
STAINLESS STEEL
NOZZLE TIP

0.052" D.
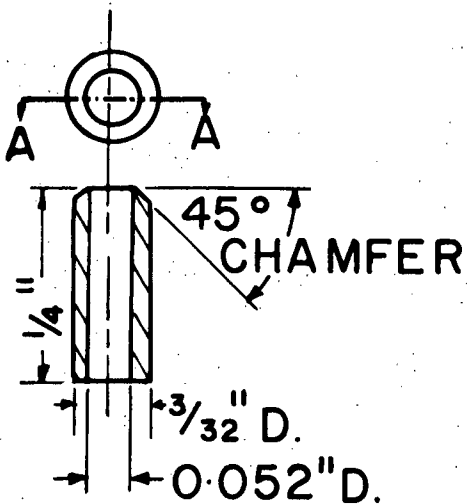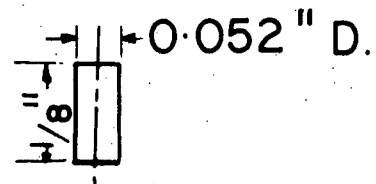
TEFLON NOZZLE
TIP PLUG

FIGURE V-8.   0.053-IN. I.D. NOZZLE TIPS, NOZZLE TIP SUPPORT PLATE, AND
NOZZLE TIP PLUGS
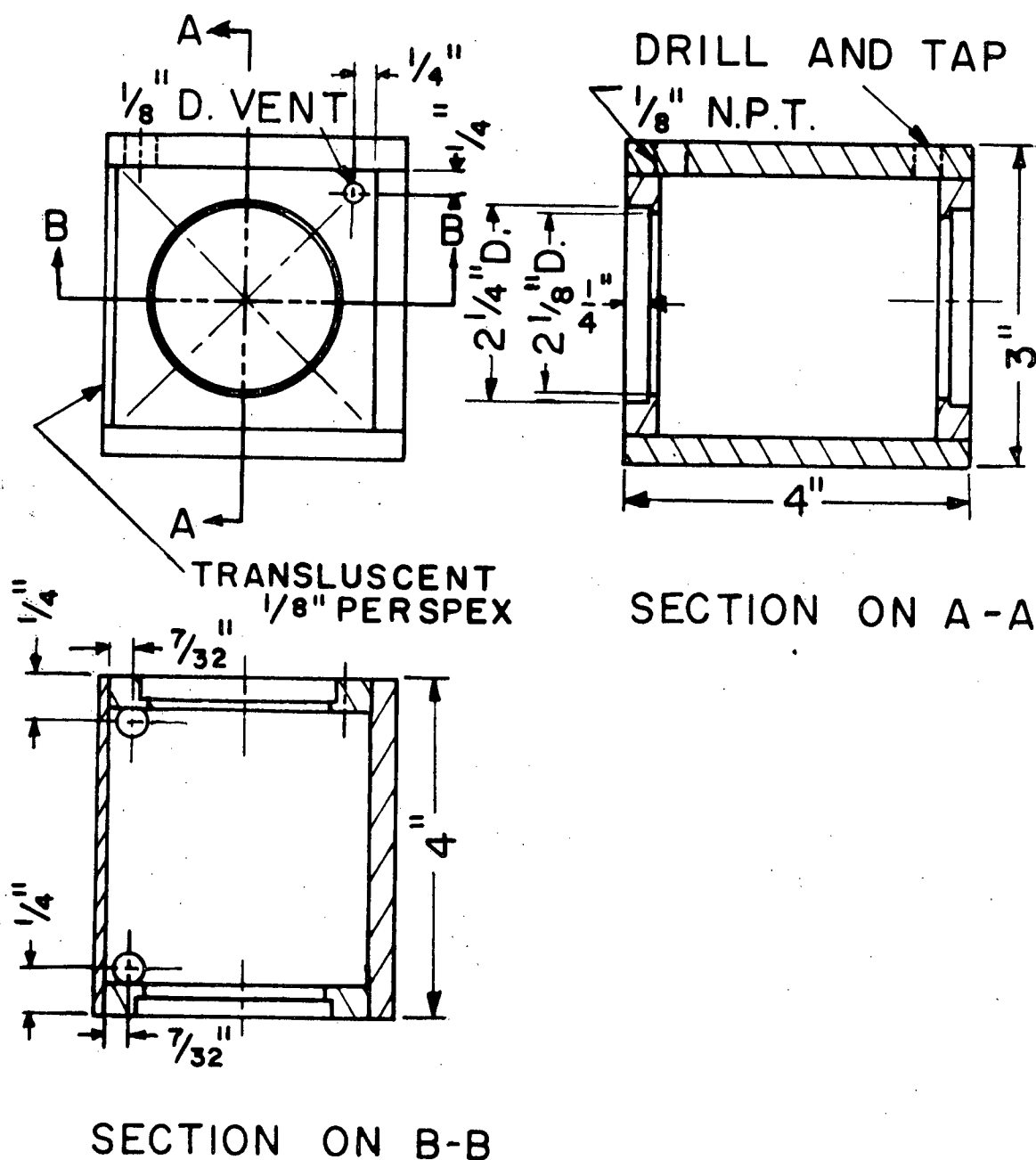
FIGURE V-9. PERSPEX BOX FOR THE 1½-IN. I.D. COLUMN PHOTOGRAPHS

8 SHEETS OF TRACING PAPER

FLASH HEAD FITS HERE

PHOTOGRAPHIC SECTION OF COLUMN FITS HERE
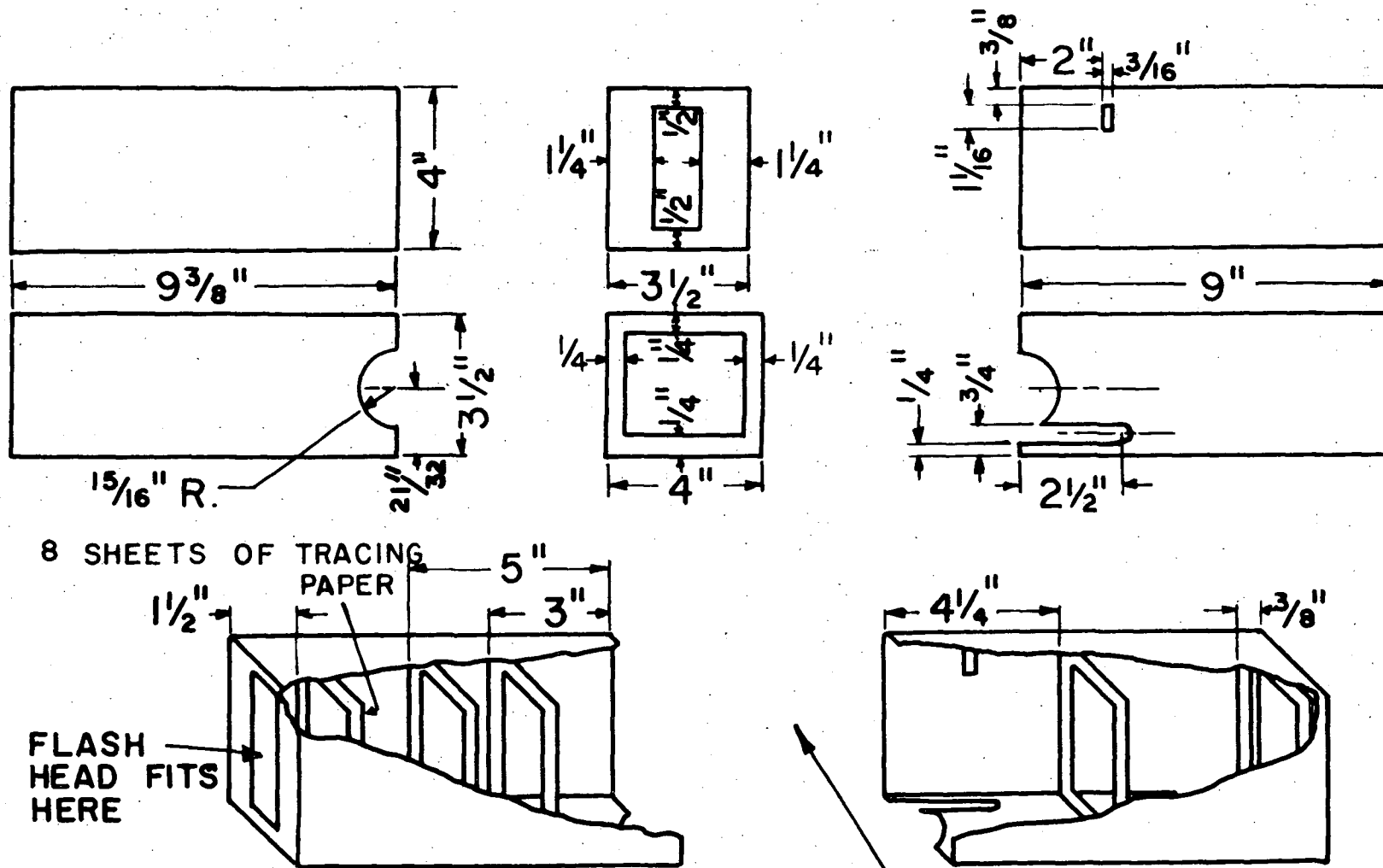
MATERIAL: $1/32$" PULPBOARD

FIGURE V-10. LIGHT SHIELD FOR THE $1\frac{1}{2}$-IN. I.D. COLUMN PHOTOGRAPHS

SPECIAL
PYREX REDUCER

NOZZLE TIPS

NOZZLE TIP
SUPPORT

NOZZLE TIP
PLUGS

NOZZLE

FLOW
STRAIGHTENER

TEFLON
GASKET

END PLATE

POLYETHYLENE GASKET

NOZZLE RETAINING NUT

NOZZLE SECURING PLATE
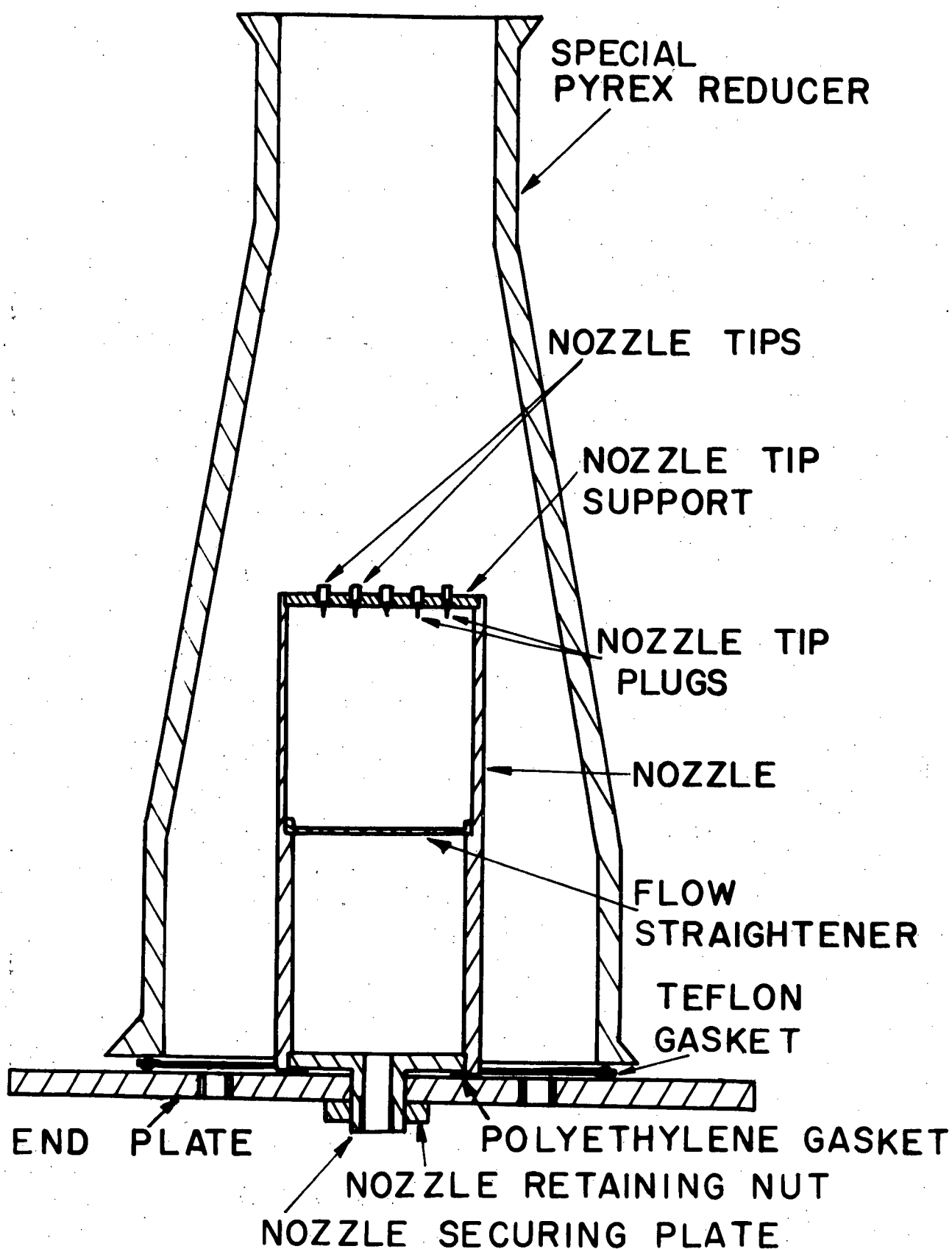
FIGURE V-11. LOWER END OF THE 3-IN. I.D. COLUMN
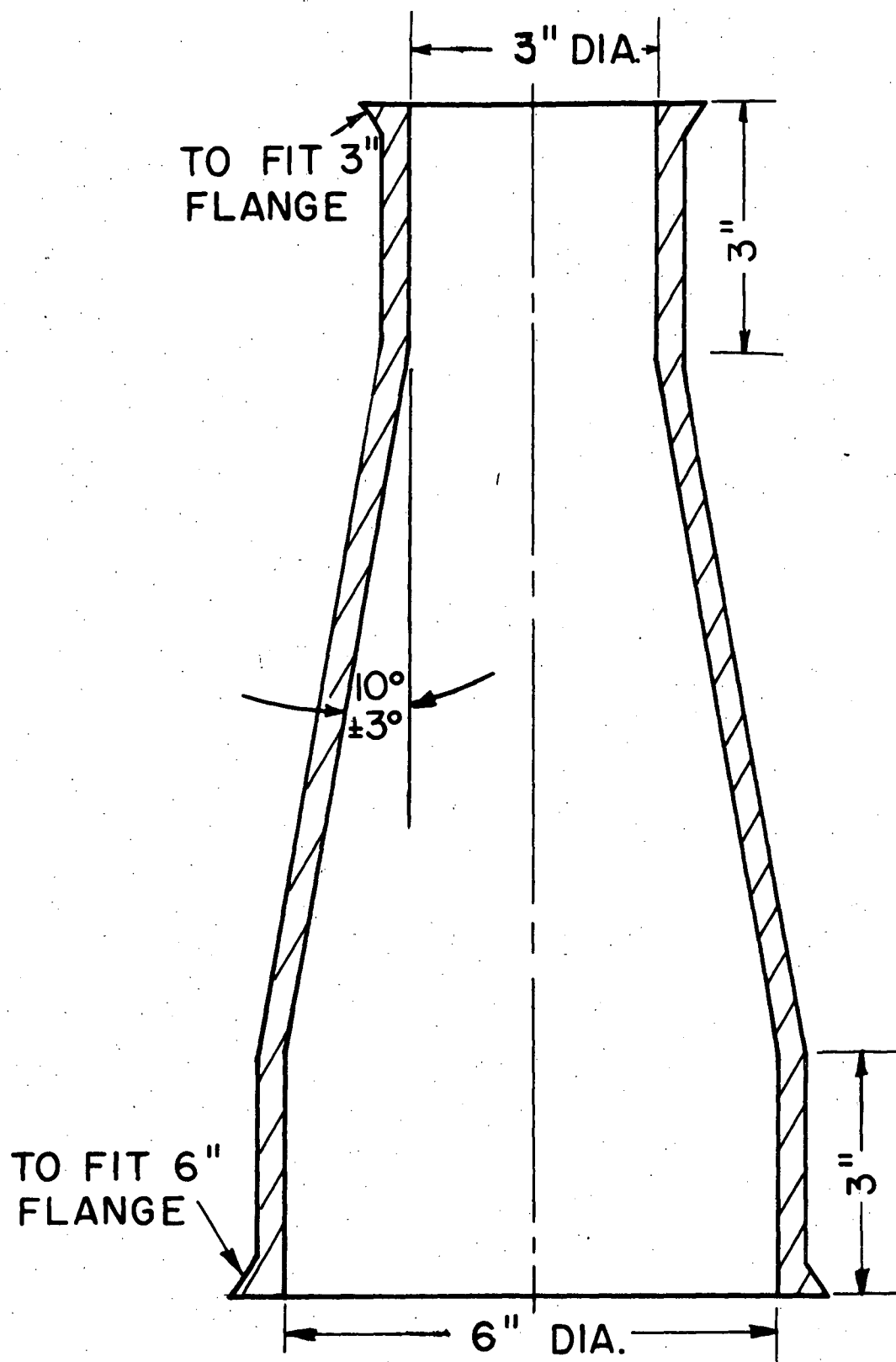
FIGURE V-12.   SPECIAL PYREX REDUCER FOR THE 3-IN. I.D. COLUMN

2·875" D.
2·719" D.
2·657" D.
2·469" D.
⅛"
3·375"
6·750"
0·250"
2½" I.D./16 T.P.I.
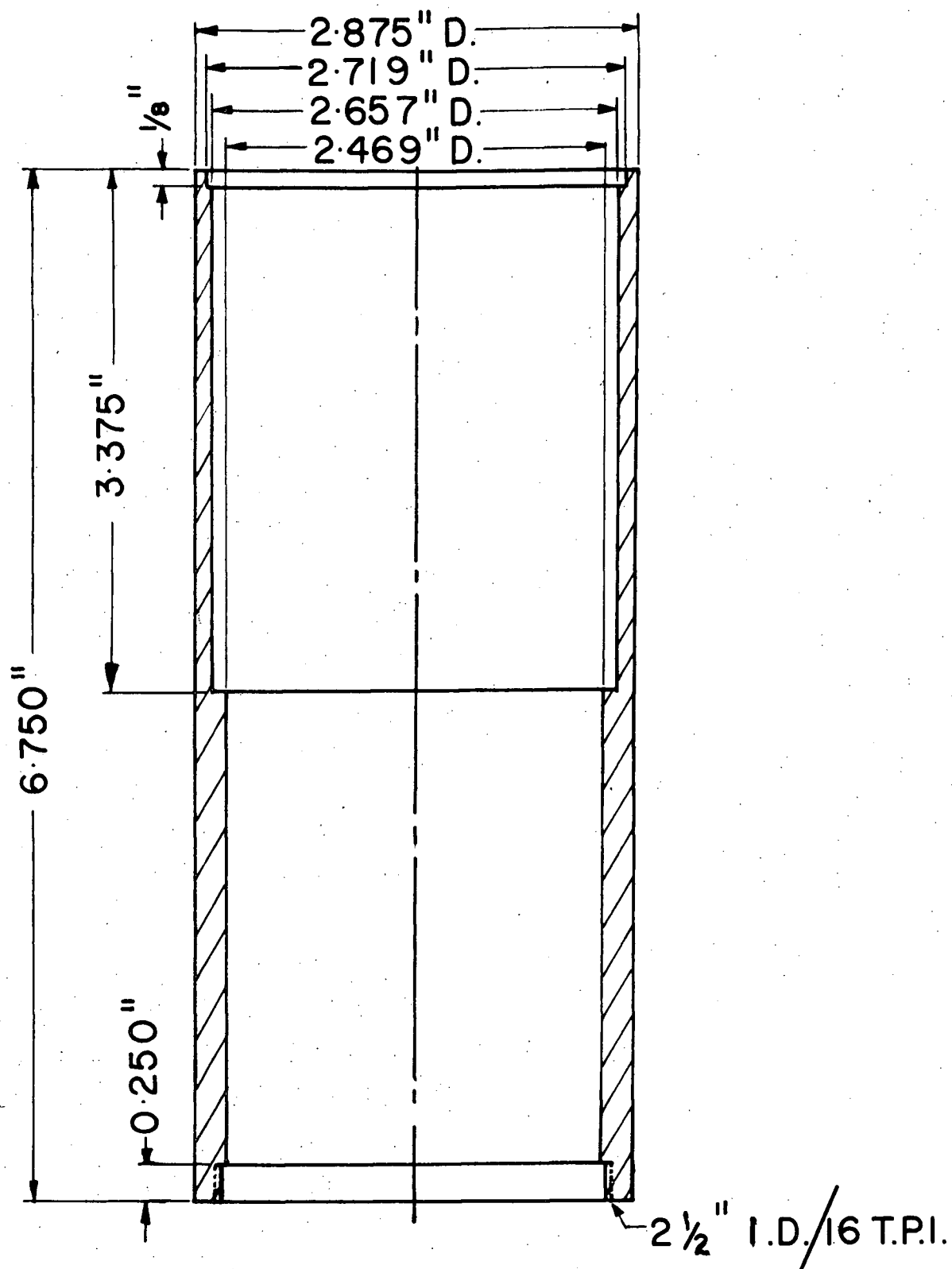
MATERIAL: STAINLESS STEEL

FIGURE V-13.   NOZZLE SHELL FOR THE 3-IN. I.D. COLUMN

$\frac{1}{8}'' \times 2\frac{23}{32}''$ D.

85 HOLES $\frac{1}{8}''$ D. ON $\frac{1}{4}''$
TRIANGULAR PITCH
STAINLESS STEEL NOZZLE TIP SUPPORT

45°
CHAMFER

$\frac{1}{4}''$

$\frac{1}{8}''$ D.

0.101" D.

SECTION ON A-A

STAINLESS STEEL
NOZZLE TIP

$\frac{1}{8}''$

0.101" D.
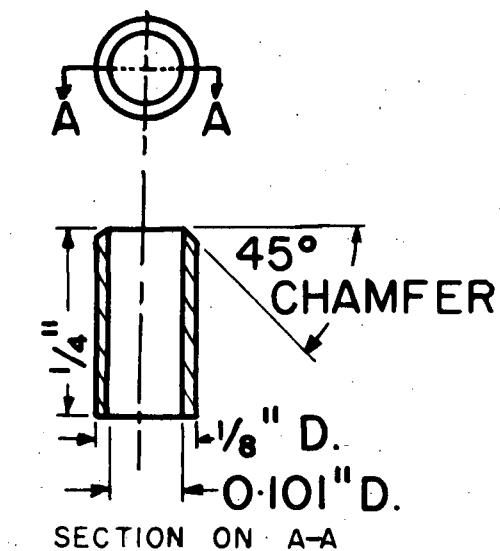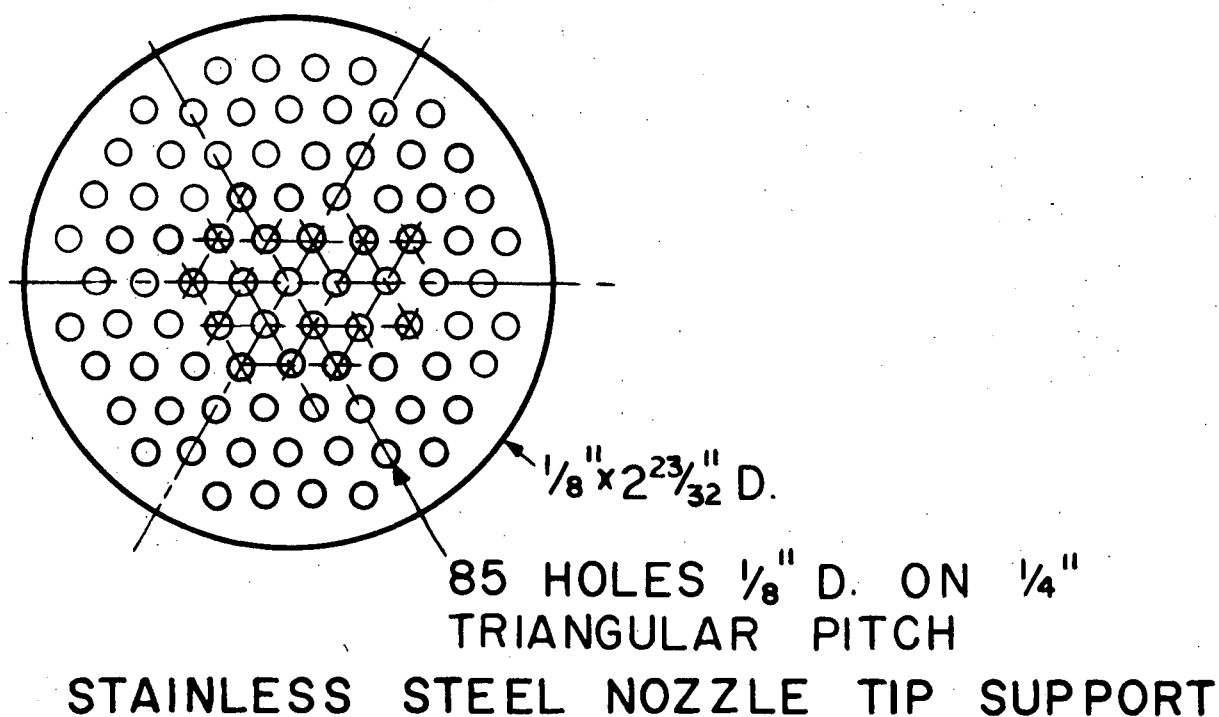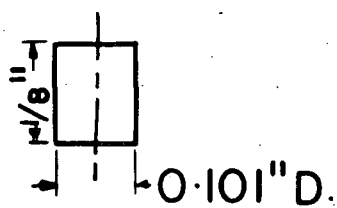
TEFLON NOZZLE
TIP PLUG

FIGURE V-14. NOZZLE TIPS, NOZZLE TIP SUPPORT PLATE, AND NOZZLE TIP
PLUGS FOR THE 3-IN. I.D. COLUMN

12 HOLES ³⁄₁₆" D.
ON 1¾" P.C.D.

4 HOLES ³⁄₁₆" D.
ON ⅞" P.C.D.

A   A

15°

2²¹⁄₃₂" D.

2¹⁵⁄₃₂" D.

SECTION ON A-A

¹⁄₁₆"

³⁄₁₆"
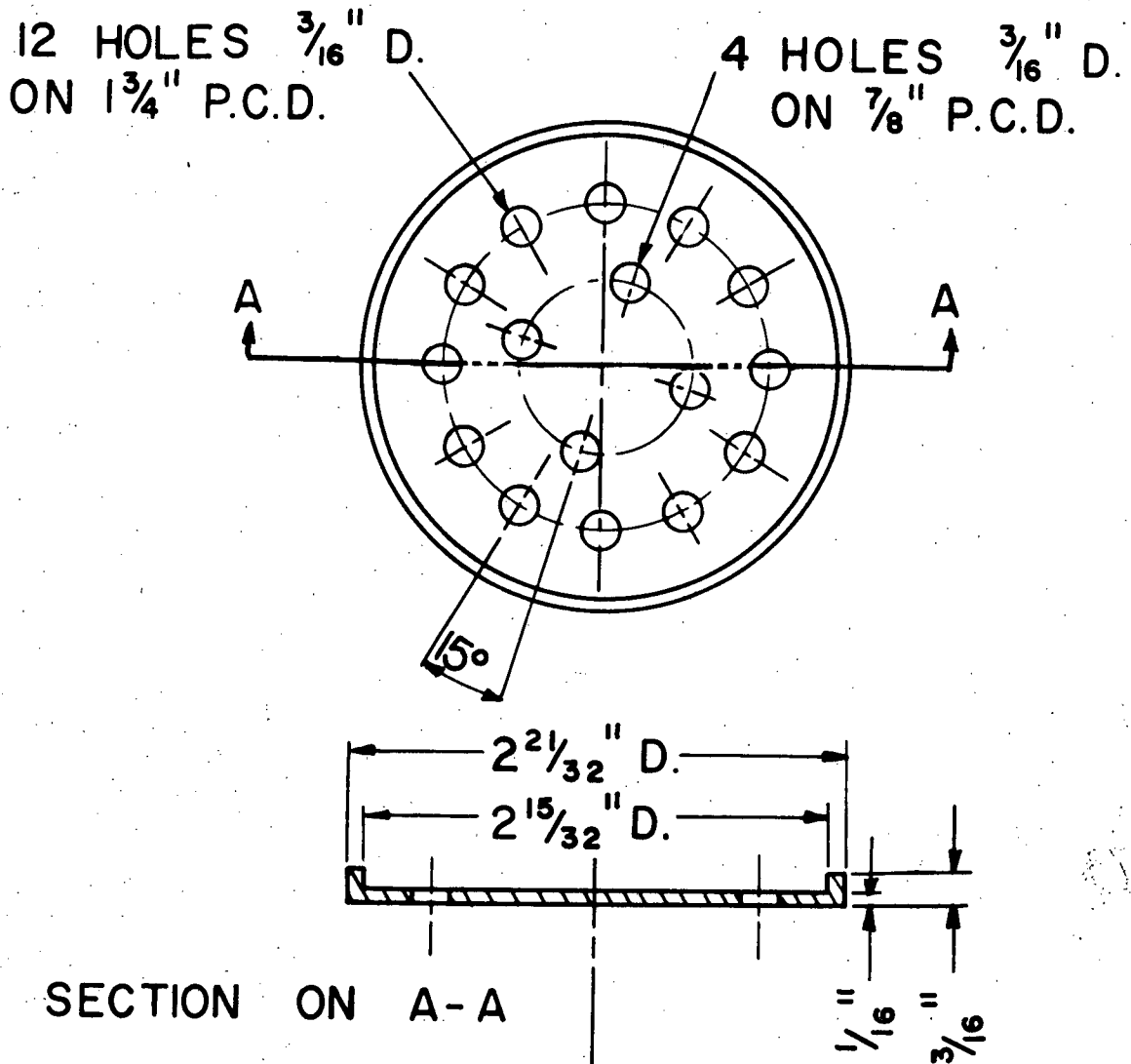
MATERIAL: STAINLESS STEEL

FIGURE V-15. FLOW STRAIGHTENER FOR THE 3-IN. I.D. COLUMN NOZZLE

2⁹⁄₁₆" O.D./16 T.P.I.

¼"

3/8"

½"   ¾"   1⅛"

⅛" N.P.T.
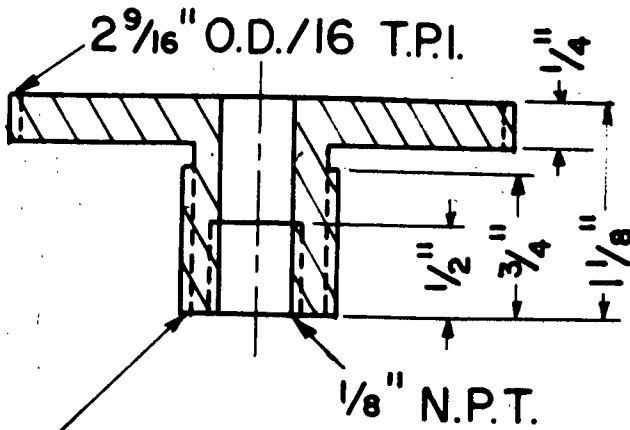
¾" O.D./16 T.P.I.

SECTION ON B-B

B

A   A

B

9⁄16"
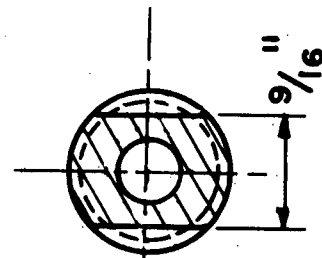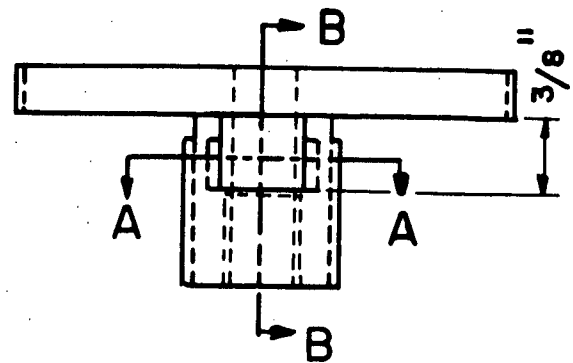
SECTION ON A-A

STAINLESS STEEL NOZZLE SECURING PLATE

C

1⁵⁄₈"

¼"

¾" O.D./16 T.P.I.
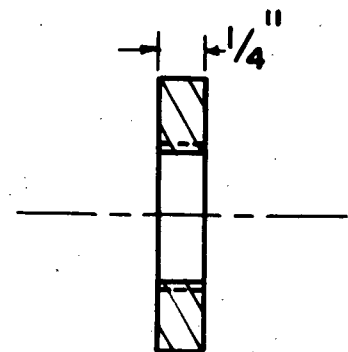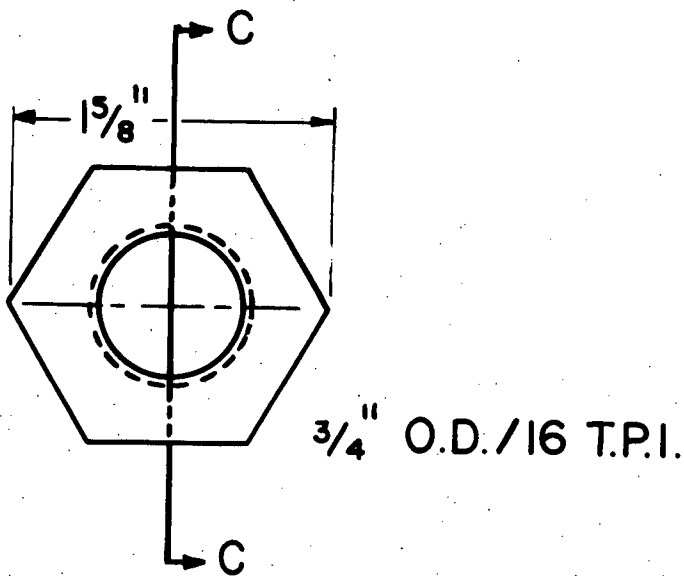
SECTION ON C-C

C

STAINLESS STEEL RETAINING NUT

FIGURE V-16. NOZZLE SECURING PLATE AND RETAINING NUT FOR THE 3-IN. I.D.
COLUMN

8 HOLES WITH
CLEARANCE FOR ⅜"
BOLTS ON 9½" P.C.D.

A — A

22½°

B B E C B B

4½" P.C.D.
B,B,B, 3 HOLES DRILL AND TAP ¼" N.P.T.
C,I HOLE DRILL AND TAP ⅛" N.P.T.
E,I HOLE ¾" D.

10½" D.

⅜"

MACHINE FLAT
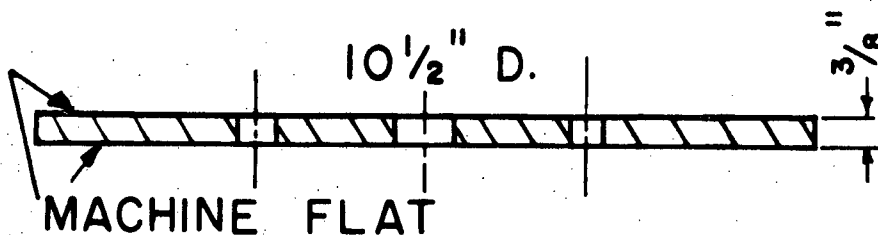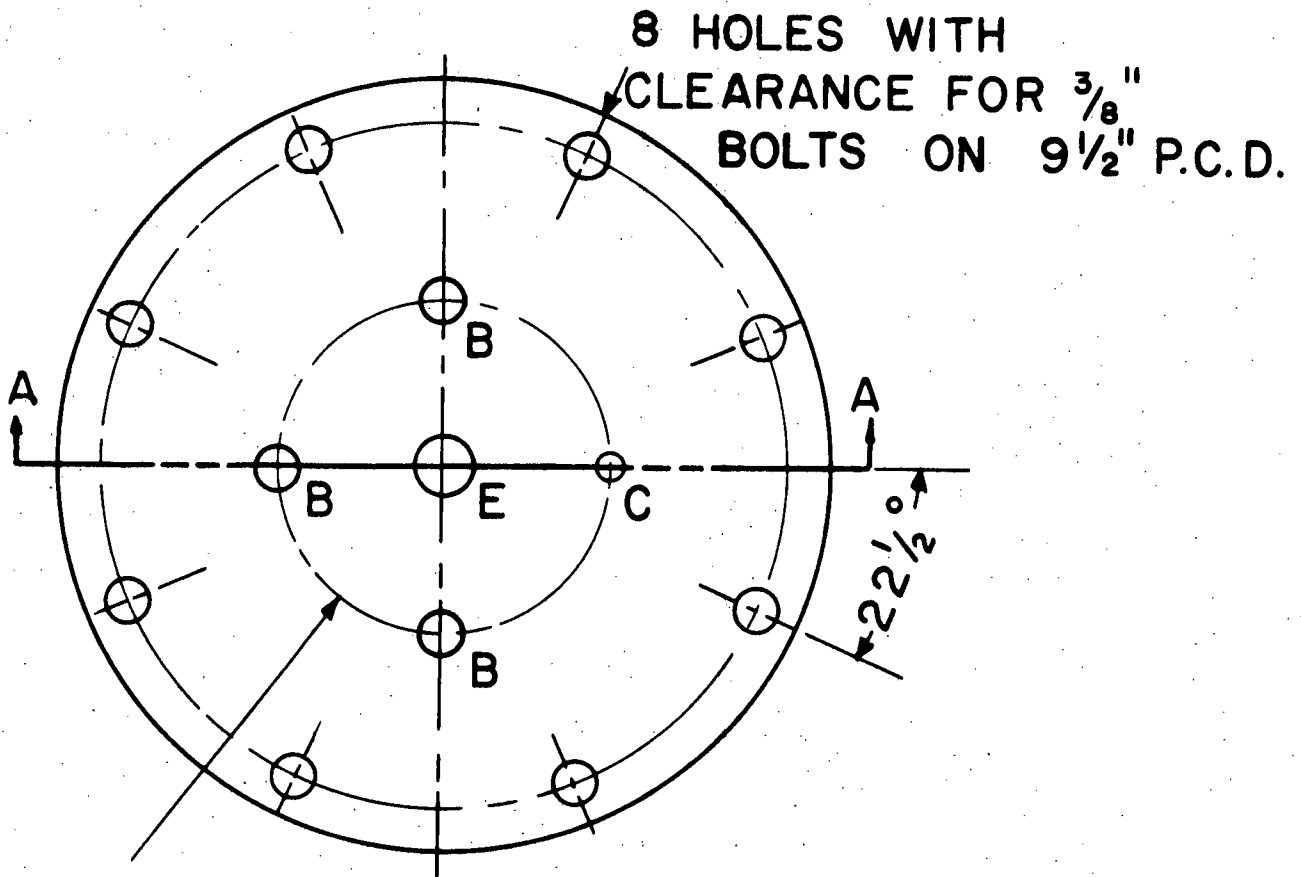
SECTION ON A-A

MATERIAL: STAINLESS STEEL
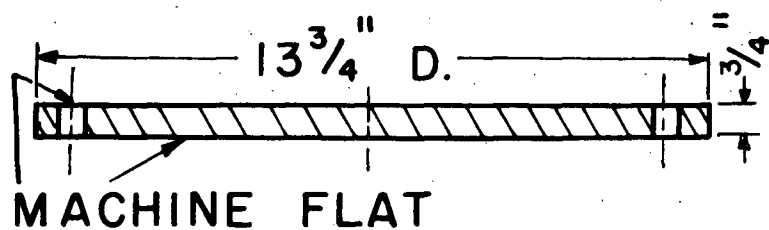
FIGURE V-17.   END PLATE FOR THE BOTTOM OF THE 3-IN. I.D. COLUMN
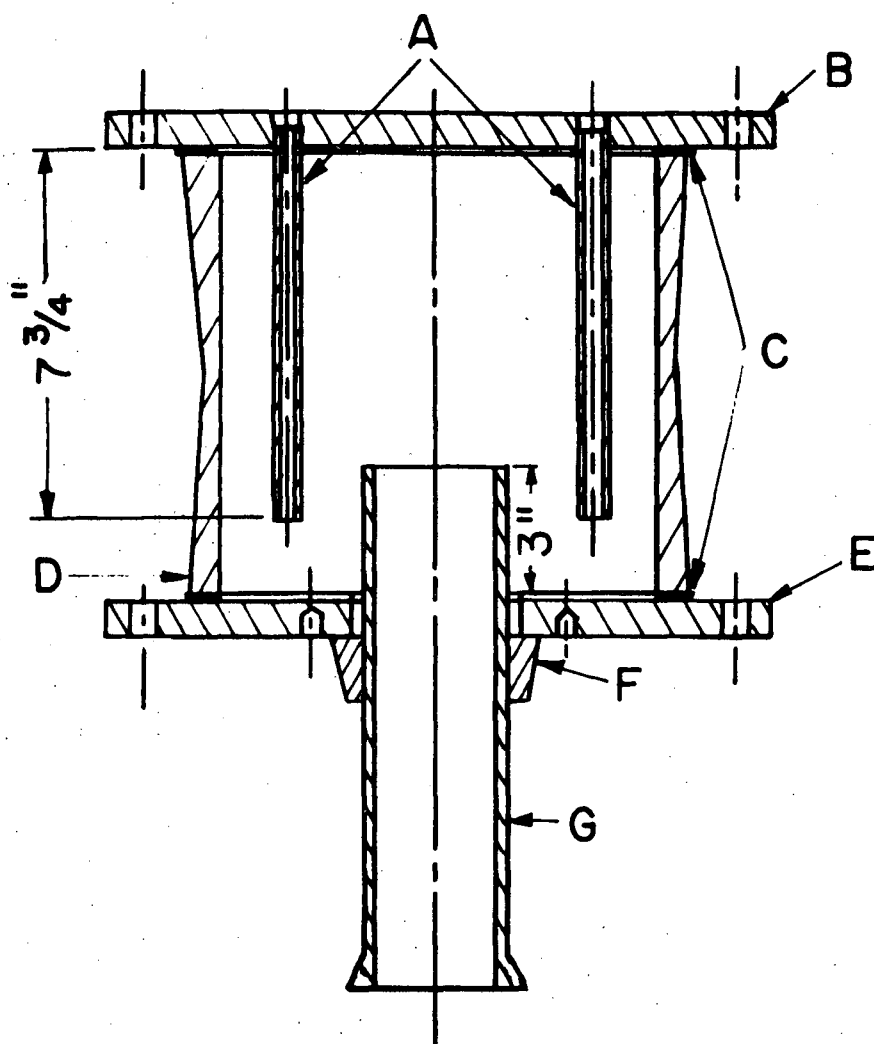
A   ¼" STAINLESS STEEL   PIPES (AQUEOUS PHASE INLET).

B   UPPER END PLATE OF ELGIN HEAD.

C   TEFLON COVERED GASKETS.

D   9" LONG, 9" I.D. Q.V.F. GLASS SECTION.

E   LOWER END PLATE OF ELGIN HEAD.

F   LOWER END PLATE PACKING.

G   10¾" LONG, 3" I.D. PYREX "DOUBLE TOUGH" PIPE WITH FLAT UNFLARED UPPER END.

FIGURE V-18.   ELGIN HEAD FOR THE 3-IN. I.D. COLUMN

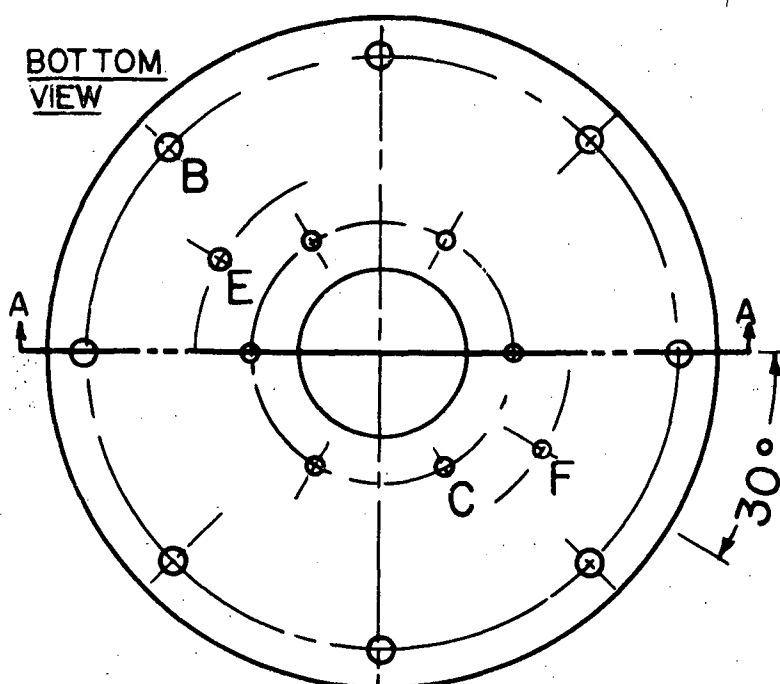8 HOLES $\frac{7}{16}$" D. ON $12\frac{3}{16}$" P.C.D.
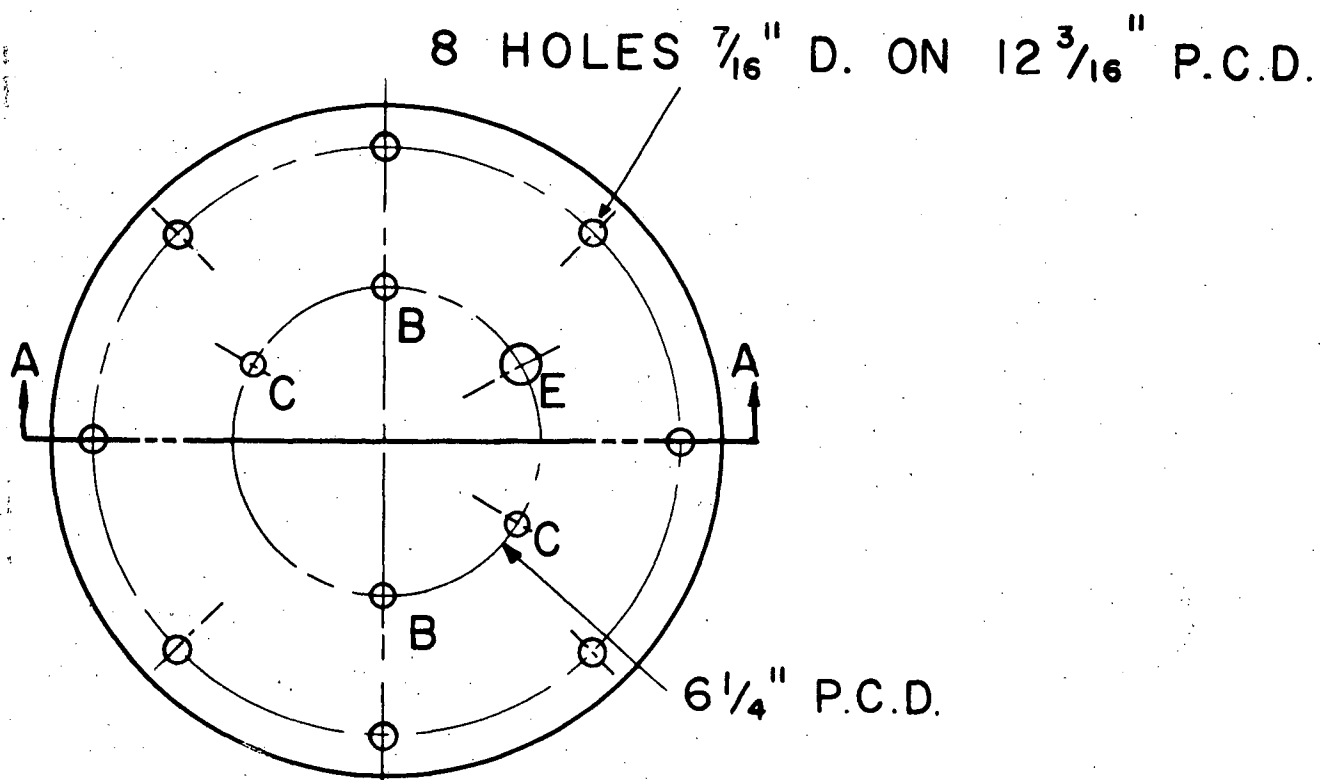
B,B, 2 HOLES DRILL AND TAP $\frac{1}{4}$" N.P.T.
C,C, 2 HOLES DRILL AND TAP $\frac{1}{4}$" N.P.T.
FROM BOTH SIDES
E, I HOLE DRILL AND TAP $\frac{1}{2}$" N.P.T.

$6\frac{1}{4}$" P.C.D.

$13\frac{3}{4}$" D.

$\frac{3}{4}$"

MACHINE FLAT

SECTION ON A-A

MATERIAL: STAINLESS STEEL

FIGURE V-19. UPPER END PLATE FOR THE ELGIN HEAD OF THE 3-IN. I.D. COLUMN
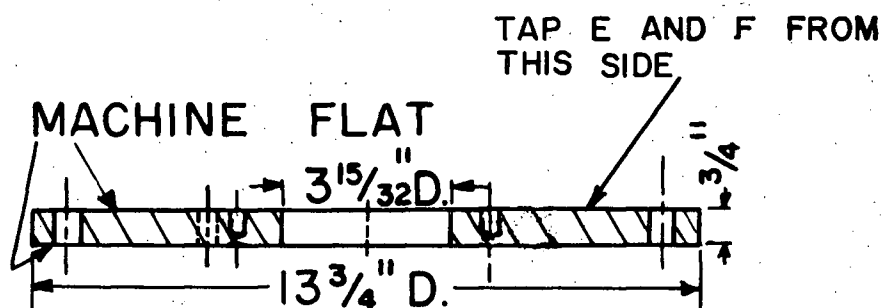
BOTTOM
VIEW

30°

B   8 HOLES $\frac{7}{16}$" D. ON $12\frac{3}{16}$" P.C.D.

C   6 HOLES DRILL AND TAP $\frac{1}{2}$"
     DEEP FOR $\frac{5}{16}$" BOLTS ON
     $5\frac{1}{4}$" P.C.D.

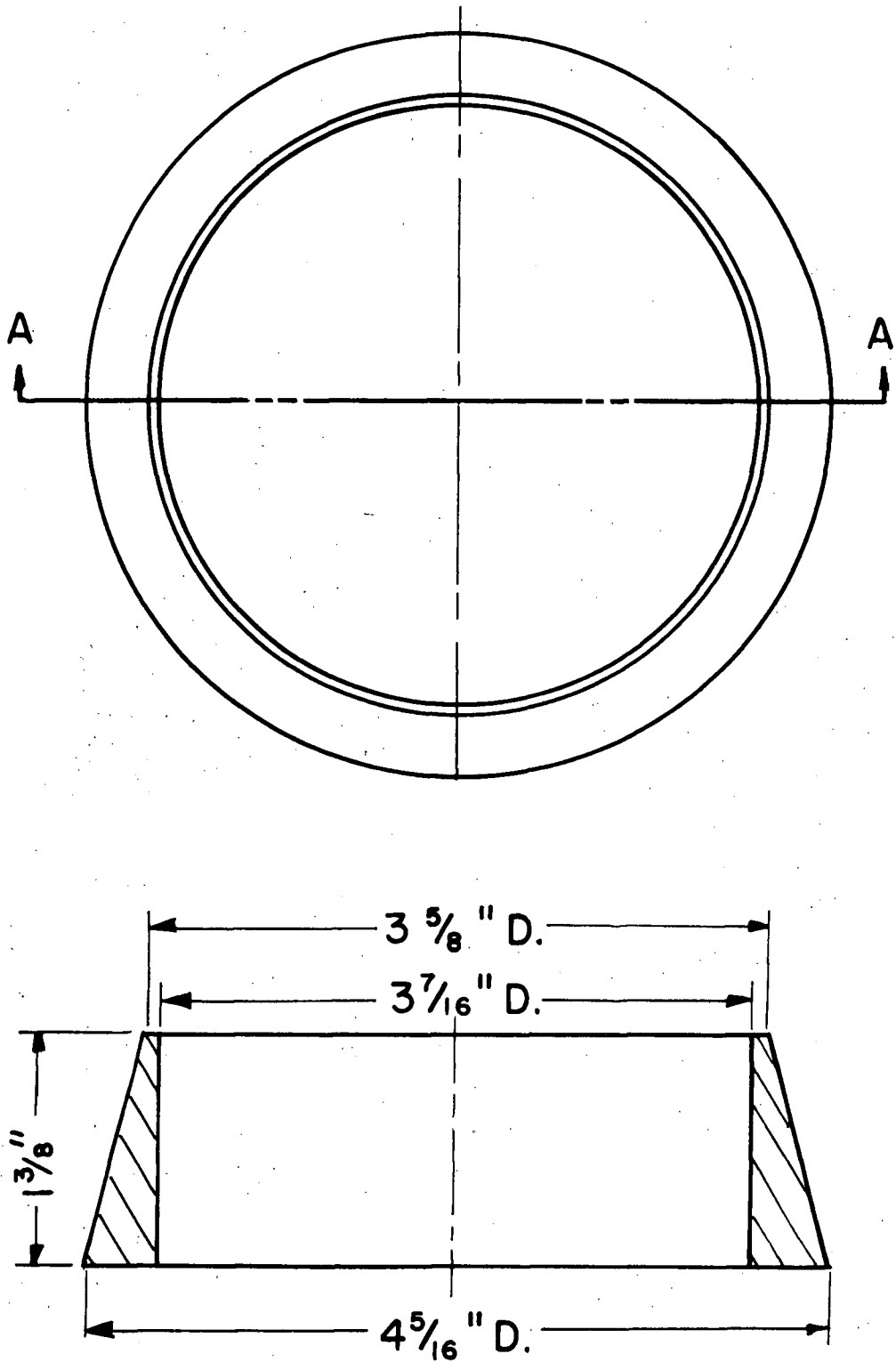E   1 HOLE DRILL AND TAP $\frac{1}{4}$"
     N.P.T. ON $7\frac{1}{2}$" P.C.D.

F   1 HOLE DRILL AND TAP $\frac{1}{8}$"
     N.P.T. ON $7\frac{1}{2}$" P.C.D.

TAP E AND F FROM
THIS SIDE

MACHINE FLAT

$3\frac{15}{32}$D.

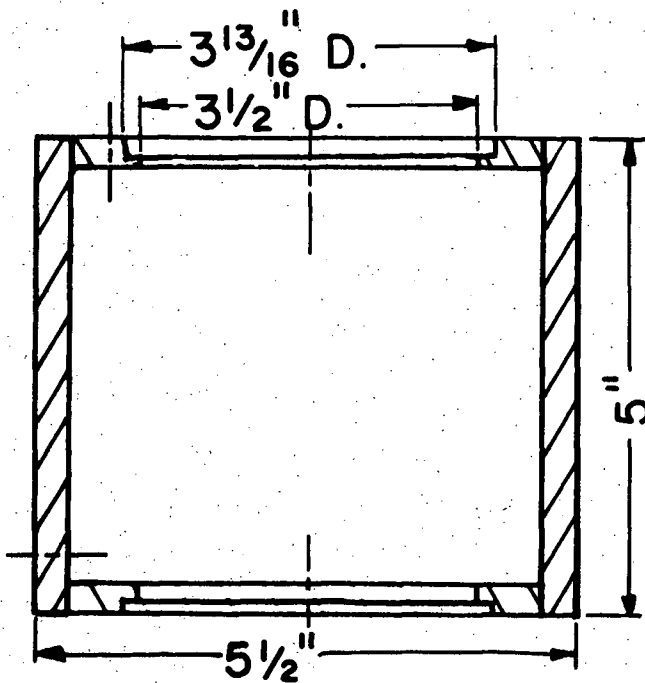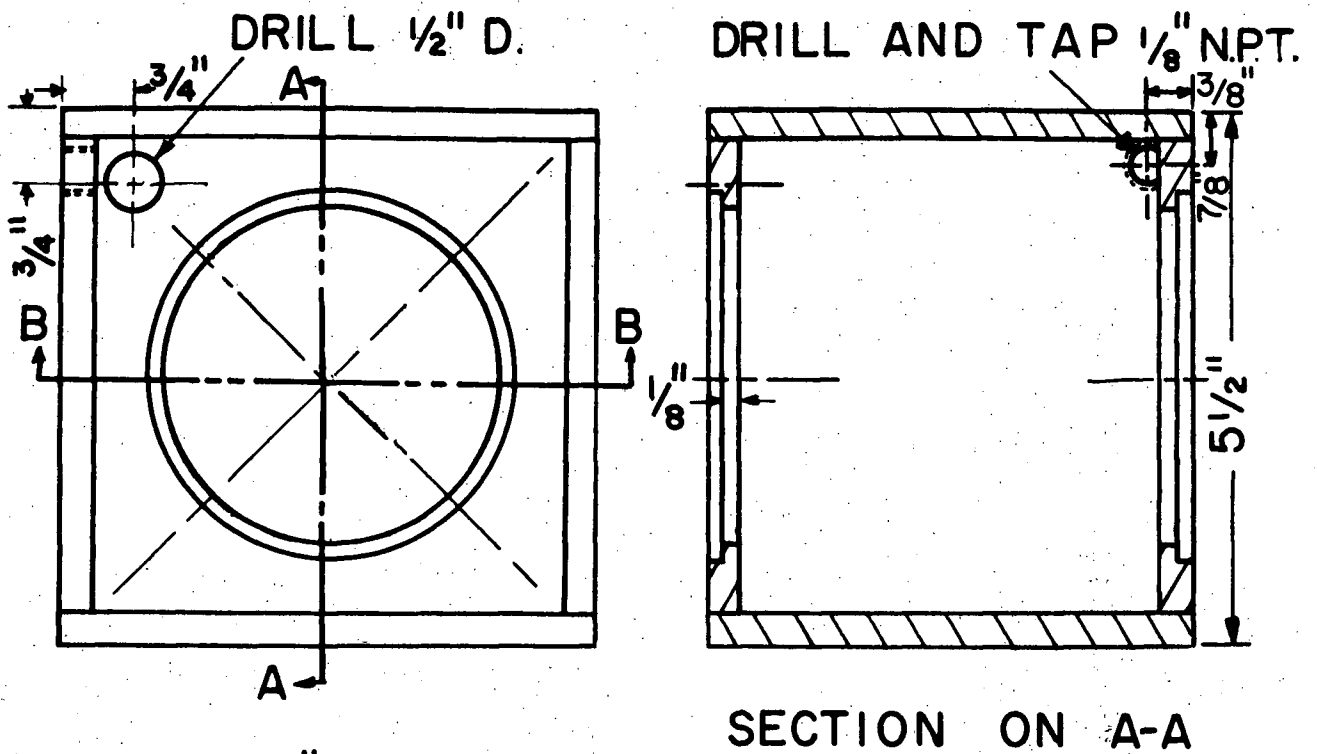$\frac{3}{4}$"

$13\frac{3}{4}$" D.

SECTION ON A-A
MATERIAL: STAINLESS STEEL

FIGURE V-20.   LOWER END PLATE FOR THE ELGIN HEAD OF THE 3-IN. I.D. COLUMN

SECTION ON A-A

MATERIAL: POLYETHYLENE

FIGURE V-21.   LOWER END PLATE PACKING FOR THE ELGIN HEAD OF THE 3-IN. I.D.
COLUMN

DRILL ½" D.

DRILL AND TAP ⅛" N.P.T.

SECTION ON A-A

SECTION ON B-B

MATERIAL: TRANSPARENT ⁵⁄₁₆" PERSPEX

FIGURE V-22.   PERSPEX BOX FOR THE 3-IN. I.D. COLUMN PHOTOGRAPHS

4 HOLES $\frac{9}{32}$" D. ON 9" P.C.D.

$4\frac{3}{8}$" D.

$3\frac{7}{8}$" D.

$\frac{3}{4}$"

$\frac{3}{8}$"

$4\frac{3}{16}$" D.

$9\frac{7}{8}$" D.

SECTION ON A-A
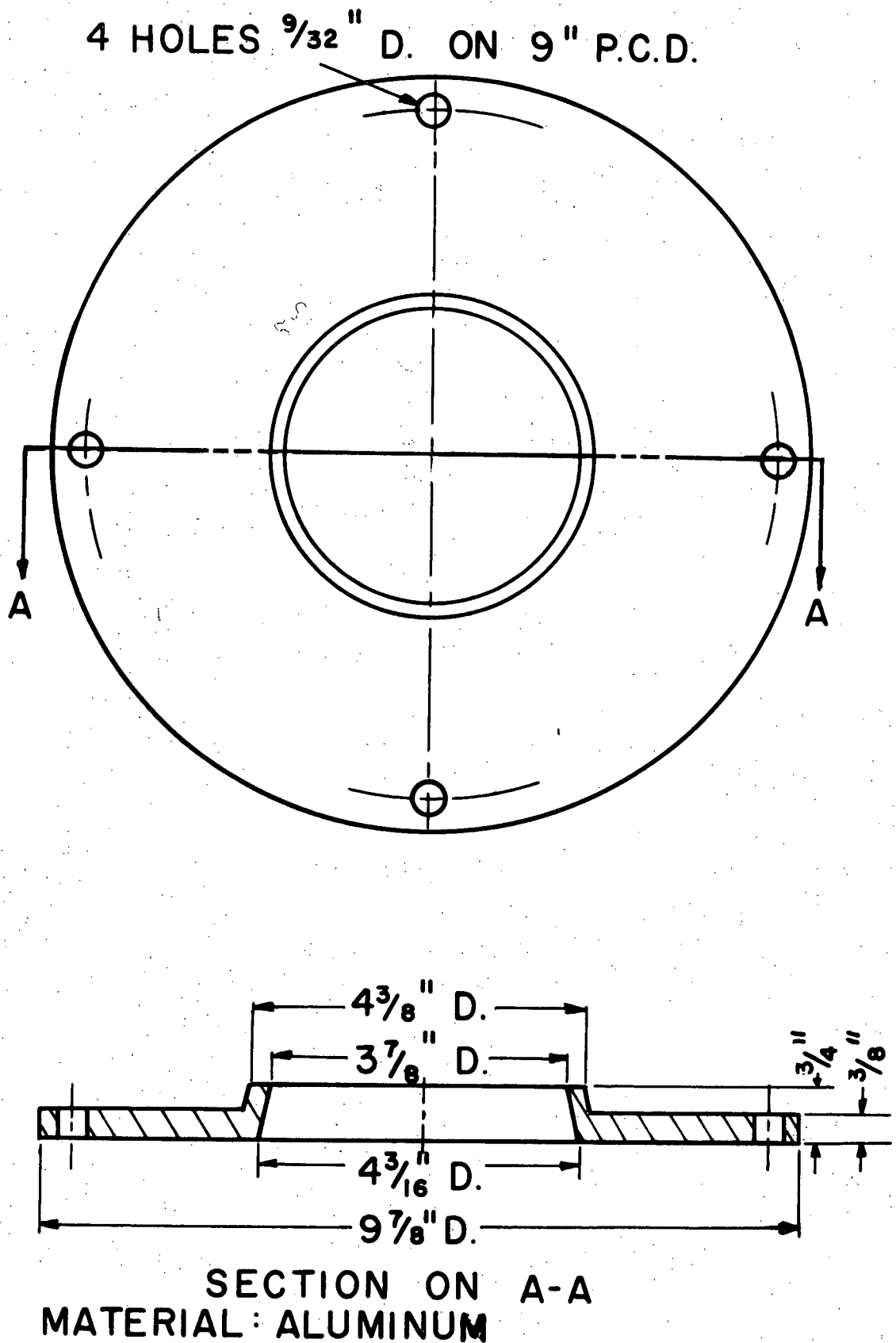## MATERIAL: ALUMINUM

FIGURE V-23.   FLANGE FOR THE PHOTOGRAPHIC SECTION OF THE 3-IN. I.D. COLUMN

APPENDIX VI

DIMENSIONS OF THE GLASS PORTIONS IN THE COLUMN TEST SECTIONS
AND MEASUREMENT OF PURGE TIMES.

a) Dimensions of the glass portions in the column test sections.

The length and inside diameter of each piece of Pyrex
"Double Tough" glass pipe in the test sections of the $1\frac{1}{2}$-in.
I.D. and 3-in. I.D. columns were measured by means of vernier
calipers. The I.D. was taken to be the average of six readings
equally spaced along the length of the glass piece. These
measurements are given in Table VI-1.

TABLE VI-1. DIMENSIONS OF THE GLASS PORTIONS IN THE COLUMN
TEST SECTIONS.

Section of column between positions (See diags. 10 and 20)	Length ($1\frac{1}{2}$-in. I.D.column) in.	I.D.($1\frac{1}{2}$-in. I.D. column) in.	Length (3-in.I.D. column) in.	I.D.(3-in. I.D.column) in.
Tracer distributor and 1	6.044	1.500	5.983	2.992
1 and 2	5.967	1.500	6.022	3.026
2 and 3	5.969	1.497	6.020	2.985
3 and 4	5.978	1.503	5.975	2.989
4 and 5	6.024	1.492	6.020	3.008
5 and 6	5.793[a]	1.497[a]	6.014	3.009
6 and 7	5.975	1.504	6.008	2.992
7 and 8	6.050	1.595	6.044[b]	3.020[b]
8 and 9	6.049	1.508	6.018	2.998
9 and 10	6.032	1.500	5.996	2.995

[a]The piston sampler block replaced a glass section.

[b]This piece of glass was used as the photographic test section. It was cut from a longer piece of Pyrex "Double Tough" pipe.

The thickness of each polyethylene gasket was measured and was found to be 1/16-in. This measurement did not change when the gasket was compressed between two pieces of glass.

b) Measurement of purge times.

i) Hook and bell-probes sampling lines.

The column was brought to steady state operating conditions with the transfer of acetic acid from the continuous phase to the dispersed phase as described under Experimental Procedure. With the probes a few inches below the interface the flow of samples into the probes and along the sampling lines was started and maintained for about 2-hr. Without altering the sampling rates the probes were lowered to about 1-ft. above the nozzle tips. Samples from each probe were collected at time intervals of about 1-min. until 30-min. after moving the probes. The bell-probe samples were shaken vigorously many times to bring the two phases to equilibrium. The hook-probe samples and the ketone phase of the bell-probe samples were analysed for acetic acid as described earlier. For each probe a plot was made of the concentration of acetic acid in each sample versus the time after moving the probes. The purge time was taken to be that time when there was no change in concentration with increasing time. Purge times were determined for various sampling rates

between 4-ml./min. and 20-ml./min. It was found that a conservative estimate of the minimum purge time for each of the sampling lines was given by the following equation.

$$\text{Purge time (min.)} = \frac{120}{\text{sampling rate (ml./min.)}}$$

ii) Hypodermic needles.

The inside diameter of a 22-gauge hypodermic needle is so small that the purge time for such a sampling device is very small. A conservative estimate of the minimum purge time was estimated in the following manner. A hypodermic needle sampler was inserted through one of the $1\frac{1}{2}$-in. I.D. polyethylene gaskets described earlier. This gasket was sandwiched between one end of a 3-ft. length of $1\frac{1}{2}$-in. I.D. Pyrex pipe and a $1\frac{1}{2}$-in. dia. disk of 1/16-in. thick polyethylene. The gasket and disk were clamped to the end of the pipe by means of an aluminum end plate and flange. The pipe was filled with water and a sampling rate of 3/4-ml./min. through the needle was established. The water was poured out of the pipe and then the pipe was filled with an aqueous solution of potassium permanganate. The flow of liquid through the hypodermic needle recommenced at 3/4-ml./min. The colour of the potassium permanganate showed up in the sample issuing from the needle in less than 45-sec. The change in colour was so rapid that the time between that when the colour first appeared and that when it reached full strength was considered to be negligible. A purge time of $1\frac{1}{2}$-min. was considered to be conservative for sampling rates of at least 3/4-ml./min.